Universidade de Aveiro Departamento de Biologia

2018

Maria João Janeiro da Silva

Selecção, genética e evolução do crescimento e do tamanho

Selection, genetics and evolution of growth and size

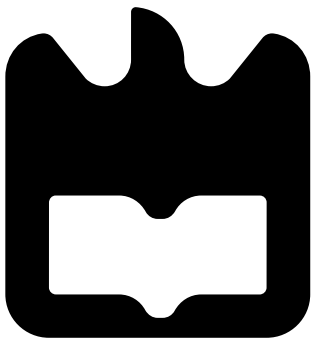

Maria João Janeiro da Silva

Selecção, genética e evolução do crescimento e do tamanho

Selection, genetics and evolution of growth and size

Tese apresentada à Universidade de Aveiro para cumprimento dos requesitos necessários à obtenção do grau de Doutor em Biologia e Ecologia das Alterações Globais, e realizada em regime de co-tutela com a Universidade de St Andrews para a obtenção do grau de Doutor em Biologia, realizada sob a orientação científica do Professor Doutor Michael Blair Morrissey, Professor Associado na *School of Biology, University of St Andrews*, do Professor Doutor Amadeu Mortágua Velho da Maia Soares, Professor Catedrático do Departamento de Biologia da Universidade de Aveiro, e do Doutor Miguel Maria Borges da Costa Guint Barbosa, investigador do Departamento de Biologia da Universidade de Aveiro.

Apoio financeiro do POCTI no âmbito do III Quadro Comunitário de Apoio.

Apoio financeiro da FCT e do FSE no âmbito do III Quadro Comunitário de Apoio (bolsa de doutoramento SFRH/BD/96078/2013)

To my grandmother

o júri / the jury

presidente / president

Luís António Ferreira Martins Dias Carlos
Professor Catedrático da Universidade de Aveiro | *Full Professor at the University of Aveiro*

vogais / committee

Ulisses Manuel de Miranda Azeiteiro
Professor Associado c/ Agregação da Universidade de Aveiro | *Associate Professor at the University of Aveiro*

Hannah Dugdale
Professor Associado da Universidade de Leeds | *Associate Professor at the University of Leeds*

Erik Postma
Professor Associado da Universidade de Exeter | *Senior Lecturer at the University of Exeter*

Michael Blair Morrissey
Professor Associado da Universidade de St Andrews (orientador) | *Reader at the University of St Andrews (supervisor)*

Amadeu Mortágua Velho da Maia Soares
Professor Catedrático da Universidade de Aveiro (co-orientador) | *Full Professor at the University of Aveiro (co-supervisor)*

agradecimentos / acknowledgements

I am immensely grateful to Michael Morrissey for everything he taught me and for his continuous guidance and support. I feel in great debt to Michael for his kind and generous willingness to always share his knowledge and I would like to express how privileged I feel to be his student. I also thank my secondary advisors, Miguel Barbosa, for his continuous support and constructive advices, and Prof. Amadeu Soares, for the opportunity to start this project.

I would like to express my gratitude to Marco Festa-Bianchet, Fanie Pelletier and Dave Coltman for their precious advice in all bighorn matters, and for setting such a great example of generosity in academia. I particularly thank Marco for welcoming me to a lovely stay in Sherbrooke.

I owe many thanks to Loeske Kruuk, Jarrod Hadfield, Luis-Miguel Chevin, Josephine Pemberton, and Graeme Ruxton for sharing insightful comments and suggestions that helped improving my work. I am also very grateful to Mick Crawley, Josephine and Jill Pilkington for having given me the opportunity to visit Hirta and to participate in the field work of the Soay sheep project.

Appreciation is also due to the members of my committee, Nathan Bailey and Will Cresswell; and also to Tom Meagher, Maria Dornelas and Laura Antão for their guidance in troubled moments during my PhD. I would like to express my gratitude to Lianne Baker and Joyce Haynes for being an incredible support to Biology students at St Andrews.

I am particularly grateful to countless volunteers that have been collecting data for the Soay and the bighorn sheep projects for decades, without whom my thesis would not have been possible.

While too many to mention by name, I feel the most fortunate to have met many kind and crazy souls in St Andrews who made *the North* feel like home.

I would like to thank my family for their encouragement and support, and I want to thank Esme, without whom the sky of St Andrews would have looked just like it is - always pretty cloudy. I thank her with all my heart for having patiently endured and supported a very difficult version of me, and for her love.

Finally, I am most grateful to Fundação para a Ciência e Tecnologia, Portugal, for financial support during the PhD.

palavras-chave

caça ao troféu, constrangimento genético, evolução, genética quantitative evolutiva, modelo baseado em indivíduos, modelo de projecção integral, *Ovies aries*, *Ovies canadensis*, paradoxo da estase morfológica, selecção natural, tamanho, trajectórias de crescimento, viés.

resumo

O paradoxo da estase morfológica (*paradox of stasis*) tem motivado avanços consideráveis na área da genética quantitativa evolutiva nas últimas décadas. Discrepâncias entre tendências temporais do tamanho de organismos em populações selvagens e previsões baseadas em teoria evolutiva devem-se necessariamente a uma compreensão deficiente dos fundamentos teóricos subjacentes à evolução num determinado sistema e/ou à adopção de ferramentas metodológicas com pressupostos que não são realistas. Embora difiram na sua natureza, estas duas explicações são difíceis de distinguir, uma vez que, muitas vezes, as ferramentas (estatísticas) da genética quantitativa têm pressupostos, implícitos ou explícitos, sobre biologia e ecologia. Na presente tese, eu investigo mecanismos de hereditariedade e/ou selecção em casos para os quais se prevê que aplicações teóricas convencionais gerem previsões enviesadas ou erróneas acerca da evolução do tamanho dos organismos. Especificamente, adopto uma metodologia para lidar com constrangimentos genéticos numa perspectiva bastante fenotípica, o que facilita a quantificação do viés que existiria se tal constrangimento não fosse tido em conta (Capítulo 3). Esta metodologia permite distinguir a selecção do peso corporal de ovelhas da raça *Soay* (*Ovies aries*) que ocorre directamente, através do efeito do peso na *fitness* (ou valor adaptativo), e indiretamente, através do seu efeito na probabilidade de gravidez durante o primeiro ano de vida. No Capítulo 4, apresento provas analíticas de várias questões com aplicações típicas de modelos de projeção integral (*integral projection models*, IPMs) que incorporam hereditariedade e desenvolvimento de caracteres, concluindo que estas aplicações são incapazes de prever alterações evolutivas, ainda que estas tenham ocorrido ou se espere que ocorram. Outro tópico importante desta tese é o desenvolvimento de um modelo baseado em indivíduos (*individual-based model*, IBM), concebido e parameterizado para o comprimento dos cornos da população de ovelhas de raça *bighorn* (*Ovies canadensis*) residente em Ram Mountain, no Canada (Capítulo 6). Este modelo, desenvolvido para ambos os sexos e equivalente a um IPM, usa teoria da genética quantitativa para modelar a transmissão genética de caracteres (com funções de desenvolvimento estimadas no Capítulo 5). Desta forma, esta abordagem permite a quantificação da resposta evolutiva à caça ao troféu, contabilizado, ao mesmo tempo, um grande número de complexidades ecológicas.

keywords

bias, evolutionary prediction, evolutionary quantitative genetics, genetic constraint, growth, individual-based models, integral projection models, natural selection, ontogenetic trajectories, *Ovies aries*, *Ovies canadensis*, paradox of stasis, size, trophy hunting.

abstract

A considerable body of work in recent decades in the field of evolutionary quantitative genetics has been motivated by the paradox of stasis. Mismatches between observed dynamics of size in wild populations and evolutionary predictions must arise from deficient understanding of the theoretical grounds underlying the evolution in a particular system, and/or the adoption of methodological tools making assumptions that are unrealistic. Although different in their nature, these classes of explanation are difficult to tear apart, as very often quantitative genetics (statistical) tools make either implicit or explicit assumptions about biology and ecology. In this thesis, I investigate inheritance and/or selection mechanisms when conventional applications of theory are expected to lead to biased or erroneous predictions of evolutionary change in size. Specifically, I adopt a methodology to handle genetic constraints in a fairly phenotypic perspective, which facilitates quantification of bias that would exist if such constraint was not accounted for (Chapter 3). I use this methodology to tear apart the selection in Soay sheep body mass that occurs directly through its effect on fitness and indirectly through its effect on pregnancy during the first year of life. Next, I provide analytical proofs of several issues with applications of integral projection models (IPMs) that incorporate inheritance and development, concluding that these will predict no evolutionary change regardless of whether it should, will, or has occurred (Chapter 4). Another main topic of this thesis is the development of a two-sex individual-based model (IBM) of horn length (Chapter 6), equivalent to an IPM, that uses quantitative genetics theory to model trait transmission (with development functions estimated in Chapter 5). This IBM, parameterised using data from the bighorn sheep (*Ovis canadensis*) of Ram Mountain, is used to quantify the evolutionary response to trophy hunting, while accounting for a large number of ecological complexities.

Contents

Jury v
Acknowledgements vii
Resumo ix
Abstract xi

1 General introduction **1**
1.1 Bias in predicting evolution and the paradox of stasis 1
1.2 Evolution of ontogenetic size trajectories 4
1.3 Population models 6
1.4 Thesis overview 7

2 Meet the sheep **9**
2.1 The Soay sheep 9
2.2 The bighorn sheep 11

3 Selection of size and early pregnancy in Soay sheep (*Ovies aries*) **15**
3.1 Introduction 15
3.2 Study system and data 17
3.3 Early pregnancy and lamb size 18
3.4 Fitness: first-year survival and lifetime rearing success 23
3.4.1 First-year survival 23
3.4.2 First-year rearing success (AReS) 27
3.4.3 First-year life history 27
3.4.4 Subsequent lifetime rearing success (LReS) 28
3.5 Formal selection analysis 31
3.6 Model estimation and reported statistics 37
3.7 Discussion 37
3.8 Summary 39

4 Towards robust evolutionary inference with integral projection models **41**
4.1 Introduction 42
4.2 Development 44
4.3 Inheritance 48
4.3.1 Inheritance across generations 49
4.3.2 Across-age inheritance functions 51
4.3.3 Parent-offspring regression with a constant intercept 54
4.4 Study case: bighorn sheep 58

4.4.1 Standard IPM approach . . . 58
4.4.2 Random regression of size . . . 59
4.4.3 Recovering resemblance within and across-generations . . . 60
4.5 Discussion . . . 64
4.6 Summary . . . 66

5 The genetics of horn length trajectories in bighorn sheep (*Ovies canadensis*) rams 67
5.1 Introduction . . . 67
5.2 Methods . . . 70
5.2.1 Study system and data . . . 70
5.2.2 Models and variance structures . . . 70
5.2.3 Model estimation and comparison . . . 74
5.3 Results . . . 75
5.3.1 Observed size trajectories and underlying cross-age population structure in horn length . . . 75
5.3.2 Model comparison . . . 76
5.4 Discussion . . . 82
5.5 Summary . . . 85

6 What evolutionary change is expected due to trophy hunting based on a heritable trait? 87
6.1 Introduction . . . 87
6.2 Study system and data . . . 90
6.3 Vital rates . . . 90
6.3.1 Annual breeding success . . . 90
6.3.2 Harvest-related survival . . . 92
6.3.3 Winter survival . . . 93
6.3.4 Horn length ontogenetic trajectories . . . 94
6.3.5 Parameter estimation and reported statistics . . . 94
6.4 The model . . . 97
6.4.1 Model description . . . 97
6.4.2 Comparison of alternative approaches to modelling horn length trajectories . . . 97
6.4.3 Measuring evolution . . . 101
6.5 Discussion . . . 104
6.6 Summary . . . 106

7 General discussion 107
7.1 Summary of findings . . . 107
7.2 Bias in inference of selection and the genetics of size . . . 108
7.3 Challenges and future work . . . 112
7.4 Conclusion . . . 113

Bibiography 130

Appendices i

Appendix A Supplementary material to Chapter 3 i

Appendix B Supplementary material to Chapter 4 **iii**

Appendix C Supplementary material to Chapter 5 **xiii**

Appendix D Supplementary material to Chapter 6 **xxvii**

Appendix Bibiography **xlv**

List of Figures

2.1 The Soay sheep of St Kilda. 11
2.2 Bighorn sheep at Ram Mountain. 13

3.1 (a) Number of Soay sheep ewes, ewe lambs and population size from 1991 to 2015 in the Village Bay study area; (b) empirical distribution of body mass in pregnant and non-pregnant ewe lambs; (c) size-dependent probability of early pregnancy; (d) lamb body mass (upper panel) and probability of early pregnancy (lower panel) across time; (e) non-parametric survival curves of Soay sheep according to mother's age at conception. 19
3.2 Probability of first-year survival and lifetime rearing success, LReS, in Soay sheep ewes as a function of lamb body mass, and both lamb body mass and early pregnancy status. 24
3.3 Probability of first-year survival in pregnant and non-pregnant ewe lambs, and AReS and LReS in Soay sheep ewes that survived their first annual cycle as a function of lamb body mass and population size. 26
3.4 Geometric diagrams with areas corresponding to the joint probabilities of early pregnancy and first-year survival for average-sized individuals experiencing average environmental conditions. 28
3.5 Developmental system representing the phenotypic landscape defined in Equation (3.11), including the probability of twinning, lamb body mass, the probability of being pregnant as a lamb, the probability of surviving the first annual cycle, first year and subsequent lifetime rearing success, as well as fitness, defined as the sum of AReS and LReS on surviving ewes weighted by the probability of first-year survival. 32
3.6 The effect of population density on the values of the traits in the path diagram in Figure 3.5, and consequently on selection of lamb body mass and early pregnancy. 34
3.7 Proportion of natural selection on lamb body mass occurring through viability selection in Soay sheep ewes as a function of population density. 35
3.8 Maximum probability of early pregnancy that maximises fitness as a function of lamb body mass in Soay sheep. 37

4.1 Path diagrams illustrating the ontogenetic development of size 45
4.2 Proportion of correlation in size among ages recovered by a typically-built IPM as a function of the square root of the repeatability (r) and number projection steps ($\Delta\prime$). . 47
4.3 Path diagrams illustrating the transmission of a quantitative trait across generations of the same age. 50

4.4 Proportion of the parent-offspring regression recovered by a same-age inheritance function as a function of the heritability and the number of generations. 51
4.5 Path diagrams illustrating the transmission of a quantitative trait between parents and offspring with two ontogenic stages, juvenile and adult. 53
4.6 Proportion of parent-offspring regression recovered by a cross-age parent-offspring regression, in juveniles and adults. 55
4.7 The consequences of assuming a constant intercept for the parent-offspring (PO) regression across generations. 57
4.8 Observed phenotypic correlation matrix for size across ages for the bighorn sheep population of Ram Mountain, and analogous matrices implied by the IPM and estimated by the RRM approaches, as well as the respective proportions of the correlation in size among ages recovered by each approach. 62
4.9 Parent-offspring regressions estimated for different ages for the bighorn sheep population of Ram Mountain, by the IPM and the RRM approaches. 63

5.1 Observed horn length trajectories of 276 rams of the bighorn sheep population of Ram Mountain. 75
5.2 Variance components contributing to the phenotypic variance in horn length up to the age of 4 years in bighorn rams from Ram Mountain, and the corresponding proportion of variance explained by each component. 76
5.3 Diagrams showing unstructured **P** and **G** variance-covariance and correlation matrices of horn length across ages in bighorn rams from Ram Mountain. 77
5.4 Mean male horn length trajectories observed and estimated for the bighorn sheep population of Ram Mountain. 78
5.5 Variance, proportion of phenotypic variance, and coefficient of variation associated with additive genetic and permanent environment effects in horn length trajectories of male bighorn sheep at Ram Mountain. 80
5.6 Proportion of the phenotypic and additive genetic correlations in horn length recovered by the random regression, the factor analytic with a single and two additive genetic common factors, and the antedependence models, according to the number of years apart between horn length measurements. 81

6.1 Annual breeding success in bighorn ewes and rams at Ram Mountain. 93
6.2 Annual survival probability as a function of age, population density and horn length in the bighorn sheep population at Ram Mountain. 95
6.3 Probability of annual winter survival as a function horn length for ages one (a), four (b), and seven (c) years, for the bighorn rams from the population at Ram Mountain. The black lines correspond to averages, whereas the areas in teal correspond to 95% credible intervals, both predicted using the model in Equation 6.7. 96
6.4 Annual cycle and dynamics of the bighorn sheep at Ram Mountain. 98
6.5 Simplified illustration of the individual-based model mimicking the life-cycle of the bighorn sheep inhabiting Ram Mountain. 98
6.6 Male horn length dynamics simulated over 200 years, of which the last 100 years correspond to a hunting period 100

6.7 Average male horn length ontogenetic trajectories for different years (iterations) after the start of the hunting period, and the relative change in horn length across the ontogeny, with respect to observed age-specific means. 101
6.8 Trajectories of the breeding values of male horn length as simulated using the random regression model over 200 iterations, of which the last 100 correspond to a hunting period. 102
6.9 Differences in horn length (phenotype and breeding values) from the beginning of the hunting period over 100 years for ages from 1 to 8 years; and yearly and relative phenotypic rate of change across the ontogeny of bighorn sheep males 103

B.2.1 Proportion of parent-offspring regression recovered by IPMs, in juveniles and adults as a function of the size-dependent growth regression and the additive genetic covariance in growth. xi

D.1.1 Observed and predicted annual breeding success in bighorn ewes of Ram Mountain. xxvii
D.1.2 Observed and predicted annual survival probability as a function of age in the bighorn sheep population of Ram Mountain. xxviii
D.3.1 Population dynamics and sex ratio obtained along 1000 iterations in a scenario with no inheritance mechanism built-in. xxx
D.3.2 Female population structured by age, observed in the bighorn sheep population of Ram Mountain and simulated over 1000 years, in a scenario with no inheritance mechanism built-in. xxxi
D.3.3 Male population structured by age, observed in the bighorn sheep population of Ram Mountain and simulated over 1000 years, in a scenario with no inheritance mechanism built-in. xxxii
D.3.4 Male horn length dynamics over 1000 years under a scenario with no inheritance mechanism built-in. xxxiii
D.3.5 Male horn length ontogenetic trajectories, observed in the bighorn sheep population of Ram Mountain and simulated over 1000 years under a scenario with no inheritance mechanism built-in. xxxiv
D.3.6 Observed and simulated average breeding success as a function of age in a scenario with no inheritance mechanism built-in. xxxv
D.3.7 Observed and simulated average winter survival as a function of age in a scenario with no inheritance mechanism built-in. xxxvi
D.3.8 Population dynamics and sex ratio obtained along 1000 years with an inheritance mechanism built-in. xxxvii
D.3.9 Female population structured by age, observed in the bighorn sheep population of Ram Mountain and simulated over 1000 years, in a scenario with an inheritance mechanism built-in. xxxviii
D.3.10 Male population structured by age, observed in the bighorn sheep population of Ram Mountain and simulated over 1000 years, in a scenario with an inheritance mechanism built-in. xxxix
D.3.11 Male horn length dynamics over 1000 years in a scenario with an inheritance mechanism built-in. xl

D.3.12 Breeding values dynamics, including intercepts, slopes and curvatures, over 1000 years for the random regression model. xli
D.3.13 Male horn length trajectories, observed in the bighorn population of Ram Mountain and simulated for 1000 years under a scenario with an inheritance mechanism built-in. xlii
D.3.14 Observed and simulated average breeding success as a function of age in a scenario with an inheritance mechanism built-in. xliii
D.3.15 Observed and simulated winter survival as a function of age in a scenario with an inheritance mechanism built-in. xliv

List of Tables

3.1 Coefficients of a binomial regression of early pregnancy on body mass in Soay ewe lambs. . . . 20

3.2 Coefficients in the latent and expected scales of the multi-response animal model on lamb body mass and early pregnancy in Soay sheep. . . . 22

3.3 Coefficients of mixed effect binomial regressions exploring the association of first-year survival with lamb size and early pregnancy in Soay ewes. . . . 25

3.4 Coefficients of a binomial regression of AReS in surviving ewe lambs that got pregnant on lamb body mass, birth and measurement dates, and population density in Soay sheep ewe lambs. . . . 27

3.5 Coefficients of Poisson regressions exploring the association between LReS in ewes surviving their first year and lamb body mass and early pregnancy. . . . 30

3.6 Coefficients of a binomial regression of the probability of twinning as a function of mean-centred population density and maternal age. . . . 32

3.7 Selection gradients of lamb body mass and early pregnancy for three different values of observed population density. Raw (η) and standardised selection gradients, either by the observed standard deviation (η_{sd}) or the observed mean (η_{μ}), are shown. For lamb body mass, selection gradients considering first-year survival as a measure of fitness are also included (η_s). . . . 36

4.1 Coefficients for the IPM standard approach, including regressions of mass at age a on mass at age $a-1$, and of lamb's mass on mother's mass at conception for the bighorn sheep population of Ram Mountain. The values correspond to posterior modes and 95% quantile-based credible intervals. . . . 59

4.2 Coefficients for the random regression animal model on body mass for the bighorn sheep ewes from Ram Mountain. . . . 60

5.1 Absolute differences (upper diagonal) and corresponding 95% credible intervals (lower diagonal) between phenotypic and additive genetic correlations in horn length of bighorn sheep rams from Ram Mountain, estimated by the multivariate model. . . . 76

6.1 Parameter estimates of the binomial and multinomial regressions of annual breeding success in bighorn sheep females and males, respectively, from the population at Ram Mountain. . . . 92

6.2 Parameter estimates of binomial regressions of winter and harvest-related survival fitted to data from the bighorn sheep population at Ram Mountain. . . . 96

6.3 Number of simulations run for each combination of growth function, inheritance and hunting settings. 98

A.1.1 Coefficients of the bivariate model of lamb body mass and early pregnancy in Soay sheep ewes. i

B.2.1 Covariances among ages i and j ($j > i$) in true and observed sizes. x
B.2.2 Covariances in size among ages i and j ($j > i$) recovered by typically-constructed IPMs. xi

C.1.1 JAGS code for the factor analytic model including a single additive genetic axis. . . . xiv
C.1.2 JAGS code for the factor analytic model including two additive genetic axes. xv
C.2.1 Parameter estimates from the multivariate model on horn length fitted to the bighorn sheep males from the population of Ram Mountain. xvi
C.2.2 Parameter estimates from the random regression model on horn length fitted to the bighorn sheep males from the population of Ram Mountain. xvii
C.2.3 Estimates of the age-specific parameters from the factor analytic model with a single additive genetic common factor on horn length fitted to the bighorn sheep males from the population of Ram Mountain. xviii
C.2.4 Estimates of the non-age-specific parameters from the factor analytic model with a single additive genetic common factor on horn length fitted to the bighorn sheep males from the population of Ram Mountain. xviii
C.2.5 Estimates of the age-specific parameters from the factor analytic model with two additive genetic common factor on horn length fitted to the bighorn sheep males from the population of Ram Mountain. xix
C.2.6 Estimates of the non-age-specific parameters from the factor analytic model with two additive genetic common factors on horn length fitted to the bighorn sheep males from the population of Ram Mountain. xix
C.2.7 Estimates of the age-specific parameters from the antedependence model on horn length fitted to the bighorn sheep males from the population of Ram Mountain. xx
C.2.8 Estimates of the non-age-specific parameters from the antedependence model on horn length fitted to the bighorn sheep males from the population of Ram Mountain. . xx
C.2.9 Estimates of the age-specific parameters from an IPM-like antedependence model on horn length fitted to the bighorn sheep males from the population of Ram Mountain. This model differs from one shown in the main text as its inheritance function is of parental horn length at conception, rather than at 3 years-old. xxi
C.2.10 Estimates of the non-age-specific parameters from an IPM-like antedependence model on horn length fitted to the bighorn sheep males from the population of Ram Mountain. This model differs from one shown in the main text as its inheritance function is of parental horn length at conception, rather than at 3 years-old. xxi
C.3.1 Additive genetic and permanent environment contributions to the phenotypic variance across the horn length ontogeny of males from the bighorn sheep population of Ram Mountain, as estimated by the different models. xxii
C.4.1 Additive genetic covariance and correlation matrix of male horn length across ages in the bighorn population of Ram Mountain, estimated with the multivariate model. . . . xxiii
C.4.2 Additive genetic covariance and correlation matrix of male horn length across ages in the bighorn population of Ram Mountain, estimated by the random regression model. xxiii

C.4.3 Additive genetic covariance and correlation matrix of male horn length across ages in the bighorn population of Ram Mountain, estimated by the factor analytic model with a single additive genetic common factor. xxiii
C.4.4 Additive genetic covariance and correlation matrix of male horn length across ages in the bighorn population of Ram Mountain, estimated by the factor analytic model with two additive genetic common factors. xxiv
C.4.5 Phenotypic covariance and correlation matrix of male horn length across ages in the bighorn population of Ram Mountain, estimated with the multivariate model. xxiv
C.4.6 Phenotypic covariance and correlation matrix of male horn length across ages in the bighorn population of Ram Mountain, estimated by the random regression model. . . xxiv
C.4.7 Phenotypic covariance and correlation matrix of male horn length across ages in the bighorn population of Ram Mountain, estimated by the factor analytic model with a single additive genetic common factor. xxv
C.4.8 Phenotypic covariance and correlation matrix of male horn length across ages in the bighorn population of Ram Mountain, estimated by the factor analytic model with two additive genetic common factors. xxv
C.4.9 Phenotypic covariance and correlation matrix of male horn length across ages in the bighorn population of Ram Mountain, implied by the antedependence model. xxv

D.2.1 JAGS code for the multinomial model fitting annual male breeding success, as described in Equations (6.2)-(6.4). xxix

CHAPTER 1

General introduction

This thesis, along with a considerable body of work produced over the last decades in the field of evolutionary quantitative genetics, is primarily motivated by the paradox of stasis and an attempt to make a contribution to its resolution. Mismatches between observed dynamics of body size in wild populations and evolutionary predictions must arise from deficient understanding of the theoretical grounds underlying the evolution in a particular system, and/or the adoption of methodological tools making assumptions that are unrealistic. The former is related to how general theory can be in the face of the complex biology and ecology of particular species or populations, while the latter relates to technical aspects of evolutionary prediction. Although different in their nature, these are difficult to tear apart, as very often quantitative genetics tools make either implicit or explicit assumptions about biology and ecology. The work contained within this thesis aims at investigating inheritance and/or selection mechanisms when conventional applications of theory are expected to lead to biased or erroneous predictions of evolutionary change. Its focus is not the paradox of stasis, in particular, but to identify and correct sources of error when predicting the evolution of size. Although I dedicate one of the technical chapters to looking at such issues at a particular age, most of the work I developed focuses on the evolution of ontogenetic size trajectories. At this particular point in time, such focus is particularly relevant, as notions of inheritance are starting to be implemented into population models. With such advances in the field of population ecology, new theoretical and methodological challenges have arisen in predicting evolutionary change that can also lead to biased predictions. The main subjects addressed in this thesis and, therefore in this introduction to the thesis, are, as a consequence, the paradox of stasis and biases in predicting evolutionary change, the genetics of function-valued traits, particularly trajectories of size-at-age, and the use of population models in the prediction of evolutionary change. I devote the last paragraphs of this introduction to providing a brief outline of the structure and contents of the thesis.

1.1 Bias in predicting evolution and the paradox of stasis

The inheritance and evolution of body size has been the subject of great interest since early in the study of evolutionary biology (Galton, 1886). Size is particularly relevant in different areas of evo-

lutionary biology as it has been shown to be associated with fitness, including fecundity, offspring quality, mating success and survival, with larger body sizes generally being beneficial. This connection between size and fitness is so widely accepted that body size is often used as a proxy for fitness when it is not possible or it is difficult to measure fitness itself (Dmitriew, 2011, but see Franklin & Morrissey, 2017). One relevant hypothesis, the tendency for organisms to evolve larger body sizes over evolutionary time (Cope, 1896), has been given particular attention by microevolutionary biologists, as quantitative genetics theory provides a perfect framework in which to formally address such hypothesis. Over decades we have witnessed microevolutionary predictions of evolution by natural selection chiefly corroborating the Cope's rule, while very little evidence exists of it (Bradshaw, 1991). In fact, the contrary, stasis (or even decreasing body size), seems to be more common, and has been argued as the predominant mode of evolution (Gould & Eldredge, 1993). Such mismatch between microevolutionary predictions and the macroevolutionary evidence from the fossil record, referred to as the *paradox of stasis* (e.g. Sogard, 1997), is an important theoretical problem in microevolution and is still largely unsolved.

When natural selection operates on genetic variability, evolution is expected to occur (Fisher, 1930). Formalisations of how evolution by natural selection occurs in terms microevolutionary dynamics, such as the breeder's equation (Lush, 1937) or the secondary theorem of selection (Robertson, 1966, 1968; Price, 1970), are used to identify the direction and quantify the magnitude of evolutionary change. Accurate estimates of evolution are obtained whenever those formalisations hold and their parameters, measures of the strength of selection and evolvability, are estimated sufficiently precisely and without bias. Estimates obtained so far suggest that directional selection towards larger size is widespread in nature (Kingsolver & Pfennig, 2004; Hereford et al., 2004), even when accounting for selection of correlated traits (Hereford et al., 2004; Perez & Munch, 2010; Morrissey et al., 2012a). Likewise, numerous studies have shown that body size is heritable across a wide range of taxa (Visscher et al., 2008; Hansen et al., 2011), including mammals (Wilson et al., 2005; Pelletier et al., 2007), birds (Noordwijk et al., 1988; Charmantier et al., 2004), amphibians (Pakkasmaa et al., 2003), fish (Gjerde et al., 2004; Shimada et al., 2007; Letcher et al., 2011), crustaceans (Thompson, 1986), insects (Gunay et al., 2011), zooplankton (Spitze, 1995) and plants (Johnson et al., 1966; Peiffer et al., 2014). Considering the positive directional selection along with the widespread heritability of body size reported for so many species, one would expect faster evolution of body size than is observed in the fossil record. Hunt (2007) analysed fossil traits and fit three evolutionary models: directional change, random walk and stasis and concluded that only 5% of the size related traits were best fit by the directional change model, suggesting that evolution in these traits was rarely sustained in a particular direction. Similarly, Estes & Arnold (2007) fitted different evolutionary models to a database of 2,639 microevolutionary, historical and paleontological evolutionary rates, concluding that an adaptive landscape model with a single displaced optimum, allowing very rare displacements, was the best fit to the data, once again corroborating stasis as a common mode of evolution. While Kingsolver & Pfennig's (2004) interpretation of directional gradients as the basis of the Cope's rule might be tempting, it actually neither holds quantitatively nor qualitatively: for the reported magnitudes of positive directional selection of body size to be consistent with Cope's rule, greater magnitudes of phylogenetic increase in body size would be necessary. Consistent evidence from extant taxa is also available, with body size being proven to be stable or decreasing, even when heritable and under positive selection (Larsson et al., 1998; Kruuk et al., 2002; Knouft & Page, 2003; Ozgul et al., 2009).

Several mechanisms have been proposed to explain the apparent lack of widespread rapid contemporary evolution of body size, and consequently the inherent bias in microevolutionary estimates. Such mechanisms are either associated with how natural selection operates or to how apparent genetic variability might not be available. Regarding the former, widespread stabilising selection and the existence of opposing selective forces (*selective constraints* or trade-offs) have been the most investigated candidates, whereas concerning the latter, *variational constraints* have been suggested, which can either be pleiotropic or epistatic in nature. Several authors have suggested that either fluctuating selection or the widespread occurrence of stabilising selection (empirically difficult to detect once populations have adapted to a fitness peak) may be the main cause of the stasis observed in body size (Perez & Munch, 2010; Estes & Arnold, 2007; Haller & Hendry, 2014). However, stabilising selection as a single explanation for stasis is a challenging theory to accept as it implies that the selective optimum varies only within a narrow range, when evidence exists suggesting that selection is variable both in space and time (e.g. Hereford, 2009; Siepielski et al., 2009; Bell, 2010; Morrissey & Hadfield, 2012). Another explanation for stasis, very tightly related to selection constraints, is based on the notion of adaptive landscape and how its shape can itself provide a constraint to evolution (Arnold et al., 2001). Natural selection, as a multivariate mechanism, might result in no adaptation if traits under different selective pressures are correlated (Hansen, 2012). As for inheritance mechanisms, the existence of genetic (or variational) constraints can also provide an explanation for stasis (Hansen & Houle, 2004; Walsh & Blows, 2009; Hansen, 2012). Although additive genetic variance may exist in a particular trait, both pleiotropic and epistatic effects may prevent adaptation or evolution. If genes that create variation in one trait also create variation in other traits that are under stabilising selection, evolution is expected to be slower. Such mechanisms result in genetic correlations among traits that are likely to be common in nature (Walsh & Blows, 2009). Likewise, interaction between genes can also modulate evolvability if genes interaction involve negative directional epistasis (Hansen & Houle, 2004; Hansen, 2012). Variational and selective constraints are sometimes difficult to tear apart and are the basis of a broader explanation for stasis, the occurrence of trade-offs, as for example between natural and sexual selection.

Despite the fact that large body sizes are known to (mostly) confer fitness advantages, regarding survival and/or reproductive success (see Honek, 1993; Sogard, 1997; Sokolovska et al., 2000), the occurrence of trade-offs as a limiting mechanism to the evolution of body size has strong support in the literature. It is generally accepted that trade-offs among body size and different components of fitness play an important role on the evolution of body size (Roff, 1981, 1986; Neems et al., 1998; Miller & Sinervo, 2007; Johnson & Hixon, 2011). This argument has its roots in sexual selection and the notion that natural and sexual selection could operate as opposing forces. Trade-offs occur when an increase in one trait that improves fitness is associated with a decrease in another trait that decreases fitness and therefore, in the absence of confounding variables, are statistically identified by a simple bivariate correlation (Roff & Fairbairn, 2007). Evidence for the occurrence of trade-offs has been documented in experimental studies, with major contributions from Stearns (1989), Roff (Roff, 1981, 1986, 2000; Roff & Fairbairn, 2007), De Jong & Van Noordwijk (1992), and van Noordwijk & de Jong (1986), regarding both their theoretical understanding and their translation to a quantitative framework (particularly under the resource acquisition-allocation model). However, observational studies in the wild rarely report negative phenotypic correlations between life-history traits such as

viability and fecundity (Kruuk et al., 2008), where strong *a priori* expectations of trade-offs exist (van Noordwijk & de Jong, 1986; De Jong & Van Noordwijk, 1992). A methodological limitation may be the cause of such apparent incoherence, as correlations cannot be expected to detect trade-offs if the values of two traits are both partially determined by a third trait (Roff & Fairbairn, 2007). The existence of trade-offs in the wild is particularly difficult to detect when both traits are determined by an overall acquisition resource, which may be largely or entirely non-genetic (De Jong & Van Noordwijk, 1992). In that case, at the phenotypic level, both traits may covary positively, despite the existence of an inherent trade-off (Morrissey et al., 2012c).

Another layer of bias that could be associated with both selection and evolvability is related to how body size is measured and what is the actual trait under selection. Larger body size at a specific age is either the result of faster growth or longer development time, and ultimately the accumulation of growth until that specific age (Roff, 2000). Although size at a specific age is the result of the entire ontogeny, empirical evidence on trade-offs among body size and fitness mostly includes data on body size at certain ages, not including information from the entire life-cycle trajectories (e.g. Neems et al., 1998; Miller & Sinervo, 2007; Xu & Wang, 2013). This approach might be limiting, as growth rates seem to play an important role on selection as well. Blanckenhorn (2000) clearly identifies costs of becoming larger, as opposed to costs of being larger, and other authors identify and discuss several advantages and disadvantages of *accelerated growth* and *extended development time* (Arendt, 1997; Dmitriew, 2011). Looking at size at a particular age, disregarding any selection and/or variational constraints between size across ages might also be a source of bias leading to inaccurate estimates of evolutionary change.

1.2 Evolution of ontogenetic size trajectories

The realisation that growth rates are rarely at their physiological maximum suggests that observed rates are the result of a compromise between the advantages and the costs of growing fast, a trade-off between age and size at maturity (Dmitriew, 2011). While faster growth rates imply shorter development time, which allows, for example, early reproductive onset, several disadvantages have been identified that limit how fast individuals grow (Blanckenhorn, 2000). These include increased viability costs associated with predation, parasitism and/or starvation, as a consequence of riskier foraging behaviours necessary to reach faster growth, or higher metabolic demands necessary for faster growth under resource limitation (reviewed by Blanckenhorn, 2000; Dmitriew, 2011). Along with the natural selection operating on size across ontogeny, abundant additive genetic variability in growth trajectories has also been documented in wild populations (e.g. Wilson et al., 2005, 2007; Hadfield et al., 2013; Huchard et al., 2014). Put together, these suggest that investigating the evolution of size at a particular age might be a limiting perspective and have the potential to be misleading. As an alternative, the genetic architecture and selection mechanisms could be evaluated throughout the life cycle of organisms.

The extension of quantitative genetics theory to encompass developmental trajectories has been accessible for nearly three decades (Kirkpatrick & Heckman, 1989; Kirkpatrick et al., 1990). These traits, referred to as function-valued, or as initially coined, *infinite-dimensional* (Kirkpatrick & Heck-

man, 1989), vary according to another continuous character (e.g. an environmental variable, or time or age), therefore being described by a function. Deriving expressions that determine the genetic architecture of function-valued traits and allow predictions of evolutionary change to be made was a very important breakthrough to both evolutionary biologists and animal breeders as it allowed overcoming serious intractability issues associated with considering size at each age as a separate trait, as when applying the classical multivariate approach proposed by Lande & Arnold (1983). Kirkpatrick & Heckman (1989) proposed describing the additive genetic variance of function-valued traits using a covariance function. As a consequence, the number of parameters of a **G** matrix corresponds to the number of parameters in the corresponding **G** function, which is independent from the number of ages analysed. Additionally, one of the grounds upon which quantitative genetics lies, the partitioning of variance components (Fisher, 1918), is readily extendable to covariance functions, such that a phenotypic covariance function of a polygenic trait can be written as the sum of the additive genetic function and functions associated with other variance components. Implementations of this theory have lead to the development of *animal models* (Henderson, 1975) being coupled to random regression of orthogonal polynomial functions (Kirkpatrick et al., 1990; Meyer, 1998). Such approach was then generalised to functions of principal components (Kirkpatrick & Meyer, 2004; de los Campos & Gianola, 2007) or even fully parametric functions (Pletcher & Geyer, 1999).

The quantitative genetics of function-valued traits has been predominantly used by animal breeders as a means to selecting for larger body mass (e.g. Lewis et al., 2002; Legarra et al., 2004; Meyer, 2005), increased milk yield (e.g. Jakobsen et al., 2002; Sesana et al., 2010), or higher food intake (e.g. Bermejo et al., 2003), for example. For evolutionary biologists working with wild populations such a framework has been important to establish, for instance, that heritabilities can be quite variable and high across the ontogeny of animals from different taxa, and that additive genetic and environmental correlations in traits such as body mass can be very substantial, providing evidence that both the genetic architecture and mechanisms of plastic adaptation play a role in defining size at each age (Wilson et al., 2005, 2007; Hadfield et al., 2013). Quantitative genetics of function-valued traits has also been valuable in collecting evidence of compensatory growth in wild populations where phenotypic variability decreases with increasing age (Wilson et al., 2005, 2007). Equally relevant, such an approach has been useful in testing for genetic constraints across ages that could be limiting evolutionary change in populations under directional selection. In Soay sheep (*Ovies aries*), for example, Wilson et al. (2007) concluded that the paradox of stasis observed in this species is not the result of a constraint imposed by genetic architecture of body mass, suggesting instead that the mismatch between observed dynamics and evolutionary predictions is likely to lie, at least partially, in how natural selection is being measured.

Although the genetic architecture of ontogenetic trajectories of size is very well described by the formulation proposed by Kirkpatrick and co-authors, and that age-specific selection gradients are also easily obtainable (Kirkpatrick et al., 1990), accounting for changes in natural selection over and within generations is not readily feasible by applying expressions as the breeder's or Lande's (Lande, 1979; Lande & Arnold, 1983) equation. Assuming that selective pressures on size and its genetic architecture across ages is constant over time results in quantitative prediction of evolutionary change to be potentially biased in natural systems that are characterised by environmental heterogeneity (Reeve, 2000; Nussey et al., 2005). Such limitation is particularly relevant given the information gathered over

the last decades suggesting that selection, in addition to evolvability, can change very dramatically with environmental conditions (Charmantier & Garant, 2005; Hereford, 2009; Bell, 2010). Furthermore, the emergence of several long-term studies of long-lived animals, in which both phenotype and life history are measured very precisely over large periods of time (Pemberton, 2008; Clutton-Brock & Sheldon, 2010), demands a solution to this problem. Population models, such as integral projection models (IPMs, Easterling et al., 2000) or individual based models (IBMs, Huston et al., 1988), modelling trait inheritance across generations might be an alternative, given their ability to explicitly model changes in ecological patterns over time, besides life history and population dynamics. In fact, the theoretical grounds of quantitative genetics of developing traits are now on the verge to be fully implemented within structured population models (Childs et al., 2016), opening the possibility to predict evolutionary change while simultaneously considering population ecology and life history.

1.3 Population models

Demographic models are often classified as *top-down* or *bottom-up* models, referring to whether they are structured from the population to the individual or *vice-versa* (e.g. DeAngelis & Grimm, 2014; Grimm, 1999). Top-down models are described by population-level parameters, such as reproduction and survival rates, whereas in bottom-up models population parameters emerge from the interactions between individuals and between individuals and the surrounding environment. Examples of top-down, or *state variable* (Huston et al., 1988), population models include matrix models (Caswell, 2001) and integral projection models (IPMs), whereas individual-based models (IBMs) belong to the second group. The technical distinction between these approaches relies on whether individual information is handled or if instead that information is reduced to a distribution function (Caswell & John, 1992). In practice, in both bottom-up and top-down models, a population increases or decreases according to fundamental processes determining the rate at which individuals are born, mature, reproduce, and die. In both cases, these processes are allowed to depend, not only on time or age, but also on one or more characteristics of interest (e.g. age- and stage-structured IPMs). As a result, both are used to track the number of individuals and their distribution according to certain characteristics, and more generally to link demography and life history to ecological aspects of populations (DeAngelis & Gross, 1992; Caswell, 2001). Given that state variable models and IBMs mimicking the life cycle of individuals within a population have the potential to rely on the exact same biological functions, their mathematical implementation is the feature that mostly distinguishes them. Differing implementations, however, have pragmatic implications that will constitute benefits or constraints depending on the characteristics of the population to be modelled. Particularly, whereas state variable models are particularly useful to derive properties of populations analytically, IBMs can incorporate more complexity and therefore be used to build models that are more realistic (Caswell & John, 1992).

From their conceptual equivalence follows that, in principle, IBMs and IPMs are equally suited to incorporate the mechanics of trait transmission among relatives. Simple formulations of IPMs explicitly modelling the genetics underlying trait transmission exist. These track allele frequencies of a trait determined by a single locus in a diploid organism (Coulson et al., 2011) and by setting the mechanics of genetic transmission in clonal organisms (Rees & Ellner, 2016). Additionally, Barfield et al. (2011) and Childs et al. (2016) have begun to set the solutions to incorporate the infinitesimal model (Fisher,

1918; Bulmer, 1980) into stage and age- and stage- structured IPMs, respectively. In opposition to IPMs, given their structural flexibility, IBMs have been widely used to study various genetic aspects, including the dynamics of trait transmission in population models (e.g. Eldridge et al., 2010; Castellani et al., 2015).

1.4 Thesis overview

Although never the very focus of any chapter, this thesis was motivated at making a contribution to resolving the paradox of stasis, looking both at biological and methodological issues that could possibly explain the mismatch between the observed dynamic of size and growth and the corresponding evolutionary predictions. I study these issues looking particularly at body mass and horn length in two species of the genus *Ovis*, the Soay sheep (*Ovis aries*) and the bighorn sheep (*Ovis canadensis*), and I dedicate Chapter 2 to a detailed description of the two study systems. This thesis comprises four chapters making novel empirical and/or theoretical contributions (Chapters 3, 4, 5, and 6). Chapter 3 addresses issues in predicting evolutionary change in a scalar trait, the body mass at a particular age, whereas the remaining address size as a developing trait, focusing on ontogenetic trajectories of body mass and horn length. In the last chapter of this thesis (Chapter 7) I provide a general discussion of the results obtained in the previous chapters. Finally, various supplementary materials that accompany each of the previous chapters are provided in the last pages of this thesis.

Chapter 2 includes a description of the Soay sheep study system in the isle of Hirta in the archipelago of St Kilda, in the Outer Hebrides, Scotland, as well as of the population of bighorn sheep inhabiting Ram Mountain, in Alberta, Canada. Details of the biology of the species, how phenotypic data were collected and how pedigrees were constructed are provided.

Chapter 3 provides evidence of a trade-off between viability and fecundity mediated by body size and pregnancy in female lambs and how it shapes the strength of selection. Larger lambs are more likely to survive their first year of life and produce more offspring over their lifetime, but are also more prone to become pregnant during their first months of life, which, in turn, is associated with lower first-year survival. I use this knowledge in a formal analysis of selection, using an extension of path analysis for nonlinear development systems, where I disentangle the selection on body mass that is occurring through the direct effect of body mass on fitness and through its effect on lamb pregnancy.

Chapter 4 encompasses theoretical proofs of four different sources of bias in common IPM implementations. These occur both in the development functions and the inheritance function and lead to serious underestimation of resemblance within individuals across time and of relatives across generations. I use the principles of path analysis to derive expression for true parameters and those implied by such implementations of IPMs, therefore allowing analytical comparisons. I finish this chapter providing an empirical example of body mass in bighorn sheep ewes.

Chapter 5 applies different modelling approaches for fitting ontogenetic trajectories of male horn length and the underlying genetic architecture in bighorn sheep from Ram Mountain. I particularly

use random regression and factor analytic structures to model both additive genetic and permanent environment correlations across ages, as well as an antedependence model as typically implemented in IPMs. I compare these three alternatives to a multivariate trait model.

Chapter 6 is dedicated to implementing a two-sex IBM of horn length in bighorn sheep, using the different development and inheritance functions estimated in Chapter 5. I first estimate the remaining vital functions (survival and breeding success of both males and females), and then simulate populations that are exposed to trophy hunting after a hunting-free period, allowing a direct comparison of phenotype and breeding values before and after hunting was applied.

Chapter 7 includes a general discussion of the previous chapters, drawing attention to the main contributions of the present thesis to resolving the paradox of stasis, including: (1) the use of a fairly phenotypic approach to deal with genetic constraints, (2) the application of population models that incorporate quantitative genetics principles (also accounting for ecological complexities such as differing selection pressures according to age structure and sex), and (3) theoretical proof of the very little correspondence between a cross-parent offspring regression and known mechanics of trait transmission across relatives.

CHAPTER 2

Meet the sheep

The empirical results included in this thesis were produced using two populations of unmanaged sheep, namely of Soay (*Ovies aries*) and bighorn (*Ovies canadensis*) sheep. Both populations have been subject to an intensive individual-level study and are predigreed, providing valuable information on both the genetic architecture of any traits of interest and the selection pressures the populations have been subjected to. The bighorn sheep population has been the target of both natural and artificial selection, as it was subject to trophy hunting until 2011. In this chapter, I provide a description of both populations as well as details on how the data were collected.

2.1 The Soay sheep

I used data from the Soay sheep population inhabiting the Village Bay study area in the island of Hirta, in the St Kilda archipelago. St Kilda is located off the north-west of Scotland, beyond the Outer Hebrides (57°49'N 08°34'W). The Soay sheep population inhabiting the island was introduced in 1932, when the landlord of St Kilda, the Marquis of Bute, moved 107 Soay sheep from the nearby island of Soay to Hirta to maintain the grazings (Clutton-Brock & Pemberton, 2004a). Since then, this population has been unmanaged and, therefore, limited by the availability of resources in the island. As a consequence, the population dynamics of the Soay sheep of St Kilda is very unpredictable, with population crashes after periods of sustained growth. These crashes, one of the most striking characteristics of this population, result in the number of individuals oscillating considerably (between 600 and 2200 individuals on the island).

The Soay sheep are a small breed compared to domestic sheep, mature female and male adults weigh, on average, 24 Kg and 32 Kg, respectively (Fig. 2.1, Illius et al., 1995; Nussey et al., 2011). This species ruts in the autumn and gives birth during the spring, with the first lambs being born in late March or early April. Depending on population density, a significant proportion of females conceive in the first November of their lives, when they are around seven months old (Clutton-Brock et al., 2004a). Additionally, Soay sheep ewes give birth to twins at a rate that can be over 20% in years of low population density (Clutton-Brock et al., 2004a). Horn-clashing fights that establish dominance

relationships between males start in September preparing for the female oestrus, occurring for one to four days during November (Clutton-Brock et al., 2004a). In winter, resources become limiting, resulting in weight loss and mortality, which occurs predominantly in February and March, and especially when population density is high and winter weather conditions are unfavourable (Clutton-Brock et al., 2004b).

The population inhabiting the Village Bay study area on Hirta has been the subject of intensive, individual-based study since 1985 (Clutton-Brock & Pemberton, 2004a). More than 95% of the individuals living in the study area have been marked with plastic ear tags shortly after birth to enable identification throughout their lifetimes. Regular censuses and mortality searches allow the survival status of individual sheep to be known. Each year in August a large portion of the Soay sheep resident in the Village Bay study area is captured and phenotyped for multiple traits. During the mating season further measurements are made on males migrating into the study area. A very comprehensive pool of information about the life cycle of most individuals in the population is therefore gathered and both biometric and life history traits are available.

The pedigree of this population was constructed through a combination of observational field data and molecular markers for maternal links, and using molecular markers only for paternal links (Johnston et al., 2013; Bérénos et al., 2014). 315 polymorphic and unlinked SNP markers were used in molecular parentage assignments (for 4371 individuals) with 100% confidence in the R package MasterBayes (Hadfield et al., 2006). Polymorphic microsatellite markers were also used when SNP genotypes were not available either for lambs or candidate fathers. In those cases, for a total of 222 lambs, 14-18 polymorphic microsatellite markers were used in assignments with confidence >95% in MasterBayes (Morrissey et al., 2012b). The resulting pedigree has a maximum depth of 10 generations and consists of 6740 individuals, of which 6336 are nonfounders (i.e. have one or two known parents).

Data used in Chapter 3 I used the Soay sheep data to investigate the effect of a trade-off between lamb body mass and the probability of becoming pregnant as lamb. Only data from 1991 to 2015 were used, as there is no systematic record of pregnancies occurring in non-surviving ewes for the early years of the study. My analyses focus on August body mass, measured in kg, pregnancy status, evaluated through the presence of lambs and lactation for ewes that survive the winter, survival status, number of offspring successfully reared, and population density (total number of individuals in the Village Bay study area). In the statistical models I present in Chapter 3, I also used birth and capture dates, birth year, twinning status (singleton or twin), maternal age at parity and maternal identity.

Figure 2.1: The Soay sheep of St Kilda. (a) lamb, (b) adult ewe, (c) adult ram, and (d) a portrait of a horn-clashing fight between two rams during the rut. Photo credits: Jill Pilkington.

2.2 The bighorn sheep

The bighorn sheep data I used in this thesis come from the population inhabiting Ram Mountain, Alberta, Canada (52°N, 115°W, elevation 1082-2173 m). The study area at Ram Mountain includes approximately 38 m^2 of alpine and subalpine habitat, surrounded largely by coniferous forest and by the North Saskatchewan River on one side. Similarly to the Soay sheep, this species is characterised by a marked sexual dimorphism, with males being considerably heavier than females - adult males weigh on average 80 Kg, whereas females weigh on average 50 Kg - and presenting larger horns (Fig. 2.2 Wilson et al., 2005). These phenotypic traits are of extraordinary importance to males, as they largely determine male reproductive success (Coltman et al., 2002). The annual cycle of this population is similar to that described for the Soay sheep. Most lambs are born from late May to early June (Festa-Bianchet, 1988), and the rut occurs in late November and early December (Festa-Bianchet et al., 1995).

This isolated population has been the subject of intensive individual-level monitoring since 1971. Sheep are captured in a corral trap (see Fig. 2.2) baited with salt and phenotyped multiple times per year between late May and late September. Most individuals are marked with unique tags as lambs, and therefore the vast majority are of known age. As births, deaths and migratory movements are closely observed, population size is known with high accuracy. At each capture, body mass and different aspects of horn size are measured. Adults and lambs are recaptured approximately 3-5 and 2-3 times per year, respectively. These measurements are used to estimate phenotype adjusted to June 5 and September 15, using the methodology proposed by Martin & Pelletier (2011), who adopted linear mixed models to standardise trait values of each individual to common environmental conditions and a given point in time.

Although maternities have been assigned from suckling behaviour since 1972, genetic assignment of paternities was initiated in 1988 based on 26 microsatellite *loci* with a confidence threshold of 95% using `Cervus` (Coltman et al., 2005; Poissant et al., 2008). By 2014, the pedigree included 864 maternal links (corresponding to 254 dams) and 528 paternal links (including 79 sampled and 37 unsampled sires). `Colony` (Wang, 2013) was used to infer full or half siblings from unsampled males.

Trophy hunting occured from late August through October in the study area from before the beginning of the study until 2011. Any resident in Alberta was allowed to purchase a trophy sheep license and the only criterion defining a *legal trophy ram* was based on phenotype, with no limit to the number of rams shot. Until 1996, rams with horns achieving four fifths of a curl (Fig. 2.2), which was described as "a male sheep with horns, 1 of which is of sufficient size that a straight line drawn from the most anterior point of the base of the horn to the tip of the horn passes in front of the eye when viewed in profile", could be legally harvested (Jorgenson et al., 1998). From 1996 the definition of *legal trophy ram* increased to a full curl. This restriction resulted in only four rams being shot between then and 2011 (Pigeon et al., 2016).

Data from the bighorn sheep study system is **used in Chapters 4, 5, and 6**. In Chapter 4, I used ontogenetic trajectories of ewe body mass to perform a comparison between IPM-like development and inheritance functions and random regression models in how well these alternatives recover similarity across ages within individuals and between individuals and their relatives. A similar comparison was performed in Chapter 5, where I compared the additive genetic and phenotypic architecture of male horn length across ages using different modelling approaches. To minimise measurement error caused by horn wear or breakage, I used the longest horn in the analyses presented in this chapter. Finally, in Chapter 6, I used the bighorn sheep data to estimate male and female breeding success and winter survival, as well as selective harvest-related survival for males. The estimates obtained, in addition to the horn length trajectories estimated in Chapter 5, were used to parameterise the IBM of horn length presented this chapter.

Figure 2.2: Bighorn sheep at Ram Mountain. (a) lamb with its mother wearing a collar; (b) adult ewes; (c) ram next to the corral trap where sheep are caught; and (d) an illustration of the legal definition of a 4/5 of a curl; Photo credits: Marco Festa-Bianchet (a,b,c) and Alberta F&W (d).

CHAPTER 3

Selection of size and early pregnancy in Soay sheep (*Ovies aries*)

Abstract

The paradox of stasis has been widely documented in the last few decades. Both theoretical and methodological grounds for the mismatch between the predictions of quantitative genetics and observed dynamics of size have been shown to occur in various species, including the Soay sheep (*Ovies aries*). Particularly, genetic correlations between traits that affect fitness can result in trade-offs between different mechanisms of selection. Here, I identify the persistence of a maladaptive behaviour, pregnancy during the first year of life, as the basis of a genetic constraint regulating body mass in ewe lambs. I demonstrate the existence of a positive additive genetic correlation between lamb body mass and early pregnancy, larger ewes are more likely to get pregnant, and investigate how this correlation provides a mechanism for regulating body size in Soay sheep. I used recent theory on nonlinear developmental systems to disentangle selection *of* and *for* body mass. The direct effect of body mass on fitness is positive, regarding both first-year survival and offspring production, whereas its pregnancy-mediated effect on fitness entails important viability costs. I thus explain why selection of body mass is not stronger (more positive) and provide evidence that substantial selection on lamb body mass occurs at older ages, suggesting that this mechanism might also play a role at regulating size at older ages.

Keywords: body size, lamb pregnancy, natural selection, non-linearity, paradox of stasis, path analysis, Soay sheep

3.1 Introduction

The *paradox of stasis* and the pattern *bigger-is-better* (Sogard, 1997) with respect to selection on body size have been the target of great attention in the last few decades amongst both macro- and microevolutionary biologists. Widespread positive directional selection (e.g. Kingsolver & Pfennig,

2004; Hereford et al., 2004) and available genetic variability (e.g. Postma, 2014) have been documented, while fossil records (Estes & Arnold, 2007; Hunt, 2007) and extant taxa data (Larsson et al., 1998; Knouft & Page, 2003; Ozgul et al., 2009) show very little change in body size. Both theoretical and methodological explanations have been identified for this mismatch (Bradshaw, 1991; Merilä et al., 2001; Hansen & Houle, 2004). One such mechanism that is expected to be common in nature is the existence of opposing selective forces, i.e. *trade-offs* between natural and sexual selection (e.g. Roff, 2000; Roff & Fairbairn, 2007). On a more methodological side, a lack of compliance with the assumptions of the breeder's equation (Lush, 1937), the most widely adopted means of predicting evolutionary change, has been argued to be a major problem in studies of natural selection in the wild (Morrissey et al., 2010). Ultimately, as information accumulates, it is becoming increasingly evident that a single explanation for stasis will not suffice, either generally, or even in a single instance.

It is widely accepted that fecundity and sexual selection are major evolutionary forces selecting for larger body size in both females and males (Fairbairn, 1997). These may eventually be counterbalanced by viability selection targeting bigger individuals (Blanckenhorn, 2000), leading to a trade-off between sexual (or fecundity) and natural (particularly viability) selection (Roff, 2000; Roff & Fairbairn, 2007). The benefits and costs associated with larger body size provide the mechanisms underlying such trade-offs and have been extensively discussed (Shine, 1988; Honek, 1993; Anderson, 1995; Sogard, 1997; Blanckenhorn, 2000; Sokolovska et al., 2000). This weighting of costs and benefits are naturally not limited to adult body size. Particularly, Blanckenhorn (2000) emphasizes the distinction between the costs of *becoming* as opposed to *being* large, and elaborates on how forces such as predation, parasitism and starvation play different roles in juveniles and adults.

Trade-offs are most likely identified through a deep understanding of the biology of a species. Once a trade-off's mechanistic basis is hypothesised, appropriate multivariate statistical methods are useful to characterise trade-offs on evolutionary quantitative genetics terms. Path analysis, developed by Wright (1921, 1934) to deal "with a system of interrelated variables" (Wright, 1960), is a natural candidate as it provides the means to disentangle the different mechanisms by which body size can affect fitness. In fact, the use of path analysis underlies the concept of *extended* selection gradient, formally defined by Morrissey (2014) as the total effects of traits on fitness, i.e, taking into account the whole system of causal associations among traits. *Extended* selection gradients are therefore akin to the concept of *selection for*, defined by Sober (1986) in opposition to that of *selection of* (the total association of traits with fitness). Also, the initial linear formulation of path analysis and *extended* selection gradients was extended to nonlinear development systems (Morrissey, 2015), such as one including variables central to the study of selection, like the probability of survival or the number of offspring.

The Soay sheep (*Ovis aries*) on St Kilda (Clutton-Brock & Pemberton, 2004b) is an example of such a species where positive directional selection (Milner et al., 2004; Morrissey et al., 2012a) and reasonably high heritability (Milner et al., 2000; Wilson et al., 2007; Bérénos et al., 2014) have been reported for body size, alongside with stasis (Ozgul et al., 2009). Growing faster may be harmful in Soay sheep female juveniles as a consequence of an association between size and fecundity, combined with a viability cost of reproduction. A non-negligible percentage of ewes get pregnant as lambs and those ewes are more likely to die during their first year of life (Clutton-Brock et al., 2004a).

I hypothesise that early pregnancy is size-dependent, with larger ewes being more likely to get pregnant and, therefore, to die. A mechanism regulating body size follows directly from this hypothesis - genetic variation in body mass could be maintained by a trade-off between fitness components in female lambs: being larger is associated with higher rates of survival and total offspring production over a lifetime (Clutton-Brock et al., 1992, 1996; Milner et al., 1999), but being pregnant as a lamb would be associated with lower first-year survival.

In this chapter, I first model lamb body mass and early pregnancy, as well as their effects on first-year survival and lifetime offspring production, showing that: (1) early pregnancy is size-dependent; (2) there is a positive additive genetic correlation between lamb body mass and pregnancy, (3) there is selection against early pregnancy through viability selection, and (4) lifetime rearing success (LReS; lambs reared to independence) in surviving ewes is size-dependent, but very similar in ewes that got and did not get pregnant. I devote a subsequent section of this chapter to a formal quantitative genetic analysis of natural selection. I estimate overall selection on body mass to be positive, and I quantify how much stronger it would be in the absence of lamb pregnancy. I also show that about half the selection on lamb body mass occurs later in life, suggesting that this trade-off is also regulating body size in adults through across-age correlation in body size.

3.2 Study system and data

The Soay sheep population of Hirta, St Kilda, was adopted as the study system to investigate the effects of lamb size and pregnancy on the evolution of body size. A comprehensive description of the population and the individual-based study is given in Chapter 2. Here, I used data on ewe lambs from 1991 to 2015, as there is no systematic record of pregnancies occurring in non-surviving ewes for the early years of the study. My analyses focus on August body mass, measured in kg, pregnancy status, evaluated through the presence of lactation and foetuses observations, survival status, number of offspring successfully reared, and population density (total number of individuals at the Village Bay study area). In the statistical models I also used birth and capture dates, birth year, twinning status (singleton or twin), maternal age at parity and maternal identity. Here, I define parental success as the number of offspring successfully reared to their first November 1st and distinguish between those offspring successfully reared as a result of early pregnancy (annual reproductive success, AReS) and subsequently (lifetime rearing success, LReS). LReS, as AReS, are conceptually intermediate to breeding success (offspring produced over a lifetime) and reproductive success (offspring successfully raised up until the age of 1) as usually used with Soay sheep. This definition was adopted in order to consider labour-related mortality as being part of the first annual cycle, while avoiding having offspring winter survival as part of parental fitness (see Thomson et al., 2017, for reasons why that is important).

Information with increasingly tighter constraints was used to perform the analyses shown in this chapter. The first level of information includes all ewes born from 1991 to 2015 (n_1 = 3916). These data were used in models of body mass and pregnancy. A second level of information was considered in analyses associating first-year survival to body mass and pregnancy. In this case, the following extra constraining criteria were considered: having known first-year survival status and to have survived until the rut, which is not a major restriction as almost no mortality occurs between August (up until

when most growth occurs) and November (n_2 = 947). To study LReS, the data were also constrained to only include ewes from cohorts that were completely phenotyped for this trait, which was achieved by excluding all ewes born after 2006 (n_3 = 542). This procedure resulted in including very few LReS records associated with ewes that were still alive by the cut-off year (2015). While these ewes lifetime fitness is underestimated, they have reared most the offspring they will rear in their lives. Excluding these records would result in stronger bias as those correspond to ewes that lived longer and therefore had potentially higher rearing success, while avoiding excluding more cohorts.

Lamb body mass in August is dependent on birth and measurement dates. Both are indicators of how long lambs had the opportunity to grow and are particularly relevant because higher growth rates occur during the warmer months (before August), when vegetation is most available (Crawley et al., 2004). As a result, birth and measurement dates were included as covariates when modelling lamb body mass or lamb body mass was used as a predictor. Fixed effects for twinning status, population density and maternal age at parity, including quadratic terms for the latter two, were included in all regressions, as well as the following linear interaction terms: between lamb body mass and population density in models including lamb body mass as predictor, between early pregnancy status and population density in models including early pregnancy as a predictor, and between these three traits in models including both lamb body mass and early pregnancy status as predictors. Likewise, random effects to estimate among-mother and among-cohort variation were included in all regressions. This fixed and random structure was applied to all statistical models except the one modelling AReS (due to a lack of statistical power). Finally, the pedigree information required to parameterise the quantitative genetic models was constructed as described by Johnston et al. (2013) and Bérénos et al. (2014), and as detailed in Chapter 2.

3.3 Early pregnancy and lamb size

Early pregnancy, here defined as a pregnancy occurring during the first year of life, occurs at a rate of 37 per year in Soay sheep (914 records documented from 1991 to 2015). The frequency of lamb pregnancy varies greatly among years, but in the raw data no apparent temporal trend is found (Fig. 3.1a). A major driver of these pregnancies seems to be body size, as early pregnancy increases significantly with body mass (Fig. 3.1b, Tab. 3.1). A lamb weighing around 10 kg has a very low chance of becoming pregnant, whereas a lamb weighing around 15 kg is more likely to become pregnant than not (Fig. 3.1c). It is well known that body mass in Soay sheep depends on population size, on average decreasing in years with higher density (Clutton-Brock & Pemberton, 2004b; Ozgul et al., 2009). Conditional on population density, there is a temporal trend for body mass to decrease in Soay sheep, including in lambs (Ozgul et al., 2009), and also in ewe lambs (Fig. 3.1d, upper panel). This trend is apparently concomitant with a decrease in the rate of early pregnancy over the years, when density is again accounted for (Fig. 3.1d, lower panel). Substantial costs and few benefits would explain this trend in early pregnancy, as, for example, ewe lamb descendants having significant lower survival when compared to offspring born to older ewes (Fig. 3.1e).

To better understand the nature of the association between lamb size and early pregnancy I used an animal model corresponding to a multi-response generalised linear mixed model (Hadfield, 2010) for

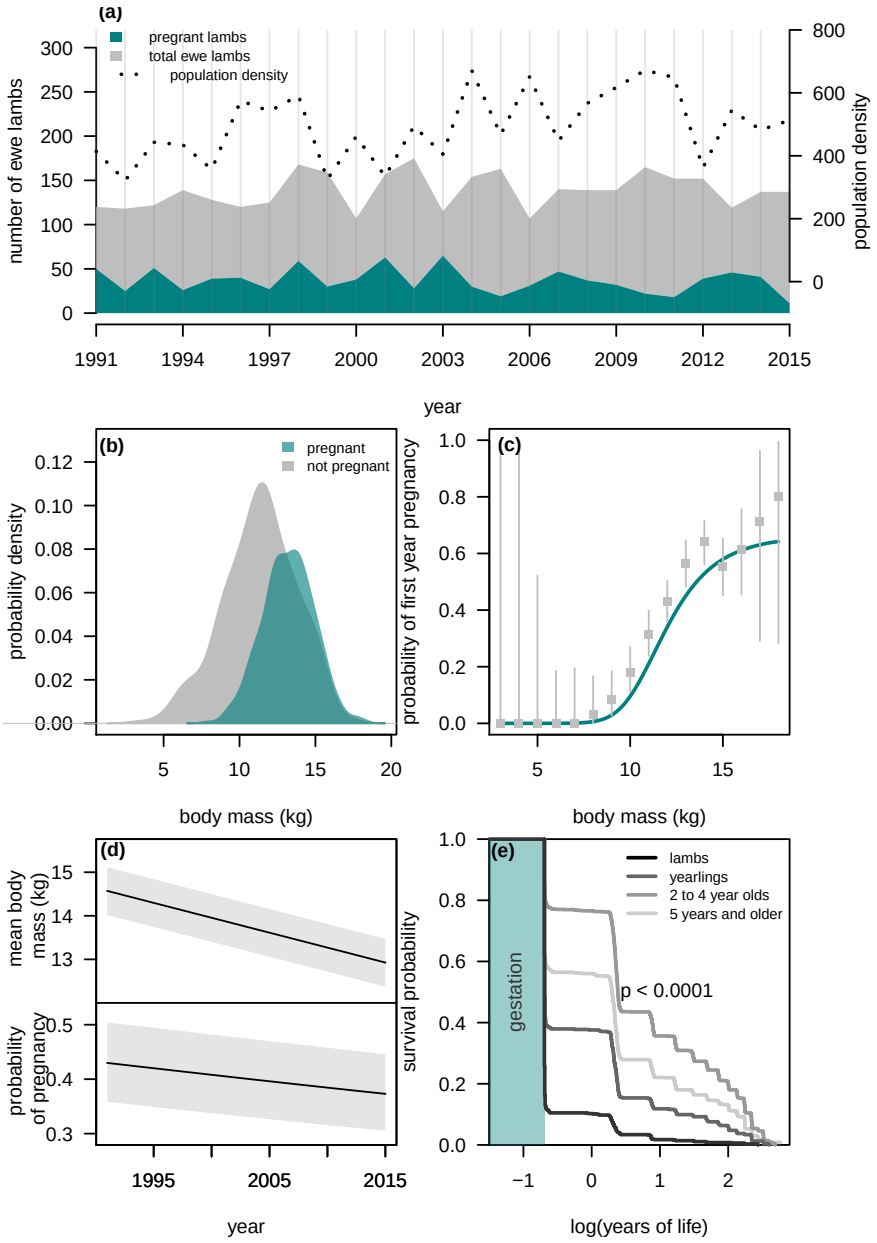

Figure 3.1: (a) Number of Soay sheep ewes, ewe lambs and population size from 1991 to 2015 in the Village Bay study area; (b) empirical distribution of body mass in pregnant and non-pregnant ewe lambs; (c) size-dependent probability of early pregnancy. The line in teal corresponds to the prediction of a binomial regression with logit link function (see Tab. 3.1 for full specification and parameter estimates), whereas the grey bars correspond to 95% confidence intervals on the binomial probability obtained from the raw data; (d) lamb body mass (upper panel) and probability of early pregnancy (lower panel) across time. The black lines correspond to predictions of a linear and a binomial model (logit link function), respectively, correcting for birth and measurement dates, maternal age and population density (slopes and curvatures for the latter two covariates). Random effects for cohort and maternal identity were also considered. The grey areas illustrate the variation in lamb body mass and probability of early pregnancy attributed to varying population density in 1 standard deviation from the mean; (e) non-parametric survival curves of Soay sheep according to mother's age at conception. The p value corresponds to a Peto & Peto test for differences among Kaplan-Meier curves.

Table 3.1: Coefficients of a binomial regression (logit link function) of early pregnancy on body mass in Soay ewe lambs. Other fixed effects include population density, twin status, and maternal age. All covariates, except for twin status, were mean-centred. Variances in random intercepts for cohorts and maternal identity were also estimated. 95% credible intervals correspond to HPD intervals. See Fig. 3.1(c).

parameter	posterior mode	95% CrI
intercept	-0.81	(-1.39; -0.12)
body mass	0.69	(0.49; 0.87)
body mass^2	-0.11	(-0.18; -0.07)
body mass^3	0.01	(-0.01; 0.02)
density $(\times 100)$	-0.45	(-0.89; -0.15)
density^2 $(\times 100)$	0.00	(0.00; 0.01)
density $\times$ body mass $(\times 100)$	0.11	(0.02; 0.23)
twin	0.76	(0.17; 1.45)
maternal age	-0.03	(-0.13; 0.07)
maternal age^2	0.00	(-0.03; 0.03)
birth date	-0.02	(-0.05; 0.02)
measurement date	-0.07	(-0.12; 0.01)
variance in cohort effects:	0.46 (0.14; 1.27)	
variance in maternal effects:	0.01 (0.00; 1.34)	
residual variance:	set to 1	

body mass, m, and the probability of lamb pregnancy, p. Although the probability of lamb pregnancy is well described by a binomial distribution, a latent scale variable, p_l, can be defined such that $p_l = ln\left(\frac{p}{1-p}\right)$. In that case, both m and p_l are assumed to be drawn from a multivariate normal distribution, with a mean vector that includes both mean mass, μ_m, and mean pregnancy probability in the logit scale, μ_{p_l}, and a variance-covariance matrix $\boldsymbol{P_l}$,

$$\begin{bmatrix} m \\ p_l \end{bmatrix} \sim \mathcal{MVN}\left(\begin{bmatrix} \mu_m \\ \mu_{p_l} \end{bmatrix}, \boldsymbol{P_l}\right). \tag{3.1}$$

Both μ_m and μ_{p_l} depend on twin status (singleton or twin), population density, and maternal age at parity, whereas the former also depends on birth and measurement dates. The corresponding parameters and their estimates are listed in Appendix A.1. Note that the subscript l denotes *latent scale*, which, in practice, refers to early pregnancy only, since August lamb body mass was modelled in its natural scale. The model in Equation (3.1) is particularly useful to study the correlation between lamb body mass and early pregnancy, providing information about its strength and its nature. To accomplish that, the genetic and environmental contributions to $\boldsymbol{P_l}$ were partitioned by including random effects on breeding values (animal model, Henderson 1975). In fact, a $\boldsymbol{G_l}$ matrix and an $\boldsymbol{E_l}$ matrix can be defined as follows

$$\boldsymbol{P_l} = \begin{bmatrix} \sigma^2_m & \sigma_{m,p_l} \\ \sigma_{m,p_l} & \sigma^2_{p_l} \end{bmatrix} = \begin{bmatrix} \sigma^2_{m_a} & \sigma_{m,p_{l\,a}} \\ \sigma_{m,p_{l\,a}} & \sigma^2_{p_{l\,a}} \end{bmatrix} + \begin{bmatrix} \sigma^2_{m_e} & \sigma_{m,p_{l\,e}} \\ \sigma_{m,p_{l\,e}} & \sigma^2_{p_{l\,e}} \end{bmatrix}, \tag{3.2}$$

where subscripts a and e denote the additive genetic and the environmental contribution to the overall (co)variances, respectively. For more information on (co)variance partition, see Falconer (1981). To simplify the notation, I do not use any extra subscript to denote phenotypic (co)variances (see matrix $\boldsymbol{P_l}$ in Equation 3.2). Besides residual variances and covariances, matrix $\boldsymbol{E_l}$ also includes

variances and covariances associated with cohort and maternal random effects. Since the overdispersion variance of a generalised linear mixed model (GLMM) is unobservable for binary data, the residual variance for p_l was set to one.

Taking into account the additive genetic and the phenotypic variances in lamb body mass, 0.78 (95% CrI 0.20; 1.27) and 4.29 (95% CrI 3.84; 5.23), respectively, the heritability of this trait is estimated to be 0.14 (95% CrI 0.04; 0.29), very similar to the estimate reported by Bérénos et al. (2014) for both sexes (0.12, SE 0.036). Up until very recently, for binomial variables, heritabilities were typically obtained by approximation, as described in Nakagawa & Schielzeth (2010). Following this approach, I obtain an estimate of 0.15 (95% CrI 0.10; 0.70) for the heritability of early pregnancy. There is a strong positive phenotypic correlation between lamb body mass and early pregnancy (0.51, 95% CrI 0.40; 0.66), the genetic contribution to that correlation being very important (0.64, 95% CrI 0.24; 0.90).

In 2016, Villemereuil et al. derived exact expressions to convert the latent scale parameters estimated in GLMMs into scales on which traits are expressed and selected. I am particularly interested in obtaining parameters in the probability scale (probability of early pregnancy), rather than in the logarithm of the odds of being pregnant as a lamb. Villemereuil et al. (2016) refer both to *expected* and *data* scales, the difference between them being the random noise that distinguishes a model from the data itself. Here, I adopt the expected scale. Following their work, the expected values for body mass and the probability of early pregnancy is given by

$$\bar{\boldsymbol{z}} = \begin{bmatrix} \bar{m} \\ \bar{p} \end{bmatrix} = \int \boldsymbol{g^{-1}(l)} f_{\mathcal{MVN}}(\boldsymbol{l}, \boldsymbol{\mu}, \boldsymbol{P_l}) dl, \tag{3.3}$$

where $\boldsymbol{g}^{-1}$ corresponds to the inverse link functions used to model body mass and the probability of early pregnancy. As the adopted link functions for these variables were the identity and the logit functions, respectively, their inverses are the identity and the logistic functions, the latter corresponding to $\frac{exp(p_l)}{exp(p_l)+1}$. $\boldsymbol{l}$ are the latent values for lamb body mass and early pregnancy. $f_{\mathcal{MVN}}(\boldsymbol{l}, \boldsymbol{\mu}, \boldsymbol{P_l})$ is the probability density of a multivariate normal distribution with vector mean $\boldsymbol{\mu}$ and variance $\boldsymbol{P_l}$. Likewise, the phenotypic variance-covariance matrix in the expected scale is given by

$$\boldsymbol{P} = \int \left(\boldsymbol{g}^{-1}(\boldsymbol{l}) - \bar{\boldsymbol{z}}\right)^2 f_{\mathcal{MVN}}(\boldsymbol{l}, \boldsymbol{\mu}, \boldsymbol{P_l}) \, \mathrm{d}l \, . \tag{3.4}$$

The $\boldsymbol{G}$ matrix in the expected scale,

$$\boldsymbol{G} = \boldsymbol{\Phi} \boldsymbol{G_l} \boldsymbol{\Phi}^T, \tag{3.5}$$

can also be derived (Villemereuil et al., 2016), where $\boldsymbol{\Phi}$ is the average derivative of the expected values with respect to the latent values,

$$\boldsymbol{\Phi} = \int \frac{\mathrm{d}\boldsymbol{g}^{-1}}{\mathrm{d}\boldsymbol{l}} f_{\mathcal{MVN}}(\boldsymbol{l}, \boldsymbol{\mu}, \boldsymbol{P_l}) \, \mathrm{d}l \, . \tag{3.6}$$

Details on how derivatives and integrals were solved are provided in Appendix A.2. The heritability in

the expected scale is obtained directly through its definition, as the proportion of the additive genetic variance relative to the phenotypic variance, using the derived values. The results obtained using the above expressions can also be found in Table 3.2. The heritability of early pregnancy in the expected scale (probability) is 0.40 (95% CrI 0.11; 0.63), higher than the approximation shown above (but note that such approximation is derived for the data scale), and corroborating the genetic basis of this trait. Using the derived values in the expected scale, I also obtained the conditional genetic variance of lamb body mass. Such measure allows to evaluate the proportion of the additive genetic variance in lamb body mass that is independent from early pregnancy. Following Hansen et al. (2003), such quantity, $\sigma^2_{m|p_a}$, is given by

$$\sigma^2_{m|p_a} = \sigma^2_{m_a} - \frac{{\sigma_{m,p_a}}^2}{\sigma^2_{p_a}}, \tag{3.7}$$

which in this particular case corresponds to 0.40 (95% CrI 0.06; 0.85). The analogous metric for early pregnancy corresponds to 0.03 (95% CrI 0.00; 0.05). Since $\sigma^2_{m_a}$ and $\sigma^2_{p_a}$ were estimated to be, respectively, 0.78 (95% CrI 0.20; 1.27) and 0.04 (95% CrI 0.00; 0.08), the additive genetic variance in lamb body mass and early pregnancy that are independent from one another corresponds to 59% (95% CrI 29%; 100%). A significant proportion of the genetic variance in lamb body mass and early pregnancy are not independent, and therefore *selection for* each one of these traits necessarily results in *selection of* the other.

Table 3.2: Coefficients in the latent and expected scales of the multi-response animal model on lamb body mass and early pregnancy in Soay sheep. Note that lamb body mass was modelled in its natural scale and therefore no distinction between latent and expected scales are made. 95% credible intervals correspond to HPD intervals. The fixed effects and the partition of the **E** matrix are not shown, but can be found in Appendix A.1.

	latent scale		expected scale	
	posterior mode	95% CrI	posterior mode	95% CrI
μ_m	13.82	(13.22; 14.26)	-	-
μ_p	0.00	(-0.85; 0.64)	0.50	(0.39; 0.59)
$\sigma^2_{m_a}$	0.78	(0.20; 1.27)	-	-
$\sigma^2_{p_a}$	0.69	(0.00; 5.86)	0.04	(0; 0.08)
σ_{mp_a}	0.31	(0.00; 1.49)	0.11	(0; 0.18)
ρ_{mp_a}	0.64	(0.24; 0.90)	0.64	(0.24; 0.9)
σ^2_m	4.29	(3.84; 5.23)	-	-
σ^2_p	3.20	(1.99; 10.12)	0.09	(0.07; 0.14)
σ_{mp}	2.34	(1.49; 3.50)	0.36	(0.26; 0.44)
ρ_{mp}	0.51	(0.40; 0.66)	0.49	(0.38; 0.64)

Note that the estimated mean log odds of being pregnant (0.00) is considerably higher than the intercept in the univariate model (-0.81, Tab. 3.1). The models differ in their fixed effect structure (the univariate version includes mean-centred body mass). As a result of the distribution of body mass being slightly left skewed those values are not expected to match.

3.4 Fitness: first-year survival and lifetime rearing success

3.4.1 First-year survival

I investigated whether early pregnancy has fitness costs by evaluating first-year survival in ewe lambs as a function of pregnancy and body mass. First-year survival was defined using the first day of May as the cut-off date to make sure that dying during labour was considered in the first annual cycle of the ewes (89% of births are before 1 May). A binomial regression with logit link function of the form

$$ln\left(\frac{\mathbb{E}[s_{ijk}]}{1-\mathbb{E}[s_{ijk}]}\right) = \alpha + \alpha_p \times I_{p_{ijk}} + \beta_m \times mass_{ijk} + \beta_{mp} \times I_{p_{ijk}} \times mass_{ijk} + \boldsymbol{\beta} \times \boldsymbol{X_{ijk}} + u_{ci} + u_{mj} + \epsilon_{ijk}, \quad (3.8)$$

was adopted to model the probability of lamb k, born in year i to mother j, survives its first year of life. α and α_p are the intercept and the pregnancy-specific contrast to the intercept, β_m and β_{mp} are the slope for lamb body mass, and its pregnancy-specific contrast, and $\boldsymbol{\beta}$ is a vector with the coefficients for the remaining fixed effects. As first-year survival, and survival in general, is highly dependent on cohort effects due to variability in winter conditions and food availability (Clutton-Brock et al., 2004a), I included cohorts as random effects (u_{ci}), as well as maternal environmental effects (u_{mj}). Variance in residuals (ϵ_{ijk}) was set to one, as overdispersion is unobservable in binomial mixed models.

I first establish that first-year survival is size-dependent by adopting a similar model to the one in Equation (3.8), but excluding the pregnancy-specific contrasts - bigger ewes have higher chance of survival ($p < 0.001$, Fig. 3.2a, Tab. 3.3a). Adopting the full model in Equation (3.8) shows that for a given body mass pregnant lambs are significantly less likely to survive their first annual cycle when compared to the ewes that were not pregnant ($p < 0.001$, Fig. 3.2c, Tab. 3.3b). Lamb pregnancy has indeed a cost to survival - the probability of survival for ewe lambs of average body mass that did not get pregnant is 50% (95% CrI 37%; 65%), an estimate that drops to 26% (95% CrI 14%; 39%) in pregnant lambs. Pregnant lambs of all sizes are more likely to die than non-pregnant ewe lambs (Fig. 3.2c). Although merely a numerical result, it is interesting to notice that the mean body mass is lower in lambs that got pregnant (14.00, 95% CrI 13.65; 14.48) than it is in the sub-group of lambs that got pregnant and survived at least a year (14.59, 95% CrI 14.11; 15.03), suggesting that if a ewe is to be big enough to get pregnant, then it is better to be as big as possible. Investigating the simultaneous effect of lamb body mass, early pregnancy and population density on first-year survival exposes an important interaction effect between the former traits and the latter. Although large population size is, in general, associated with lower survival, it is evident that pregnant ewe lambs (Fig. 3.3a) are more susceptible to variation in population density than lambs that do not get pregnant (Fig. 3.3b). In general, investigating the simultaneous effect of body mass and population density on first-year survival exposes the importance of the effect of population density on this trait. It also shows that first-year survival in pregnant ewes is very low (below 10%) across most possible values of population density, unless body mass is relatively very high (Fig. 3.3a), whereas such low survival rates are much less likely in non-pregnant ewes (Fig. 3.3b).

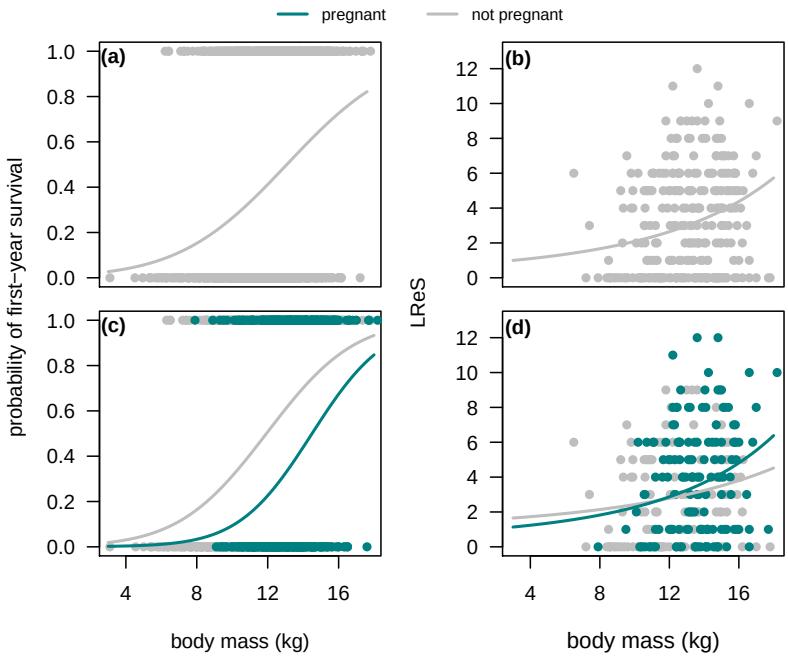

Figure 3.2: Probability of first-year survival (a, c) and lifetime rearing success, LReS, (b, d) in Soay sheep ewes as a function of lamb body mass (a, b), and both lamb body mass and early pregnancy status (c, d). Dots correspond to observed data and curves to model predictions. Binomial regressions for first-year survival with logit link function were fit to the data (see Tab. 3.3 for model parameters). LReS was estimated in ewes that survived their first year of life. Poisson regressions with exponential link function were fit to the data (see Tab. 3.5 for model parameters). In all models, population density and maternal age were included as covariates (slopes and curvatures were estimated for both), as well as birth and measurement dates. Variance among cohorts and maternal identities were also estimated.

Table 3.3: Coefficients of mixed effect binomial regressions with logit link function exploring the association of first-year survival with lamb size and early pregnancy in Soay ewes; (a) size-dependent first-year survival, (b) first-year survival as a function of size and pregnancy. Covariates except for twin status and pregnancy status were mean-centred.

parameter	posterior mode	95% CrI
(a)		
intercept	-0.55	(-1.59; 0.38)
body mass	0.50	(0.36; 0.66)
density $(\times 100)$	-1.38	(-1.95; -0.72)
density^2 $(\times 100)$	0.01	(0.00; 0.01)
density $\times$ body mass $(\times 100)$	-0.06	(-0.18; 0.05)
twin	0.06	(-0.70; 0.74)
maternal age	-0.02	(-0.12; 0.12)
maternal age^2	0.01	(-0.03; 0.05)
birth date	0.02	(-0.02; 0.05)
measurement date	-0.10	(-0.20; -0.03)
variance in cohort effects: 0.78 (0.78; 4.18)		
variance in maternal effects: 1.82 (0.61; 4.22)		
residual variance: set to 1		
(b)		
intercept	0.14	(-0.95; 1.23)
pregnancy	-2.15	(-2.73; -1.35)
body mass	0.69	(0.47; 0.89)
body mass $\times$ pregnancy	0.19	(-0.18; 0.43)
density $(\times 100)$	-0.89	(-1.75; -0.28)
density^2 $(\times 100)$	0.00	(0.00; 0.01)
density $\times$ pregnancy $(\times 100)$	-1.35	(-2.04; -0.70)
density $\times$ body mass $(\times 100)$	0.10	(-0.07; 0.24)
density $\times$ body mass $\times$ pregnancy $(\times 100)$	-0.04	(-0.34; 0.27)
twin	0.19	(-0.74; 0.88)
maternal age	0.04	(-0.12; 0.14)
maternal age^2	0.00	(-0.04; 0.04)
birth date	0.01	(-0.03; 0.05)
measurement date	-0.15	(-0.23; -0.04)
variance in cohort effects: 2.04 (0.98; 5.11)		
variance in maternal effects: 2.23 (0.85; 4.89)		
residual variance: set to 1		

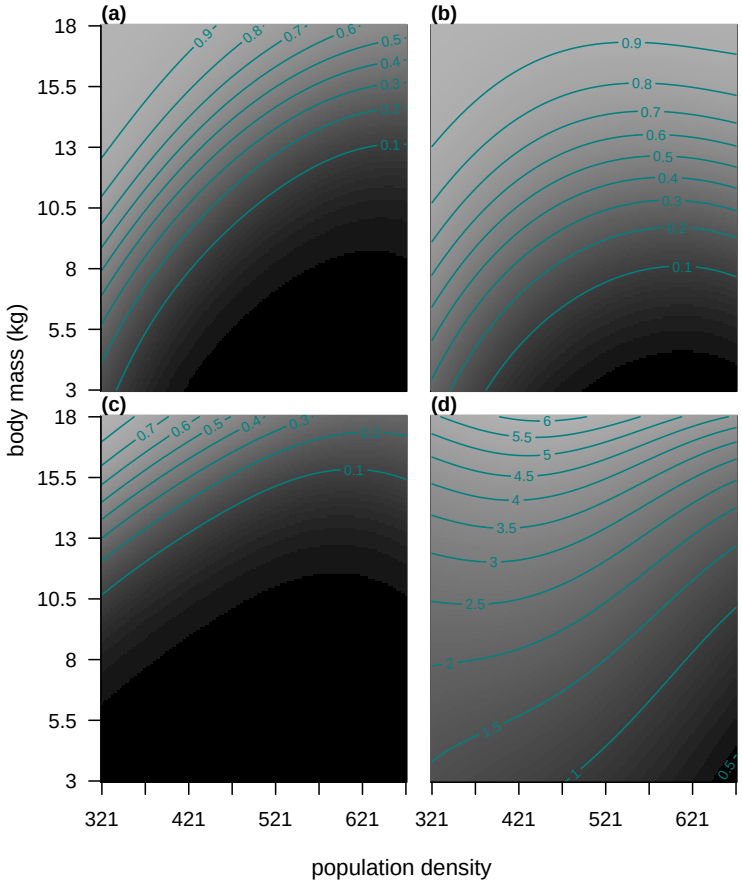

Figure 3.3: Probability of first-year survival in pregnant (a) and non-pregnant (b) ewe lambs, and AReS (c) and LReS (d) in Soay sheep ewes that survived their first annual cycle as a function of lamb body mass and population size. These are predictions based on models in Tables 3.3, 3.4 and 3.5.

3.4.2 First-year rearing success (AReS)

Having established that pregnant ewe lambs are more likely to die when compared to same sized non-pregnant ewe lambs, it is important to understand what is the fate of those pregnancies. From the 914 documented early pregnancies only 97 resulted in offspring surviving until the winter (AReS), and only 36, less than 5%, resulted in recruitments to the population, i.e. offspring that survived until their first April 1st. For modelling purposes, I only considered phenotyped mothers and those cases where their offspring had a chance of surviving, particularly looking at the cases where the mothers were known to have survived. As a result, only 50 offspring surviving until the winter were available. I estimated the AReS of ewe lamb i fitting a binomial regression with a logit link function of the form

$$ln\left(\frac{\mathbb{E}[AReS_i]}{1-\mathbb{E}[AReS_i]}\right) = \alpha + \beta_m \times mass_i + \boldsymbol{\beta} \times \boldsymbol{X_i} + \epsilon_i, \tag{3.9}$$

where α is the model intercept, β_m is a slope for lamb body mass, and $\boldsymbol{\beta}$ is a vector with the coefficients associated to the covariates in $\boldsymbol{X}$, which includes capture and birth dates, as well a linear and a quadratic term for population density. The variance in the model residuals, ϵ_i, was set to one. Due to sample size limitations, I did not include any random effects. I estimate that only 2.2% (95% CrI 0.57%; 6.17%) of the offspring born to ewes getting pregnant as average-sized lambs in average-density years survive until the winter (Tab. 3.4). It is interesting to note that the slope for body mass is positive and significantly different from zero, showing that larger ewe lambs are more likely to have surviving offspring, and suggesting that, as for first-year survival, if a ewe lamb is to get pregnant, than the larger the better. Overall, AReS not only increases with ewe body mass, but also significantly decreases as population size increases (Fig. 3.3c).

Table 3.4: Coefficients of a binomial regression (logit link function) of AReS in surviving ewe lambs that got pregnant on lamb body mass, birth and measurement dates, and population density in Soay sheep ewe lambs. All covariates were mean-centred and the 95% credible intervals correspond to HPD intervals.

Parameter	Posterior mode	95% CrI
intercept	-4.00	(-5.08; -2.94)
body mass	0.64	(0.43; 1.02)
density $_{(\times 100)}$	-1.06	(-2.41; -0.11)
density^2 $_{(\times 100)}$	0.00	(0.00; 0.01)
birth date	0.03	(-0.04; 0.10)
measurement date	0.06	(-0.11; 0.16)
residual variance: set to 1		

3.4.3 First-year life history

Given the dependency of first-year survival on pregnancy and mass, a diagram combining these events can be built that covers all the possible outcomes of the first year of life of Soay sheep ewes, and even extend it to include the fate of lamb pregnancy (Fig. 3.4a). Such a comprehensive diagram illustrates both the joint and the conditional distributions of these events on an average cohort. I

present such an exercise for average conditions, including average body mass and population density. The most evident feature is that the most common events are not getting pregnant and surviving and not getting pregnant and dying (32%), whereas the less likely event is for a ewe lamb to get pregnant and survive (9.49%). Also interesting, is that even though the major fraction of the average-sized ewe lambs do not get pregnant, pregnant and non-pregnant ewes contribute similarly to the yearly ewe lamb mortality (26.62%, and 31.83%, respectively). By looking at the first year of life only, the costs of lamb pregnancy in terms of survival seem huge when compared to the marginal benefits in terms of rearing success. Only 0.21% of all the ewes will successfully rear an offspring at least until the winter, corresponding to 2.21% of the pregnant ewes that get pregnant and survive. After the first annual cycle, in any given cohort, the ewe yearlings will correspond to the 32.06% of surviving non-pregnant lambs plus the 9.49% of pregnant ones, where 2.21% of these will have contributed with an offspring.

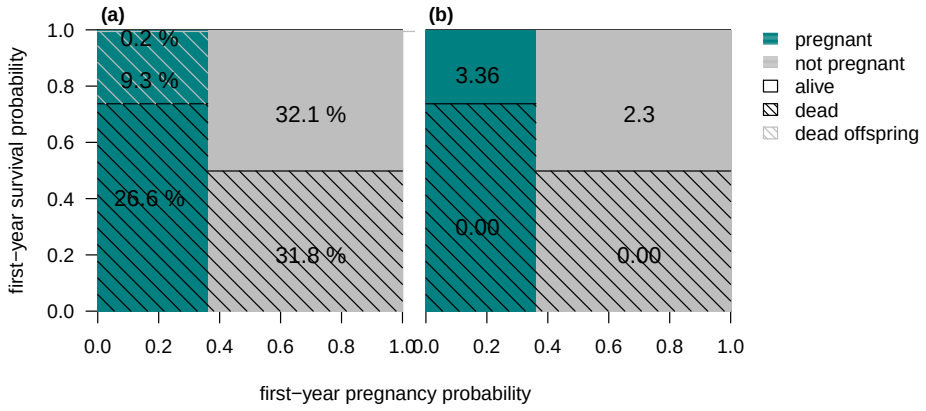

Figure 3.4: Geometric diagrams with areas corresponding to the joint probabilities of early pregnancy and first-year survival for average-sized individuals experiencing average environmental conditions. Areas in teal and grey correspond to early pregnancy and non-early pregnancy probabilities, respectively, and black-dashed and non-dashed areas correspond to non-surviving and surviving probabilities. Values within areas correspond to (a) joint probabilities of early pregnancy, survival, and AReS (grey-dashed area); and (b) LReS in ewes surviving their first year of life. The values shown in these plots were obtained using the models in Tables 3.1, 3.3(b), 3.4, and 3.5(b).

3.4.4 Subsequent lifetime rearing success (LReS)

I also investigated the effect of lamb body mass and early pregnancy on LReS. As the LReS of ewes dying during their first year of life is known to be zero, analyses presented here only include ewes that survived their first winter. The LReS of ewe i, born in year j to mother k was modelled with a Poisson mixed model with a $\log$ link function of the form

$$ln(\mathbb{E}[LReS_{ijk}]) = \mu + \mu_p \times I_{p_{ijk}} + \beta_m \times mass_{ijk} + \beta_{mp} \times I_{p_{ijk}} \times mass_{ijk} + \boldsymbol{\beta X} + u_{c_j} + u_{m_k} + \epsilon_{ijk}, \quad (3.10)$$

where μ is the model intercept and μ_p is the early pregnancy specific contrast to the intercept, with

$I_{p_{ijk}}$ being an indicator variable for early pregnancy. β_m is the slope for lamb August mass, β_{mp} the slope contrast for pregnant ewes, and $\boldsymbol{\beta}$ a vector with the slopes of the remaining fixed effects, $\boldsymbol{X}$. $\boldsymbol{u_c}$ and $\boldsymbol{u_m}$ are random effects, assumed to be drawn from independent normal distributions, for cohort and maternal identity. Finally, ϵ_{ijk} is the residual of individual i.

I applied the model in Equation (3.10) without the coefficients associated with early pregnancy and established that LReS is dependent on lamb size (Fig. 3.2b, Tab. 3.5a). Rearing success is an increasing function of lamb August body mass, with bigger animals being more likely to rear more offspring. Results from the full model suggest that rearing success is not determined by early pregnancy status (Fig. 3.2d, Tab. 3.5b), although it is unclear whether under particular conditions of population density this trait could have an effect on LReS that is independent from its correlation to lamb body mass. Neither the contrast to the intercept (0.37; 95% CrI -0.06; 0.82) nor the interaction terms with body mass (0.02; 95% CrI -0.05; 0.07) and population density (0.34; 95% CrI -0.09; 0.75, ($\times 100$)) are significantly different from zero, however these pregnancy-related coefficients are close to being considered so. Such numeric differences result in distinct expected number of offspring successfully reared in ewes that were and were not pregnant as lambs. In averaged-sized individuals living under average environmental conditions, 2.48 (95% CrI 1.57; 4.00) offspring are expected to be reared by ewes that survived their first year of life, which is broken down to 3.36 (95% CrI 1.87; 5.54) and 2.30 (95% CrI 1.40; 3.46) in ewes that got and did not get pregnant as lambs, respectively (Fig. 3.4b). As no strong statistical support is found for these differences nor any biological justification is known for such an effect of early pregnancy, LReS will be assumed to be independent from this trait in further analyses. The simultaneous effect of body mass and population density on LReS, independent of early pregnancy, is presented in Fig. 3.3(d), showing not only that LReS is highest in ewes born at low population densities, but also that the effect of lamb body mass on LReS is stronger in ewes that were also born in years of low population density.

Table 3.5: Coefficients of Poisson regressions with logarithm link functions, exploring the association between LReS in ewes surviving their first year and lamb body mass and early pregnancy; (a) size-dependent LReS, and (b) LReS as a function of lamb August body mass and early pregnancy. Covariates except for twin status and early pregnancy status were mean-centred, and 95% credible intervals correspond to HPD intervals.

parameter	posterior mode	95% CrI
(a)		
intercept	0.64	(0.12; 0.99)
body mass	0.14	(0.04; 0.23)
density $(\times 100)$	-0.15	(-0.49; 0.01)
density^2 $(\times 100)$	0.00	(0.00; 0.00)
density $\times$ body mass $(\times 100)$	0.04	(-0.06; 0.09)
twin	0.07	(-0.38; 0.52)
maternal age	0.00	(-0.08; 0.06)
maternal age^2	0.01	(0.00; 0.03)
birth date	0.01	(-0.02; 0.03)
measurement date	0.01	(-0.06; 0.07)
variance in cohort effects:	0.00 (0.00; 0.37)	
variance in maternal effects:	0.38 (0.00; 0.68)	
residual variance:	0.45 (0.20; 0.86)	
(b)		
intercept	0.38	(-0.07; 0.83)
pregnancy	0.37	(-0.06; 0.82)
body mass	0.14	(0.03; 0.27)
pregnancy $\times$ body mass	0.02	(-0.28; 0.09)
density $(\times 100)$	-0.25	(-0.52; 0.06)
density^2 $(\times 100)$	0.00	(0.00; 0.00)
density $\times$ pregnancy $(\times 100)$	0.34	(-0.09; 0.75)
density $\times$ body mass $(\times 100)$	0.10	(0.00; 0.21)
density $\times$ body mass $\times$ pregnancy $(\times 100)$	-0.24	(-0.39; -0.06)
twin	0.14	(-0.34; 0.57)
maternal age	0.00	(-0.08; 0.07)
maternal age^2	0.02	(0.00; 0.04)
birth date	0.00	(-0.02; 0.03)
measurement date	0.02	(-0.05; 0.07)
variance in cohort effects:	0.00 (0.00; 0.38)	
variance in maternal effects:	0.30 (0.00; 0.60)	
residual variance:	0.51 (0.26; 0.91)	

3.5 Formal selection analysis

The analyses shown so far establish that (1) early pregnancy is size-dependent, (2) there is a fairly strong positive additive genetic correlation between lamb body mass and early pregnancy, (3) there is selection against early pregnancy through viability selection, (4) ultimate fitness benefit of early pregnancy is very small, and (5) subsequent LReS in surviving ewes is size-dependent, but very similar in ewes that got and did not get pregnant. In this section, I use the information presented so far in a formal selection analysis to investigate *selection for* and *selection of* lamb size in Soay sheep ewes. Particularly, I use a path analysis involving all pertinent traits (Fig. 3.5), allowing the estimation of an *extended selection gradient* (Morrissey, 2014) for lamb body mass. Using the path rules for developmental systems set by Wright (1934) and expanded to non-linear variables by Morrissey (2015) one can infer the component of the effect of lamb body mass on fitness and that that occurs via early pregnancy and otherwise. The path diagram shown in Figure 3.5 includes twining, t, mass, m, pregnancy, p, survival, s, AReS, $ares$, subsequent LReS, $lres$, and fitness, W, and can be represented by a vector-valued function of the following form

$$z_{ijk} = \begin{bmatrix} t \\ m \\ p \\ s \\ ares \\ lres \\ W \end{bmatrix}_{ijk} = \boldsymbol{f(l)}_{ijk} = \begin{bmatrix} \frac{e^{\alpha+\boldsymbol{\beta X_{ijk}}+u_{cj}+u_{mk}+\epsilon_{ijk}}}{1+e^{\alpha+\boldsymbol{\beta X_{ijk}}+u_{cj}+u_{mk}+\epsilon_{ijk}}} \\ \alpha + \alpha_t \times I_{t_{ijk}} + \boldsymbol{\beta X_{ijk}} + a_i + u_{cj} + u_{mk} + \epsilon_{ijk} \\ \frac{e^{\alpha+\alpha_t \times I_{t_{ijk}}+\beta m_1 \times m_{ijk}+\beta m_2 \times m^2_{ijk}+\beta m_3 \times m^3_{ijk}+\boldsymbol{\beta X_{ijk}}+u_{cj}+u_{mk}+\epsilon_{ijk}}}{1+e^{\alpha+\alpha_t \times I_{t_{ijk}}+\beta m_1 m_{ijk}+\beta m_2 m^2_{ijk}+\beta m_3 m^3_{ijk}+\boldsymbol{\beta X_{ijk}}+u_{cj}+u_{mk}+\epsilon_{ijk}}} \\ \frac{e^{\alpha+\alpha_t \times I_{t_{ijk}}+\alpha_p \times I_{p_{ijk}}+\beta m \times m_{ijk}+\boldsymbol{\beta X_{ijk}}+u_{cj}+u_{mk}+\epsilon_{ijk}}}{1+e^{\alpha+\alpha_t \times I_{t_{ijk}}+\alpha_p \times I_{p_{ijk}}+\beta m \times m_{ijk}+\boldsymbol{\beta X_{ijk}}+u_{cj}+u_{mk}+\epsilon_{ijk}}} \text{ (Eqn. 3.8)} \\ \frac{e^{\alpha+\beta m \times m_{ijk}+\boldsymbol{\beta X_{ijk}}+\epsilon_{ijk}}}{1+e^{\alpha+\beta m \times m_{ijk}+\boldsymbol{\beta X_{ijk}}+\epsilon_{ijk}}} \text{ (Eqn. 3.9)} \\ e^{\alpha+\alpha_t \times I_{t_{ijk}}+\alpha_p \times I_{p_{ijk}}+\beta_m \times m_{ijk}+\boldsymbol{\beta X_{ijk}}+u_{cj}+u_{mk}+\epsilon_{ijk}} \text{ (Eqn. 3.10)} \\ s_{ijk}\ (ares_{ijk} + lres_{ijk}) \end{bmatrix}. \quad (3.11)$$

As before, although corresponding to different quantities, I use the same Greek letters for equivalent coefficients in all models: α represents the intercepts, α_t and α_p the twinning and pregnancy-specific contrasts to the intercept, respectively, β_m (and β_{m_1}), β_{m_2}, and β_{m_3} the slope, curvature, and cubic term for mass, β_{mp} the pregnancy-specific contrast to the slope and, finally, $\boldsymbol{\beta}$ is a vector containing the effects associated with the remaining covariates, population density and maternal age at parity, including quadratic terms for both. $\boldsymbol{\beta}$ also includes interaction terms for body mass and population density in all models including body mass as predictor, interaction terms between early pregnancy status and population density in all models including early pregnancy as a predictor, and between these two and body mass in the models including both lamb body mass and early pregnancy status as predictors. u_{cj} and u_{mk} are random effects associated with cohort j and mother k, and ϵ_{ijk} is the residual of individual i. The model for mass also includes breeding values, a, allowing to segregate the additive genetic variance from other sources of variation. Twinning, pregnancy, survival, and AReS were assumed to follow binomial distributions, mass to follow a Gaussian distribution, whereas LReS was assumed to be Poisson distributed with additive overdispersion. Fitness was defined as the sum of AReS and LReS of ewes surviving their first annual cycle weighted by the probability of first-year survival. The estimates of the parameters in the vector-valued function are found in the

tables shown so far, except for the parameters explaining the probability of twining, which can be found in Table 3.6. Note that although population density is not included in the path diagram of Figure 3.5, all the results presented in this section were obtained by marginalising over the observed population density in all cohorts. Particularly, population densities were marginalised by averaging over predicted values, i.e. Equation (3.11) was evaluated for the values of population density of each cohort and the mean value taken as the best estimate of $\bar{z}$.

Table 3.6: Coefficients of a binomial regression (logit link function) of the probability of twinning as a function of mean-centred population density and maternal age. 95% credible intervals correspond to HPD intervals.

parameter	posterior mode	95% CrI
intercept	-2.47	(-3.37; -1.43)
density $(\times 100)$	-0.07	(-0.47; 0.55)
density^2 $(\times 100)$	-0.01	(-0.01; 0.00)
maternal age	0.90	(0.69; 1.14)
maternal age^2	-0.15	(-0.20; -0.08)
variance in cohort effects:	0.72 (0.15; 2.59)	
variance in maternal effects:	9.25 (5.02; 14.35)	
residual variance:	set to 1	

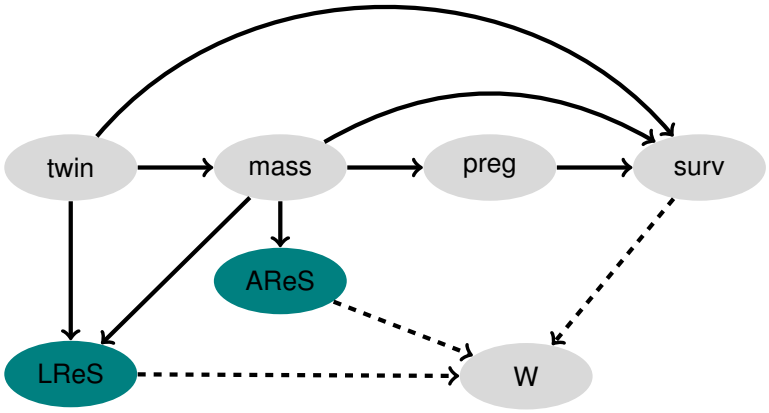

Figure 3.5: Developmental system representing the phenotypic landscape defined in Equation (3.11). The probability of twinning, *twin*, has an effect in all the other traits, lamb body *mass* affects the probabilities of being pregnant as a lamb, *preg*, surviving the first annual cycle, *surv*, and also first year (conditional on early pregnancy) and subsequent lifetime rearing success, *AReS* and *LReS*; and *preg* affects *surv*. Fitness, *W*, is defined as the sum of AReS and LReS on surviving ewes weighted by the probability of first-year survival.

Mean phenotype, $\bar{z}$, and the phenotypic variance-covariance matrix, $\mathbf{P}$, in the expected scale were obtained using Equation (3.3) and Equation (3.4), and correspond to

$$\bar{\boldsymbol{z}} = \begin{bmatrix} \bar{t} \\ \bar{m} \\ \bar{p} \\ \bar{s} \\ a\bar{r}es \\ l\bar{r}es \\ \bar{W} \end{bmatrix} = \begin{bmatrix} 0.20\ (0.16; 0.25) \\ 12.71\ (12.54; 12.87) \\ 0.48\ (0.46; 0.49) \\ 0.57\ (0.55; 0.59) \\ 0.06\ (0.05; 0.06) \\ 3.00\ (2.50; 3.54) \\ 1.95\ (1.61; 2.31) \end{bmatrix},$$

and

$$\boldsymbol{P} = \begin{bmatrix} 0.09\ (0.06; 0.11) & -0.25\ (-0.34; -0.16) & -0.01\ (-0.02; -0.01) & -0.02\ (-0.02; -0.01) & 0.00\ (0.00; 0.00) & -0.05\ (-0.13; 0.01) & -0.09\ (-0.15; -0.04) \\ -0.43\ (-0.49; -0.34) & 3.92\ (3.54; 4.55) & 0.31\ (0.27; 0.36) & 0.25\ (0.20; 0.29) & 0.04\ (0.03; 0.05) & 1.26\ (0.86; 2.02) & 1.45\ (1.17; 2.18) \\ -0.14\ (-0.22; -0.08) & 0.57\ (0.48; 0.64) & 0.08\ (0.07; 0.09) & 0.01\ (0.00; 0.02) & 0.00\ (0.00; 0.00) & 0.10\ (0.04; 0.18) & 0.09\ (0.04; 0.15) \\ -0.21\ (-0.27; -0.13) & 0.42\ (0.33; 0.51) & 0.11\ (0.03; 0.19) & 0.09\ (0.07; 0.11) & 0.00\ (0.00; 0.00) & 0.08\ (0.03; 0.16) & 0.31\ (0.23; 0.40) \\ -0.12\ (-0.17; -0.06) & 0.31\ (0.25; 0.36) & 0.15\ (0.09; 0.21) & 0.14\ (0.08; 0.19) & 0.00\ (0.00; 0.01) & 0.01\ (0.00; 0.04) & 0.02\ (0.01; 0.04) \\ -0.05\ (-0.11; 0.00) & 0.19\ (0.11; 0.26) & 0.10\ (0.03; 0.16) & 0.08\ (0.02; 0.13) & 0.05\ (-0.01; 0.13) & 11.39\ (4.93; 36.23) & 8.51\ (3.74; 25.96) \\ -0.09\ (-0.15; -0.05) & 0.27\ (0.18; 0.35) & 0.10\ (0.03; 0.16) & 0.34\ (0.24; 0.43) & 0.11\ (0.03; 0.18) & 0.87\ (0.79; 0.93) & 7.55\ (3.88; 23.60) \end{bmatrix},$$

respectively. Note that, as reported here, the diagonal of $\boldsymbol{P}$ corresponds to variances, the upper off-diagonal to covariances and the lower off-diagonal to correlations among traits. As variance in breeding values was only estimated for lamb body mass, which was modelled in its natural scale, the additive genetic variance in mass in the expected scale is the one estimated in the model, 0.67 (95% CrI 0.07; 1.14). The fact that the correlations between lamb body mass and first-year survival (0.42, 95% CrI 0.33; 0.51) and between early pregnancy and first-year survival (0.11, 95% CrI 0.03; 0.19) are both non-negative suggests that the equilibrium between lamb body mass affecting first-year survival positively (direct effect) and negatively (through its effect on early pregnancy) is leaning towards the former. To investigate the consequences of this trade-off in the selection of lamb body mass, I calculated its *extended* directional selection gradient. For trait z, the extended directional selection gradient is defined as the average derivative of expected fitness with respect to latent value (Morrissey, 2015; Villemereuil et al., 2016),

$$\eta_z = \frac{\partial \bar{W}(\bar{\boldsymbol{l}})}{\partial \bar{l}_j} \bar{W}^{-1}. \tag{3.12}$$

For mass, I calculate η_m to be positive, 0.25 (95% CrI 0.24; 0.27), whereas for lamb pregnancy, η_p is negative, -0.56 (95% CrI -0.67; -0.46). Importantly, the conflict between viability and fecundity is density-dependent, and is almost nonexistent when population density is very low. In such circumstances, virtually all ewe lambs survive, and therefore early pregnancy does not have a significant cost. As a consequence, η_p is higher when population density is at its lowest and decreases with population density (Fig. 3.6, Tab. 3.7). In contrast, at high densities, when the probability of first-year survival is lowest, selection favouring larger body size is stronger. The directional selection gradient, β_m, as opposed to the *extended* directional selection gradient, η_m, is blind to the positive correlation that exists between lamb body mass and early pregnancy (and therefore to the pregnancy induced viability selection), and as a consequence is expected to be larger than η_m. On average, however, these two quantities do not differ much, and β_m is only marginally larger (0.29; 95% CrI 0.26; 0.31). The reason for that lies again in the dependency of these quantities on population density. At its limit, no differences between η_m and β_m are expected when population density is very low, as viability

selection tends to zero and, therefore, there is no cost to early pregnancy. Indeed, I show that η_m and β_m become increasingly dissimilar with increasing population density (Fig. 3.6).

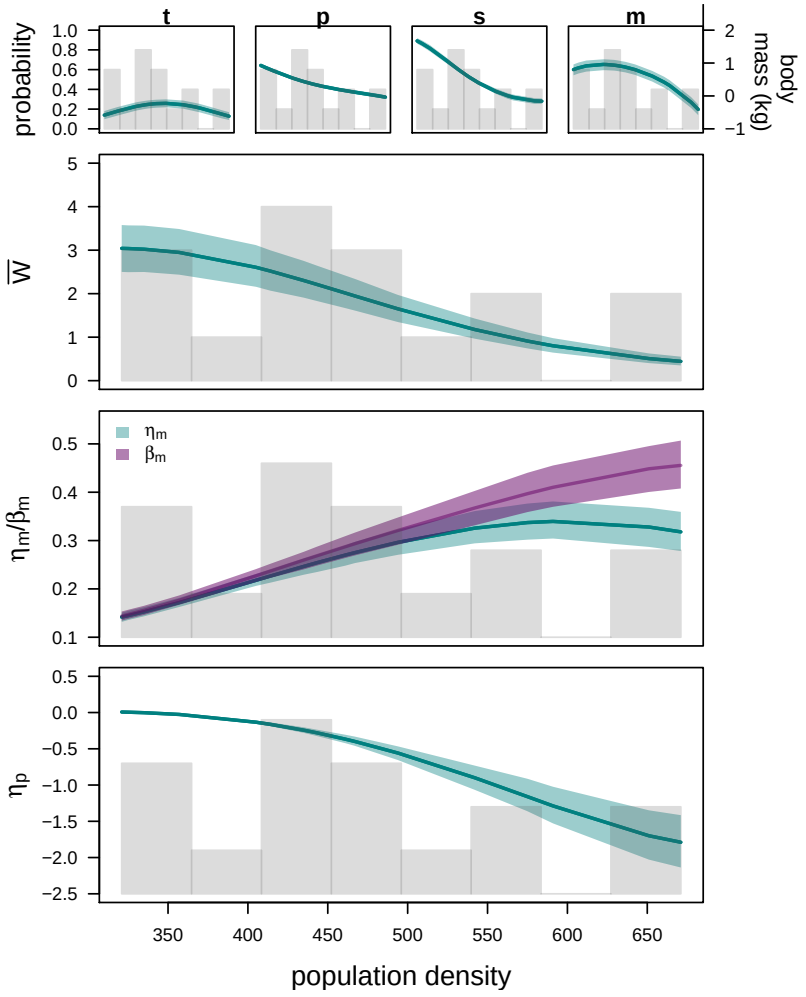

Figure 3.6: The effect of population density on the values of the traits in the path diagram in Figure 3.5, and consequently on selection of lamb body mass and early pregnancy. The upper panel shows variation in mean twinning (t), early pregnancy (p), and first-year survival (s) probabilities, and in mean-centred lamb body mass (m). The three lower panels include functions of mean fitness, selection of lamb body mass, and selection of early pregnancy on population density. All plots include an histogram showing the empirical distribution of population density. Areas in teal correspond to 95% HPD credible intervals.

The path analysis represented by Figure 3.5 assumes a definition of fitness that includes the entire life of the Soay ewes, encompassing the selection on lamb body mass that occurs throughout the entire lifetime. However, the mechanisms through which selection acts, survival and fecundity, tend to occur predominantly at different points of the life of these ewes. Viability selection is particularly strong in the first annual cycle, whereas most offspring are reared at older ages. To evaluate the strength of the two mechanisms is, therefore, also to understand in which period selection is the strongest. I quantify the contribution of selection on lamb body mass that occurs during the first year of life using a path diagram similar to the one in Figure 3.5, but defining fitness as first-year survival. Measured this way, η_m is 0.12 (95% CrI 0.11; 0.14), and therefore corresponds to 48% (95% CrI

44%; 52%) of the overall selection on body mass. Such relative strength of first-year survival and lifetime fecundity in shaping the selection on lamb body mass varies with environmental conditions (Fig. 3.7, Tab. 3.7). Selection acting on lamb body mass through viability costs during the first year of life is proportionally very low when population density is lowest (around 30%), is highest at intermediate populations densities and decreases when population density is very high. A slightly different pattern is obtained if β_m, instead of η_m, is used to quantify the strength of selection. In this case, the relative importance of viability selection does not decrease when population density is at its highest. These two trajectories, put together, suggest that at low densities, when both fecundity and survival are very high (Fig. 3.6), fecundity governs selection on lamb body mass, as mothers will successfully rear several offspring. As population size increases and first-year survival decreases (Fig. 3.6), viability selection becomes proportionally more important as it occurs before any opportunity for reproduction. Under exceptional high population density, the probability of survival is very low. As most ewes die, fecundity selection becomes slightly more important. That is not observed when the correlation between lamb body mass and early pregnancy is dismissed, probably because the pregnancy-related viability costs are not considered. Overall, the fact that about half the selection on lamb body mass does not occur in the first year of life of these ewes, strongly suggests that the trade-off between viability and fecundity selection in ewe lambs might also play a role in regulating body mass at older ages.

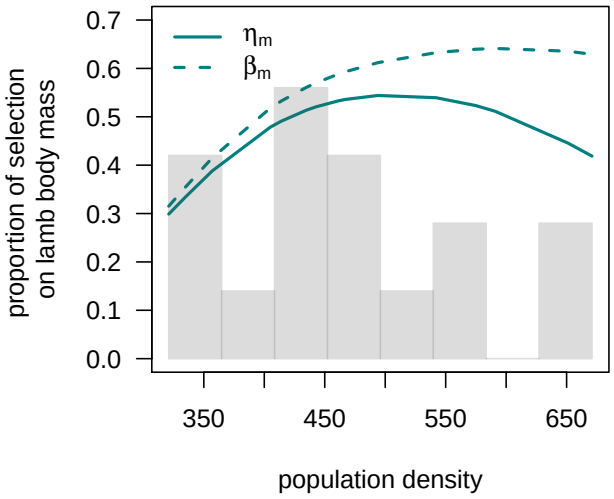

Figure 3.7: Proportion of natural selection on lamb body mass occurring through viability selection in Soay sheep ewes as a function of population density. This proportion was obtained both using the extended (η_m) and non-extended (β_m) directional selection gradient of lamb body mass. The histogram in grey shows the empirical distribution of population density.

Finally, I investigated in which conditions of population size and body mass early pregnancy could be advantageous, or at least not maladaptive, to Soay sheep ewes. Such knowledge could contribute to understand why early pregnancy occurs in this population despite its large viability cost. To accomplish this I used a modified version of Equation (3.11) where instead of the expression for lamb body mass I used a range of values comprising all observations of lamb body mass and where I also

Table 3.7: Selection gradients of lamb body mass and early pregnancy for three different values of observed population density - minimum, mean and maximum (321, 452, and 671, respectively). Raw (η) and standardised selection gradientes, either by the observed standard deviation (η_{sd}) or the observed mean (η_{μ}), are shown. For lamb body mass, selection gradients considering first-year survival as a measure of fitness are also included (η_s).

		d=321	d=452	d=671
mass	η	0.14 (0.13; 0.15)	0.28 (0.25; 0.30)	0.32 (0.28; 0.36)
	η_{sd}	0.33 (0.30; 0.35)	0.64 (0.59; 0.69)	0.73 (0.64; 0.83)
	η_{μ}	1.76 (1.64; 1.87)	3.42 (3.15; 3.70)	3.95 (3.46; 4.47)
	η_s	0.04 (0.04; 0.05)	0.15 (0.13; 0.17)	0.13 (0.11; 0.16)
	$\eta_{s_{sd}}$	0.10 (0.08; 0.11)	0.34 (0.30; 0.39)	0.31 (0.25; 0.37)
	$\eta_{s_{\mu}}$	0.53 (0.45; 0.59)	1.83 (1.60; 2.08)	1.66 (1.33; 2.00)
pregnancy	η	0.01 (0.00; 0.02)	-0.40 (-0.46; -0.33)	-1.79 (-2.14; -1.42)
	η_{sd}	0.00 (0.00; 0.01)	-0.20 (-0.23; -0.17)	-0.90 (-1.07; -0.71)

modified the expression used to fit the probability of early pregnancy. I simplified the latter expression by dropping the polynomial terms associated to body mass, leaving only the slope and by substituting the intercept and the slope for lamb body mass by a fixed range of values that would allow probabilities of early pregnancy to vary from zero to one. I, then, evaluated this modified expression for all observed values of population density. For each combination of lamb body mass and population density, a matrix for each trait, including early pregnancy and fitness, was obtained that corresponded to the possible combinations of intercepts and slopes associated to early pregnancy. As a result, for each combination I could derive the probability of pregnancy that maximised fitness. Often this maximisation was not singular, and various values of early pregnancy (various combinations of intercepts and slopes) would result in maximum fitness. In such cases, I selected the combination resulting in highest probability of early pregnancy, as my aim was to assess the conditions under which early pregnancy would not be selected against. Such approach resulted in reaction norms of probability of pregnancy across values of lamb body mass for different population densities (Fig. 3.8). I conclude that early pregnancy is only adaptive in particular combinations of environmental and body mass conditions. Specifically, early pregnancy is only adaptive when population density is low and/or lamb body mass is particularly high. Although population density ranged from 321 to 671 individuals, only when population density corresponded to 410 individuals or less, there were conditions of body mass for which probabilities of pregnancy higher than zero would maximise fitness. Also interesting is the fact that when population density is particularly low, early pregnancy can be advantageous in ewes whose mass is even below average. Given these results, it would be particularly relevant to understand if there is variation in these reaction norms and, if so, how much of that variation has an additive genetic basis.

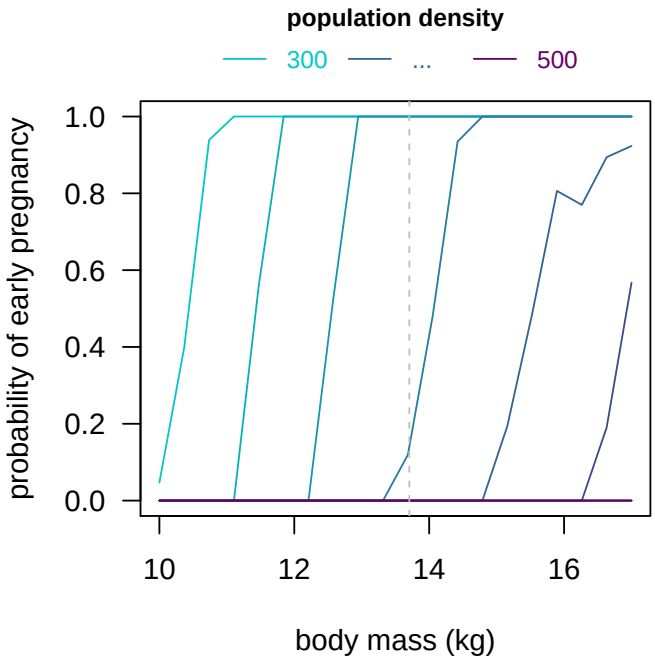

Figure 3.8: Maximum probability of early pregnancy that maximises fitness as a function of lamb body mass in Soay sheep. Results are shown for different values of population density, ranging from 300 to 500 individuals, by intervals of 20. The vertical grey line represents average body mass.

3.6 Model estimation and reported statistics

All statistical models were fit using a Bayesian framework, using MCMCglmm (Hadfield, 2010). Inverse gamma distributions were adopted for residual variances (of non-binary traits), whereas inverse Wishart distributions were adopted for the remaining (co)variance components associated with random effects, using parameter expansion to increase convergence efficiency (Gelman, 2006; Hadfield, 2010). While parameter estimates from statistical models were defined as corresponding to the modes of the respective posterior distributions, when presenting derived quantities I used means instead. The reason for that was because these derived quantities not always were expected to be normally distributed. Uncertainty on parameter estimates and derived quantities is presented using Highest Posterior Density credible intervals at the 95% level. Adopting a Bayesian framework allowed for uncertainty to be propagated when calculating composite statistics such as heritabilities and selection gradients.

3.7 Discussion

Results from this chapter provide evidence of a trade-off between viability and fecundity selection of body size in Soay sheep ewe lambs. Larger lambs are more likely to get pregnant during their first annual cycle, and pregnant lambs are more likely to die. As a consequence, natural selection acts on lamb body mass through two distinct pathways, through the direct effect of lamb body mass on fitness, independent of early pregnancy status, and through its effect on early pregnancy. Selection

on lamb body mass would, therefore, be stronger (more positive) if not for the relationship between this trait and early pregnancy. As a result, this correlation provides a mechanism that contributes to the regulation of body size in Soay sheep.

Although I do not directly test the impact of the identified trade-off in body mass of males or older females, any existing genetic correlation in body mass across sexes and ages would, in principle, facilitate that effect. In Soay sheep, both kinds of genetic correlations are known to exist. On the one hand, Robinson et al. (2009) have shown that there is very strong additive genetic correlation in body mass between ewes and rams, and, additionally, Wilson et al. (2007) showed that body mass is highly correlated across ages. This last finding is consistent with the fact that, as I have shown, nearly half the selection on lamb body mass occurs through subsequent lifetime rearing success, rather than through first-year survival. Overall, evidence suggests that the correlation between lamb body mass and early pregnancy in females plays a role in the selection of body mass in the entire population of Soay sheep. It is also noteworthy that this mechanism is expected to become increasingly important if the population of Hirta continues to increase (Clutton-Brock et al., 2004a).

I used recent theory on nonlinear development systems to decompose selection on body mass, which essentially correspond to systems of path analyses that allow for non-linear effects and interactions (Morrissey, 2015). As a result, I was able to disentangle and quantify the direct effect of lamb body mass on fitness and that through its effect on early pregnancy. Alternatives to this approach are the use of traditional path analysis (developed for linear traits, e.g. Scheiner et al., 2000; Morrissey, 2014) or multi-response (linear or generalised linear) models that explicitly estimate (additive genetic) correlations among traits (e.g. Bonnet et al., 2017). Although each approach was designed for slightly different purposes, these are equally suitable to decompose selection into its different mechanisms and therefore to identify and quantify putative evolutionary constraints. My approach specifically harnesses the phenotypic relationship between lamb body mass and early pregnancy, and builds it into a formal model of selection. Such an approach has the potential to be particularly useful when analytical power is a limiting constraint to infer the genetic architecture among traits. If the existence of genetic trade-offs, alongside with the lack of directional selection, is indeed a major explanation for the widespread mismatch between predicted evolutionary change and observed dynamics of body size (Blanckenhorn, 2000; Hansen & Houle, 2004; Kruuk et al., 2008), why are these methods not more frequently adopted? Information available suggests that the most considerable obstacle in dealing with the selection of correlated traits is far from being purely methodological. Detecting such correlations seems to be a limiting step, with evidence for genetic constraints in the wild being rather scarce (Kruuk et al., 2008). Reasons for this may include insufficient knowledge about the biology and ecology of a species (Pemberton, 2010), but also the existence of confounding effects between genes and environment. A negative genetic covariation between two traits might be obscured at the phenotypic level by patterns of environmental covariation among traits (Roff & Fairbairn, 2007; Morrissey et al., 2012c). Put together, the information gathered so far supports the hypothesis that the paradox of stasis will not in most cases have a single and simple solution and that a deep understanding of the biology and ecology of the species being studied is of instrumental importance.

Finally, the work presented here does not to explain why early pregnancy occurs in Soay sheep,

given the significant selection against this trait and its fairly high heritability. It is clear that to some extent it is a non-adaptive correlated response to lifetime selection for larger body size, but there is some additive genetic variance that is independent of mass. As a result, although at a slow pace, reduced pregnancy can evolve despite selection for larger body size. An explanation for its persistence might lie in the dynamics of this population. The Soay sheep were reintroduced in Hirta in 1932, when one hundred and seven individuals were brought from the neighbouring island of Soay (Clutton-Brock & Pemberton, 2004a), and evidence suggests that population density is still increasing (Clutton-Brock et al., 2004a). In the first decades after the reintroduction, the population size was much below its carrying capacity, potentially favouring behaviours that would increase reproductive success. The non-negative selection gradients for early pregnancy obtained here for low population densities support the hypothesis that this was once an adaptive behaviour. A second explanation could be related to gene introgression. Given that early pregnancy is actually common in domestic sheep, its occurrence in Soay sheep could be a result of introgression of domesticated genes back into the Soay sheep population of Hirta. There is some evidence supporting this hypothesis, as admixture is known to have happened between Soay sheep and a more modern breed approximately 150 years ago (Feulner et al., 2013).

3.8 Summary

The results presented in this chapter provide evidence of a trade-off constraining the evolution of lamb body mass in an unmanaged population of an ungulate species. The Soay sheep population of Hirta has been established as an example of the paradox of stasis, which exists beyond the genetic constraint here identified. Nonetheless, I show that selection towards larger body sizes would be stronger if not for the positive correlation between lamb body mass and early pregnancy, and their opposing association to fitness. Large lamb body mass is associated with higher rates of first-year survival and lifetime rearing success, but also with higher chance of early pregnancy. The latter has a very large viability cost. Furthermore, I present results that strongly suggest that this mechanism might also be involved in the regulation of adult body size in females, as half the selection on ewe lamb body mass occurs at older ages. Additive genetic correlations among sexes and across ages might also facilitate a broader scope of action for this mechanism, which might play a role at regulating the body size in the entire population.

CHAPTER 4

Towards robust evolutionary inference with integral projection models

Note: The work presented in Chapter 4 was presented in the form of a peer-reviewed article: **Towards robust evolutionary inference with integral projection models** (2017). M. J. Janeiro, D. W. Coltman, M. Festa-Bianchet, F. Pelletier & M. B. Morrissey. *Journal of Evolutionary Biology*, 30: 270-288.

Abstract

Integral projection models (IPMs) are extremely flexible tools for ecological and evolutionary inference. IPMs track the full joint distribution of phenotype in populations through time, using functions describing phenotype-dependent development, inheritance, survival and fecundity. For evolutionary inference, two important features of any model are the ability to (i) characterise relationships among traits (including values of the same traits across age) within individuals, and (ii) characterise similarity between individuals and their descendants. In IPM analyses, the former depends on regressions of observed trait values at each age on values at the previous age (development functions), and the latter on regressions of offspring values at birth on parent values as adults (inheritance functions). I show analytically that development functions, characterised this way, will typically underestimate covariances of trait values across ages, due to compounding of regression to the mean across projection steps. Similarly, I show that inheritance, characterised this way, is inconsistent with a modern understanding of inheritance, and underestimates the degree to which relatives are phenotypically similar. Additionally, I show that the use of a constant biometric inheritance function, particularly with a constant intercept, is incompatible with evolution. Consequently, one should expect typical constructions of IPMs to predict little or no phenotypic evolution, purely as artefacts of their construction. I present alternative approaches to constructing development and inheritance functions, based on a quantitative genetic approach, and show analytically and by empirical example, using a population of bighorn sheep, how they can potentially recover patterns that are critical to

evolutionary inference.

Keywords: integral projection models, regression to the mean, inheritance, development, body size, evolutionary responses, bighorn sheep

4.1 Introduction

Evolutionary and ecological dynamics converge at the scale of generation-to-generation change in populations (Pelletier et al., 2009; Coulson et al., 2010). When traits cause fitness variation, the distributions of those traits, weighted by fitness, necessarily changes within generations (Godfrey-Smith, 2007). If differences among individuals have a genetic basis, then genetic changes will be concomitant with phenotypic changes. Such genetic changes are the basis for the transmission of within-generation change due to selection, to genetic change between populations, i.e. evolution (Lewontin, 1970; Endler, 1986). The fundamental nature of this relationship between phenotypic change due to selection, and associated genetic and thus evolutionary change, has motivated the development of various expressions relating selection to genetic variation and evolution in quantitative terms (Lush, 1937; Robertson, 1966, 1968; Lande, 1979; Lande & Arnold, 1983; Morrissey, 2014, 2015). Important recent advances in population demography, particularly the introduction (Easterling et al., 2000) and popularisation (e.g. Childs et al., 2003; Ellner & Rees, 2006; Coulson et al., 2010; Ozgul et al., 2010; Coulson, 2012; Merow et al., 2014) of integral projection models (IPMs), can potentially allow the construction of very flexible models of changes in phenotype, and of associated demographic implications (Coulson et al., 2010).

In principle, IPMs track the full joint distribution of phenotype through time. These are very general models capable of calculating many biological parameters through the estimation of four sets of functions, termed fundamental functions or fundamental processes (Coulson et al., 2010): (i) survival, (ii) fertility, (iii) ontogenetic development of size conditional on surviving (development functions), and (iv) distribution of offspring trait as a function of parent's (inheritance functions). As discussed by Coulson et al. (2010), these processes underly the high flexibility of IPMs and their ability to link different aspects of population ecology, evolutionary biology and life history.

A key aspect of the distribution of phenotypes is how traits covary at the level of individuals. Genetic and phenotypic covariances among traits are key determinants of evolution (Lande, 1979). In the context of IPMs, which often consider single traits (e.g., mass), age-specific values of a given trait can be thought of as separate, age-specific traits, the covariances among which are key determinants of evolutionary processes. For example, if viability selection acts on juveniles, the influence of that selection on future generations can only occur if there is covariance between trait values at juvenile ages and at ages when reproduction occurs. In IPMs as parameterised to date (e.g. Childs et al., 2003; Ellner & Rees, 2006; Coulson et al., 2010; Ozgul et al., 2010), covariance across ages depends on correctly estimating regressions of observed trait values at each age on trait values at the previous age. In practice, such regressions will typically be underestimated due to regression to the mean (Campbell & Kenny, 1999; Barnett et al., 2005; Kelly & Price, 2005). This statistical phenomenon occurs if phenotypic measurements of predictor variables imperfectly reflect relevant

biological quantities. This problem has been implied in the context of IPMs (Chevin, 2015), and it is likely to be very general. A theoretical analysis of development functions in IPMs may help to determine the scope of the problem, and suggest potential solutions.

In age-size-structured IPMs, size-dependent transition functions of the fundamental demographic processes are used to project size distribution from one age to the next, and across generations. The inheritance function has been defined as an association between the phenotype of the offspring as newborns or juveniles and that of the parents at the time the offspring was produced (Coulson et al., 2010; Schindler et al., 2013; Traill et al., 2014; Bassar et al., 2016). Essentially, it is a cross-age parent-offspring regression, which is a peculiar measure of resemblance. The concept of biometric heritability, outside of the IPM framework, is defined by comparing parent and offspring at the same age (e.g. Galton, 1886). In fact, no theory exists for this concept of heritability as used in IPMs. Body size, commonly the focal trait in IPMs, is typically a dynamic trait - in opposition to static, as defined by Vindenes & Langangen (2015) - and therefore its value at a certain age is the result of the accumulation of growth until that age, causing differences among individuals to accumulate over the ontogeny due to environmental and genetic variation in size trajectories (Chevin, 2015). Genes are inherited, or as put by Simpson (1944, p. 30), "what is inherited is a complex of potentialities for development", not the phenotypes (or functions of phenotypes) resulting from development. As such, parental phenotype (as an adult) is an imperfect predictor of the adult's (genetic) contribution to the phenotype of the offspring. In effect, a phenotype at a given age is generally an imperfect measure of genetic value for phenotype at any age. As a consequence, regression to the mean occurs and results in the underestimation of resemblance between parents and their offspring, and therefore of the genetic contribution to phenotypic change (Chevin, 2015).

In this chapter, I construct simple but realistic models of development and inheritance. For both processes, I construct corresponding models of how conventional IPMs will use data on size-at-age of relatives, and what across-age and across-generation population structure in continuous traits IPMs can recover. Aspects of the distribution of traits through time, other than over single iteration steps (in size-dependent development and inheritance functions), are not used to parameterise IPMs. Also, the way IPMs are typically iterated means that once the population structure at time $t+1$ is generated, the state of the population at time t is discarded. Consequently, while IPMs owe their generality to tracking the distribution of phenotype through time, they do not output aspects of the population structure that allow their performance to be checked. Critically, aspects of the distribution of traits across time for any inference, particularly evolutionary inference, requires that correlations of individual trait values across ages, and of trait values of relatives across generations, are adequately reflected.

I use path analysis to generate analytical expressions that isolate growth and inheritance in IPMs, providing insight into their behaviour in structuring populations. These exercises demonstrate that typical parameterisations of IPMs generally recover only a small fraction of similarity within individuals across ages, and that IPMs recover only a small fraction of similarity between relatives. These patterns have severe consequences for evolutionary inference with IPMs. I discuss potential solutions that may prove useful in fully realising the potential of IPMs. I give an empirical example where I use random regression of developmental trajectories to develop a quantitative genetic analysis to model variation in mass in a pedigreed wild population of bighorn sheep (*Ovis canadensis*). I compare this

analysis to the inheritance function based on the cross-age parent-offspring regression and standard regression methods for growth functions normally implemented into IPMs. I show a large difference between the two parameterisations in the ability to capture similarity within individuals across ages, which results in standard regression methods normally used in IPMs not capturing the across-age structure in growth. Similar conclusions are reached across generations, with most similarity among relatives being missed by IPMs, corresponding to a failure of the typical IPM inheritance function to predict evolution.

4.2 Development

Regression to the mean is particularly relevant to IPMs due to how size-dependent growth coefficients are typically - although not necessarily - estimated. Transition rates between size classes for surviving individuals are modelled by regressing observed size at age $a + 1$ on observed size at age a, observed size being therefore a predictor. Either linear models (e.g. Childs et al., 2003; Coulson et al., 2010), or extensions of such models, including generalised linear or additive (mixed) models and nonlinear models (e.g. Ozgul et al., 2010; Rees et al., 2014; Traill et al., 2014) have been used for this purpose. All these methods assume that predictors are measured without error. When this assumption is violated, downwardly biased estimates are obtained (for a review on problems and proposed models to deal with measurement error see Thompson & Carter, 2007). Measurements of most traits, including size, will virtually always be made with non-trivial error, for two reasons. First, limitations in the measurement process caused by different measuring conditions (e.g. different levels of stomach fill when measuring the mass of a sheep), or limitations of instruments used for measurement, tend to occur. Second, size, like most other variables of ecological interest, is an abstract concept and therefore is not directly measurable. As such, proxy variables that do not perfectly represent size are measured instead, such as mass or some skeletal measure. The complexity of *size* is such that the covariation between any proxy at time t and $t + 1$ is also determined by the other components of size, which are highly correlated with each other. Importantly, the mechanics underlying IPMs neither imply measurement error nor regression to the mean. Rather, the application of standard regression methods that do not account for measurement error within an autoregressive structure on size (subsequent sizes being used as predictors) promotes the occurrence of regression to the mean due to measurement error.

As the measurement error that causes regression to the mean is random rather than systematic, this problem can be modelled by thinking of true size, the trait we want to measure, as a latent variable, z, that cannot be measured (e.g. McArdle, 2009; Little, 2013, p. 43). In such a scenario, instead of the true values z, a proxy, the trait we actually measure, x, is recorded, which differs from z by a measurement error, σ^2_ϵ, and is related to it by a repeatability, r^2. x can, therefore, be written as $x = z + \sigma^2_\epsilon$. In Figure 4.1a, I illustrate such model of the ontogenetic development of size, which I named *latent true size model*, using a path diagram. In this diagram, true size at age 1, z_1, determines true size at age 2, z_2. z_2 is then a predictor of true size at age 3, z_3, and so on until size at age n, z_n, is predicted. In contrast, the kinds of regression analyses implemented to date in IPMs (e.g. Childs et al., 2003; Coulson et al., 2010; Ozgul et al., 2010; Rees et al., 2014; Traill et al., 2014) assume that true size z is being measured when in fact the measured variable is x. This model, which I termed

observed size model, is illustrated in Figure 4.1b. The autoregressive structure in this model is very similar to that in Figure 4.1a, but is built on observed sizes rather than true ones. I use the theoretical models in Figure 4.1 to illustrate the consequences of this conceptual mismatch and to inspect how regression to the mean affects inference about development. I show that the correlations, and therefore the regression coefficients, estimated using IPMs do not correspond to the true latent ones. I then derive a generic analytical expression for how much correlation an IPM can recover given a certain repeatability and number of projection steps (number of IPM iterations).

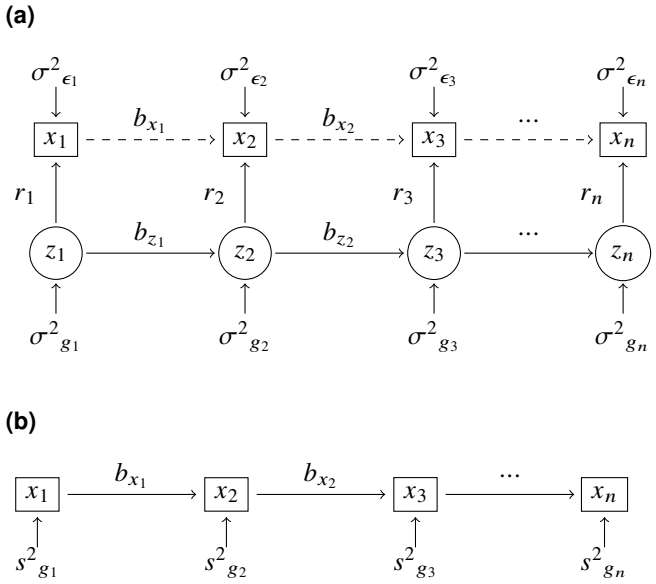

Figure 4.1: Path diagrams illustrating the ontogenetic development of size. **(a)** Latent true size model; **(b)** Observed size model implemented into IPMs. z_a and x_a are, respectively, the true and observed sizes at age a. r_a, linking true and observed sizes, are defined such that repeatabilities are r_a^2. In these antedependence models, $\sigma^2_{g_a}$ and $s^2_{g_a}$ are exogenous variances in growth for true and observed values, respectively, except when they refer to $a = 1$. In this case, $\sigma^2_{g_1}$ and $s^2_{g_1}$ also correspond to variances in size. $\sigma^2_{\epsilon_a}$ are exogenous errors associated with observed sizes. b_{z_a} and b_{x_a} are growth regressions (path coefficients) for true and observed values, respectively. Dashed lines, as opposed to solid lines, do not belong in the path diagram. Although b_{xa} correspond to the same quantities in both models, the two models result in covariance structures that are very different (see Appendix B.1.1).

If we consider linear size-dependent growth functions, we can express the true biometric relationships (i.e. true theoretical expressions) among traits z (e.g. size at different ages), as well as the relationships captured by standard regression methods typically used in IPMs to describe development, using the principles of path analysis (McArdle & McDonald, 1984). Developed by Wright (1921, 1934) for estimating causal path coefficients, path analysis mathematically decomposes correlations (or covariances) among the variables in a path diagram. For convenience, in the path diagrams that I show I assume that all variables are standardised (mean centred and variance of 1). In such circumstances, the expected correlation between two variables is the product of the standardised path coefficients that link them. Some notational details are worth summarising: σ denotes several aspects of true covariation (covariance in growth among ages), whereas σ^2 represents true variances. Variances estimated by IPMs are denoted by s^2. Since the models in Figure 4.1 are antedependence

models (or autoregressive, as the response variable depends on itself at a previous time), σ_g^2 in Figure 4.1a and s_g^2 in Figure 4.1b correspond to variances in growth associated with the regressions of true size on true size at a previous time and observed size on observed size at a previous time, respectively. Finally, the path coefficients b correspond to regressions of size on size and r^2 to the square of the regression coefficient of observed size at age a, x_a, on true size at the same age, z_a. Following the principles of path analysis, I used a variance-covariance matrix with the variances in growth, ${\sigma^2}_{g_a}$, and errors associated with observed sizes, ${\sigma^2}_{\epsilon_a}$, for each age a, and a matrix with path coefficients ($b_{z\,a}$ and r_a) matching Figure 4.1a to obtain a variance-covariance matrix for sizes at different ages (Appendix B.1.1). From this matrix, I then extracted the covariances among ages for both true and observed sizes (Tab. B.2.1 in Appendix B.2). As an example, according to the path rules, the correlation and covariance in true size between ages 1 and 3 are given by $b_{z\,1} \cdot b_{z\,2}$ and ${\sigma^2}_{g_1} \cdot b_{z\,1} \cdot b_{z\,2}$, respectively. Analogous quantities were obtained similarly for IPMs (Tab. B.2.2 in Appendix B.2). Since regressions of observed size on observed size, b_{x_a}, are estimated from the data (rather than implied), these quantities are necessarily recovered correctly, and therefore the b_{x_a} estimated in IPMs (Fig. 4.1b) are equivalent to the analogous quantities in Figure 4.1a. In contrast, variances in growth estimated with observed sizes, ${s^2}_{g_a}$, do not correspond to variances in growth estimated with true latent sizes, $\sigma^2_{g_a}$, nor to the measurement error associated with observed sizes, $\sigma^2_{\epsilon a}$. Consequently, since these quantities are crucial to estimate covariances in size among ages, the across-age distribution of phenotype that occurs in a typically-constructed IPM does not generally recover the across-age distribution of either a measured aspect of phenotype (e.g. correlations in the x variable across ages) or of an underlying quantity (e.g. correlations in the z variable across ages). An across-age distribution of phenotype, which includes correlations among ages, is not typically tracked by an IPM (e.g. Childs et al., 2003; Ellner & Rees, 2006; Coulson et al., 2010; Ozgul et al., 2010). Yet, an IPM's utility for any ecological and evolutionary inference depends on its ability to track this distribution through time. In a typical implementation, the distribution of phenotype at age $a-1$ is discarded once the distribution at age a is generated, so such correlations cannot easily be outputted and checked against data. As such, I use path analysis to mimic basic IPM mechanics and to extract the across-age dynamics that are not otherwise easily tracked. In contrast, an IPM can easily be interrogated for the distribution of phenotype at any given time. These distributions generally closely match data (Ozgul et al., 2010; Childs et al., 2011, also see fig3(a) in Chevin, 2015 for a simulation example).

For tractability, I demonstrate that IPMs do not in general recover the across-age structure of phenotype using a simplified case of the path diagram in Figure 4.1a as the true model. Specifically, I focus on a static trait, as it renders the basic principles more clearly without loss of generality. I assume that all size-dependent growth coefficients are one ($b_{z_a} = 1, \forall a$), that the variance in true growth at age one - which also corresponds to the variance in true size at age one - is one (${\sigma^2}_{g_1} = 1$) and that the subsequent variances are zero (${\sigma^2}_{g_a} = 0, \forall a > 1$). Finally, all repeatabilities, r_a, and measurement errors, ${\sigma^2}_{\epsilon_a}$, take the same value, r and $1 - r^2$, respectively. Applying the path rules and these assumptions results in the particular case of all true phenotypic variances and covariances being 1 and variances and covariances for phenotypic observed size being 1 and r^2, respectively (see Appendix B.1.1 for details). Standard regression methods typically used in IPMs underestimate regressions for true growth in any instance where $r < 1$, by a factor of r^2. Whenever true and observed sizes differ, which is true for virtually every attempt to measure size, instead of 1 (value set for all b_{z_a}), b_{x_a} take the value r^2 for any consecutive pair of ages (both in Fig. 4.1a and Fig. 4.1b). As mentioned

before, covariances in size across ages are in general not reported when building an IPM. However, the implied covariances can be calculated using path analysis (see Appendix B.1.1 for both the general and the simplified cases). Since that according to the path rules of standardised variables correlations between two variables correspond to the product of the path coefficients linking them, in this example correlations in size among two ages will be r^2 to a power equivalent to the number of links between them. As such, since $r < 1$, these correlations will be underestimated. As for the covariances, these are obtained by multiplying the correlations by the variance in growth at age 1, which corresponds to the variance in growth at age one, s_{g_1}. Variances in size are well recovered in IPMs because these quantities are directly estimated from the data. Therefore, in this example, s_{g_1}, which also corresponds to variance in size at age one, corresponds to one, resulting in covariances in size implied by the growth functions normally implemented in IPMs being given by

$$cov_{IPM}(x_i, x_j) = \left(r^2\right)^{\Delta\ell}, \tag{4.1}$$

where $\Delta\ell$ is the number of projection steps (or path coefficients) connecting ages i and j $(j - i)$.

The standardised conditions set in this simplified example illuminate how much correlation between sizes at different ages the standard IPM formulation will miss. As true correlations (or covariances) in size across ages were set to one, subtracting the correlation in Equation (4.1) to that theoretical value corresponds to the amount of correlation a standard regression fails to recover,

$$\text{missed correlation} = 1 - \left(r^2\right)^{\Delta\ell}. \tag{4.2}$$

The theoretical result of Equation (4.2) shown in Figure 4.2 demonstrates that this quantity is far from negligible, increasing rapidly with the number of projection steps and decreasing values of r.

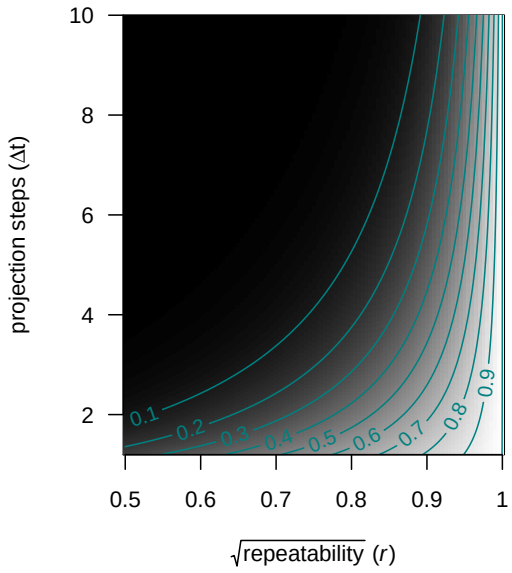

Figure 4.2: Proportion of correlation in size among ages recovered by a typically-built IPM as a function of the square root of the repeatability (r) and number projection steps ($\Delta\ell$). The true values were used as reference.

Many IPM analyses to date have focused on long-lived organisms. In these systems, age differences (projection steps) of 5 to 10 years may correspond to the gap between juvenile stages, which are often subject to the strongest viability selection, and ages of greatest fecundity. Even for traits with high repeatabilities (e.g. $r = 0.9$), correlations over such age differences will be underestimated by more than 60% (Fig. 4.2). Ultimately, size is estimated as an accumulation of growth through an autoregressive process that discards the distribution of size at time $t - 1$ at each iteration (when the distribution at t is obtained). This results in measurement error at each iteration not being accounted for in the next, and therefore the effect of regression to the mean rising with the number of IPM projection steps. Serious consequences can be expected both for evolutionary and ecology studies, whenever differences in individual growth are of interest. Curiously, all else being equal, IPMs with narrower projection intervals (e.g. monthly, rather than yearly) will suffer more from regression to the mean than models constructed with wider projection intervals. Finally, it is important to note that asserting that the observed quantities, rather than underlying variables, are the target of interest in any given IPM application does not solve the fundamental problem. In any scenario where the covariance of observed values through time is caused (in part or in whole) by quantities other than the observed values themselves (Fig. 4.1a) a model of sequential regressions of observed values on one another (Fig. 4.1b) will not recover the resulting covariance structure.

4.3 Inheritance

The modern understanding of how genes contribute to similarity among relatives (Fisher, 1918, 1930; Wright, 1922, 1931) has a very different structure from the inheritance function typically included in IPMs (e.g. Coulson et al., 2010; Traill et al., 2014; Bassar et al., 2016). Fisher and Wright showed how Mendelian inheritance at many loci influencing a trait generates the observed biometric relationships among relatives, including the relationships of a quantitative character between parents and offspring. Here, I use the basic mechanics of inheritance of a polygenic trait, which have well-known relationships to selection and evolution (Lynch & Walsh, 2018), and use it as simple background to see if IPM mechanics are generalisations of these principles. The notion of breeding value, or genetic merit, of an individual is central to the current theory of the inheritance of quantitative traits, and has its roots in Fisher's (1918) and Bulmer's (1980) infinitesimal model (see Falconer, 1981; Lynch & Walsh, 2018, Chapter 15). Each parent passes half of its genes and therefore half of its breeding value on to the offspring. As such, the expected breeding value of offspring i, $\mathbb{E}[BV_i]$, corresponds to half the sum of parental breeding values, as follows

$$\mathbb{E}[BV_i] = \frac{(BV_{m_i} + BV_{f_i})}{2}, \tag{4.3}$$

where BV_{m_i} and BV_{f_i} are the maternal and paternal breeding values, respectively. The true breeding value, BV_i, follows a normal distribution,

$$BV_i \sim \mathcal{N}(\mathbb{E}[BV_i], \frac{\sigma^2_{\mathscr{A}}}{2}), \tag{4.4}$$

with its expected value as mean and $\frac{\sigma^2_{\mathscr{A}}}{2}$ as variance, corresponding to the variance in breeding values in the absence of inbreeding, conditional on mid-parent breeding values, resulting from seg-

regation (Bulmer, 1980). The variance in the breeding values divided by the phenotypic variance is defined as heritability, h^2, a measure of evolutionary potential. The degree of resemblance between relatives provides the means for distinguishing the different sources of phenotypic variation and therefore for estimating heritabilities and other quantitative genetic parameters (Falconer, 1981). The simplest way of doing so is by using correlations of close kin, for example, of parents and their offspring, as h^2 corresponds to the slope of the offspring trait regressed on the midparent's (Lynch & Walsh, 1998, Chapter 7). In fact, Jacquard (1983) defines the heritability estimated with a parent-offspring regression as a biometric heritability, as opposed to broad- and narrow-sense heritabilities, for which the genetic and additive genetic variances are, respectively, explicitly estimated. Any genetic architecture, i.e. broad- and narrow-sense heritability, determines the biometric relationships among kin (Lynch & Walsh, 1998, Table 7.2). In IPMs, heritabilities have been estimated using parent-offspring regressions. Specifically, inheritance has been defined as a regression of the phenotype of the offspring as newborns or juveniles on that of the parents at the time the offspring was produced (Coulson et al., 2010; Schindler et al., 2013; Traill et al., 2014; Bassar et al., 2016). In this section, I investigate whether this cross-age biometric notion of inheritance is compatible with what is known about trait transmission across generations.

4.3.1 Inheritance across generations

I start by addressing consequences of regression to the mean related to the biometric concept of inheritance when applied across multiple generations. I define a true model for trait transmission across four generations of the same age, according to Fisher's and Wright's understanding of trait transmission (Fig. 4.3a), and a comparable model reflecting the biometric concept of inheritance typically used in IPMs (Fig. 4.3b). As for the development models, I used path diagrams and path analysis to compare the correlations implied by both models. In Figure 4.3a, breeding values, the underlying units that are inherited, are passed on across generations: from great-grandparents to grandparents, from grandparents to parents, and from these to the offspring. Since each parent passes on half its breeding value to the next generation, the regression coefficient linking generations is $\frac{1}{2}$. The variance associated with the breeding values is $\frac{3}{4}$, which corresponds to $\frac{1}{2}$ from the other parent and $\frac{1}{4}$ from segregation. h corresponds to the correlation between the breeding values and phenotypic values (Wright, 1921; Falconer, 1981) and, in a standardised path analysis, to the corresponding regression coefficient as well. If observed size is standardised (variance of 1), then according to the path rules its exogenous variance corresponds to $1 - h^2$. Finally, if any regression was to be made between the observed sizes, x, the coefficient would be half the heritability. There is a close analogy with the path diagrams in Figure 4.3a and Figure 4.1a. Not only do they share the same structure (sizes at different generations instead of sizes at different ages), but other analogies can be taken. For example, as the regression coefficient of phenotype on breeding values, the square root of the heritability expresses the reliability of the phenotype to represent the underlying genetics, which in Figure 4.1a was represented by the square root of the repeatability. In Figure 4.3b I show a series of parent-offspring regressions based on phenotype, rather than genetics. The slope of the parent-offspring regression for a single parent is known to be $\frac{1}{2}h^2$ and in a standardised path analysis, the associated variance is $1 - \frac{1}{4}h^4$. Similarly, the path diagram in Figure 4.3b relates to the one in Figure 4.1b.

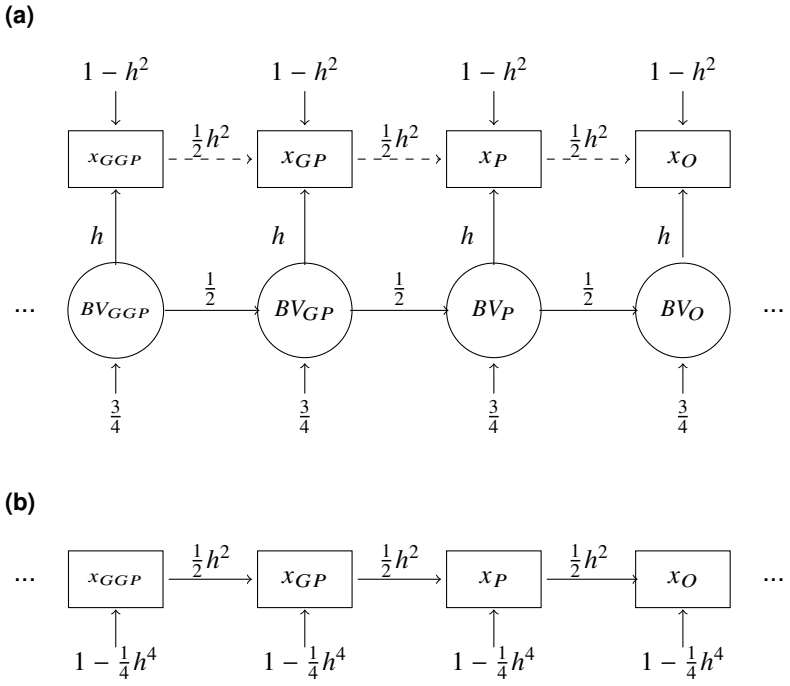

Figure 4.3: Path diagrams illustrating the transmission of a quantitative trait across generations of the same age. **(a)** Model based on the fundamentals of quantitative genetics; **(b)** model corresponding to a purely biometric notion of inheritance. BV and x correspond to breeding values and the observed phenotype, respectively. The exogenous inputs to BVs include contributions from the other parent and segregation. The subscripts GGP, GP, P and O denote great-grandparent, grandparent, parent and offspring, respectively. h^2 corresponds to the heritability and therefore h and h^4 to its square root and square, respectively. Dashed lines, as opposed to solid lines, do not belong in the path diagram. While the observed parts of the two models look very similar, they imply different correlation structures among relatives more than one generation apart (see main text).

With this single age set up, I can isolate the regression to the mean that occurs as a result of a purely biometric approach to the inheritance function. As for the true regressions, parent-, grandparent-, great-grandparent-offspring regressions are given by $\frac{1}{2}h^2$, $\frac{1}{4}h^2$, $\frac{1}{8}h^2$, respectively (Lynch & Walsh, 1998). The extension for arbitrary ancestral regressions is given by

$$\beta_{\Delta_{\mathscr{g}}} = \frac{1}{2^{\Delta_{\mathscr{g}}}}h^2, \tag{4.5}$$

where $\Delta_{\mathscr{g}}$ is number of generations between two relatives. I used path analysis to obtain the analogous regressions that are implied when applying a biometric inheritance function repeatedly within an autoregressive process (Fig. 4.3b). The structure of the path diagrams in Figures 4.1b and 4.3b are equivalent and therefore the reasoning for obtaining covariances and regressions for size presented in Appendix B.1.1 also applies in this case. As such, according to the path rules, IPMs, as usually parameterised, will estimate these regressions as

$$\beta_{\Delta_{\mathscr{g}}IPM} = \left(\frac{1}{2}h^2\right)^{\Delta_{\mathscr{g}}}, \tag{4.6}$$

which does not correspond to Equation (4.5). As an example, tracing the regression of grand-

offspring size (x_O) on grandparent size (x_{GP}) in this standardised path diagram involves two paths with coefficient $\frac{1}{2}h^2$, resulting in $\frac{1}{4}(h^2)^2$ instead of the true regression $\frac{1}{4}h^2$. Equation (4.6) implies that trait transmission between same-age relatives is not fully recovered when the gap between generations ($\Delta_{\mathscr{g}}$) is greater than one. For ancestral regressions other than of offspring on parent to be correctly recovered the heritability of this trait would have to be one, which tends not to happen in nature for most ecologically interesting traits. The proportion of the true regressions recovered by the biometric inheritance function is given by $h^{2(\Delta_{\mathscr{g}}-1)}$, as illustrated in Figure 4.4. For example, if a trait has a heritability of 25%, the grandparent-grandoffspring regression will be estimated as $\frac{1}{4}h^4 = \frac{1}{64}$ rather than its true value of $\frac{1}{4}h^2 = \frac{1}{16}$, which corresponds to only recovering 25% of the regression. This proportion drops to 6.25% for great-grandparents and their offspring.

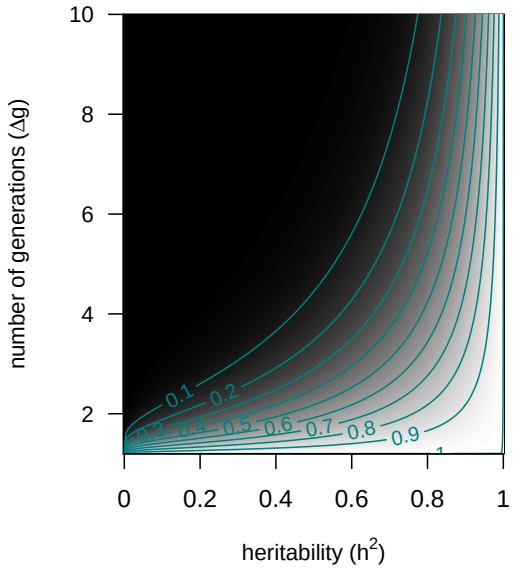

Figure 4.4: Proportion of the parent-offspring regression recovered by a same-age inheritance function as a function of the heritability (h^2) and the number of generations ($\Delta_{\mathscr{g}}$). The true values were used as reference.

4.3.2 Across-age inheritance functions

There is a second mechanism by which regression to the mean affects inference with the inheritance function, particularly resulting from its cross-age structure. It is important to note that although an individual's genetic constitution is constant throughout life, the genetic variants relevant at one life stage need not affect other life stages. Genetic variants acting late in life may be latent early in development. Such variants may be inherited and contribute to similarity among relatives, even if they contribute neither to covariance of traits within individuals, through time, nor to covariance of parents, as adults, with their offspring, at young, or arbitrary, life stages. Consequently, there is potential for the concept of inheritance applied to date in IPMs to neglect a major fraction of how genetic variation can generate similarity among relatives (Hedrick et al., 2014; Chevin, 2015). Chevin (2015) illustrated this issue with numerical demonstrations. Here I formalise his findings analytically to explore the generality and the magnitude of his conclusions. I examine what would happen to two cohorts (parents and offspring) with two ontogenetic stages (juvenile, J, and adult, A, Figure 4.5). I choose a

simple model with only two ontogenetic stages, since extending it to include more age classes would correspond exactly to what was described for development in the previous section. I explore two different perspectives of trait transmission - first using basic quantitative genetic principles and then a cross-age biometric approach typical of IPMs. The first path diagram (Fig. 4.5a) reflects the former, with phenotype being a result of the breeding values, BV, and the environment, $\sigma_e{}^2$. To account for the fact that different genes may influence different traits or the same traits across ages, I use different symbols for breeding values in the juvenile and adult stages. In this path diagram, parent phenotype as a juvenile determines parent phenotype as an adult through the regression coefficient b. I also represent segregation and mating, through which the offspring receives paternal breeding values that, together with the environment, define offspring phenotype as juveniles, O_J. Finally, offspring phenotype as juvenile also determines its phenotype as an adult, O_A. I use the subscripts z, a and e to distinguish between phenotypic variance, σ^2, and covariance, σ, and their additive genetic and environmental components, respectively. The diagram in Figure 4.5b illustrates a cross-age phenotypic transmission between parents and offspring normally used in IPMs (e.g. Coulson et al., 2010; Traill et al., 2014; Bassar et al., 2016). In this diagram, parent phenotype as a juvenile determines parent phenotype as an adult (through the regression coefficient for development, b_{dev}), which determines offspring phenotype as a juvenile (through the regression coefficient for inheritance, b_{inh}). Finally, growth also occurs in the offspring, resulting in its adult stage. As before, I consider linear size-dependent growth functions, and additive genetic effects on juvenile size and subsequent growth, so that path analysis can be used to obtain the biometric relationships among traits (true theoretical expressions), as well as the relationships captured by the cross-age inheritance function implemented in IPMs (see Appendix B.1.2 for details).

First, I defined true hypothetical additive genetic and environmental variance-covariance matrices for growth at each age, as well as true path coefficients that match the path diagram in Figure 4.5a. Subsequently, I used path analysis to obtain the true phenotypic variance-covariance matrix for size, a matrix that quantifies both direct and indirect effects of size at each age. Finally, the slopes of the regressions of offspring size on parent size were obtained analytically from the model, corresponding to the true parent-offspring regressions for both juveniles,

$$\beta_{O_J,P_J} = \frac{1}{2}\frac{\sigma^2_{a\,J}}{\sigma^2_{z\,J}} = \frac{1}{2}h^2_J, \tag{4.7}$$

and adults,

$$\beta_{O_A,P_A} = \frac{1}{2}\frac{\sigma^2_{a\,J}b^2 + 2\sigma_{a_{J,A}}b + \sigma^2_{a\,A}}{\sigma^2_{z\,J}b^2 + 2\sigma_{z_{J,A}}b + \sigma^2_{z\,A}} = \frac{1}{2}h^2_A. \tag{4.8}$$

Note that the numerator and denominator in Equation (4.8) are simply reconstructions of the additive genetic and phenotypic variances in size, respectively, given the additive genetic and phenotypic variances in juvenile size, growth to adult size, and the covariance between them. Two other expressions are required, as they are used in constructing IPMs, namely for the regression of adult offspring size on juvenile offspring size, or adult parent size on juvenile parent size,

$$\beta_{O_A,O_J} = \beta_{P_A,P_J} = \beta_{A,J} = \frac{\sigma^2_{z\,J}b + \sigma_{z_{J,A}}}{\sigma^2_{z\,J}}, \tag{4.9}$$

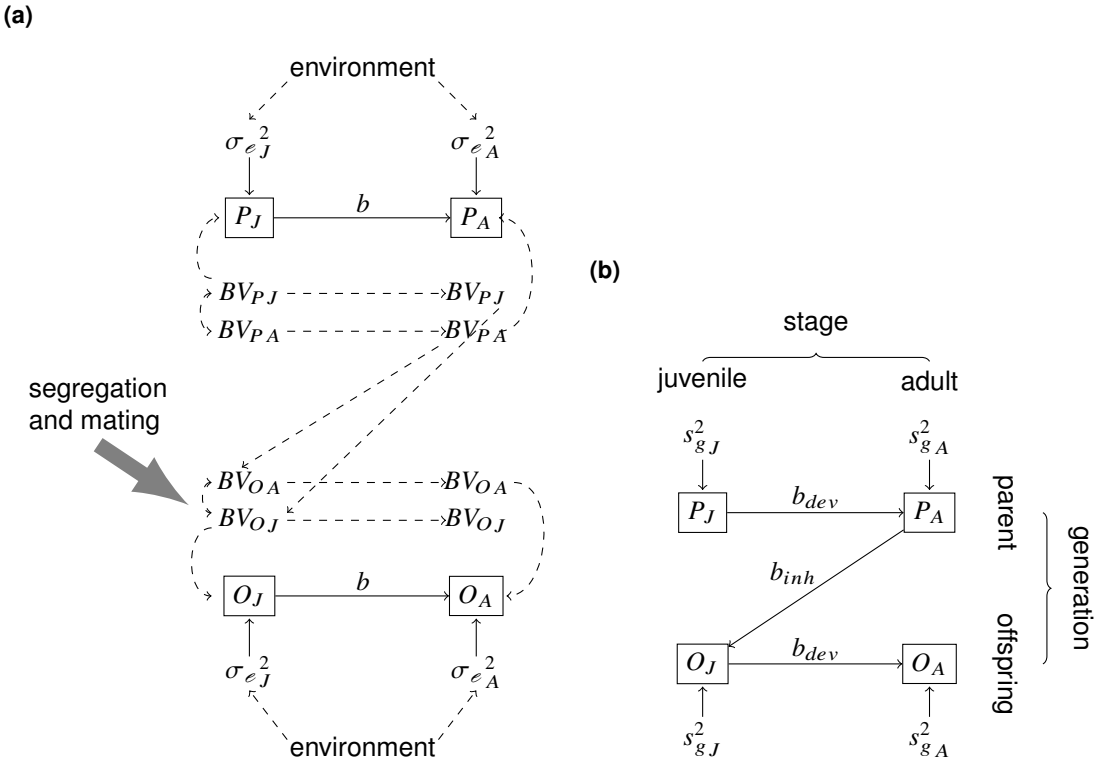

Figure 4.5: Path diagrams illustrating the transmission of a quantitative trait between parents, P, and offspring, O, with two ontogenic stages, juvenile, J, and adult, A. **(a)** Model based on the fundamentals of quantitative genetics; **(b)** model corresponding to a cross-age concept of trait transmission. P_J and P_A correspond to parental trait as juvenile and adult, respectively, and likewise for the offspring (O_J and O_A). σ^2_e and s^2_g correspond to the exogenous variances of size at birth, and of growth until the juvenile stage ($\sigma^2_{e\,J}$ and $s^2_{g\,J}$) and of growth ($\sigma^2_{e\,A}$ and $s^2_{g\,A}$). b, b_{dev} and b_{inh} correspond to regressions, namely for development (b and b_{dev}) and inheritance (b_{inh}). Finally, BV are breeding values. Although the genetic constitution is constant over an individual's life, different genes are activated throughout life, which is denoted by distinguishing BV for both juvenile and adult stages.

which models the ontogenetic development of size, and for the regression of juvenile offspring size on adult parent size,

$$\beta_{O_J,P_A} = \frac{1}{2}\frac{\sigma^2_{a\,J}b + \sigma_{a\,J,A}}{\sigma^2_{z\,J}b^2 + 2\sigma_{z\,J,A}b + \sigma^2_{z\,A}}, \tag{4.10}$$

which corresponds to the cross-age inheritance function.

As shown in Figure 4.5b, typical IPMs adopt β_{O_J,P_A} (b_{inh}) as the inheritance function. I use the path rules to obtain the covariances among same-age parent and offspring that are implied by this quantity, and therefore to obtain expressions for the same-age parent-offspring slopes. In practice, I then compare the theoretical results presented above, in particular the true parent-offspring regressions in Equations (4.7) and (4.8), to those that occur with the cross-age inheritance function, allowing us to derive the conditions under which IPMs recover the population structure of continuous traits between parents and offspring. According to the path rules, IPM-based inference for parent-offspring regression at both juvenile and adult stages, β_{O_J,P_J} and β_{O_A,P_A}, respectively, corresponds to the

product of $\beta_{J,A}$ (Eqn. 4.9) and β_{O_J,P_A} (Eqn. 4.10, see Appendix B.1.2 for details), as follows

$$\frac{1}{2}h^2_{(IPM)} = \beta_{O_J,P_{J(IPM)}} = \beta_{O_A,P_{A(IPM)}} = \frac{1}{2}\frac{\sigma^2_{z_J}b + \sigma_{z_{J,A}}}{\sigma^2_{z_J}}\frac{\sigma^2_{\mathscr{a}_J}b + \sigma_{\mathscr{a}_{J,A}}}{\sigma^2_{z_J}b^2 + 2\sigma_{z_{J,A}}b + \sigma^2_{z_A}}. \tag{4.11}$$

As a result, in a two-stage case, an IPM as typically built implies the same value of the parent-offspring regression for both stages, which is not the case for the true values (Eqn. 4.7 and Eqn. 4.8). Also, and even more importantly, the IPM-based inference corresponding to the expression in equation (4.11) does not correspond to the true values for either age (Eqn 4.7 and Eqn. 4.8). Thus, IPMs do not, in general, recover parent-offspring regressions.

The comparison between IPM-based inference and true values becomes more straightforward in the simplified case of no covariances of growth across ontogenetic stages (additive genetic, $\sigma_{\mathscr{a}_{J,A}}$, and more generally, phenotypic, $\sigma_{z_{J,A}}$). In such circumstances, the IPM implies a parent-offspring regression, for both juveniles and adults, of

$$\frac{1}{2}h^2_{(IPM)} = \beta_{O_J,P_{J(IPM)}} = \beta_{O_A,P_{A(IPM)}} = \frac{1}{2}\frac{\sigma^2_{\mathscr{a}_J}b^2}{\sigma^2_{z_J}b^2 + \sigma^2_{z_A}}, \tag{4.12}$$

which is always less than the corresponding true values. This is a best-case scenario for IPMs, as covariances of growth across ages are in general not modelled when estimating size transitions in such models. Even in such unrealistic conditions, a standard IPM can only recover the true parent-offspring regressions under very specific conditions. According to Equation (4.12), for parent-offspring regression in juveniles to be fully recovered by a model using a cross-age biometric inheritance function, the phenotypic variance in growth, $\sigma^2_{z_A}$, must be zero. When that is not the case, the proportion of regression recovered decreases with decreasing size-dependent size regression, b (Eqn. 4.7, Fig. 4.6a). The same condition holds for the parent-offspring regression in adults (Eqn. 4.8, Fig. 4.6b). These quite narrow conditions are unlikely to occur in nature. I obtained similar results for the case where covariance in growth exists (Appendix B.2). Indeed, although IPMs were developed to model dynamic traits, the conditions for which they are guaranteed to recover parent-offspring regression, particularly the absence of variance in growth, essentially constrain a dynamic trait to be static.

4.3.3 Parent-offspring regression with a constant intercept

The preceding analysis shows that regression to the mean prevents the inheritance function from capturing most aspects of covariance between individuals and their descendants. In language typically used to describe properties of IPMs, a cross-age biometric inheritance function does not fully capture the most important ways in which inheritance influences the dynamics of a population through time. Importantly, however, as shown above, the biometric inheritance notion does capture the correct covariance of parents and offspring, at least of a static trait (or a model with a single age class). In itself, this may imply that a purely biometric notion of inheritance can be used, at least in simple cases, to track some important features of a population. Nonetheless, the use of the concept of biometric inheritance that is extensively recommended for IPMs (Coulson et al., 2010; Coulson, 2012; Rees et al., 2014) does not correctly employ the concept. This recommendation is based on two misconceptions

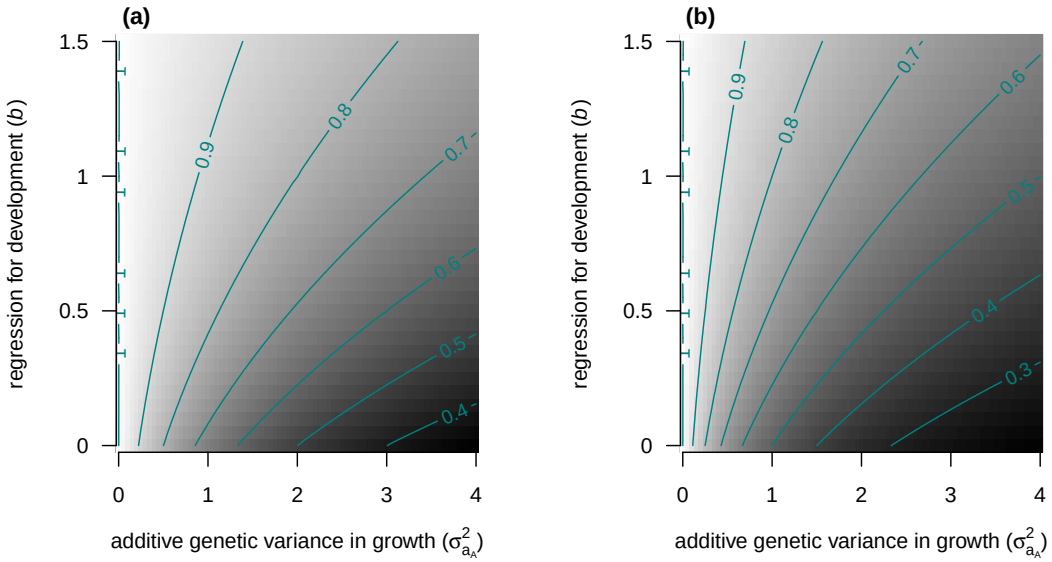

Figure 4.6: Proportion of parent-offspring regression recovered by a cross-age parent-offspring regression, in juveniles, **(a)**, and adults, **(b)**. In both cases, correlation in growth, genetic ($\sigma_{a_{J,A}}$) and environmental ($\sigma_{e_{J,A}}$), was assumed to not exist, and the remaining parameters were set as follows $\sigma^2_{a_J} = 1$, $\sigma^2_{e_J} = 1$, and $\sigma^2_{e_A} = 0$. The true values were used as reference in both plots.

about biometric inheritance, both of which lead to failures to characterise even the simplest aspects of phenotype (e.g. the dynamic of mean phenotype). The first misconception, shown above, is the assumption that theory underlying the biometric relations among kin can be applied to a non-static trait when parents and offspring are of different ages. This includes the assumption that iteration of the purely phenotypic relations of parents and offspring across multiple generations can recover biometric relationships among more distant kin, e.g. arbitrary ancestral regressions. The second misconception is that the biometric inheritance concept, and its known relationships to quantitative genetic parameters (Lynch & Walsh, 1998, Chapter 7), implies that biometric functions are constant. A constant genetic basis (e.g. an assumption that h^2 is constant over a period of time) to a trait is commonly assumed in quantitative genetic studies, and implies that the slope of the parent-offspring regression is constant. However, should a trait evolve, changing the mean phenotype, then the intercept of the parent-offspring regression necessarily changes. If the intercept is assumed to not change, or a model is constructed where the intercept cannot change, then the dynamic of mean phenotype will be highly restricted. Therefore, even the simplest possible IPM constructed with a typical inheritance function, which has not only a constant slope, but also a constant intercept, will necessarily fail in describing the evolution of mean phenotype.

As an example, consider a non-age structured population, with no class structure other than that associated with some focal trait, z. I denote the mean trait value in generation g by $\bar{z}_g$ and its heritability as h^2. Without loss of generality, I assume that during a period of equilibrium z is measured such that its mean is 10. I also assumed that z is heritable ($h^2 = 0.5$) but, since there is no selection, no phenotypic change is observed (Fig. 4.7a). Suppose that the equilibrium is then disrupted and that both sexes experience the same selection, which represents a change in mean phenotype for the first generation ($\Delta\bar{z}'_1$) of 1 unit (Fig. 4.7b). The offspring on mid-parent regression is then $\mathbb{E}[z_2] = \alpha + h^2 \frac{z_{1m}+z_{1f}}{2}$, where α is the intercept and z_{1m} and z_{1f} denote maternal and paternal pheno-

types, respectively. An IPM constructed using this regression (appropriately handling the two sexes) yields a mean phenotype in the next generation of $\bar{z}_2 = \int \alpha + h^2 \cdot z \cdot p_1(z)dz = \alpha + h^2 \left(\bar{z}_1 + \Delta\bar{z}'_1\right)$. The first expression corresponds to the integral that would be solved (typically numerically) by an IPM corresponding to this example, and $p_1(z)$ is the probability density function of phenotype after selection but before reproduction in generation 1. The second expression is the analytical solution for this integral, made possible by assuming a linear function. Under the conditions set for this example, this expression would be $\bar{z}_2 = 5 + 0.5 \cdot (10 + 1) = 10.5$. This change satisfies the breeder's equation for the change in mean phenotype across generations $\bar{z}_{i+1} - \bar{z}_i = h^2\Delta\bar{z}'$. The problem arises in the next generation.

Let us suppose that selection is now relaxed, such that the within-generation change in phenotype due to selection, $\Delta\bar{z}'_2$, is zero. In the absence of selection, drift, immigration and mutation, we expect no change in allele frequencies (Wright, 1937) and therefore no evolution. Consequently, we expect no change in mean phenotype (Fig. 4.7c). In a very simple non-age structured IPM, we would use the current distribution of trait values ($\not{z} = 2$) and the same inheritance function to obtain the mean phenotype in generation 3, and that would correspond to $\bar{z}_3 = \int \alpha + h^2 \cdot z \cdot p_2(z)dz = \alpha + h^2\,(\bar{z}_2)$, which in this case would be 10.25 (Fig. 4.7d). In this example, an IPM would predict the trait moving back 0.25 phenotype units, which corresponds to reverting back to half of the initial response to selection. If z_2 is any value other than 10, the static biometric inheritance function results in changes in mean phenotype in the absence of selection, drift, mutation and migration. Continuing the analytical iteration of the mean phenotype in this simple IPM, I show that with each subsequent generation (iteration step, in this simple argument), the mean phenotype regresses further toward a value determined by the nature of the static biometric inheritance function (Fig. 4.7e). If selection is sustained, then the dynamic of the mean phenotype even in this very simple IPM will be wrong, representing a component associated with the response to selection, and a spurious change due to the misconception of biometric inheritance associated with a parent-offspring regression with a fixed intercept. A biometric inheritance function with a constant slope and intercept is inconsistent with evolution.

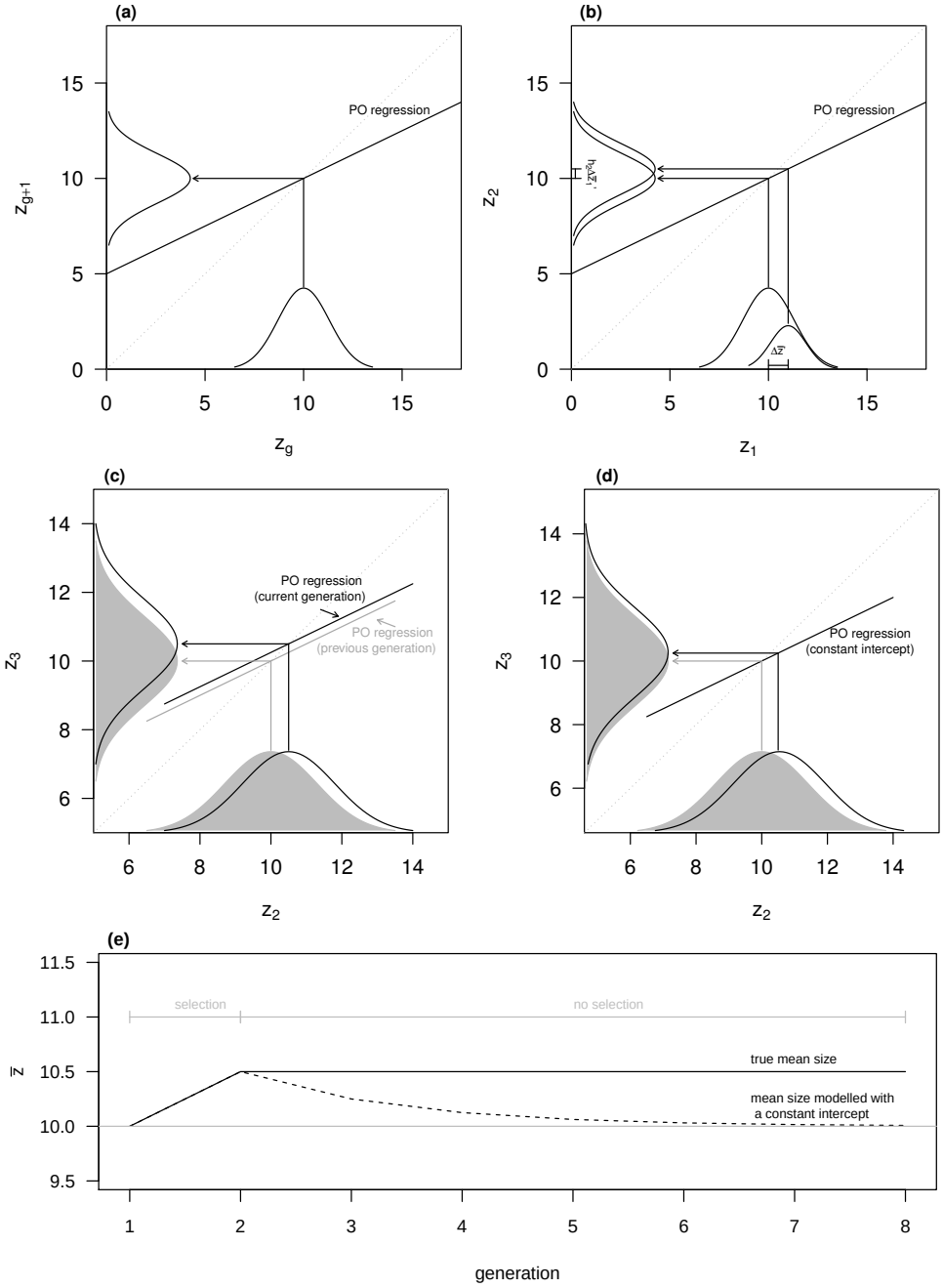

Figure 4.7: The consequences of assuming a constant intercept for the parent-offspring (PO) regression across generations. **(a)** Population at equilibrium, where mean phenotype is 10; **(b)** Period of selection. Selection before reproduction causes mean parental size to change from 10 to 11 ($\Delta\bar{z}'_1 = 1$). Mean offspring phenotype (z_2) is 10.5, which implies a parent-offspring regression given by $\bar{z}_2 = 5 + 0.5 \cdot (\bar{z}_1 + \Delta\bar{z}'_1)$, and therefore $h^2 = 0.5$ and an intercept of 5; **(c)** Relaxed selection. When mean phenotype changes across generations, in this case from 10 to 10.5, the intercept of the parent-offspring regression necessarily changes as well. In a case of no selection in generation 2, the parent-offspring regression is given by $\bar{z}_3 = 5.25 + 0.5 \cdot \bar{z}_2$; **(d)** Relaxed selection with constant intercept. If the intercept is assumed to remain constant, and the first parent-offspring regression is used to estimate the mean phenotype in generation 3 (z_3), instead of the true value 10.5, 10.25 is obtained instead; **(e)** Iteration of mean phenotype to subsequent generations of relaxed selection, both under a model with a genetical notion of inheritance and an analytical iteration of a simple IPM with a biometric inheritance function with a fixed intercept. In **(c)** and **(d)** the distribution in grey corresponds to the previous generation.

4.4 Study case: bighorn sheep

I used a pedigreed population of bighorn sheep from Ram Mountain, Alberta, Canada (52° N, 115° W) to assess the performance of the development and inheritance functions as implemented in standard IPMs. Both quantitative genetic (e.g. Coltman et al., 2003; Wilson et al., 2005) and IPM analyses (Traill et al., 2014) have been conducted for this study system. For detailed information on the study system see Chapter 2. I analysed individual age-specific masses adjusted to September 15 (see Martin & Pelletier, 2011) for 461 ewes captured from 1975 to 2011 and aged up to 10 years (2002 ewe-years). I built two statistical models, one reflecting how the ontogenetic development of size and inheritance have been typically modelled in IPMs, and the other corresponding to a possible alternative to estimating these two key functions, a random regression animal model of body size (Kirkpatrick et al., 1990, 1994; Meyer & Hill, 1997; Meyer, 1998; Wilson et al., 2005). I chose random regression because it is widely used to study the genetics of developmental trajectories and it satisfies a number of criteria, namely: (i) it accommodates across-age covariance, over and above that attributable to measured values of focal traits, (ii) it incorporates the known fundamentals of quantitative genetics, (iii) it is economical in terms of the number of parameters that need to be estimated, and (iv) its basic structure is compatible with IPMs. Criteria (i) and (ii) result in random regression analysis providing an approach for characterising development and inheritance that should be robust to regression to the mean, as imperfectly measured quantities are not used as predictor variables, and as it uses a modern notion of inheritance of quantitative traits. Nonetheless, other options can also avoid regression to the mean, including a formulation of an explicit genetic autoregressive size-dependent model that accounts for measurement error. Also, although the random regression approach, and potentially other models using quantitative genetic approaches characterising variation in phenotype and its inheritance, could profitably be integrated into the broader IPM framework, for simplicity I refer to the former approach as “IPM" and to the latter as “RRM". Both models were fitted in a Bayesian framework, using MCMCglmm (Hadfield, 2010), and diffuse inverse gamma priors for all (co)variance components.

4.4.1 Standard IPM approach

I used a linear model to estimate the development and inheritance functions used in typical IPMs. I modelled observed ewe mass at each age as a function of mass at the previous age, with separate intercepts and slopes for each age. For lambs, I estimated a regression of lamb mass on the mass of their mother two months before conception (previous September). Formally, the model is described as

$$x_{i,a} \sim \mathcal{N}\left(u_a + b_{dev_a} \times I_{adult_i} \times x_{i,a-1} + b_{inh} \times I_{lamb_i} \times mothermass_i, e_{i,a}\right), \tag{4.13}$$

where $x_{i,a}$ is the observed mass of individual i at age a, u_a age-specific intercepts, b_{dev_a} age-specific size slopes and b_{inh} is the inheritance function coefficient. I_{lamb} and I_{adult} are indicator variables for lambs and older individuals, respectively. Finally, e_a are heterogeneous residuals per age. The estimated fixed effects and variance parameters are presented in Table 4.1.

Table 4.1: Coefficients for the IPM standard approach, including regressions of mass at age a on mass at age $a-1$, and of lamb's mass on mother's mass at conception for the bighorn sheep population of Ram Mountain. The values correspond to posterior modes and 95% quantile-based credible intervals.

Age	Intercept	Slope	Residuals
1	17.30 (13.61 - 21.16)	- (- - -)	17.87 (15.63 - 20.80)
2	25.62 (21.41 - 29.63)	0.71 (0.56 - 0.87)	20.66 (17.43 - 25.04)
3	25.91 (21.45 - 30.56)	0.70 (0.59 - 0.79)	17.51 (14.83 - 21.30)
4	35.01 (29.42 - 40.77)	0.51 (0.41 - 0.60)	18.04 (15.15 - 21.98)
5	26.75 (19.78 - 34.07)	0.62 (0.52 - 0.74)	15.13 (12.51 - 18.69)
6	28.04 (19.07 - 36.47)	0.62 (0.49 - 0.75)	17.79 (14.80 - 22.32)
7	28.05 (19.97 - 35.28)	0.62 (0.51 - 0.73)	12.63 (10.35 - 16.17)
8	27.34 (17.14 - 37.05)	0.63 (0.49 - 0.77)	15.04 (12.31 - 19.43)
9	23.04 (13.72 - 32.60)	0.68 (0.55 - 0.81)	11.48 (9.17 - 15.10)
10	20.30 (7.56 - 33.20)	0.72 (0.54 - 0.90)	15.14 (11.83 - 21.05)
Posterior mode and 95% credible interval for the inheritance regression: 0.12 (0.07 - 0.18)			

4.4.2 Random regression of size

To model the family of size-at-age functions in bighorn sheep ewes, its genetic basis, and associated phenotypic and genetic covariances of size across age, I fitted a random regression animal model (Kirkpatrick et al., 1990, 1994; Meyer & Hill, 1997; Meyer, 1998; Wilson et al., 2005) of the form

$$x_{i,a} \sim \mathcal{N}\left(\mu_a + f_1(d_i, n_1, a) + f_2(BV_i, n_2, a), e_{i,a}\right), \tag{4.14}$$

where $x_{i,a}$ is the mass of individual i at age a and μ_a are age specific intercepts. f_1 and f_2 are random regression functions on natural polynomials of order n, for permanent environment effects and additive genetic values, respectively. The permanent environment effect refers to all consistent individual effects other than the additive genetic effect (see Kruuk & Hadfield, 2007). In both f_1 and f_2, n was set to 2, allowing the estimation of random intercepts, slopes, and curvatures. Polynomials were applied to mean-centred and standard deviation-scaled ages to improve convergence. Finally, heterogeneous residuals across ages were estimated ($e_{i,a}$). d and BV, vectors with individual and pedigree values, respectively, were assumed to follow normal distributions, $d \sim \mathcal{N}(\mathbf{0}, \boldsymbol{D})$ and $BV \sim \mathcal{N}(0, \boldsymbol{G} \otimes \boldsymbol{A})$. Both $\boldsymbol{D} = \boldsymbol{I}\sigma_i^2$, where σ_i^2 is the permanent environment effect of individual i, and the additive genetic variance-covariance matrix, $\boldsymbol{G}$, are 3×3 matrices, $\boldsymbol{A}$ is the pedigree-derived additive genetic relatedness matrix, and $\otimes$ denotes a Kronecker product. More information on partitioning phenotypic variance into different components of variation using pedigrees and the animal model is provided by Lynch & Walsh (1998), Kruuk (2004) and Wilson et al. (2010). To obtain the genetic variance-covariance matrix for the 10 ages, the following equation is used

$$\boldsymbol{G_{10}} = \boldsymbol{\Phi G \Phi}^T, \tag{4.15}$$

where $\boldsymbol{G_{10}}$ is the resulting 10×10 genetic matrix, $\boldsymbol{G}$ is the 3×3 genetic matrix estimated by the model and $\boldsymbol{\Phi}$ is a 10×3 matrix with the polynomials evaluated at each age (Kirkpatrick et al., 1990; Meyer, 1998). A 10×10 matrix, $\boldsymbol{D_{10}}$, for individual effects at the 10 ages can be obtained similarly. The estimated fixed effects and variance parameters are presented in Table 4.2.

Table 4.2: Coefficients for the random regression animal model on body mass for the bighorn sheep ewes from Ram Mountain, including age-specific fixed intercepts and residuals (upper part), as well as estimates for the intercept, slope (Age) and curvature (Age^2) of the random effects on breeding values (BV) and permanent environment (d, lower part). The values correspond to posterior modes and 95% quantile-based credible intervals.

Age-specific intercepts and residuals		
Age	Intercept	Residuals
1	25.77 (25.18 - 26.36)	8.19 (4.75 - 11.68)
2	44.22 (43.48 - 44.94)	14.01 (10.83 - 17.23)
3	57.05 (56.26 - 57.83)	16.21 (12.90 - 19.73)
4	63.64 (62.85 - 64.42)	11.45 (8.80 - 14.20)
5	66.76 (65.93 - 67.59)	9.78 (7.41 - 12.32)
6	69.15 (68.29 - 70.03)	10.20 (7.55 - 12.99)
7	70.32 (69.47 - 71.16)	6.84 (4.91 - 8.96)
8	71.09 (70.20 - 71.99)	8.72 (6.27 - 11.31)
9	71.36 (70.44 - 72.30)	6.90 (4.50 - 9.43)
10	71.34 (70.14 - 72.48)	10.0 (5.95 - 14.56)
Random regression on age		
Term	BV	d
$Intercept$	7.59 (1.52 - 13.29)	8.60 (2.00 - 15.93)
$cov(Intercept, Age)$	2.29 (0.24 - 4.29)	0.46 (-1.45 - 2.56)
$cov(Intercept, Age^2)$	-1.44 (-3.11 - 0.19)	-1.12 (-2.94 - 0.45)
Age	2.07 (0.71 - 3.37)	0.53 (0.01 - 1.38)
$cov(Age, Age^2)$	-1.13 (-1.90 - -0.36)	-0.01 (-0.48 - 0.39)
Age^2	0.89 (0.20 - 1.57)	0.34 (0.02 - 0.80)

4.4.3 Recovering resemblance within and across-generations

I compare the correlations in mass among ages implied by the development functions typically adopted in IPMs and those derived from a RRM, to the observed phenotypic correlations (Fig. 4.8A-C). I used the path rules, as described for the theoretical models, to obtain the correlation matrix for size at different ages implied by the IPM approach. There was no need to do the same for the RRM, as these correlations were recovered with Equation (4.15). I also analyse the proportion of correlation recovered for different gaps between ages (projection steps, Δt) by both models (Fig. 4.8D). The RRM estimates a phenotypic correlation matrix (Fig. 4.8C) that is much more similar to that observed (Fig. 4.8A) than the correlation matrix implied by the IPM approach (Fig. 4.8B). Across-age correlations are better recovered by the RRM than by the IPM approach (Fig. 4.8D). The proportion of correlation in size among ages recovered by an IPM follows the pattern predicted in Figure 4.2, with high recoveries for a single projection step, and then rapidly decaying to near zero (Fig. 4.8D). As predicted by the theory presented in this chapter, typical parameterisations of the development functions severely underestimate similarity of trait values within individuals across ages.

Second, I show the parent-offspring regressions recovered by the RRM and the IPM, and use the “observed" regressions as reference (Fig. 4.9). These latter values correspond to regressions of daughter mass on maternal mass for all matching ages, also including random intercepts for mother identity by age, year and cohort, as well as heterogeneous residuals by age. The cross-age biometric inheritance function implemented in IPMs recovers parent-offspring regression for lambs (age 1), but for older ages most similarity between parents and offspring is missed (Fig. 4.9). In contrast, the

patterns of parent-offspring similarity recovered by the RRM are of the observed order of magnitude throughout most of the life cycle (Fig. 4.9).

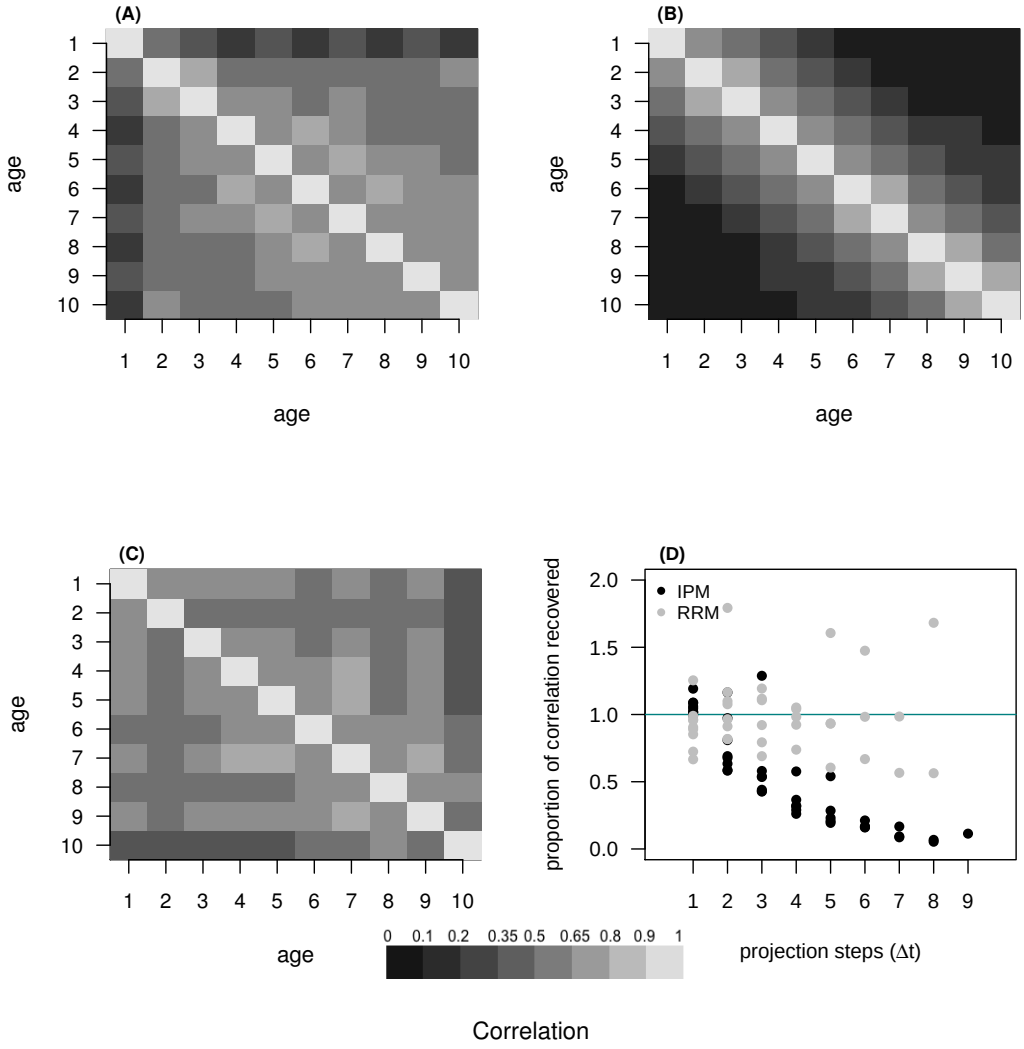

Figure 4.8: Observed phenotypic correlation matrix for size across ages for the bighorn sheep population of Ram Mountain (**A**), and analogous matrices implied by the IPM (**B**) and estimated by the RRM (**C**) approaches. Proportion of the correlations in size among ages recovered by the IPM (black dots) and RRM (grey dots) for different age gaps (projection steps, Δt), using the observed phenotypic correlations as reference (**D**). In (**D**), a porportion of 1 (horizontal line) corresponds to a perfect recovery of the observed correlation.

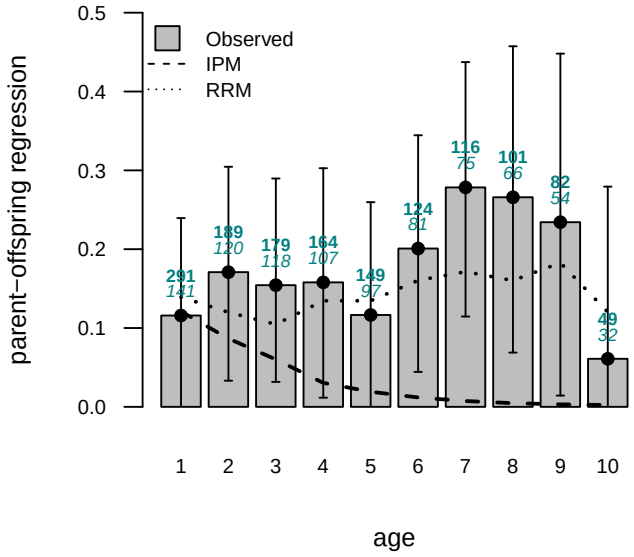

Figure 4.9: Parent-offspring regressions estimated for different ages for the bighorn sheep population of Ram Mountain, by the IPM and the RRM approaches. The observed values, and the corresponding 95% credible intervals, were estimated by a linear mixed model of daughters' mass on mothers' mass for matching ages, with random intercepts for the mother identity by age, year, and cohort. The values on top of the bars correspond to the number of offspring (top, bold) and mothers (bottom, italic) available for each age.

4.5 Discussion

I have shown analytically that IPMs, as typically implemented, will generally, and often severely, underestimate quantities that are critical to evolutionary inference. Both my theoretical results and my empirical example show that phenotypic covariances within and across individuals can be effectively zero in these models, due purely to artefacts of their construction. Additionally, the static nature of the inheritance function (parent-offspring regressions with fixed intercept) artificially reverses any response to selection. Consequentially, IPMs, as typically constructed, will inevitably suggest that evolution is not an important aspect of the dynamics of traits over time. I suggest, and demonstrate empirically, alternative approaches that could be used to characterise some key functions in IPMs. IPMs in principle are extremely useful and highly flexible, and their original conceptualisation (Easterling et al., 2000; Ellner & Rees, 2006) should be broadly compatible with a variety of alternative ways of characterising variation in growth and inheritance.

The main reason why development functions in IPMs fail to recover within-generation covariances of traits is regression to the mean. This problem is well-understood in evolutionary and ecological studies (e.g. Kelly & Price, 2005). In IPMs, this problem is particularly severe because the multiple age-specific projection steps compound the effect of measurement error to reduce covariance among predictor and response variables. Consequently, covariance between non-adjacent ages, which can be substantial (Fig. 4.8A, Wilson et al., 2005), is severely underestimated (Fig. 4.8B), even when measurement error is relatively small (Equations 4.1 and 4.2).

The failure of biometric inheritance functions to predict phenotypic similarity among relatives is partially also a direct manifestation of regression to the mean. Indeed, it is the canonical manifestation of regression to the mean - coined in exactly this context by Galton (1886). What we now understand is that Mendelian factors are inherited, and that, in terms of statistical mechanics of quantitative genetics, environmental variation can be regarded as measurement error obscuring the influence of breeding values. Any model of inheritance that does not include our understanding of how inheritance drives similarity among relatives in quantitative traits (Fisher, 1918, 1930; Wright, 1922, 1931) cannot be expected to suffice for even the most basic evolutionary predictions. Another issue arises from assuming that the biometric inheritance function is constant. Whenever the mean phenotype changes, the intercept of the parent-offspring regression necessarily changes as well. To presume that the intercept of the parent-offspring regression is constant across generations constrains the mean phenotype to be able to respond only transiently to selection, as I show by analytically iterating the mean phenotype in a simple IPM model structure (Fig. 4.7d). I reiterate that my criticism of a constant inheritance function is not a criticism of models assuming a constant heritability, whether that heritability is modelled using a genetical (i.e. using constant $\sigma^2_{\mathscr{a}}$ and σ^2_z) or a biometric approach (i.e. using a parent-offspring regression with a constant slope). Rather, the key point is that the mean phenotype cannot evolve in a model where a parent-offspring regression has a fixed intercept.

In my theoretical models, I use simple but general development and inheritance functions that are specifically designed to isolate these two fundamental processes from each other. In practice, however, the undesirable behaviours that I have modelled separately will interact. Importantly, in iteroparous organisms, where multiple episodes of reproduction occur over the lifetime, regression to

the mean in development functions will further obscure relationships between parents and offspring, with increasing effects as parents age (Chevin, 2015). Additionally, biased estimates of covariance of parents and offspring are compounded across multiple generations. The underestimation of similarity between parents and offspring will be compounded at each generation, leading to increasingly severe undervaluation of the relevance of relationships among more distant relatives to the evolutionary process. This interaction is very evident in the empirical example I present. Parent-offspring regressions recovered with the development and inheritance functions generally used in IPMs (Fig. 4.9) could not be predicted by the two-age theoretical model presented here, and specifically by Equation (4.11).

IPMs with typical cross-age biometric inheritance functions have been recommended for studying evolutionary responses to selection (Coulson et al., 2010; Coulson, 2012; Rees et al., 2014). Some studies applying this approach have concluded that non-evolutionary changes in trait distributions are the major contributors to temporal changes in phenotype (Ozgul et al., 2010; Traill et al., 2014). My theoretical findings do not indicate that these conclusions are wrong. Rather, I demonstrate that these are the conclusions that this kind of model must inevitably generate when applied to any system, regardless of whether evolutionary change is important or not. Since typical parameterisations of IPMs neglect the vast majority of similarity between parents and offspring, they cannot attribute phenotypic change to evolution. Concern about how IPMs model the transmission of dynamic traits had been previously raised (Hedrick et al., 2014; Chevin, 2015; Vindenes & Langangen, 2015; Benthem et al., 2017). Particularly, Chevin (2015) identified some issues addressed in this chapter, presenting insightful numerical examples that illuminate the main concern with the cross-age structure of the inheritance function. Besides my analytical demonstrations, and the numerical examples made available by Chevin (2015), I also provide an empirical example, using random regression analysis to address the issues presented here. The random regression model provided substantial improvement in recovering both correlations across ages within a generation (Fig. 4.8D), and parent-offspring regressions reflecting how breeding values are transmitted over generations (Fig. 4.9).

Vindenes & Langangen (2015) discuss joint models of static traits (constant through life) and dynamic traits (such as those typically handled in IPMs) in the general IPM framework. They suggest that incorporation of static traits could solve some of the problems that had begun to be acknowledged about evolutionary inference with IPMs (Hedrick et al., 2014; Chevin, 2015). The authors propose that the static trait, birth mass in their example, could be modelled as influencing mass at all other ages and demographic rates, which would allow covariances among birth mass and older ages to be well recovered. In a sense, using random regression animal models as I suggest treats breeding values (as opposed to some realised phenotypic value) as a static trait, but critically also models the inheritance of breeding values, not as some observed function, but according to the principles of quantitative genetics. It is noteworthy to mention that a genetic notion of trait transmission has already been implemented into an IPM for a single Mendelian locus (Coulson et al., 2011). The authors constructed an IPM that describes the dynamics of body mass and a biallelic gene determining coat color in wolves (*Canis lupus*). In contrast to biometric IPMs of quantitative traits, Coulson et al. (2011) conclude that the genetic variance within the study population is enough for natural selection to cause evolution. In fact, it is in principle relatively straightforward to implement an IPM that uses the basic principles of inheritance of polygenic quantitative traits to define inheritance functions of breeding values; such exercises have indeed begun for a single trait (Childs et al., 2016). It is easy

to conceive of multivariate extensions of such inheritance functions (based on multivariate versions of equations 4.3 and 4.4), whereby one could treat age-specific sizes as different characters, and estimate genetic variances and covariances from data. Nonetheless, a great deal of work is still required. For long-lived organisms, genetic covariance matrices of age-specific traits would be very challenging to estimate with useful precision (Wilson et al., 2010). Furthermore, the dimensionality of resulting phenotypes would overwhelm typical strategies for implementing IPMs (Coulson et al., 2010; Rees et al., 2014; Merow et al., 2014). In practice, a key challenge, but a surmountable one, will be to develop sufficiently flexible, low-dimensional characterisations of the genetic basis of development for practical estimation and subsequent modelling. The function-valued trait approach I adopted with a random regression model of bighorn sheep ewe mass is just one such possibility. Other approaches could possibly be even more useful; for example, uses of various autocorrelation functions (Pletcher & Geyer, 1999; Hadfield et al., 2013), or factor-analytic mixed model (de los Campos & Gianola, 2007; Meyer, 2009; Walling et al., 2014).

4.6 Summary

I have shown analytically and using and empirical example that standard implementations of integral projection models will generally severely underestimate the likelihood of evolutionary change. IPMs to date have been constructed using characterisations of development and inheritance that would not stand up to scrutiny in studies focusing on development and inheritance. It is not surprising that more complex models built on such functions behave poorly. In fact, insofar as the ability of IPMs to track the full joint distribution of phenotype has been suggested as their main quality for ecological inference, the problems that preclude their typical use for evolutionary inference should be of equal concern to ecologists. Importantly, I have suggested ways in which more nuanced models of development, and a modern understanding of inheritance, can be incorporated into the general IPM approach. A great deal more work is required before IPMs based on adequate models of development and inheritance will be field-ready. As a next step, careful studies of the performance of different approaches for characterising the genetic basis of developmental trajectories, with particular focus on approaches that could be incorporated into an IPM framework, are needed.

CHAPTER 5

The genetics of horn length trajectories in bighorn sheep (*Ovies canadensis*) rams

Abstract

Modelling the genetic contribution to the variation in traits that develop over time is still a challenge, due to data and computational limitations. Even a reduced dimensional approach can prove to be challenging when usual methods of quantitative genetics are to be implemented within complex population models, such as integral projection models (IPMs). Here, I first describe variation in horn length trajectories in bighorn sheep (*Ovies canadensis*) in terms of relevant components, including additive effects, and characterise similarity within individuals across the ontogeny and between individuals and their relatives. After establishing such characterisation, using a full-ranked multivariate model, I compare different models in their performance at recovering those relationships. IPMs have been implemented including a concept of inheritance that does not match the rules of how genes are passed through generations. I find that such parameterisation recovers nearly zero additive genetic variance in a trait that was shown to be heritable across the ontogeny of bighorn rams, whereas a random regression coupled with the animal model closely matches the saturated model. A very poor fit was obtained with factor analytic models with one and two common factors fitting the **G** matrix, implying that two principal components were not sufficient to model the additive genetic architecture in horn length across ages. A reason for this result might lie in how different models handle horn breakage, which is a common consequence of horn-clashing fights during the rut.

Keywords: additive genetic (co)variance, bighorn sheep, integral projection models, factor-analysis, function-valued trait, ontogeny, random regression

5.1 Introduction

Three decades have passed since Kirkpatrick and collaborators extended the canonical notion of quantitative genetics, generalising it to comprise *function-valued* traits (Kirkpatrick & Heckman, 1989; Kirkpatrick et al., 1990), i.e. traits that change over the ontogeny (e.g. size). This development was

critical in overcoming intractability issues associated with the use of classical quantitative genetics of multivariate traits (Lande & Arnold, 1983), also providing a means to describe a continuous trait over all its range (infinite points), rather than at arbitrary and finite landmarks. With the emergence of several long-term studies of long-lived animals and molecular tools to infer pedigree structure (Pemberton, 2008; Clutton-Brock & Sheldon, 2010), this framework has become particularly popular to investigate the genetics of ontogenetic trajectories of size in the wild (e.g. Wilson et al., 2005, 2007), using the so-called *animal model* (Henderson, 1975). Additionally, advances in genotyping technology continue to widen the scope of systems to which these models can be applied (Bérénos et al., 2014; Morrissey et al., 2018). All these accomplishments in the theoretical grounds of quantitative genetics of developing traits are now on the verge to be fully implemented within structured population models (Childs et al., 2016), opening the possibility to predict evolutionary change while simultaneously considering population ecology and life history.

Function-valued traits, initially coined *infinite-dimensional* (Kirkpatrick & Heckman, 1989), are traits that vary according to another continuous quantity, therefore being described by a function. Size through time or age, i.e., the ontogenetic trajectory of size, is an example of such a function. The variation associated with size across ages is itself described by a function, specifically a *covariance function*. The covariance function concept applies to the phenotypic variance, but also to any partition within total variance, including the variance in additive genetic values. As a result, an additive genetic covariance function, $\boldsymbol{\mathcal{G}}$, can be estimated. In fact, one of the grounds upon which quantitative genetics lies, the partitioning of variance components introduced by Fisher in 1918, is readily extendable to covariance functions, such that a phenotypic covariance function of a polygenic trait can be written as the sum of an additive genetic covariance function and an uncorrelated non-additive genetic (residual) covariance function, $\boldsymbol{\mathcal{P}} = \boldsymbol{\mathcal{G}} + \boldsymbol{\mathcal{R}}$ (see Kirkpatrick & Heckman (1989) for details). For practical reasons, however, additive genetic variance-covariance matrices, $\mathbf{G}$, are often derived, simply by evaluating $\boldsymbol{\mathcal{G}}$ at specific ages i and j, $\boldsymbol{G}_{i,j} = \boldsymbol{\mathcal{G}}_{(i,j)}$. In its initial formulation, Kirkpatrick adopted random regression on orthogonal polynomials as a function to model the genetic structure across the ontogeny of individuals, but since then other modelling approaches have been adopted, such as the estimation of autoregressive (Pletcher & Geyer, 1999; Hadfield et al., 2013) or factor analytic (Kirkpatrick & Meyer, 2004; de los Campos & Gianola, 2007; Meyer, 2009) genetic structures.

A fairly recent breakthrough in terms of potentially expanding application of quantitative genetics of developing traits happened with the extension of integral projection models (IPMs, Easterling et al., 2000) to include inheritance functions (Coulson et al., 2010). These are structured models designed to study the dynamic of populations when individuals' vital rates (e.g. survival, growth, reproduction) depend on one or more continuous state variables (e.g. horn length). To achieve this, IPMs make population projections from regression models that define the underlying vital rates as functions of the state variables. By combining evolutionary biology to different aspects of population ecology and life history, these models are potentially very flexible and an advantageous framework to study evolutionary change. However, controversy has been raised as to a concept of inheritance that has been implemented in several IPMs (Chapter 4, Hedrick et al., 2014; Chevin, 2015). Peculiarly, cross-age parent-offspring regressions (offspring trait at birth or recruitment regressed on parental trait at conception or parity) have been adopted (e.g. Coulson et al., 2010; Schindler et al., 2013; Traill et al., 2014; Bassar et al., 2016) as matching the concept of *biometric heritability* (Jacquard, 1983). The

concept of *biometric heritability*, however, has been defined since Galton (1886) as a parent-offspring regression evaluated at the same age. Such implementation is highly problematic because: (1) there are no theoretical grounds to a concept of inheritance matching a cross-age parent-offspring regression; and (2) such implementation leads to a systematic underestimation of the resemblance across relatives and, therefore, of evolution (see Chapter 4 and Chevin, 2015 for details). Moreover, another concern regarding IPM implementations is related to how mean trajectories have been estimated so far, through a series of antedependent regressions of subsequent observed sizes, and its consequences to the phenotypic variance-covariance matrix implied in all IPMs to date. By using multiple subsequent regressions on observed size, bias occurs through regression to the mean, leading to an underestimation of the resemblance within individuals across ages (Chapter 4).

Of particular interest is an IPM developed for the bighorn sheep (*Ovis canadensis*) population at Ram Mountain in Alberta, Canada, due to its role in an ongoing controversy about the effect of trophy hunting in the evolution of horn size (Traill et al., 2014). Such debate is of critical concern as a result of this being the only hunted population of ungulates for which a pedigree and horn measurements are available. Bighorn sheep rams at Ram Mountain were subject to trophy hunting until 2011, while shooting was allowed of any ram whose horns reached a certain phenotypic criteria based on the *curl* of the horn (for details, see Chapter 2). The curl of a horn is highly correlated with its length, a trait that is known to be positively associated to the reproductive success of rams beginning at 6-7 years of age (Coltman et al., 2002; Festa-Bianchet et al., 2004). As rams from the age of 4 years start to reach legal trophy status, and are thus vulnerable to hunting mortality, selective harvest of males with larger horns could, consequently, result in reproductive advantage to rams with smaller horns, potentially leading to a change in the allele frequency in this population. The first analyses addressing this hypothesis (Coltman et al., 2003; Traill et al., 2014, although the IPM developed by Traill et al. used body mass rather than horn length) reached opposite conclusions as to the role of evolution in the phenotypic decrease in horn size and were both subject to criticism (Postma, 2006; Hadfield et al., 2010; Hedrick et al., 2014; Chevin, 2015, Chapter 4). Recently, Pigeon et al. (2016) presented a similar analysis to Coltman et al. (2003), addressing the issues raised to the initial analysis and provided evidence of evolutionary change. As a result, there is particular interest in assessing the performance of a cross-age parent-offspring regression of horn length, rather than body mass, and comparing it to quantitative genetics models.

This chapter serves, in large part, as an intermediate step to developing an individual-based model (IBM) of horn length, which is presented in the next chapter (Chapter 6). Nonetheless, two distinct goals were set for Chapter 5. The first aim includes characterising the contribution of additive genetic effects in the variability of horn length along the ontogeny of bighorn sheep rams, as well as quantifying the similarity in horn length among ages and among individuals and their descendants. Although estimates of the heritability of male horn length in bighorn sheep exist in the literature (Coltman et al., 2003, 2005; Poissant et al., 2012; Pigeon et al., 2016), those are specific to particular ages or age ranges, and the genetic and phenotypic architecture of correlations across ages is unknown for this trait. The second aim of this chapter involves testing alternatives to the cross-age parent-offspring regression that simultaneously: (1) could be implemented into IPMs - or into alternatives to IPMs that are more feasible to implement with realistic models of component biological processes, such as IBMs, and (2) match known theory of how genes are inherited. As such alterna-

tives, which also should be relatively economical in terms of the number of parameters used, I adopt random regression and factor analysis, both coupled with the *animal model*. The former is possibly the most frequently used approach to investigate the genetics of size ontogeny among evolutionary biologists, whereas the latter is primarily adopted by animal breeders. I compare the ability of the three approaches in recovering both across-generation and across-age resemblance and conclude that random regression is the option that shows better performance.

5.2 Methods

5.2.1 Study system and data

I used the pedigreed population of bighorn sheep at Ram Mountain, Alberta, Canada (see details in Chapter 2), to investigate the mechanisms underlying resemblance in horn length across the ontogeny of bighorn males and among individuals and their relatives, as well as to assess the performance of alternative models in their ability to recover such patterns. I used yearly measurements of horn length, information on population density (number of females in the study area), age and year of measurement, maternal identity and cohort of each individual, as well as the pedigree of the population. To minimise measurement error caused by horn wear or breakage, I used the longest horn in the analyses presented here. Also, prior to any data analysis, horn length was adjusted to predicted individual values on September 15 using a mixed model approach (Martin & Pelletier, 2011). As data becomes very scarce for older ages, the corresponding sample sizes are not enough for the unstructured estimation of all age-specific additive genetic variances, and all covariances between ages. For that reason, I focused on horn length estimated for rams aged between 1 and 8 years old. Most rams achieve their asymptotic horn length by that age (Fig. 5.1, Schindler et al., 2017). Furthermore, for tractability, a multivariate model, (*sensu* Lande & Arnold, 1983), was fitted to ages 1 to 4 years only. I analysed 819 records of individual age-specific horn lengths of 276 rams captured from 1972 to 2015. For detailed information on the study system and on how the data were collected, see Chapter 2.

5.2.2 Models and variance structures

The genetics of horn length trajectories was modelled using three different approaches: random regression (`rr`, Kirkpatrick et al., 1990, 1994; Meyer & Hill, 1997; Meyer, 1998), factor analysis (`fa`, Kirkpatrick & Meyer, 2004; de los Campos & Gianola, 2007; Meyer, 2009), and an antedependence model (`ant`), as implemented for, example, in Traill et al. (2014) and advised by Coulson et al. (2010) or Rees et al. (2014). Although both the `rr` and the `fa` models are low dimensional alternatives to a multivariate approach (Lande & Arnold, 1983), only the former is implemented within the function-valued trait framework. As a result, covariance functions were obtained with the `rr` model, whereas matrices were instead derived with the `fa` and `ant` models. Regardless of this conceptual difference, phenotypic (co)variances were obtained as the sum of additive genetic, permanent environment, maternal, cohort, year of measurement and residual effects. While additive genetic, permanent environment, and phenotypic covariance functions were denoted by $\boldsymbol{\mathcal{G}}$, $\boldsymbol{\mathcal{E}}$, and $\boldsymbol{\mathcal{P}}$, respectively, matrices

were denoted by the corresponding bold capital letter (e.g. **G** for the additive genetic covariance matrix). I use the term *permanent environment* to refer to all consistent individual effects other than the additive genetic effects (Kruuk & Hadfield, 2007). To simplify model comparison, covariance matrices were derived from covariance functions in the `rr` model. In the IPM-like `ant` model, covariance matrices are not explicitly estimated, but the phenotypic variance-covariance matrix and heritabilities at each age implied by the model can be derived (see Chapter 4).

I fitted the `rr`, `fa`, and `ant` models sharing several consistent features. Age-specific intercepts, μ_t, and different slopes for population size, β_{pop}, according to a four-level categorical variable to characterise age were fitted. Yearlings, 2 year-olds, 3 year-olds and individuals of older ages were the classes considered. Additionally, I estimated random intercepts for maternal, u_m, cohort, u_c, and year of measurement, u_y, effects. A structure that is common to all models is represented by

$$z_{it} \sim \mathcal{N}\left(\mu_t + \sum_{j=1}^{4} I_{j_{it}} \times \beta_{pop_j} \times pop_{it} + u_{m_i} + u_{c_i} + u_{y_i} + \boldsymbol{U}, \epsilon_{it}\right), \tag{5.1}$$

where $z_{i,t}$ corresponds to the horn length of individual i at age (or time) t. As t takes values from 1 to 8, eight different μ were estimated in each model. $I_{j_{it}}$ is an indicator variable for age class j and pop are observed values of population density. To simplify model notation, indexing refers to individuals and ages only, resulting in u_{m_i} corresponding to the effect associated to the mother of ram i, rather than the effect of mother i. u_m, u_c, u_y, and ϵ_{it}, the model residuals, were assumed to be independent and normally distributed with mean zero and variances σ^2_m, σ^2_c, σ^2_y, σ^2_r, respectively. Finally, $\boldsymbol{U}$ includes any approach to modelling across-age resemblance within individuals and among relatives and is specific to each model.

Random regression models To model the family of size-at-age functions and associated phenotypic and genetic covariances of horn length across ages using random regression, I set up Equation (5.1) as follows

$$z_{it} \sim \mathcal{N}\left(\mu_t + \sum_{j=1}^{4} I_{j_{it}} \times \beta_{pop_j} \times pop_{it} + u_{m_i} + u_{c_i} + u_{y_i} + f_1(d_i, n_1, t) + f_2(a_i, n_2, t), \epsilon_{it}\right). \tag{5.2}$$

f_1 and f_2 are random regression functions on natural polynomials of order n, of permanent environment and additive genetic values, respectively. In both f_1 and f_2 n was set to 2, allowing the estimation of random intercepts, slopes, and curvatures. Polynomials were applied to mean-centred ages to improve convergence. d_i and a_i, vectors with individual permanent environment and breeding values, respectively, were assumed to follow normal distributions, $d \sim \mathcal{N}(\boldsymbol{0}, \boldsymbol{I} \otimes \boldsymbol{\mathcal{E}})$ and $a \sim \mathcal{N}(0, \boldsymbol{A} \otimes \boldsymbol{\mathcal{G}})$, where $\boldsymbol{I}$ and $\boldsymbol{A}$ are identity and pedigree-derived relatedness matrices, respectively. Random regressions imply correlation structures among ages that are described by their coefficients, variances in intercepts, slopes and curvatures and by the covariances among them. Both the permanent environment, $\boldsymbol{\mathcal{E}}$, and the additive genetic, $\boldsymbol{\mathcal{G}}$, covariance functions are defined by those coefficients and can be represented by 3×3 symmetrical matrices. Importantly, a covariance matrix, such as the 8×8 **G** matrix with the additive genetic covariances among ages from 1 to 8 years, can be decomposed as $\boldsymbol{G} = \boldsymbol{\Phi}\boldsymbol{\mathcal{G}}\boldsymbol{\Phi}^T$. In that case, $\boldsymbol{\Phi}$ is a 8×3 matrix with natural polynomials of order n evaluated at each age

(Kirkpatrick et al., 1990; Meyer, 1998). A covariance matrix associated to permanent environment effects, **E**, is obtained similarly using the corresponding covariance function, $\boldsymbol{\mathcal{E}}$. More information on partitioning the phenotypic variance into different components of variation using general pedigrees and the animal model is provided by Lynch & Walsh (1998), Kruuk (2004) and Wilson et al. (2010). Finally, I estimated heterogeneous residual variances for each of the age classes defined above.

Factor analytic model In a factor analysis, a vector of q random variables, for example of additive genetic effects at q different ages, is described as a linear combination of m, fewer, unobservable random variables called common factors and the variance not explained by these is modelled separately by fitting corresponding specific effects (de los Campos & Gianola, 2007; Meyer, 2009). As I aim to identify low dimensional approaches that could possibly be implemented into population models, I adopted a particularly parsimonious version of this factor analytic setting, often referred to as a *reduced rank model*, in which the specific effects are not estimated (Kirkpatrick & Meyer, 2004; Meyer, 2009). I modelled the breeding values at 8 different ages as $\boldsymbol{a} = \boldsymbol{\Lambda} \times \boldsymbol{c}$, in which each c_i is a vector of $m \times 1$ common factors characteristic of individual i and $\boldsymbol{\Lambda}$ corresponds to an $8 \times m$ matrix with the loadings for each of the m common factors. The variance in the common factors is assumed to be unitary and the covariance matrix associated with a factor analytic structure is simply obtained by $\boldsymbol{G} = \boldsymbol{\Lambda} \times \boldsymbol{\Lambda}^T$. I fitted two different models, `fa(1)` and `fa(2)`, where I set m to 1 and 2, respectively. In both `fa(1)` and `fa(2)`, I modelled permanent environment effects also adopting a factor analytic structure, setting $m = 1$. These models can be represented as

$$z_{it} \sim \mathcal{N}(\mu_t + \sum_{j=1}^{4} I_{j_{it}} \times \beta_{pop_j} \times pop_{it} + u_{m_i} + u_{c_i} + u_{y_i} + \boldsymbol{\lambda_{a_t} c_{a_{it}}} + \lambda_{e_t} c_{e_{it}}, \epsilon_{it}), \tag{5.3}$$

where subscripts a and e refer to additive genetic and permanent environment structures, respectively. When more than one common factor is fitted, orthogonality constraints must be considered. Specifically, $m \times q - m(m-1)/2$ parameters are estimated, where $m(m-1)/2$ are constrained to ensure orthogonality among the common factors (Meyer, 2009). As a result, in model `fa(2)` I fixed the first loading (referring to age 1) of the second factor to zero. Finally, as in the random regression model, I estimated heterogeneous residual variances for ages 1, 2, 3 and older.

Antedependence model I used a linear model to estimate the development and inheritance functions used in typical IPMs (see Chapter 4). I modelled observed horn length at each age as a function of observed horn length at the previous age, with separate intercepts and slopes for each age. For yearlings, I estimated a regression of yearling horn length on sire horn length at the age of 3 years, z_{s3_i}. Formally, the model is described as

$$\begin{aligned} z_{it} \sim \mathcal{N}(\mu_t + \sum_{j=1}^{4} I_{j_{it}} \times \beta_{pop_j} \times pop_{it} + b_{dev_t} \times z_{i,t-1} \times (1 - I_{year_{it}}) + b_{inh} \times I_{year_{it}} \times z_{s3_{it}} + \\ u_{e_i} + u_{m_i} + u_{c_i} + u_{y_i}, \epsilon_{it}), \end{aligned} \tag{5.4}$$

where b_{dev_t} are age-specific horn length slopes and b_{inh} is the inheritance function coefficient. I_{year} is an indicator variable for yearlings and u_{e_i} is a random intercept for individual i. As for the remain-

ing random effects, u_e are assumed to be normally distributed with mean zero and a certain variance (σ^2_e). To match the rational of autoregressive growth functions in IPMs, which can be fitted separately, heterogeneous residual variances were estimated for each age.

In order to derive the phenotypic covariances implied by this model, it is useful to perceive the antedependence model, i.e. the subsequent regressions of trait value on trait value at a previous age, as a path diagram (see Fig. 4.1 in Chapter 4). In that case, b_{dev} correspond to path coefficients and the phenotypic variances associated with growth at each age to the exogenous variances. To apply the rules of path analysis (McArdle & McDonald, 1984; Gianola & Sorensen, 2004; Morrissey, 2014), I define $\boldsymbol{\Psi}$ as the matrix of total causal effects of each trait on every other as

$$\boldsymbol{\Psi} = (\boldsymbol{I} - \boldsymbol{b})^{-1}, \tag{5.5}$$

where $\boldsymbol{b}$ is a matrix with all path coefficients. The phenotypic covariance matrix, $\boldsymbol{P}$, is then obtained as

$$\boldsymbol{P} = \boldsymbol{\Psi}\boldsymbol{P}_{\boldsymbol{\epsilon}}\boldsymbol{\Psi}^T, \tag{5.6}$$

where $\boldsymbol{P}_{\boldsymbol{\epsilon}}$ includes all exogenous variances, which in the case of the model in Equation (5.4) includes permanent environment, maternal, cohort, year of measurement and residual effects. For more details on how to obtain covariance matrices in causally covarying traits see Morrissey (2014). Regarding the inheritance function, note that although a single regression coefficient is estimated, it is possible to derive the same-age parent-offspring regression coefficient (and, therefore, heritability) that is implied at each age. According to the path rules, such quantities are obtained as the product of the inheritance function coefficient by the development path coefficients up until the age of interest. Using these parent-offspring covariances it is then straightforward to derive the implied age-specific additive genetic variances, using the phenotypic variances as denominator.

As implemented in Coulson et al. (2010) or Traill et al. (2014), the inheritance function, used jointly with the antedependence model of development, uses parental phenotype at the age of conception. In the particular case of these data, this regression is negative (-0.14, 95% CrI -0.22; -0.07, see Appendix C.2 for the remaining parameters). This negative cross-age inheritance function is itself a clear indication of the inadequacy of this approach to handling inheritance. Nonetheless, some comparison of this approach with the random regression and factor analytic approaches is clearly desirable. Consequently, the solution I adopt, a parent-offspring regression using parental measurements at the age of 3 years, should be regarded as a particularly conservative approach to typical IPM implementations with respect to the criticisms identified in Chapter 4. Highest breeding success occurs at older ages (Chapter 6, Coltman et al., 2002), resulting in an age gap between parents and their offspring that is larger than the one considered here (between yearlings and 3 years-old). As a result, the cross-age parent-offspring regression using paternal age at conception is expected to recover less resemblance between generations (Chapter 4).

Multivariate model

Ideally one would compare the above models, and particularly the phenotypic and genetic architec-

ture they recover, with the corresponding true ones. The closest to that is to fit a model that estimates each parameter of the **G** and **E** matrices, a multivariate model (`mvt`, *sensu* Lande & Arnold, 1983). Such approach will entail no bias due to any constraints imposed by the low-dimensional approaches, but suffers from having the most parameters, and therefore is prone to being imprecise. In fact, it implies estimating $n \times (n+1)/2$ parameters for each $n \times n$ covariance matrix and is often impossible to accomplish as the number of traits (or times at which traits are evaluated) increases. Formally, I define the `mvt` model as

$$z_{i,t} \sim \mathcal{N}\left(\mu_t + \sum_{j=1}^{4} I_{j_{it}} \times \beta_{pop_j} \times pop_{it} + u_{m_i} + u_{c_i} + u_{y_i} + a_{i,t}, \epsilon_{i,t}\right), \tag{5.7}$$

where $a_{i,t}$ is the breeding value of individual i at age t. The breeding values are assumed to follow a multivariate normal distribution with zero mean vector and the direct product of $\boldsymbol{A}$ and an unstructured $\boldsymbol{G}$ matrix as covariance. In such a saturated model, permanent environment effects and residuals are confounded, as once a residual unstructured covariance matrix is estimated, there are no degrees of freedom left to model among-individual variation. Due to insufficient observations at later ages, I could not fit the model in Equation (5.7) to ages from 1 to 8 years. Instead, I fitted a phenotypic version of this model (i.e. excluding the estimation of the **G** matrix) to all ages and the full model to ages from 1 to 4 years only.

5.2.3 Model estimation and comparison

All models were fitted using Bayesian statistics in R (R Core Team, 2014). The multivariate, random regression and antedependence models were estimated using MCMCglmm (Hadfield, 2010), whereas the factor analytic models were estimated using JAGS (Plummer, 2003) with the R package *rjags* (code is provided in Appendix C.1). I assumed diffuse normal prior distributions for the fixed effects, including the factor loadings, and inverse (multivariate) Wishart distributions for residuals and random effects. For the latter, parameter expansion was adopted to improve model convergence (Gelman, 2006; Hadfield, 2010).

Model outputs correspond to means of the posterior distributions and Highest Posterior Density credible intervals (CrI). Matrix comparison was performed by taking absolute differences of posterior samples of each parameter estimated by different models. This procedure results in posterior distributions of differences, which allowed inference on the likelihood of those differences being different from zero. The proportion of variation explained by both additive genetic (narrow-sense heritability) and permanent environment effects at each age were calculated from the **G** and **E** matrices, as well as the additive genetic and permanent environment coefficients of variation, as these measures tend to be less sensitive to scale effects than unstandardised variance components (Houle, 1992).

5.3 Results

5.3.1 Observed size trajectories and underlying cross-age population structure in horn length

Variation in horn length trajectories of bighorn rams (Fig. 5.1) is a result of both genetic and environmental contributions (Fig. 5.2). According to the multivariate model, heritability in horn length is very high in bighorn rams during the first four years of age, as additive genetic variance amounts for up to 57% of the observed variation (at the age of 4 years), and never corresponds to less than 29% (at the age of 1, Appendix C.3) of the phenotypic variance. Differences among cohorts are also an important source of variation, contributing to up to 50% of total variation (in yearlings). Effects associated to the maternal environment and year of measurement account for the smallest contributions to the phenotypic variation in horn length during the first four years of life of bighorn males, representing less than 5% of total variation. Finally, although "permanent environment" effects are not distinguishable from the residual variance in the multivariate model, since there is one measurement per individual of each age-specific trait, the associated variance is not particularly large (up to 10%), leading to the conclusion that most variation is captured by the remaining components.

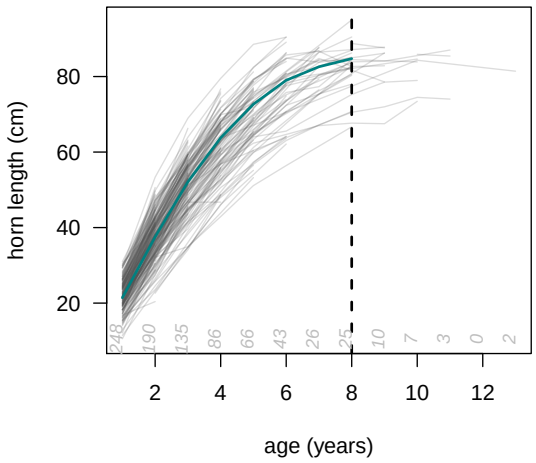

Figure 5.1: Observed horn length trajectories of 276 rams of the bighorn sheep population of Ram Mountain. Measurements were adjusted to September 15, and values in grey correspond to the number of observations available at each age. The line in teal corresponds to the mean trajectory estimated by the multivariate model, adjusted for average population size. The vertical line illustrates the adopted cut-off for data inclusion (up to the age of 8 years), suggesting that in most individuals maximum size has been reached by that age.

G matrices, as well as $\boldsymbol{\mathcal{G}}$ functions, of function-values traits are often difficult to estimate due to data or computational limitations. Moreover, as the sample size available to estimate **G** depends on kinship, whereas the accuracy in estimating **P** depends on the number of observations only, **P** matrices have smaller sampling error, and are sometimes adopted as proxies for **G** (Willis et al., 1991; Steppan et al., 2002; Agrawal & Stinchcombe, 2009). Given that the additive genetic contribution to the phe-

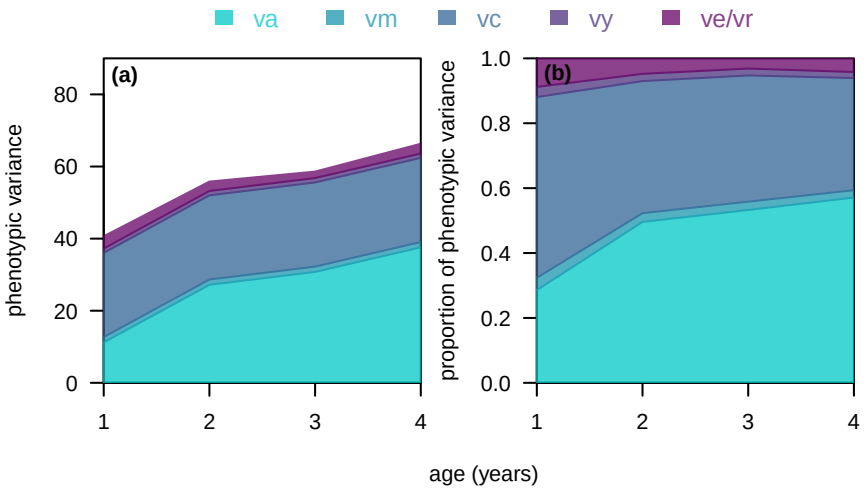

Figure 5.2: Variance components contributing to the phenotypic variance in horn length up to the age of 4 years in bighorn rams from Ram Mountain (a); and the corresponding proportion of variance explained by each component (b), as estimated by the multivariate model in Equation (5.7). `va`, `vm`, `vc`, `vy`, and `ve/vr` correspond to the additive genetic, maternal, cohort, year of measurement and permanent environment/residual components of the phenotypic variance.

notypic covariation in horn length among ages is quite substantial in this species, it is not surprising that the correlation pattern of **P** is very similar to that of **G** (Fig. 5.3), and that none of the differences between phenotypic and additive genetic correlations are statistically different from zero (Tab. 5.1).

Table 5.1: Absolute differences (upper diagonal) and corresponding 95% credible intervals (lower diagonal) between phenotypic and additive genetic correlations in horn length of bighorn sheep rams from Ram Mountain, estimated by the multivariate model.

	1	2	3	4
1		0.06	0.08	0.12
2	(0.00; 0.14)		0.04	0.07
3	(0.00; 0.20)	(0.00; 0.08)		0.03
4	(0.00; 0.25)	(0.00; 0.12)	(0.00; 0.06)	

5.3.2 Model comparison

Recovering mean trajectories

Although all models include age as a categorical fixed effect, the mean values across the ontogeny will not necessarily correspond exactly among the models, due to intrinsic differences in their structure (Fig. 5.4, see Appendix C.2 for parameter estimates). The main difference in how models estimate mean trajectories is associated with how each model copes with data incompleteness. Due to (1) mortality before the age of 8 years, (2) rams not having reached that age by the cut-off year for data inclusion, and (3) recapture success being necessarily lower than 100%, most individuals will have incomplete trajectories. When data is missing at random, modelling among-individual variation

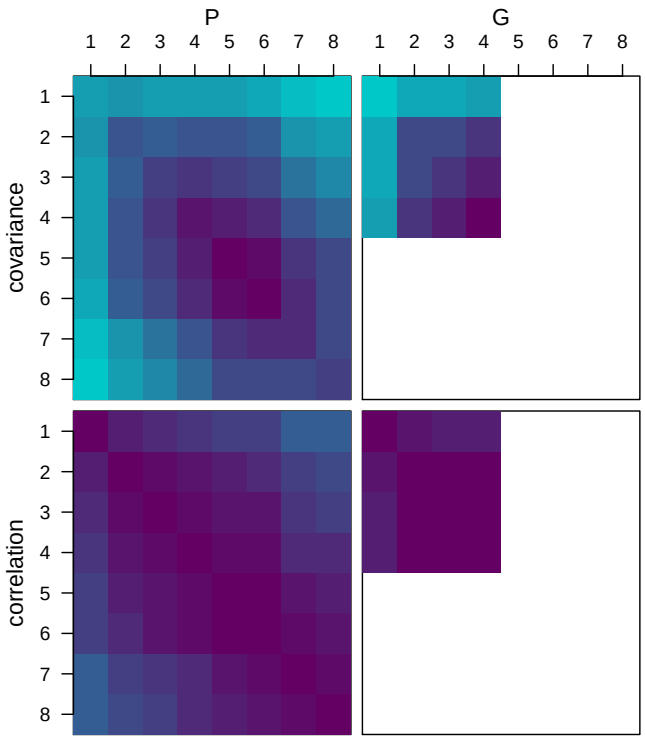

Figure 5.3: Diagrams showing unstructured **P** and **G** variance-covariance and correlation matrices of horn length across ages (years) in bighorn rams from Ram Mountain. Values correspond to estimates from the multivariate model in Equation (5.7) (due to insufficient statistical power, a genetic version was estimated only considering ages up until 4 years). Colour varies according to the minimum (green) and maximum (purple) values of each covariance matrix and from 0 (green) to 1 (purple) in the correlation matrices. Matrix estimates can be found in appendix C.4.

might be a solution to deal with incompleteness of data (Hadfield, 2008). This very reason explains why the multivariate model apparently overestimates horn length when compared to observed mean values (Fig. 5.4c). Such differences accumulate over the ontogeny, and by the age of 8 years reach 3.09 cm. All models presented in this chapter include structures fitting among-individual variation, either by including random effects on individual rams (all models but the factor analytic) or by including a factor analytic structure on individual variation (factor analytic models). The extent to which those structures were included in different models aimed at mimicking common uses of these models and will impact how each model copes with information missing at random.

Mean horn length trajectories are modelled similarly in all models, except for the antedependence model, which is conceptually distinct from the other models. All remaining models fit size-at-age, whereas as the *antedependence* function models size-dependent growth: observed trait values at a certain age are regressed on observed trait values at the previous age (development functions, e.g. Ellner & Rees, 2006). In principle, such conceptual differences between *size-at-age* and *autoregressive* modelling strategies do not necessarily affect how well the mean trajectory is recovered. The fact that the `ant` model appears to underestimate horn length at older ages (in comparison to the multivariate model), simply suggests that random intercepts at the individual level are not enough to cope with information missing at random (Fig. 5.4b). The remaining models use more parameters to model among-individual variation, therefore outperforming the antedependence model.

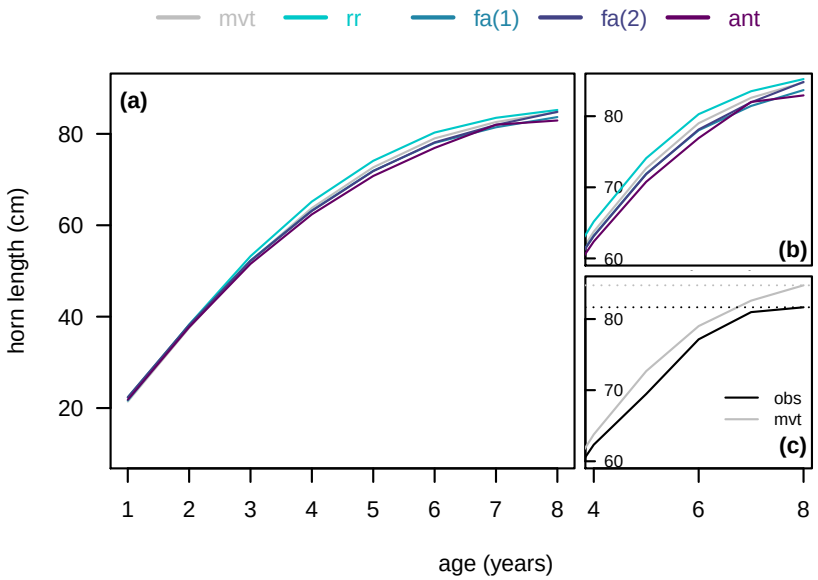

Figure 5.4: Mean male horn length trajectories observed and estimated for the bighorn sheep population of Ram Mountain. Lines are estimates from the multivariate (`mtv`), random regression (`rr`), factor analytical (with one and two additive genetic common factors, `fa(1)` and `fa(2)`), and antedependence (`ant`) models, for average population size (a, b), and also observed (`obs`) mean values at each age (c). In (a) the full trajectory is shown, whereas in (b) and (c) a close-up to older ages is presented.

Recovering age-specific aspects of variation

The contribution of the additive genetic effects to the phenotypic variance in horn length was estimated (or derived) for ages from 1 to 8 in all models. The number of parameters each model used to retrieve those effects varied considerably, from one (`ant`) to fifteen (`fa(2)`). Note that an unstructured matrix would have 36 free parameters. The additive genetic variances implied by the `ant` model (corresponding to twice the implied parent-offspring covariance) were not significantly different from zero at any age (Fig. 5.5a, Appendix C.3), showing that the cross-age parent-offspring regression implemented is not appropriate to recover similarity in horn length across relatives at any stage of the ontogeny of bighorn rams (see also Chapter 4, Hedrick et al., 2014; Chevin, 2015). The model that best recovered the additive genetic contribution to the phenotypic variation in horn length was the `rr` model. Using 6 parameters to model the additive genetic (co)variation across ages, this model closely matched the pattern obtained with the saturated model, a result that holds regardless of the adopted scale (Fig. 5.5 a, c, e). Finally, both models using factor analytic structures to approximate the **G** matrix did considerably worse than the `rr` model, and underestimated significantly the additive genetic variance in most ages. Adding a second additive genetic common factor did improve the amount of variation recovered of this component, but rather insufficiently when compared to the `rr` model. On the contrary, the factor analytic models, and particularly the `fa(1)`, overestimated permanent environment effects (Fig. 5.5 b), which, put together, suggests that the first two principal components of the **G** matrix are not sufficient to explain the genetic architecture of horn length across the ontogeny, resulting in the the additive genetic and permanent environment factors being confounded.

Given that the development functions adopted in IPMs usually use at most a single parameter to model among-individual variance (e.g. Traill et al., 2014), that was the strategy adopted in this chapter. Variance in random intercepts for permanent environment was estimated by the `ant` model as 1.22 (95% CrI 0.32; 2.20). As a result, heterogeneous variances in permanent environment effects across the ontogeny of bighorn rams were only estimated in the random regression and factor analytic models (Fig. 5.5 b, d, f). Although values are also shown for the saturated (multivariate) model, these quantities are confounded with residual variances and, as a result, these correspond to upper limits of the true underlying among-individual variances.

Recovering resemblance within and across generations

In this section, I compare the different models in terms of their ability to recover similarity in horn length among ages, considering both only the additive genetic contribution to such similarities and all sources of variation. Those comparisons rely on the assumption that the parameter estimates (covariances) of the multivariate model are very close to the underlying true ones (see Appendix C.4 for covariance matrices). I quantified the resemblance across ages recovered by each model by analysing the proportion of the correlations in horn length between ages recovered by each model (Fig. 5.6). In reality, the multivariate model, and in particular the one including additive genetic parameters, estimate parameters with substantial sampling error. As a result, this comparison is mainly an exercise checking for consistency, rather than a procedure that would lead to categorically reject any of the models. Overall, all models recover better phenotypic and additive genetic correlations be-

tween closely related ages. Regarding the phenotypic architecture of horn length across ages, both the `rr` and the `fa(2)` recover correlations that are very close to the ones estimated by the `mvt` model, whereas the `fa(1)` and the `ant` model seriously underestimate correlations between distant ages. In fact, the pattern shown by the `ant` model in recovering phenotypic correlations follows the theoretical prediction derived in Chapter 4 (Fig. 4.2), decaying rapidly to almost zero. Notably, correlations involving older ages are not systematically more difficult to recover, as long as relative to a closer age. Additionally, both the `rr` and the factor analytic models estimate additive genetic correlations between ages up to four years that are very close to the ones obtained with the multivariate model.

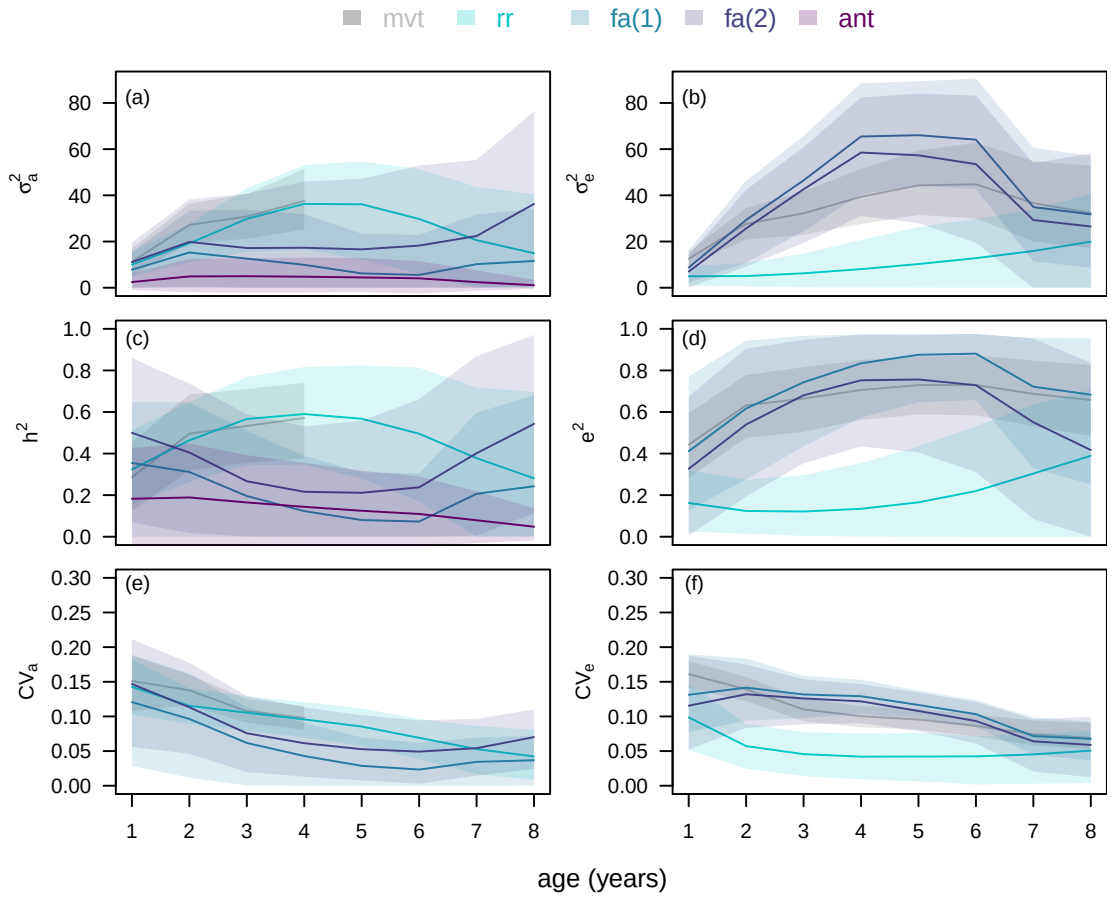

Figure 5.5: Variance (a, b), proportion of phenotypic variance (c, d), and coefficient of variation (e, f) associated with additive genetic (a, c, e) and permanent environment (b, d, f) effects in horn length trajectories of male bighorn sheep at Ram Mountain. Estimates are shown for the multivariate (`mvt`), random regression (`rr`), factor analytic with a single genetic common factor (`fa(1)`), factor analytic with two genetic common factors (`fa(2)`), and antedependence (`ant`) models. Note that for the `mvt` model residual effects that include permanent environment effects are shown, therefore corresponding to upper limits of underlying among-individual variances. CV_a estimates were not obtained for the `ant` model, as it implied obtaining the squared root of negative values. All estimates and associated uncertainty are available in Appendix C.3.

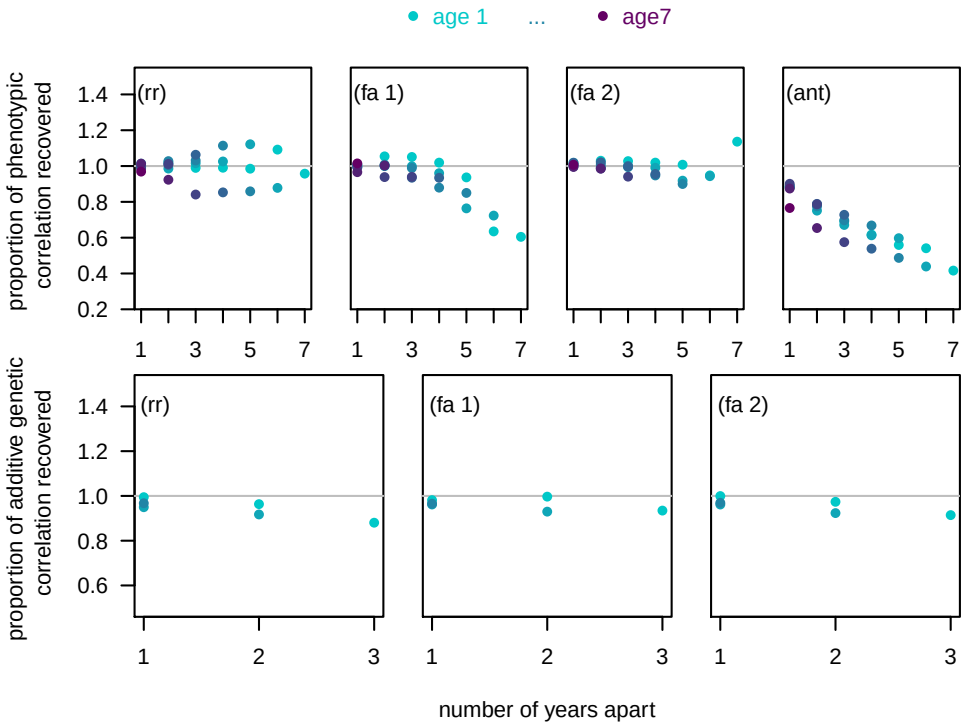

Figure 5.6: Proportion of the phenotypic and additive genetic correlations in horn length recovered by the random regression, `rr`, the factor analytic with a single, `fa(1)`, and two, `fa(2)`, additive genetic common factors, and the antedependence, `ant`, models, according to the number of years apart between horn length measurements. Different colours are used to show the lowest age involved the correlation (for example, if age 7 is the lowest, only the correlation in horn length between ages 7 and 8 can be shown). Proportions were obtained adopting the estimates from the multivariate model as reference.

5.4 Discussion

Horn length is very heritable across the ontogeny of bighorn sheep rams, varying from 0.29 (95% CrI 0.12; 0.45) to 0.57 (95% CrI 0.38; 0.74) up to the age of four years. After the age of four, the random regression model suggests a decrease in the proportion of variance explained by additive genetic effects, reaching 0.28 (95% CrI 0.00; 0.70) by the age of 8 years. Several studies had already shown that horn length is heritable in this (Coltman et al., 2003, 2005; Poissant et al., 2012; Pigeon et al., 2016) and other species of ungulates, where horn and antler size is also known to be heritable (Kruuk et al., 2002; Johnston et al., 2010). However, no age-specific estimates were available, nor was information on additive genetic correlations among ages. According to the multivariate model, correlations among ages are, overall, positive and strong, both at the additive genetic and phenotypic levels, therefore suggesting that rams that have larger horns early in life tend to be the ones with larger asymptotic horn length. I also provide evidence that both additive genetic and phenotypic variances decrease at older ages. Such pattern could be a misleading result of lower sample size at older ages due to incomplete trajectories, but also an indication of *compensatory growth* (Monteiro & Falconer, 1966), a mechanism that has been suggested for body mass in this species (Wilson et al., 2005).

Phenotypic and additive genetic correlations of horn length across ages are very similar. Such pattern seems to be very common in nature, as many examples exist where the phenotypic correlation matrix matches its additive genetic counterpart, not only in sign, but also in magnitude (Cheverud, 1988; Roff, 1995, 1996). Here, I have estimated additive genetic correlations in horn length across ages that are slightly stronger than the corresponding phenotypic correlations. Such pattern has also been commonly found by other authors and is likely to be related with differing accuracies in estimating **P** and **G** (Ponzi et al., 2018). Effective sample size corresponds to the number of observations when estimating **P**, whereas for **G** it depends on the number of families present in the data. As these are necessarily fewer, sampling errors can be considerably larger in **G**, resulting in more biased estimates (Lynch & Walsh, 1998, Ch. 21).

Heritability estimates of bighorn sheep horn length available in the literature refer to different age ranges and were obtained from models that are not equivalent, therefore varying quite significantly (from 0.26 (Poissant et al., 2012) to 0.69 (Coltman et al., 2003)), and providing a good example of heritability not being generalised across different studies (Wilson, 2008), even within the same study system. The models I adopted to estimate the additive genetic contribution to the phenotypic variance in horn length are particularly distinct from any of the the models previously adopted, not only because the corresponding heritability estimates are conditioned on a different set of fixed effects, but also because, contrarily to the previous approaches, I estimated age-specific values, rather then grouping ages together. As a check to the analyses presented here, I fitted a similar model to the one fitted by Pigeon et al. (2016), estimating an additive genetic variance of 18.07 (95% CrI 6.24; 27.09, model not shown), closely matching the results of these authors.

Other than describing the genetic architecture underlying horn length trajectories in bighorn sheep, I also aimed at evaluating alternatives to the cross-age biometric inheritance function that could also be implemented into population models such as IPMs or IBMs. Although certainly other options could

have been considered (see Pletcher & Geyer, 1999), I provided results of random regression and factor analytic models. The reasons for having selected these methods are two-fold: (1) their potential to make use of very few parameters to model both the genetic and the among-individual architecture of horn length ontogenetic trajectories, and (2) because these are extremely popular statistical tools amongst evolutionary biologists and animal breeders, therefore being available in a range of different software. As implemented in several IPMs to date (e.g. Traill et al., 2014), the cross-age parent-offspring regression requires inference of a single parameter to characterise trait transmission across generations. Other than being very economical in terms of the number of parameters used, such inheritance requires a linear regression and therefore is easily estimated. Nonetheless, I have shown here that this function recovers a resemblance in horn length across ages between fathers and their male offspring that is essentially zero, despite the high age-specific heritabilities estimated by the multivariate model. Such an empirical result is not surprising given the theoretical results presented in Chapter 4, where I show analytically that the phenotypic covariances within and across individuals can be effectively zero, due purely to artefacts of how the growth and inheritance functions are typically built in IPMs. The theoretical results from Chapter 4, put together with the empirical evidence presented here, strongly suggest that the cross-age parent-offspring regression (of *body mass*) adopted by Traill et al. (2014) to infer on the role of trophy hunting in the evolution of *horn length* in bighorn sheep is not appropriate. The consequence of using such model is that their result, that evolution does not result from selection, was inevitable, regardless of the underlying reality.

Three alternative models were assessed for their ability to recover the additive genetic and phenotypic architecture of horn length ontogenetic trajectories. Formal approaches to matrix comparison include, for example, the use of genetic covariance tensors (Hine et al., 2009), which by corresponding to higher order structures of matrices allow characterising the variation among multiple matrices. In this chapter, I preferred using metrics corresponding exactly to the quantities of interest to perform matrix comparison. As a result, model comparison was performed informally, by assessing how well each model recovered different variance components at each age and how much similarity within individuals across ages and between individuals and their relatives was recovered. The random regression model was particularly fit at recovering both age-specific additive genetic variances and the additive genetic and phenotypic architecture among ages, whereas the structures adopted in the factor analytic models seemed insufficient to achieve even close results. Particularly, results from these models suggest that there was no clear separation between the additive genetic and permanent environment sources of variation, resulting in a significant underestimation of the former and a possible overestimation of the latter. An explanation for these results obtained with the factor analytic models might lie on horn breakage. Horns break often in bighorn males, resulting in damage that tends to increase with age and can be very substantial (Pigeon et al., 2016). Such a phenomenon is expected to have a smaller effect when function-valued approaches, such as random regression, are adopted given that a trend defined by a function with a particular shape is imposed on the data. Although random regression is adopted very often among evolutionary biologists, several criticisms have been raised towards this approach (Pletcher & Geyer, 1999). Some of the concerns raised by Pletcher & Geyer (1999) are common to other methods, such as matrices not being automatically positive semidefinite, or parameters not having theoretical justification and being estimated potentially in large numbers. More specific to random regression, Pletcher & Geyer mention that polynomials do not fit covariance functions well, mainly as a consequence of not having asymptotes, which covariance functions tend to. Although acknowledging these limitations, random regression, when properly

applied is seen as being vastly advantageous in many circumstances (Stinchcombe & Kirkpatrick, 2012).

The alternative models assessed in this chapter differ considerably in the number of parameters estimated. Both the random regression and the factor analytic models were used to derive additive genetic and permanent environment (co)variance matrices among ages from one to eight years. In the random regression model, each of the two 8×8 matrices was characterised by a covariance function, through the estimation of random intercepts, slopes, and curvatures of breeding and individual values across ages, as well as the correlations between these parameters. In the two factor analytic models, one and two additive genetic common factors were used to model the **G** matrix, whereas a single axis was used to estimate the among-individual variation. As a result, the **G** matrix was modelled using 6 (random regression), 8 (factor analysis with a single genetic common factor) and 15 (factor analysis with two genetic common factors) parameters. The **E** matrix was fitted using 6 parameters in the random regression model and 8 in both factor analytic models. The number of parameters needed to describe the horn length trajectories is of crucial relevance in determining their utility to population models, and particularly to IPMs, which, as matrix models, easily become intractable (Caswell & John, 1992). In factor analytic models, I followed the approach adopted by de los Campos & Gianola (2007) and Meyer (2009), who described the **G** and **E** matrices using their most important eigenvectors. Alternatively, implementations of factor analysis are possible where eigenfunctions are estimated instead, potentially using fewer parameters, a rational that is similar to using random polynomial functions in random regression (Kirkpatrick & Meyer, 2004; Meyer & Kirkpatrick, 2005).

The bighorn sheep data used in this chapter imposes a serious limitation in the estimation of unbiased ontogenetic horn length trajectories, as the population of Ram Mountain was subject to trophy hunting until 2011 (Festa-Bianchet et al., 2014). Any ram whose horns reached a certain phenotypic criterion of minimum horn curl was allowed to be harvested (see Chapter 2, Pelletier et al., 2012). Importantly, horn curl and horn length are very correlated in bighorn sheep (Festa-Bianchet et al., 2014), resulting in horn length trajectories of rams with larger horns being more likely to be missing due to artificial selective pressure (Schindler et al., 2017). In such circumstances, the missing data mechanism is said to be non-ignorable, as selection is not ignorable in the completeness of the data (Hadfield, 2008, and references therein). In reality, there are different processes generating missing data in the used data set: (1) less than perfect recapture rate, (2) individuals not having reached 8 years old at the last year of data considered, and (3) death before reaching 8 years-old. The latter process encompasses trophy hunting, and is the only that produces incompleteness of data that is necessarily not missing at random (as the largest individuals are targeted). Both Restricted Maximum Likelihood (REML) and Markov chain Monte Carlo (MCMC) Bayesian methods are useful in accounting for data missing at random, through the use of random effects at the individual level (Hadfield, 2008). In the case of bighorn sheep horn length trajectories, such approach results in observed and estimated trajectories differing considerably (Fig. 5.4), which suggests that processes (1) and (2) are significant in the data. Nonetheless, the results presented here are not free from bias due to missing information not at random, which could be addressed by explicitly modelling the drop-out mechanism, in this case, size-dependent harvest of male bighorn sheep (Hadfield, 2008).

5.5 Summary

Horn length is very heritable across most of the lifespan of bighorn sheep males and both additive genetic and phenotypic correlations in this trait across the ontogeny tend to be positive and strong, despite some evidence for compensatory growth. As a result, rams with larger horns at early ages tend to be the ones with larger asymptotic horn length. Here, I show that a cross-age parent-offspring regression - analogous to those implemented in several IPMs to date - recovers similarity in horn length between fathers and their male offspring that is not significantly different from zero. The adoption of random regression coupled with the *animal model* provides a robust alternative as it recovers additive genetic and phenotypic architectures of horn length across ages that are similar to the ones estimated by a multivariate model (*sensu* Lande & Arnold, 1983). Additionally, since random regression is reasonably economical in terms of the parameters to be estimated, it may be generally useful for: (1) inference from limited data, and (2) integrating inheritance and development into more comprehensive models of population ecology and evolution.

CHAPTER 6

What evolutionary change is expected due to trophy hunting based on a heritable trait?

Abstract

When acting on heritable traits, selective harvest has the potential to cause evolution. Assessing and quantifying such evolution is a challenging task in wild populations due to concomitant plastic responses to selection and also due to technical challenges arising from integrating microevolutionary, demographic and life history theory. Population models providing robust estimates of evolutionary response to selection can be particularly useful to assess human-induced exploitation of natural resources, which is known to have resulted in rapid and dramatic changes in phenotype. A particular case of interest is trophy hunting, as management decisions should be based on unbiased quantification of demographic *versus* genetic responses. Here I build a two-sex individual-based model of horn length mimicking the life cycle of the hunted population of bighorn sheep (*Ovis canadensis*) from Ram Mountain, Canada. I incorporate different approaches to modelling trait transmission across generations, including random regression and a cross-age parent-offspring regression that has been used in several population models. As the latter has been shown inadequate to recover the genetic architecture of horn length across the ontogeny of bighorn rams, I focus my attention on the former. I present results from simulations comprising 200 years, where hunting is allowed in the last 100 years, providing strong evidence of evolutionary response to selective harvest, as measured by change in breeding values.

Keywords: bighorn sheep, breeding success, evolutionary change, horn length, individual-based models, function-valued trait, survival

6.1 Introduction

Evolution through natural selection is an emergent process in a population, a manifestation of the effect of a changing environment in the life history of individuals and therefore in the dynamics of the population they belong to. Due to the complexity of the association between population dynamics,

life history and change in allele frequency over generations, i.e. evolution, the latter is often very difficult to quantify in the wild (Kruuk et al., 2014). An appropriate balance between modelling complexity and parsimony is a study-specific decision of critical importance and multiple solutions exist that explore a wide range of this trade-off. Structured population models or simply computational simulations of populations are often used as a means of integrating different aspects of the ecology and life history traits and have begun to additionally be used to predict evolutionary change in microevolutionary terms (Barfield et al., 2011; Childs et al., 2016). Such advances in population models have the potential of being very useful also to evolutionary biologists, particularly to test hypotheses on the causality of any aspects of the environment on evolutionary change.

Demographic models are used to track the number of individuals and their distribution according to certain characteristics, and more generally to link demography and life history to ecological aspects of populations (DeAngelis & Gross, 1992; Caswell, 2001). Different approaches have been developed to achieve this purpose, leading to the appearance of models as distinct as integral projection models (IPMs, Easterling et al., 2000) and individual-based models (IBMs) applied in ecology (Huston et al., 1988). In both approaches, a population increases or decreases depending on the rates at which individuals are born, mature, reproduce, and die, all of which processes depending on time (or age) and one or more characteristics of interest (named *state variables*, e.g. horn length). Although very similar in the kinds of information they provide, IPMs and IBMs are operationally very distinct from each other (Caswell & John, 1992). While IPMs (and their precursor, matrix models, Caswell, 2001) are structured by *top-down* population parameters, such as birth and death rates, in individual-based models those population level parameters emerge from interactions among individuals and between individuals and the surrounding environment and are said *bottom-up models* (DeAngelis & Grimm, 2014). This distinction is at the basis of the strengths and weaknesses that characterise each approach in relation to one another. IPMs are a generalisation of matrix models to continuous state variables, and as for matrix models, algebra can be used with IPMs as a means to describe the dynamics of populations. Such characteristic is extremely powerful, allowing for generalisations that are not possible with simulations (Caswell & John, 1992). Nonetheless, although IPMs can potentially be very general in the kinds of complexity they allow (e.g. stochasticity, density- and frequency dependent populations), they very easily become intractable, in which case simulation models like IBMs are the alternative.

Both IPMs and IBMs are, in principle, equally suited to, aside from modelling demography, life history and ecology, also incorporating the principles of trait transmission among relatives. In IPMs, solutions leaning towards such purpose have begun to be developed. The first IPM used to predict evolutionary change was of body weight and coat colour in the population of wolves (*Canis lupus*) from the Yellowstone National Park (Coulson et al., 2011). As coat colour is determined by a single locus with two alleles this was a simplified genetic IPM, not directly extendable to polygenic traits. For polygenic traits, Barfield et al. (2011) and Childs et al. (2016) have started to set the theoretical grounds to incorporate the infinitesimal model (Fisher, 1918; Bulmer, 1980) into stage- and age- and stage- structured IPMs, respectively. Computer simulations, on the contrary, allow further flexibility in terms of model implementation and have been used to model trait transmission across generations in different contexts and use different approaches to model inheritance (e.g. Castellani et al., 2015; Benthem et al., 2017).

Population models incorporating the principles of trait transmission across generations are extremely useful for testing hypotheses about the effects of different selection pressures on evolutionary change. A particular interest exists in investigating the impact of human activities in the evolution of wild populations (e.g. Hutchings & Fraser, 2008; Allendorf & Hard, 2009; Pigeon et al., 2016). Artificial selection has been used for the purpose of understanding the mechanisms underlying evolution, intentionally as a means to select for particular characteristics of plants and animals, but also unintentionally, as consequence of human activities such as animal or plant harvesting (Harris et al., 2002). The consequences of the latter, typically in wild populations, have been difficult to quantify (Kuparinen & Merilä, 2007). A very important example is associated with intensive fishing, which in addition to being responsible for fish population colapses, is also believed to have resulted in evolutionary change in wild populations (Hutchings & Fraser, 2008; Kuparinen & Festa-Bianchet, 2017). Trophy hunting of ungulates is another selective pressure that is expected to result in evolution (Allendorf & Hard, 2009; Festa-Bianchet et al., 2014). A particular case of interest is the population of bighorn sheep resident at Ram Mountain, in Alberta, Canada, as it was subject to selective harvest, while being intensively monitored and also having been pedigreed (Coltman et al., 2002). Until 2011, males meeting a certain phenotypic criterion of minimum horn curl were considered *trophy rams* and could be legally harvested (Chapter 2, Festa-Bianchet et al., 2014). Horn curl is closely correlated to horn length, which, in turn is of critical importance in horn clashing fights during the rut and, therefore, to male breeding success (Coltman et al., 2002). While males showing fast-growing horns reached legal status from the age of four years (Jorgenson et al., 1998), the reproductive peak is not reached until the age of 8-10 years (Coltman et al., 2002). As a result, many rams were shot before fulfilling most of their reproductive potential (Festa-Bianchet et al., 2004). Through its effect on the reproductive success of rams with larger horns, trophy hunting has operated as selection favouring smaller horn size and has lead, as consequence, to evolutionary change (Coltman et al., 2003; Pigeon et al., 2016).

In this chapter, I develop a two-sex individual-based model of horn length mimicking the population of bighorn sheep inhabiting Ram Mountain. I first derive the vital rates (breeding success, winter mortality, and trophy hunting-related harvest) which, along with the models of development and inheritance of horn length estimated in Chapter 5, are used to simulate the life-cycle of individuals belonging to this population. Such a model has the potential to enlighten as to the consequences of trophy hunting in the evolution of horn size. The advantage of such approach when compared to, for example, predicting evolution with the breeder's equation is its flexibility to incorporate ecological complexity. I present results from simulations obtained using the three alternatives to modelling size trajectories examined in the previous chapter, namely random regression, factor analytic and antedependence models, the latter including a cross-age parent-offspring regression typical of several IPMs (Coulson et al., 2010; Traill et al., 2014; Bassar et al., 2016). In accordance to the results from Chapter 4, I provide strong evidence of the inability of the antedependence solution to identify evolutionary change when it is known to have occurred. Taking into account that random regression was the only alternative capable of recovering similarity across ages within individuals and between individuals and their relatives (Chapter 5), I used this approach to quantify changes in breeding values over 100 years of selective harvesting and along the ontogenetic trajectory of male horn length.

6.2 Study system and data

The IBM built for this chapter is based on the annual cycle of the bighorn sheep population inhabiting Ram Mountain, for which a description is presented in Chapter 2. I used data from 1972 to 2015 to estimate breeding success and winter survival of both males and females, as well as trophy hunting-related survival in males. For male breeding success, I used a subset of the data encompassing years from 1998 to 1992 and from 1996 to 2014, as those are the years when DNA samples were collected and paternities were assigned. All hunters harvesting rams were required by law to register their kill, which enabled an accurate count of harvested individuals. Mortality caused by predation, particularly by cougars (*Puma concolor*), but also from wolves (*Canis lupus*) and black bears (*Ursus americanus*), was disregarded when estimating winter mortality. While this mortality is relevant, much of it results from one cougar that specialised on bighorn sheep during a period of low population size (Festa-Bianchet et al., 2006). Consequently, it generated a pattern of positive density dependent survival, which would have ultimately precluded the implementation of the IBM with a reasonable population dynamic. Although polynomial functions of age were used to fit both breeding success and survival, age classes were adopted to estimate heterogeneous residual variances and slopes for population density, defined as the number of females in the study area, in which case the levels *lambs*, *yearlings*, *2 year-olds*, *3 year-olds* and *older* were considered. Detailed information on how information was collected and how the pedigree was reconstructed is also available in Chapter 2.

6.3 Vital rates

As both the breeding success and the survival of the sheep inhabiting Ram Mountain have already been described in detail (Coltman et al., 2002; Festa-Bianchet et al., 1998; Festa-Bianchet & King, 2007; Jorgenson et al., 1997; Loison et al., 1999), this section serves the single purpose of deriving the functions required to construct the IBM. Note that I use the same symbol to represent parameters with analogous meaning across different models. This solution, although mathematically imprecise (symbols get re-used), was adopted to simplify model interpretation. Model validation via predictions plotted against observed values are shown in Appendix D.1.

6.3.1 Annual breeding success

The nature of annual breeding success (defined as the number of offspring born) differs between male and female bighorn sheep. Whereas a ewe can only produce a single offspring per year, a ram can father multiple lambs. Female annual breeding success was assumed to follow a binomial distribution, whereas for males a multinomial model was adopted. As described by Festa-Bianchet & King (2007), offspring production begins at the age of 2 years in bighorn sheep ewes, is higher for ewes aged 4 to 12 years than for ewes aged 2 or 3 years, and senescence begins at 13 years of age. As a result, I adopted a second-order polynomial function to describe the age-breeding success association in bighorn ewes. The log odds of the probability of ewe i producing an offspring at age t

(abs_{it}) was modelled as follows

$$log\left(\frac{\mathbb{E}[abs_{it}]}{1-\mathbb{E}[abs_{it}]}\right) = \alpha + \beta_{t_s} \times (t_{it} - \bar{t}) + \beta_{t_c} \times (t_{it} - \bar{t})^2 + \sum_{j=2}^{4} I_{j_{it}} \times \beta_{pop_j} \times pop_{it} + u_{pe_i} + u_{m_i} + u_{c_i} + u_{y_i} + \epsilon_{it}, \tag{6.1}$$

where α is the model intercept, β_{t_s} and β_{t_c} are the slope and curvature for mean centred-age $(t - \bar{t})$ and β_{pop_j} is the slope for mean-centred female density (pop) estimated for age class j (*2 year-olds*, *3 year-olds*, or *older*). $I_{j_{it}}$ is an indicator variable for age class j. Note that since the rut occurs in the previous calendar year to the birth of the offspring, population density of the year corresponding to the rut was used. u_{pe_i}, u_{m_i}, u_{c_i}, and u_{y_i} are random intercepts associated with permanent environment, mother, cohort, and year of measurement, respectively. To simplify model notation, indexing in this and the following models refers to individuals and ages only, resulting in u_{m_i} corresponding to the effect associated to the mother of ram i, rather than the effect of mother i. Each random effect was assumed to be drawn from a normal distribution with mean zero and variance σ^2_{pe}, σ^2_m, σ^2_c, and σ^2_y, depending on the source of variation (individual, mother identity, cohort, or year of measurement, respectively). $\boldsymbol{\epsilon}$ are the model residuals, which variance was set to one, as overdispersion is unobservable in binomial mixed models.

Annual breeding success in males is upwardly constrained by the number of available breeding ewes (and more directly by the number of lambs produced each year), and that number is (negatively) correlated to the number of offspring the remaining rams father. The probability p that a particular ram fathers n out of N offspring is well described by a multinomial distribution. For each year k, I define a variable corresponding to the number of offspring fathered by each ram out of the total lambs born that year. The number of lambs fathered by a particular ram i in year k follows a multinomial distribution with parameters N_k and $\vec{p_k}$,

$$n_k \sim Multinomial(N_k, \vec{p_{ik}}), \tag{6.2}$$

where $\vec{p_{ik}}$ is a vector with the probabilities of each ram i fathering n_k offspring as a proportion of the offspring fathered by all the rams. Therefore, each of these probabilities is defined as follows

$$p_{ik} = \frac{p'_{ik}}{\sum_i p'_{ik}}. \tag{6.3}$$

p'_{ik}, the number of offspring fathered by ram i when he is of age t in a particular year k, can be modelled, for each year, as a function of any covariates of interest, as follows

$$p'_{it} = e^{\beta_{ts} \times (t_{it} - \bar{t}) + \beta_{hs} \times hl_{it} + \beta_{t,h} \times (t_{it} - \bar{t}) \times hl_{it} + u_{pe_i} + u_{m_i} + u_{c_i} + u_{y_i}}, \tag{6.4}$$

where β_{t_s} and β_{h_s} are the slopes for mean-centred age $(t - \bar{t})$ and mean-centred horn length (hl), respectively, and $\beta_{t,h}$ corresponds to a linear interaction term between age and horn length. Note that since the rut occurs in the previous calendar year to the birth of the offspring, horn length of the year corresponding to the rut was used. As in the model for females, u_{pe_i}, u_{m_i}, u_{c_i}, and u_{y_i} are random

effects associated with permanent environment, mother identity, cohort, and year of measurement, respectively. The residuals in this model are unobservable.

While female breeding success clearly shows the effect of senescence, with a significant negative quadratic effect for age (Fig. 6.1, Tab. 6.1, Festa-Bianchet & King, 2007), breeding success in males increases with age along the entire lifespan and with horn size (Fig. 6.1, Tab. 6.1, Coltman et al., 2002). The effect of population density was not explicitly estimated in the multinomial model because it is implicitly incorporated by construction - the probability of n out N lambs being fathered by a certain ram is estimated, where N is very closely related to the number of ewes present in the study area in each year. As for females, breeding success is higher under low population densities (Fig. 6.1, Tab. 6.1, Martin & Festa-Bianchet, 2011).

Table 6.1: Parameter estimates of the binomial and multinomial regressions of annual breeding success in bighorn sheep females and males, respectively, from the population at Ram Mountain. Logit and exponential link functions were adopted. Results correspond to means of posterior distributions and 95% HPD credible intervals.

		females		males	
	parameter	mean	95% CrI	mean	95% CrI
fixed effects	intercept	2.04	(1.57; 2.50)	-	-
	age	0.05	(-0.01; 0.10)	0.03	(-0.36; 0.44)
	age^2	-0.07	(-0.09; -0.06)	-	-
	population$_2$	-0.03	(-0.06; -0.01)	-	-
	population$_3$	-0.04	(-0.06; -0.01)	-	-
	population$_{older}$	-0.01	(-0.02; 0.01)	-	-
	horn length	-	-	0.04	(-0.01; 0.10)
	age $\times$ horn length	-	-	0.00	(-0.01; 0.01)
random effects	permanent environment	0.35	(0.00; 0.64)	0.12	(0.00; 0.38)
	mother	0.08	(0.00; 0.27)	0.05	(0.00; 0.19)
	cohort	0.09	(0.00; 0.28)	0.11	(0.00;0.48)
	year	1.37	(0.63; 2.16)	-	-
	residual	set to 1		-	-

6.3.2 Harvest-related survival

As detailed in Chapter 2, trophy hunting was allowed at Ram Mountain from before the beginning of the study until 2011. Until 1996, rams could be harvested when describing at least four-fifths of a curl, which was limited from then on to rams presenting a full-curl. This latter criterion is very restrictive resulting in only four rams being shot since 1996 (Pigeon et al., 2016). Here, I mimicked the harvest intensity that existed at Ram Mountain during the $4/5$ criterion period, and therefore I used data until 1996 only. The probability, h, of ram i not being harvested at age t was modelled with the following binomial model

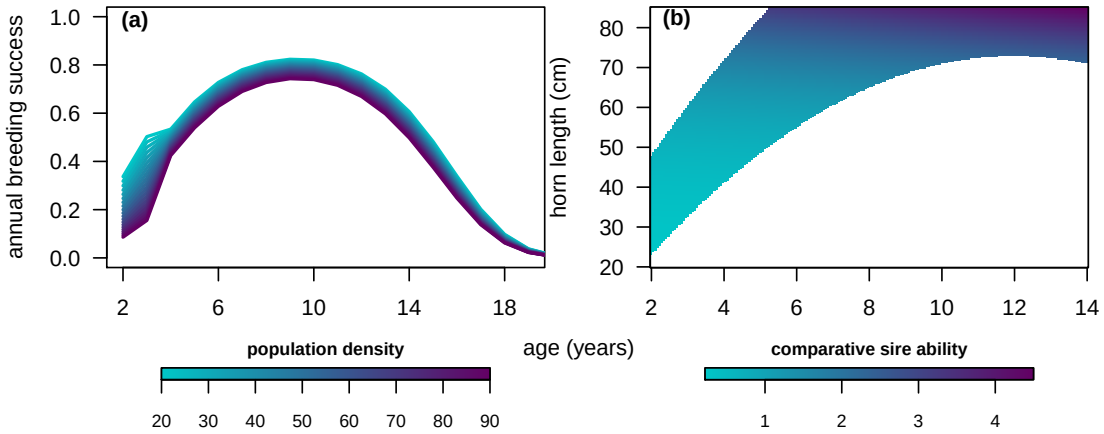

Figure 6.1: Annual breeding success in bighorn ewes (a) and rams (b) at Ram Mountain, as a function of age and population density (females) and age and horn length (males). The predictions are based on the models in Equation (6.1), and Equations (6.2-6.4), for which estimates are shown in Table 6.1. Sire breeding success is compared to that of 7 year-old males with horn length of 60 cm.

$$log\left(\frac{\mathbb{E}[h_{it}]}{1-\mathbb{E}[h_{it}]}\right) = \alpha + \alpha_{lamb} \times I_{lamb_{it}} + (1 - I_{lamb_{it}}) \times (\beta_{t_s} \times (t_{it} - \bar{t}) + \beta_{t_c} \times (t_{it} - \bar{t})^2 + \beta_{h_s} \times hl_{it} + \beta_{h_c} \times hl_{it}^2 + \beta_{t,h} \times (t_{it} - \bar{t}) \times hl_{it}) + I_{4_{it}} \times \beta_{pop_4} \times pop_{it} + u_{m_i} + u_{c_i} + u_{y_i} + \epsilon_{it}, \quad (6.5)$$

where α is the intercept of the model and α_{lamb} is the intercept contrast for lambs (I_{lamb} is an indicator variable for lambs, which takes the value 1 if age is 0 and the value 0 otherwise). β_{t_s} and β_{t_c} are the slope and curvature associated with mean-centred age $(t - \bar{t})$, whereas β_{h_s} and β_{h_c} are the slope and curvature associated with mean-centred horn length (hl). These parameters and a linear interaction term between age and horn length, $\beta_{t,h}$, were not estimated for lambs. Finally, a slope for female density (β_{pop_4}) was also estimated. Given that the youngest age at which rams were shot by hunters was 4 years, this slope was only estimated for the age class *older*, which includes 4 year-olds and older individuals. u_{m_i}, u_{c_i}, and u_{y_i} are random effects associated with maternal identity, cohort, and year of measurement, respectively. Those effects were assumed to be drawn from independent normal distributions with variances σ_m^2, σ_c^2, and σ_y^2, respectively. As in the model of female breeding success, the variance in the residuals ($\boldsymbol{\epsilon}$) was set to one, as overdispersion in unobservable in binomial mixed models. The model predicts that trophy hunting leads to mortality of rams with particularly long horns and that virtually does not occur in young individuals, which corresponds to a good description of reality (Tab. 6.2, Fig. 6.2a), as described by Jorgenson et al. (1998).

6.3.3 Winter survival

As for breeding success, winter survival was modelled separately for males and females. In females, survival was assumed to be a function of age and population density, and therefore a binomial model

with a logit link function of the following form was adopted

$$log\left(\frac{\mathbb{E}[s_{it}]}{1-\mathbb{E}[s_{it}]}\right) = \alpha + \alpha_{lamb} \times I_{lamb_{it}} + (1 - I_{lamb_{it}}) \times (\beta_{t_s} \times (t_{it} - \bar{t}) + \beta_{t_c} \times (t_{it} - \bar{t})^2) + \sum_{j=0}^{4} I_{j_{it}} \times \beta_{pop_j} \times pop_{it} + u_{m_i} + u_{c_i} + u_{y_i} + \epsilon_{it}, \tag{6.6}$$

where s_{it} is the probability of ewe i surviving the winter at age t, α is the model intercept and α_{lamb} a contrast to the intercept for lambs. The remaining parameters have a similar interpretation as described in previous models. Winter survival in males was modelled similarly to harvest-related survival, described in Equation (6.5), aside from the slopes for population density estimated for each age class, as follows

$$log\left(\frac{\mathbb{E}[s_{it}]}{1-\mathbb{E}[s_{it}]}\right) = \alpha + \alpha_{lamb} \times I_{lamb_{it}} + (1 - I_{lamb_{it}}) \times (\beta_{t_s} \times (t_{it} - \bar{t}) + \beta_{t_c} \times (t_{it} - \bar{t})^2 + \beta_{h_s} \times hl_{it} + \beta_{h_c} \times hl_{it}^2 + \beta_{t,h} \times (t_{it} - \bar{t}) \times hl_{it} + \sum_{j=0}^{4} I_{j_{it}} \times \beta_{pop_j} \times pop_{it} + u_{m_i} + u_{c_i} + u_{y_i} + \epsilon_{it}. \tag{6.7}$$

The probability of winter survival is lower for lambs (only shown for females as no records of horn length were used for male lambs) and is very high in early ages, particularly in females (Tab. 6.2, Fig. 6.2c, d, e). Senescence in females starts around the age of 8 years while in males lower rates of survival are observed earlier in life, a pattern that has been described by Loison et al. (1999). Interestingly, there is a viability cost to carrying large horns in males (Fig. 6.3), an effect that is more evident in years of high population density (Fig. 6.2b3).

6.3.4 Horn length ontogenetic trajectories

Horn length at each age and the underlying correlations among ages within individuals and between individuals and their relatives were modelled as described in Chapter 5. In this chapter I show simulations using the random regression model, the factor analytic model with a single additive genetic axis, and the antedependence model coupled with the cross-age parent-offspring regression as the inheritance function.

6.3.5 Parameter estimation and reported statistics

The statistical models introduced in this chapter were fitted in a Bayesian framework, using JAGS (Plummer, 2003, male breeding success; code available in Appendix D.2) and MCMCglmm (Hadfield, 2010, remaining models). Diffuse normal distributions were used as prior distributions for the fixed effects, whereas inverse Wishart and inverse gamma were adopted as prior distributions for the variance components associated with the random effects, using parameter expansion to increase

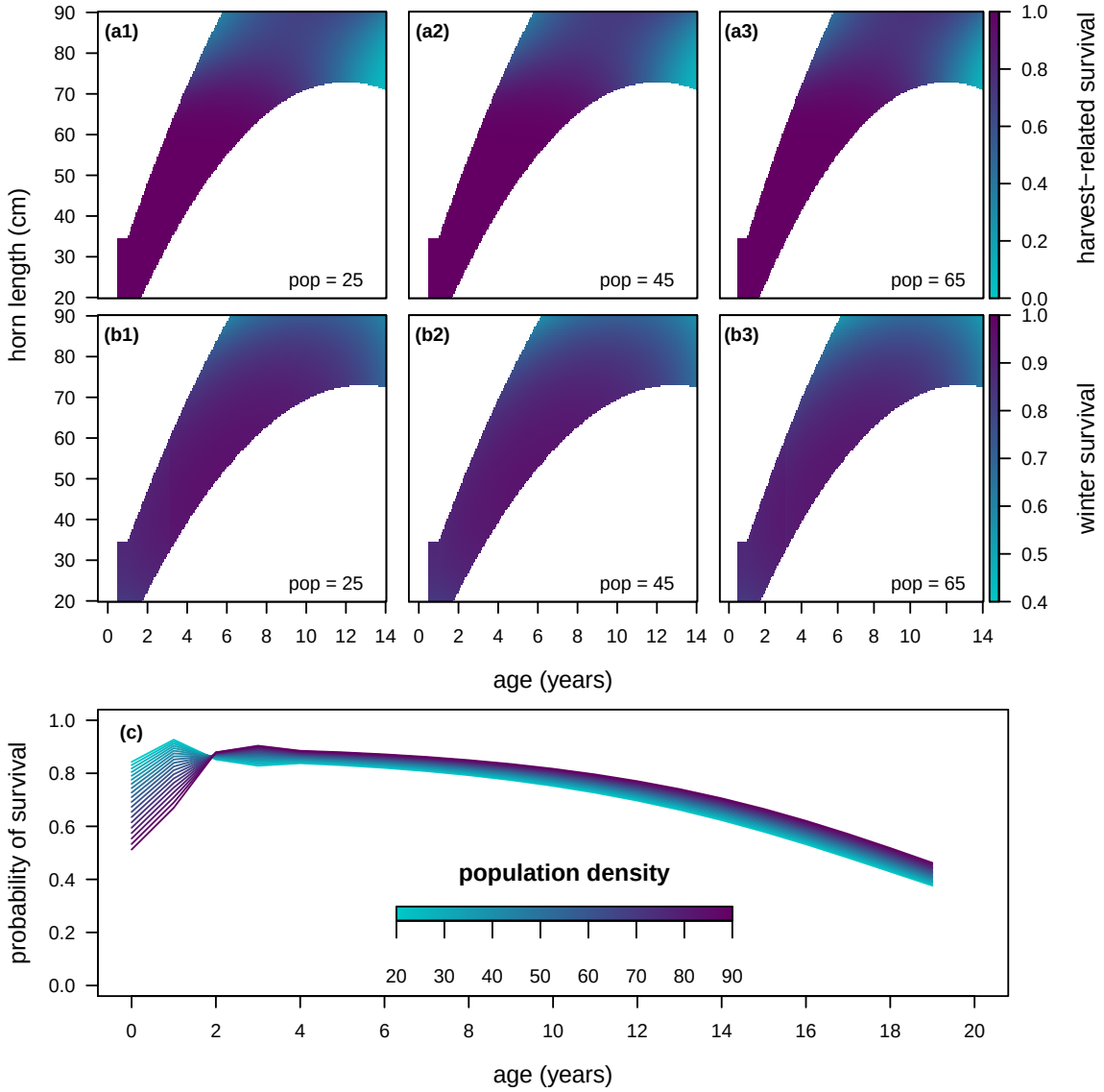

Figure 6.2: Annual survival probability as a function of age, population density and horn length in the bighorn sheep population at Ram Mountain; male harvest-related survival (a), and male (b) and female (c) winter survival are shown. For harvest-related and winter survival in males, results are shown for three different population densities (25, 45, and 65 females). Coloured lines in (c) corresponds to prediction for different values of population density.

Table 6.2: Parameter estimates of binomial regressions of winter and harvest-related survival fitted to data from the bighorn sheep population at Ram Mountain. Logit link functions were adopted, and results correspond to means of posterior distributions and 95% HPD credible intervals.

		females				males	
		winter survival		harvest survival		winter survival	
parameter		mode	95% CrI	mode	95% CrI	mode	95% CrI
fixed effects	intercept	1.87	(1.44; 2.26)	9.06	(-0.15; 21.12)	3.31	(1.76; 4.74)
	lamb	-0.39	(-0.82; 0.01)	79.90	(59.66; 101.78)	-2.44	(-3.99; -0.94)
	age	-0.15	(-0.21; -0.10)	-1.02	(-4.12; 2.39)	-0.07	(-0.67; 0.54)
	age^2	-0.01	(-0.02; 0.00)	-0.18	(-0.47; 0.09)	-0.06	(-0.19; 0.06)
	horn length	-	-	-0.43	(-1.44; 0.23)	-0.02	(-0.13; 0.08)
	$horn\ length^2$	-	-	0.00	(-0.01; 0.02)	-2.0e-03	(-4.2e-03; 2.8e-05)
	age $\times$ horn length	-	-	0.07	(-0.09; 0.21)	0.01	(-0.02; 0.05)
	$population_0$	-0.03	(-0.05; -0.02)	-	-	-0.02	(-0.04; -0.01)
	$population_1$	-0.03	(-0.05; -0.01)	-	-	0.00	(-0.02; 0.02)
	$population_2$	0.00	(-0.01; 0.03)	-	-	-0.01	(-0.04; 0.01)
	$population_3$	0.01	(-0.01; 0.03)	-	-	-0.01	(-0.04; 0.01)
	$population_{older}$	0.01	(-0.01; 0.02)	0.02	(-0.04; 0.08)	-0.01	(-0.03; 0.01)
random effects	maternal ID	0.15	(0.00; 0.41)	7.10	(0.00; 22.16)	0.08	(0.00; 0.30)
	cohort	0.21	(0.00; 0.47)	2.22	(0.00; 10.40)	0.48	(0.00; 1.11)
	year of measurement	0.67	(0.24; 1.21)	3.39	(0.00; 11.70)	0.39	(0.00; 0.89)
	residual		set to 1		set to 1		set to 1

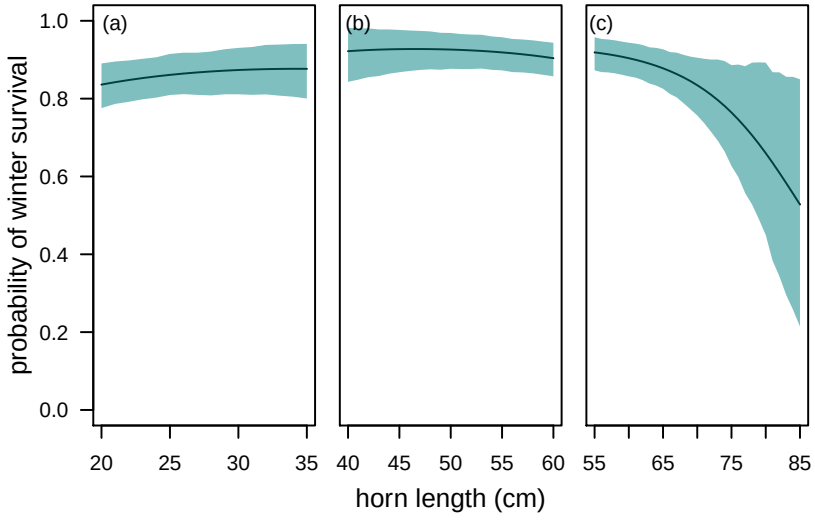

Figure 6.3: Probability of annual winter survival as a function horn length for ages one (a), four (b), and seven (c) years, for the bighorn rams from the population at Ram Mountain. The black lines correspond to averages, whereas the areas in teal correspond to 95% credible intervals, both predicted using the model in Equation 6.7.

convergence (Gelman, 2006; Hadfield et al., 2010). Parameter estimates were defined as corresponding to means of the posterior distributions and uncertainty around those estimates was reported using Highest Posterior Density (HPD) credible intervals.

6.4 The model

6.4.1 Model description

I built a stochastic simulation model mimicking populations of bighorn sheep, and structured according to the annual cycle of the population from Ram Mountain (Fig. 6.4a). At Ram Mountain, bighorn sheep are born during the spring, most growth occurs until August, after which the breeding season occurs mainly from October to December (Festa-Bianchet, 1988; Festa-Bianchet et al., 1995). Most natural mortality occurs during the winter, until March (Schindler et al., 2017). In this annual cycle, I also considered that a hunting season could occur, from August to October, as it used to at Ram Mountain until 2011, and is the case throughout Alberta. So as to take into account this sequence of events, I defined the time step of the model to be one year, with the cycle beginning with the birth of a new cohort during the spring. In the simulations I present in this chapter, the population in each simulation run was represented at the first year step, $year = 1$, by 50 males and 50 females (see Fig. 6.4b for observed population dynamics of bighorn sheep inhabiting Ram Mountain). Both males and females could reproduce for the first time from the age of two years, and were assumed to live up to 15 and 20 years, respectively. The mechanics of horn length inheritance were implemented according to the growth functions estimated in Chapter 5. As a result, breeding values were passed on from parents to their offspring (see Eqn. 4.3 and Eqn. 4.4 in Chapter 4) in scenarios using random regression or factor analysis, whereas trait transmission was purely phenotypic in scenarios using the antedenpendence model, in which the cross-age parent-offspring regression was adopted. Particularly, intercepts, slopes and curvatures defining ontogenetic trajectories of breeding values were passed on to the offspring in scenarios using random regression, whereas in scenarios using the factor analytic model age-specific breeding values were transmitted. Results of simulations where no mechanism of inheritance is built-in are also shown, reflecting the average state of the population at Ram Mountain. A burn-in of 200 years (iterations) was adopted for scenarios with no inheritance, whereas a burn-in of 1000 iterations was used in scenarios with a functional inheritance mechanism (see Appendix D.3 for details regarding how the burn-in periods were defined and supplementary information on simulated dynamics and vital rates). I show results of simulations run for 200 years after the burn-in period, corresponding first to a set of 100 years of no harvest and the subsequent 100 years with harvest simulated using Equation 6.5. The number of simulations run for each scenario is shown in Table 6.3 and a description of how the model was implemented is presented in Figure 6.5.

6.4.2 Comparison of alternative approaches to modelling horn length trajectories

The statistical models fitting the ontogenetic trajectories of horn length introduced in the previous chapter were used, together with the remaining vital rates, to simulate populations similar to the

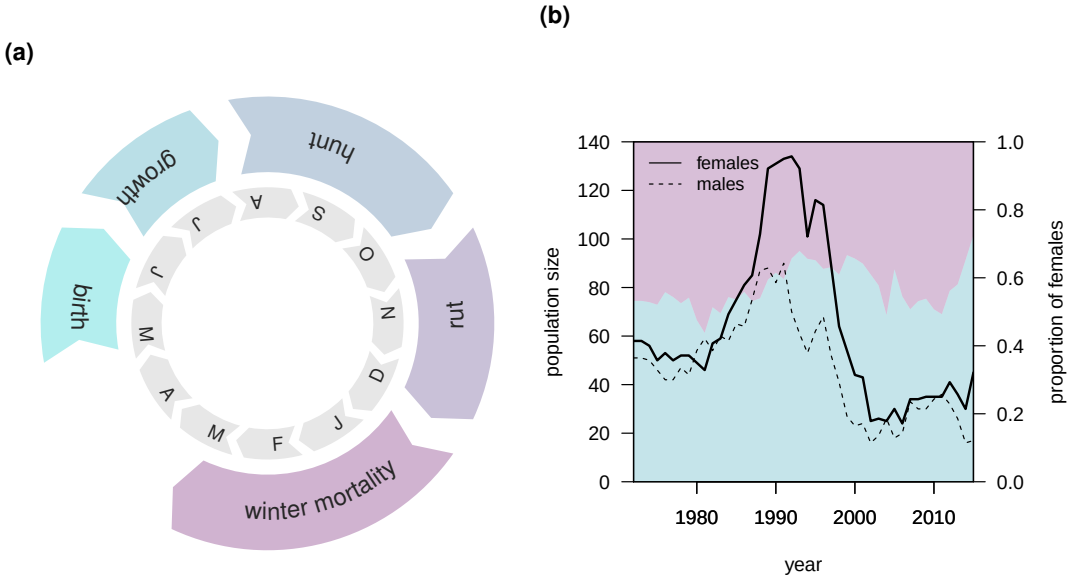

Figure 6.4: (a) Annual cycle of the bighorn sheep at Ram Mountain, illustrating the time of the year at which the main events occur, including the hunting season. The letters in the inner circle represent the months of the year. (b) Population dynamics and sex-ratio from 1972 to 2015.

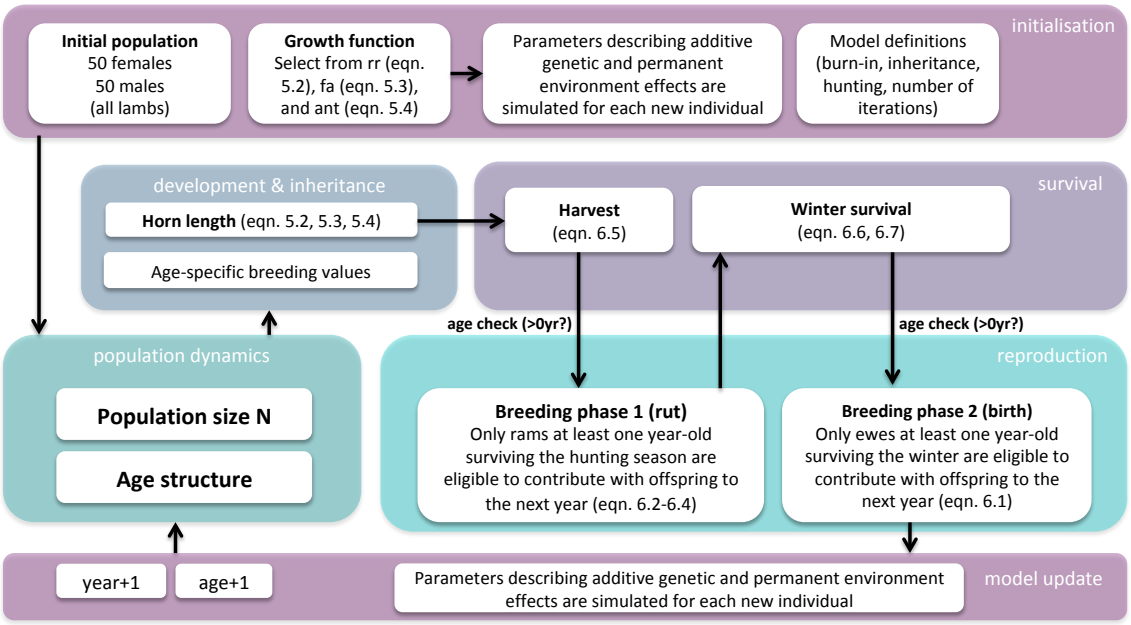

Figure 6.5: Simplified illustration of the individual-based model mimicking the life-cycle of the bighorn sheep inhabiting Ram Mountain.

Table 6.3: Number of simulations run for each combination of growth function, inheritance and hunting settings.

	no inheritance	inheritance	inheritance + hunting
`rr`	100	200	200
`fa`	50	50	50
`ant`	50	50	50

bighorn sheep population at Ram Mountain and, ultimately, to assess the phenotypic and genetic responses to selective hunting. As I show in Chapter 5, only the random regression model was adequate to recover similarity across ages between individuals and their relatives. As a consequence, only this solution has the potential to reflect a putative evolutionary response to trophy hunting. This is indeed suggested by horn length trajectories simulated over a period of 200 years, the last 100 of which under a selective pressure similar to that observed at Ram Mountain until 1996 (Fig. 6.6). All three alternatives show some kind of phenotypic decrease in horn length later in life, which corresponds at least partially to a (within generation) demographic response, as rams with larger horn are more likely to be removed from the population. While the responses observed in scenarios using factor analysis and the antedependence model are very modest and only apparent by the age of 7 years, responses predicted by the random regression scenario are more prominent and evident starting at the age of one year. This latter result suggests an evolutionary response to trophy hunting, given that any demographic response mediated by a decrease in population density would have the opposite effect. In light of these and last chapter's results, response to trophy hunting will be further investigated using the random regression approach.

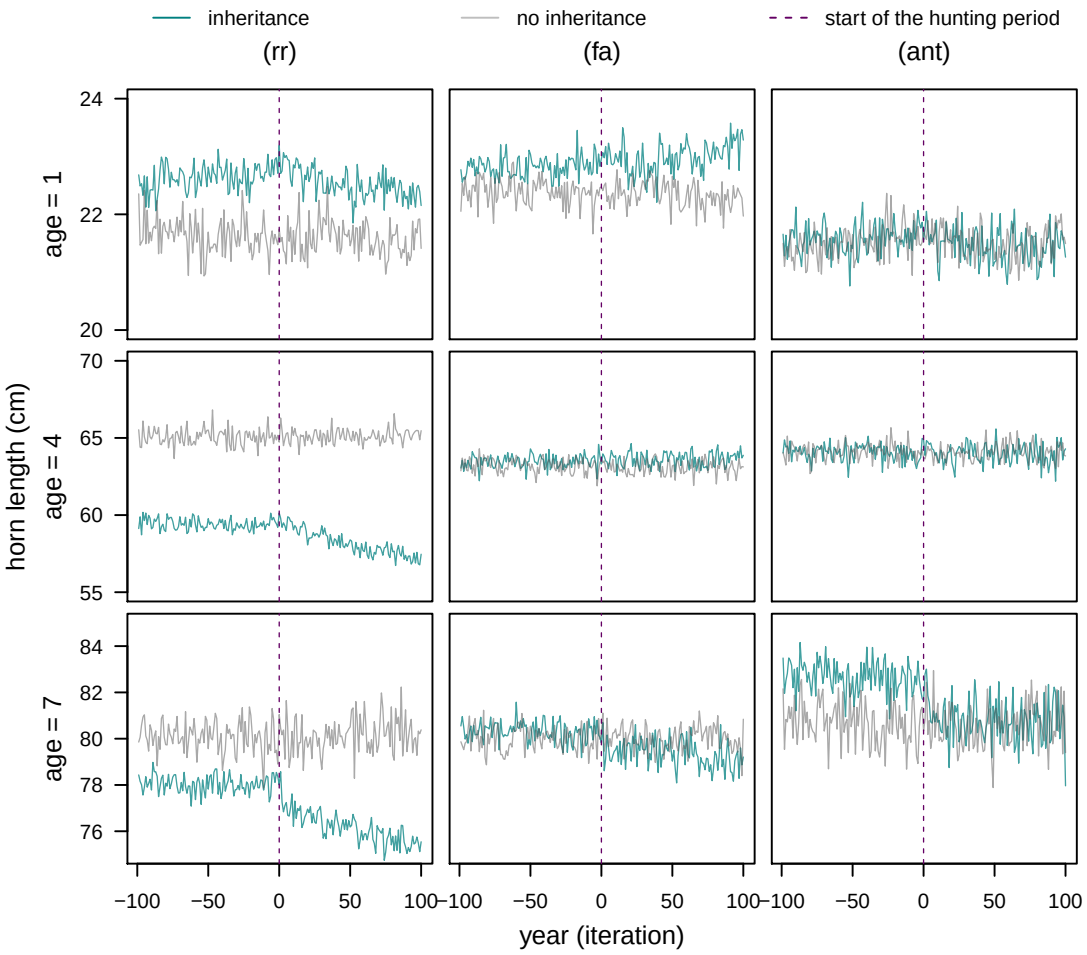

Figure 6.6: Male horn length dynamics simulated over 200 years, of which the last 100 years correspond to a hunting period. Results are shown for the three approaches to modelling horn length trajectories, random regression (`rr`), factor analysis (`fa`) and the antedependence model (`ant`), and for three different ages (1, 4, and 7 years). Each plot also includes a scenario with no inheritance, establishing the average state of the population at Ram Mountain.

6.4.3 Measuring evolution

The central aim of this chapter is to quantify the genetic contribution to the observed change in horn length due to trophy hunting. As a consequence, this particular model was not built to quantify the demographic response to such selective pressure. The demographic component of the response, which acts via two distinct effects, a plastic response to density reduction (as a consequence of ram removal) and within-generation response to selection, is therefore not shown. Nonetheless, given that the yearly rate of removal is very low (average of 2.4 males per year, Jorgenson et al., 1993), these effects are not expected to be particularly consequential. Phenotypic and additive genetic changes are, therefore, presented. The response to selective harvest is apparently very fast, occurring immediately after hunting is applied (Fig. 6.6, `rr`). The observed response in lambs and four year-olds suggest that the response to artificial selection starts very early in life, rather than involving older ages only, which is corroborated by assessing the entire ontogenetic trajectory (Fig. 6.7). As noted before, this effect occurs very few generations after hunting is started. Additionally, there are considerable changes in the mean intercept, slope and curvature defining the ontogenetic trajectories of breeding values after hunting is applied (Fig. 6.8). The value of the intercept decreases by 44% and both the slope and the curvature increase. As a consequence, age-specific breeding values decrease markedly since the age of one year (Fig. 6.9).

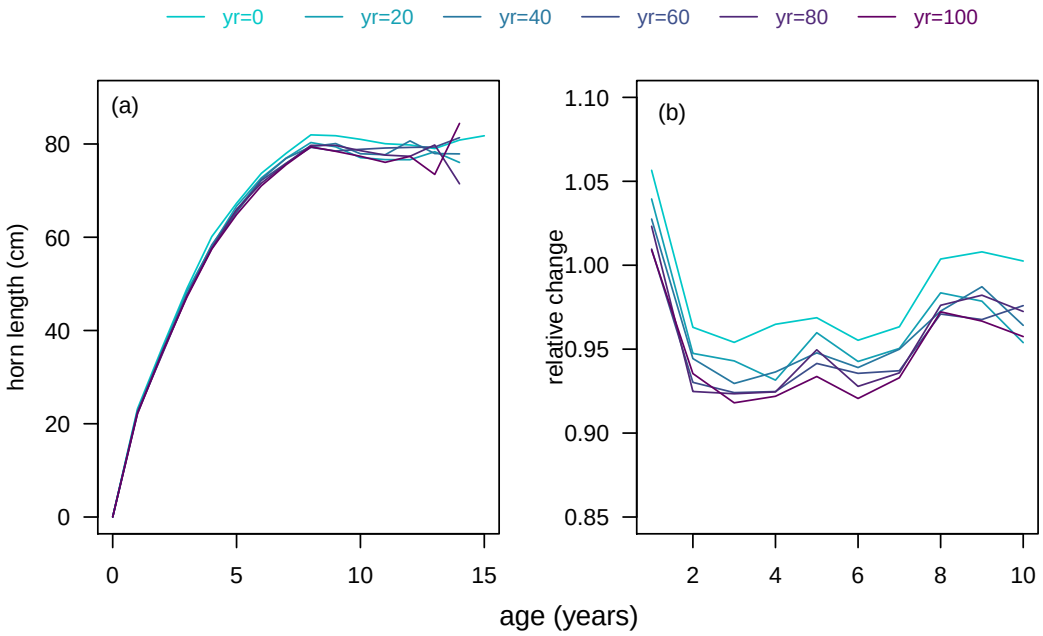

Figure 6.7: Average male horn length ontogenetic trajectories for different years (iterations) after the start of the hunting period (a), and the relative change in horn length across the ontogeny, with respect to observed age-specific means (b).

From a purely technical perspective it is also interesting to note that before simulated harvest started at $year = 1$, horn length was not evolving towards larger lengths, or it was doing so at a very slow rate (Fig. 6.6, `rr`). More importantly, horn length had evolved already to an optimum that is slightly

smaller than currently observed horn sizes. This result suggests that the approach adopted here, which considers different ecological complexities, might have been able to avoid the paradox of stasis, in particular by capturing opposing selection pressures at different stages of the life cycle.

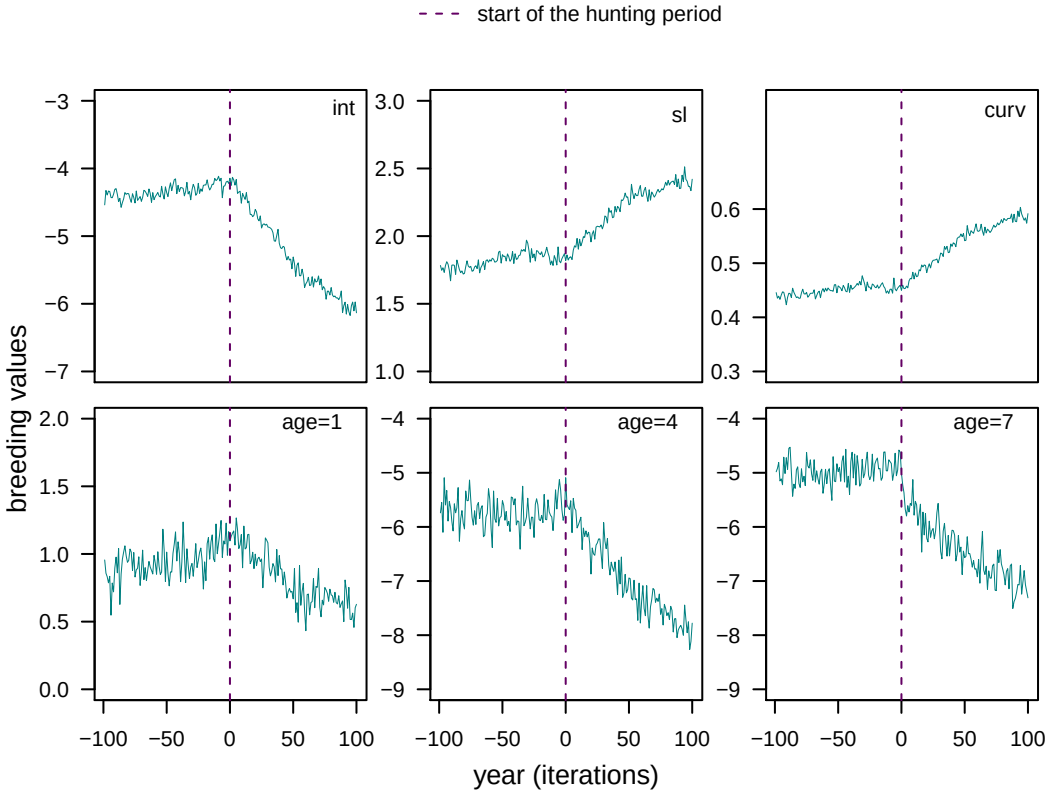

Figure 6.8: Trajectories of the breeding values of male horn length as simulated using the random regression model over 200 iterations, of which the last 100 correspond to a hunting period. Results are shown for the intercept (`int`), slope (`sl`) and curvature (`curv`) used to describe the ontogenetic trajectories of breeding values, as well as age-specific breeding values for ages 1, 4 and 7 years.

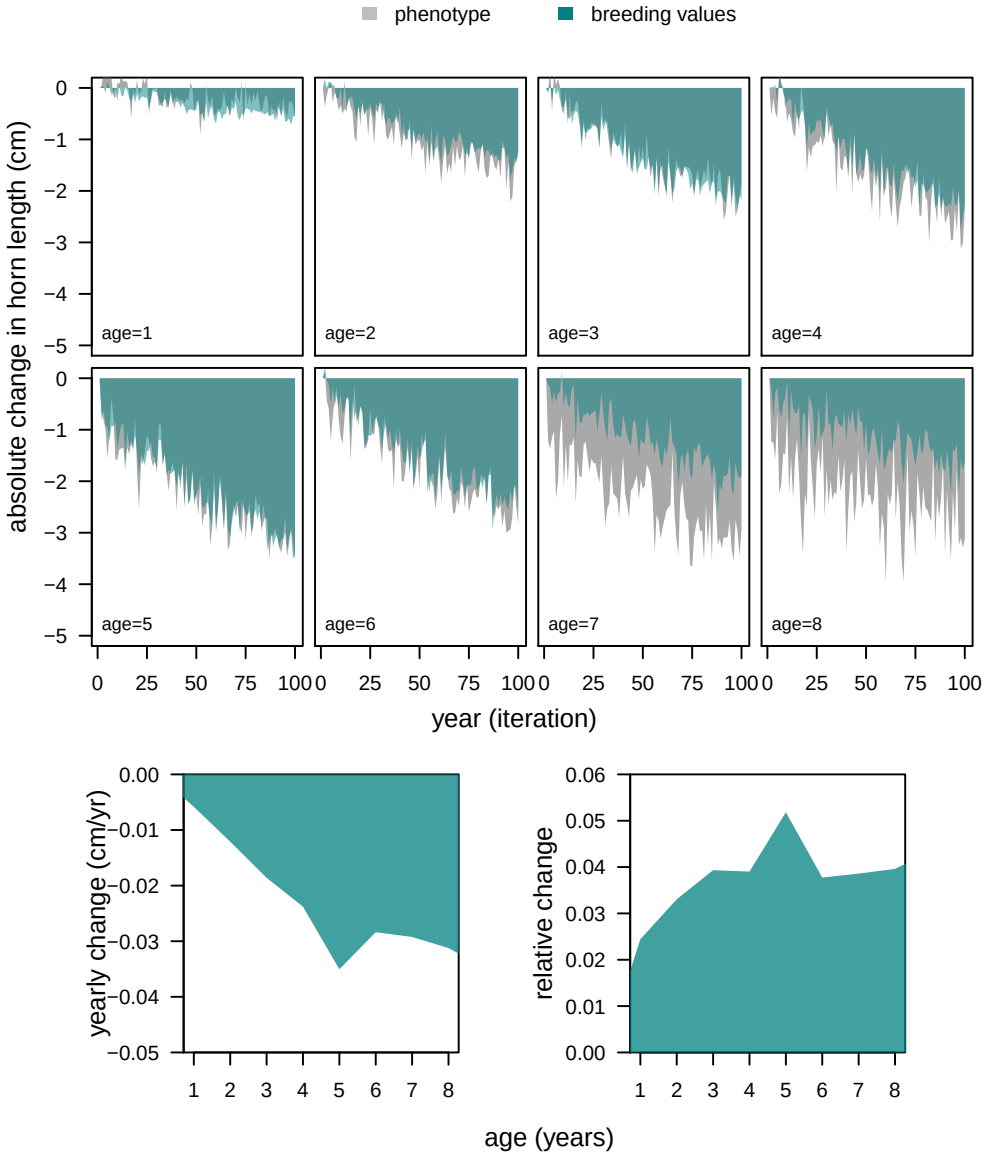

Figure 6.9: Differences in horn length (phenotype and breeding values) from the beginning of the hunting period over 100 years for ages from 1 to 8 years (upper panels). Yearly and relative phenotypic rate of change across the ontogeny of bighorn sheep males, corresponding to changes between year 1 and year 100, after hunting was started (lower panel). Relative changes correspond to the difference between horn length at year 1 and year 100 divided by the value at year 1.

6.5 Discussion

The simulations presented in this chapter provide strong evidence that selective harvesting: (1) has the potential to result in rapid evolutionary change (*sensu* Fussmann et al., 2007), and (2) is very likely to have resulted in evolutionary change in the bighorn sheep population at Ram Mountain, until 1996. Human-mediated disturbances, which have been argued as the *world's greatest evolutionary forces* (Palumbi, 2001), can take different shapes, from pollution and habitat fragmentation to climate change. From these disturbance contexts (reviewed by Hendry et al., 2017), hunting or harvesting animals and plants have been particularly associated with creating strong and consistent directional selection, therefore having the potential to result in evolutionary change (provided traits are evolvable). Virtually all hunting or harvesting involves a selective process of some kind, as the largest individuals of each generation are very often targeted and disproportionately removed (Allendorf & Hard, 2009; Kuparinen & Festa-Bianchet, 2017). As a result, selective harvesting is believed to have many times resulted in *rapid evolution* (Schoener, 2011), the bighorn sheep population of Ram Mountain constituting one of such examples (Coltman et al., 2003; Pigeon et al., 2016).

The genetic consequences of hunting have been grouped in (1) alterations of population structure, (2) loss of genetic variation, and (3) evolutionary response to selection (Harris et al., 2002; Allendorf et al., 2008). In this chapter, I focused my attention on the latter by quantifying the genetic change in horn length, provided that strong selection against large horn length had been documented for this population as a result of trophy hunting (rams with *legal* horns had a probability of 40% of being harvested each year, including each of the approximately 3-4 years between becoming legal and reaching prime reproductive age, Coltman et al., 2003, 2005; Bonenfant et al., 2009b). The simulations I ran corroborate the findings by Coltman et al. (2003) and Pigeon et al. (2016), strongly suggesting that in the presence of selective harvesting, bighorn rams evolve smaller horns. In general, although evidence of phenotypic change due to harvest is very conspicuous in the literature (Darimont et al., 2009), quantification of genetic change using quantitative genetic tools is scant for wild populations (but see Swain et al., 2007), possibly a result of the nature of the data needed to use these tools. Additionally, given the evidence demonstrating a decrease in age-specific breeding values since very early ages, evolving shorter horns seems to have occurred by decelerating growth rates (Fig. 6.7 and Fig. 6.8). Further evidence supporting this hypothesis comes from the decline in the proportion of harvested rams in Alberta that are aged 4 or 5 years, from about 25% in the 1980's to less than 10% in recent years (Festa-Bianchet et al., 2014). These results are in agreement with the notion that growth rates are rarely at their physiological maximum and therefore are the result of a trade-off between benefits and costs of growing faster (Blanckenhorn, 2000; Dmitriew, 2011). In fact, change in horn length in bighorn males under harvesting selection not only constitutes an example of suboptimal growth rates, but also provides an example of genetic adaptation of ontogenetic trajectories.

The IBM used in this chapter was parameterised using empirical data from to the population of bighorn sheep at Ram Mountain and, as a result, the conclusions reached here apply primarily to this population. The rates of phenotypic and evolutionary change in horn length due to selective harvesting varied across the ontogeny of bighorn rams, reaching its maximum at the age of 5 years (Fig. 6.8, upper panels). Both horn length and the corresponding breeding values decreased up to

approximately -0.035 cm/year, which corresponds to up to around 5% change from the phenotype observed prior to harvesting (Fig. 6.8, lower panels). Previously, Coltman et al. (2003) estimated a much steeper phenotypic trend of -0.35 cm/year, from which -0.075 cm was attributable to evolutionary change. Additionally, Pigeon et al. (2016), improving the methodology adopted by Coltman et al. (2003) in light of Postma (2006) and Hadfield et al. (2010), estimated a rate of change in breeding values of male horn length of -0.119 cm/year. Although the change in breeding values estimated in this chapter is qualitatively very consistent with the previous estimates, the dynamic approach I used is expected to yield results that are distinct from these previous estimates (Benthem et al., 2017), which rely on the direct application of the animal model (Henderson, 1975). While the animal model produces estimates that reflect the average state of the population, a dynamic approach allows quantitative genetics tools like the animal model to be incorporated with population dynamics so that microevolutionary dynamics are predicted under realistic assumptions of population structure and individual life histories. A dynamic approach as the one adopted in the present chapter can prove very powerful by simultaneously handling complexities such as age-structure, overlapping generations, sexual antagonism or environmental heterogeneity on selection in a particularly efficient manner. Also, previous results report estimates of changes in breeding values that actually occurred. These will have a component attributable to a response to selection, but also a component due to drift. There is an equal chance of drift occurring in the same *versus* opposite direction as the partial change owing to the response to selection. My inferences average over many runs to estimate the component due only to the response to selection. Thus, it is quite possible that the apparent discrepancy is mostly due to drift.

In addition to the results of Coltman et al. (2003) and Pigeon et al. (2016), Darimont et al. (2009) reviewed phenotypic rates of change associated to harvesting that were considerably higher than the estimates provided in this chapter. Darimont et al. (2009), arguing that the pace of change is exceptionally high under *harvest selection* (exerted by fishers, hunters, and plant harvesters), estimated an overall decrease in morphological traits of 18.3%. Although there is a clear and pragmatic interest in obtaining statistics like this one, interpretation should not go beyond the phenotype towards evolutionary change. In systems subject to heterogeneous environmental conditions, overlapping generations and density-dependent responses, demographic models coupled with quantitative genetics tools have the potential to provide the means to infer about what evolutionary change may be contributing to such phenotypic trends.

The individual-based model adopted here is a compromise between describing the complexity of the ecology and life history of the bighorn sheep and parsimony attending to computational limitations. As a result, several limitations can be identified. The model presented is particularly useful in tracking changes in breeding values when population dynamics are changing over time. However, it does not quantify the demographic contribution to phenotypic adaptation. For each individual a record of its horn length and associated breeding values is generated, but the scope for population density-mediated response is not quantified. Males are known to grow longer horns or antlers at low density because of weaker intraspecific competition (Jorgenson et al., 1998; Festa-Bianchet et al., 2004), and the Ram Mountain bighorn sheep population has gone through larger fluctuations in ecological conditions than my IBM is designed to study. Additionally, despite the high flexibility of computer simulations, I simplified the implementation of the IBM by not making entire use of the variance partition

I used in the statistical models of horn length, annual breeding success and annual survival. Additive genetic and permanent environment (co)variation were implemented but other sources of variation, e.g. heterogeneity in vital rates among cohorts, were grouped together as residual variance. Finally, the results presented in this chapter are based in a modest number of simulations, leading to estimates that, although clear, are *noisier* than one would consider ideal.

6.6 Summary

The individual-based model parameterised according to the life history of the bighorn sheep population at Ram Mountain corroborates the results by Coltman et al. (2003) and Pigeon et al. (2016), showing that selective harvest in this population should result in evolutionary change towards smaller horn length. Under a selective pressure with the magnitude of that imposed at Ram Mountain until 1996, a yearly decrease of up to -0.035 cm is expected in breeding values. This rate of change is smaller than previous estimates for the same population. The reason for such difference might lie in the use of a population model that can predict microevolutionary dynamics under realistic assumptions of population structure and individual life histories. In the IBM adopted in this chapter, life history traits vary yearly according not only to horn length, but also to population size and structure, which is challenging, if not impossible in practice, in non-dynamic approaches.

CHAPTER 7

General discussion

7.1 Summary of findings

The ultimate goal of this thesis is to identify potential sources of bias and error in the prediction of evolutionary change in size and to provide methodological alternatives that could alleviate those biases and errors. In Chapter 3 I provide evidence that a trade-off between viability and fecundity selection is regulating body mass in Soay sheep (*Ovies aries*) female lambs. Mechanistically, this trade-off lies on the additive genetic correlation between pregnancy during the first year of life and body mass. I determined that failing to recognise and account for such correlation leads to an overestimation of the strength of the selection acting on body mass, an effect that increases with population density, potentially contributing to the paradox of stasis observed in this species (Ozgul et al., 2009). While Chapter 3 refers to a single age only, there is evidence that this mechanism could play a role at regulating body mass in the entire population, an effect that would be mediated by correlations among ages and sexes that are known to exist in this species (Wilson et al., 2007; Robinson et al., 2009).

The remaining chapters of the thesis focus on the ontogenetic trajectories of size, and particularly of body mass and horn length. Chapter 4 identifies sources of error in estimating similarity across ages within individuals and between individuals and their relatives in typical applications of integral projection models (IPMs). Rather than being a generalisation of the notion of inheritance, the cross-age parent-offspring regression (Coulson et al., 2010; Coulson, 2012; Rees et al., 2014; Schindler et al., 2013; Traill et al., 2014; Bassar et al., 2016) represents an extremely limited mathematical model of inheritance, with little or no relation to known biological mechanics of inheritance (Fisher, 1918, 1930; Wright, 1922, 1931). This lack of correspondence emerges from three different features: a) regression to the mean acting on ancestral regressions other than offspring on parent, b) the slope of a cross-age biometric inheritance function does not correspond to half the heritability, as does the slope of a same-age parent-offspring regression of a single parent (Falconer, 1981, Ch. 9), and c) the static nature of the inheritance regression does not allow evolution to occur. I also show that regression to the mean occurs in the antedependence structure of the development functions and is compounded over ages, also diminishing the degree of similarity among ages recovered. I provide an empirical example using female body mass in bighorn sheep (*Ovies canadensis*) that follows closely the theoretical predictions.

In Chapter 5, the analytical results of Chapter 4 were subjected to further empirical testing using, once again, the bighorn sheep population from Ram Mountain, Canada. In this chapter, I compared different statistical approaches to modelling the genetics of ontogenetic trajectories of horn length in males, including the development and inheritance functions used in IPMs, but also pedigree-based methods, like random regression and factor analysis coupled to the animal model (Henderson, 1975), which estimate quantitative genetics parameters with known interpretation (Fisher, 1918; Bulmer, 1980). In addition, I used a multivariate model (*sensu* Lande & Arnold, 1983), which, together with the random regression model, provided strong evidence of horn length being heritable across the lifespan of bighorn rams. Contrarily to these approaches, the cross-age parent-offspring regression, coupled with the antedependence structure typical of IPMs, implies heritabilities across ages from 1 to 8 years that are essentially zero. The random regression model, which also outperformed two implementations of factor analytic models, was fitted using a total of 12 parameters to describe both the additive genetic and the among-individual covariance functions. Although unquestionably less economical in terms of the number of parameters used (compared to typical implementations of IPMs), random regression is likely to be much more tractable then, for example, unstructured models, when confronted with finite data.

Finally, in Chapter 6 I built a two-sex IBM of horn length mimicking the bighorn sheep population from Ram Mountain. I used this model to assess the effect of trophy hunting in the evolution of horn length. After estimating the vital rates, annual breeding success and annual winter survival for both males and females, as well as the probability of being shot for rams of particular age and horn length, I adopted the modelling strategies for horn length estimation from Chapter 5 in the simulations. As expected, given the results from the previous chapter, only the random regression model predicted a significant change in horn length compatible with evolutionary change, provided a selective pressure similar to that existing at Ram Mountain until 1996. Adopting the random regression approach, I could quantify a decrease of up to -0.035 cm/year in the breeding values for horn length (corresponding to the change at age of 5 years). Although the amount of change in horn length (phenotype and breeding values) varies across the ontogeny of bighorn sheep rams, it is observable from very early ages (as early as horn length was recorded, i.e., by the age of one year), suggesting that this genetic adaptation occurs by decreasing the rate at which horns grow. In fact, both breeding values for slopes and curvatures become more positive with hunting, also suggesting delayed growth.

7.2 Bias in inference of selection and the genetics of size

Explanations for the frequently observed mismatch between actual dynamics of body size and theoretical predictions lie on the estimation of the strength of operating natural selection or on how apparent genetic variability might not be available (Merilä et al., 2001). The former is investigated in Chapter 3, where I provide evidence of the existence of a trade-off between viability and fecundity selection involving an additive genetic correlation between body size and pregnancy in female Soay sheep lambs. Genetic correlations among traits might increase or decrease the rate of adaptive evolution, depending on the sign of the correlation with respect to the fitness landscape (Arnold et al., 2001). Nonetheless, complexity, or the number of correlated traits responding to selection, tends to

slow down the rate of adaptation (Fisher, 1930; Orr, 2000), which is shown to occur in Chapter 3, through the comparison between selection *of* and *for* lamb body mass (Sober, 1986). The existence of correlated responses to selection is potentially a conspicuous source of bias, mainly because these are very difficult to detect in the wild (Kruuk et al., 2008), particularly when the traits involved are determined by an overall acquisition resource, which may be largely or entirely non-genetic (De Jong & Van Noordwijk, 1992). In that case, at the phenotypic level, both traits may covary positively, despite the existence of an inherent trade-off (Morrissey et al., 2012c). Indeed, at very low population densities, lamb body mass and the probability of pregnancy are both maximised and are associated with increased first-year survival. The existence of trade-offs adds a layer of methodological complexity in predicting evolutionary change. As theory and methods addressing multivariate problems sustains substantial advances since the last decades, it is the lack of sufficient data usually the limiting condition. In Chapter 3, I use a methodology that handles genetic constraints in a fairly phenotypic perspective and therefore has the potential to be very useful when estimating **G** is not feasible.

One of the key explanations for the paradox of stasis is that studies often focus on specific components of the life cycle, but opposing selection at different stages may cause net stabilising selection, or at least little net directional selection (Schluter et al., 1991; Rollinson & Rowe, 2015). Particularly, antagonist selection across different phases of the life cycle has been attributed to stronger directional selection for larger size in juveniles than in adults (Rollinson & Rowe, 2015). The individual-based model built in Chapter 6 explicitly handles this potential source of bias by incorporating the entire life cycle of the bighorn sheep. Notably, in this particular case, before hunting is applied, a stable horn length at each age is predicted by the model, hence, avoiding the paradox of stasis. Indeed, variation in the strength of selection across the ontogeny has been observed in the bighorn rams from Ram Mountain. Nonetheless, the opposite pattern to that suggested by Rollinson & Rowe (2015) has been detected, with both overall and sexual selection on horn length being stronger (more positive) in mature than young males, as horn size plays a much smaller role in the success of younger males (Martin et al., 2016).

The third chapter of the thesis draws attention to another challenge in measuring natural selection. The above-mentioned trade-off between viability and fecundity selection in the Soay Sheep is mediated by the covariation between body mass and pregnancy occurring during the first year of life of these sheep. As correlations exist between lamb body mass and the body mass at older ages (Wilson et al., 2007) and between female and male body mass (Robinson et al., 2009), this mechanism is expected to also affect traits expressed in males and older individuals of both sexes. Nonetheless, lamb pregnancy, which is associated with low probability of first-year survival, is only expressed during the first annual cycle of females. In fact, the viability selection that occurs in juveniles leading to adult trait not being measured was coined by Grafen (1988) as *invisible fraction*, referring to the individuals that are missing from the adult data set. This is essentially a missing data problem (Hadfield, 2008), not limited to ontogenetic incompleteness, but also affecting sex-limited characters. As Grafen (1988) outlines, if the focal trait is genetically correlated with other characters in the sex they are not expressed, the whole sex may belong to the invisible fraction. As a result, measuring the strength of selection in Soay sheep body mass in adults and/or males will potentially lead to upwardly biased estimates. Incompleteness of information not at random has not been given much attention in

observational studies, where it is more prone to occur. However, experimental work has shown that the unmeasured component of selection can be very strong (e.g. Mojica & Kelly, 2010), suggesting it can represent a serious bias when estimating the strength of selection in wild populations (Hadfield, 2008; Nakagawa & Freckleton, 2008).

The last potential bias in estimating natural selection that was briefly covered in this thesis relates to variability in selection, which has the potential to convolute the interpretation of the strength of selection. Chapter 3, and implicitly Chapter 6 given the density-dependent effect of horn length on survival and breeding success, constitute empirical examples of density-dependent selection. In Chapter 3 I explicitly provide selection gradients of body mass and pregnancy across different values of population density, showing that, accordingly to general theory (reviewed by Mueller, 1997), selection is stronger in years of higher population density. In fact, this had already been demonstrated for different size-related traits in Soay sheep (Milner et al., 1999). In general, variation in selection implies variation of optimal trait values and, therefore, that trait values within populations are rarely at the adaptive optimum at any given point in time (Bell, 2010). This rational has been identified as a possible explanation for the general lack of response to documented selection (Merilä et al., 2001), given that the selection measured at one point in time may not persist across generations or even across life stages within generations (Merilä et al., 2001). Nonetheless, this argument should be carefully investigated, as evidence exists suggesting that most observed temporal variation in selection is accounted for by sampling error, precluding that temporal variation in the actual underlying selection coefficients is low (Morrissey & Hadfield, 2012).

Although analytical solutions extending the Lande's equation (Lande, 1979) to allow the prediction of evolutionary change under some of the non-standard conditions mentioned above exist (e.g. Russell, 1980; Lande, 1982; Kirkpatrick & Lande, 1989; Lande et al., 2017), population demographic models coupled with quantitative genetics tools can prove very useful in overcoming these challenges (e.g. Reeve, 2000). Population models, as IPMs and IBMs, provide a very convenient solution to handle the simultaneous effect of complexities such as age-structure, overlapping generations, sexual antagonism or environmental heterogeneity on selection in a particular efficient manner. An example of such a solution is provided in Chapter 6, where I used an individual-based model to infer what evolution of horn length is expected to have taken place while the bighorn population of Ram Mountain was subject to trophy hunting (Festa-Bianchet et al., 2014). In bighorn sheep, as in other ungulates, high population densities are associated with higher mortality, stronger selection and smaller horn size (Kruuk et al., 2002; Bonenfant et al., 2009a; Hunter et al., 2018). This model transparently accommodates age structure, sex structure, density-dependent fitness functions, and multi-dimensional phenotype. This could explain why the evolutionary predictions of Chapter 6, although quantitatively very similar in magnitude, are lower when compared to previous studies (Coltman et al., 2003; Pigeon et al., 2016). This would be in agreement with results from simulations of fish populations, precluding rates of evolution that are lower than observed rates (Audzijonyte et al., 2013). These results, put together, suggest that plastic responses to harvesting may also account for an important fraction of documented trends at the level of the phenotype (Kuparinen & Festa-Bianchet, 2017).

The study system of the bighorn sheep population at Ram Mountain is of particular relevance due to political considerations in shaping policy related to trophy hunting in Alberta, Canada, as the only

population simultaneously subject to trophy hunting, individual-based monitoring, and having a pedigree available (Pelletier et al., 2012). Science-based policy making has had the contribution of an IPM, using this population, aiming at evaluating the contribution of evolution to the observed phenotypic decrease in horn size due to trophy hunting (but in fact using body mass as a proxy, Traill et al., 2014). This IPM was built using a cross-age parent-offspring regression as a measure of inheritance, maintaining (necessarily) that the observed change in horn length in bighorn rams was purely demographic. Although I have not aimed at providing a formal comparison between the exact model used by Traill et al. (2014) and an alternative based on quantitative genetics, the joint results of Chapters 4, 5, and 6 strongly suggest that the conclusions reached by these authors are an artefact of an erroneous analysis. Theoretical demonstration of the lack of correspondence between a cross-age parent-offspring regression and known biological mechanics of inheritance (Fisher, 1918, 1930; Wright, 1922, 1931) is the preeminent contribution of this thesis regarding errors in estimating the genetic contribution to evolutionary change (Chapter 4). This finding has important consequences to the implementation of IPMs and eventually other population models. Most empirical applications of IPMs incorporating inheritance have been based on the cross-age regression of offspring values at birth or recruitment on parental values at conception or parity (Coulson, 2012; Schindler et al., 2013; Traill et al., 2014; Bassar et al., 2016), which is superficially particularly efficient as it uses a single parameter. This feature is particularly convenient in IPMs, as these models rely on discretising distributions by approximating them with large matrices, which increase in size exponentially (Caswell & John, 1992). In Chapter 5 I model the ontogenetic trajectories of horn length in the bighorn rams at Ram Mountain as an intermediate step to building an IBM also aiming at quantifying the genetic contribution to the observed decrease in horn length that occurred in this population as a result of selective harvesting (Coltman et al., 2003; Festa-Bianchet et al., 2014; Pigeon et al., 2016). Potential management implications of these analyses are: (1) male horn length is heritable across the entire ontogeny, as shown in Chapter 5 and previously established (Coltman et al., 2003, 2005; Poissant et al., 2012; Pigeon et al., 2016), in contrast to the predictions of a cross-age parent-offspring regression for the same data (also shown in Chapter 5); (2) as illustrated in Chapters 4 and 6, an IPM or an IBM using a cross-age parent offspring regression as its concept of inheritance is bound to predict no evolutionary change; and (3), also as illustrated in Chapter 6, an IPM or an IBM using an adequate quantitative genetic approach as its concept of inheritance predicted that evolutionary change has occurred in the horn length of the population at Ram Mountain population.

Data availability is still of concern in the field of evolutionary quantitative genetics. As the prediction of evolutionary change shifts from using a single heritability estimate to **G** matrices (Arnold, 1994), this becomes an increasingly relevant concern. Data availability determines sampling errors in the estimation of genetic quantities and selection, and the power to infer on various evolutionary questions (Lynch & Walsh, 1998, Ch. 21; Steppan et al., 2002; Jones et al., 2004). An example of practical application is the ongoing controversy about the relative constancy of the **G** matrix (see Steppan et al., 2002; Jones et al., 2004; Arnold et al., 2008), which in turn determines the suitability of various expressions used to predict evolutionary change (Arnold, 1994). Although this thesis is not concerned with the technical aspects of estimating **G**, Chapter 3 provides a means of predicting evolutionary change in correlated traits while avoiding estimating the genetic architecture among traits. Such approach could be of potential advantage where estimating **G** matrices with usable precision is not possible, as it specifically takes advantage from the phenotypic relationship between lamb body mass and early pregnancy, and builds it into a formal model of selection.

7.3 Challenges and future work

An important limitation of the results presented here is associated with measurement and data availability, either due to information not missing at random (Chapters 3 and 5) or due to the particular effect of horn breakage in estimating ontogenetic trajectories of horn length and how it constitutes measurement error (Chapter 5). The analyses presented in Chapter 5, and possibly in Chapter 3, are potentially biased by not accounting for a fraction of individuals missing not at random. In Chapter 3 only around half the pregnant lambs were phenotyped for body mass and, therefore, included in the analyses, mostly due to neonatal mortality. Although there is no obvious mechanism generating missing information not at random, as the August catch is likely to be highly non-random with respect to body mass and subsequent pregnancy, given the important fraction excluded, an opportunity for bias should be acknowledged. In Chapter 5 most of the ontogenetic trajectories of horn length are incomplete. I identified three different processes generating missing data, where one produces incompleteness of data that is known not to be at random - selective harvesting of rams with larger horns. As a result, alternatives to these analyses should be considered. Instead of the path analysis presented in Chapter 3, a similar approach could be adopted using breeding values rather than realised lamb body mass, as no phenotype would be necessary in the analysis (accounting for prediction error, see Hadfield et al., 2010). A similar approach has been implemented by Sinervo & McAdam (2008), who quantified selection acting on an invisible fraction by measuring selection on predicted breeding values for clutch size in lizards. Regarding the data missing not at random in Chapter 5, the incompleteness in horn length trajectories could be addressed by explicitly modelling the drop-out mechanism, in this case, size-dependent harvest of male bighorn sheep (Hadfield, 2008).

An unexpected result in this thesis is the poor performance obtained by modelling ontogenetic trajectories using factor analytic models (Chapter 5). The particular implementation of this methodology might have been inadequate given that an important fraction of trajectories are likely to have been shaped by horn breakage, and the factor analysis might have been more affected by this than other approaches. During the rut, bighorn rams display different types of social interactions, including front kicking and mounting, but also frontal horn clashing, to establish social ranking (Pelletier & Festa-Bianchet, 2006). This latter behaviour leads to horn breakage, a damage that tends to increase with age and can be very substantial (Pigeon et al., 2016). Factor analysis was implemented as a mere description of the variability in the data, simply relying on principal components, and not assuming any shape for the additive genetic architecture of horn length. In a situation where the size of the horn that would have existed if not for breakage is of interest, such approach might have been disadvantageous. Alternatively, implementations of factor analysis where eigenfunctions are used instead of eigenvectors, in a rational that is similar to using random polynomial functions in random regression (Kirkpatrick & Meyer, 2004; Meyer, 2005) are expected to yield better results. Another alternative would be modelling the process of horn breakage itself, which would allow to disentangle additional aspects of sexual selection in bighorn rams.

7.4 Conclusion

Application of evolutionary quantitative genetic theory to empirical problems relies on a collection of statistical tools, used either to measure the strength of selection or the genetic aspects of the potential populations have to evolve. Any statistical inference approach can only be unbiased within a certain number of assumptions. When applied to wild populations, those assumptions are frequently not guaranteed to hold due to the complexity of natural systems, and the effects of such violations are often difficult to assess. In this thesis I aimed at providing a contribution to identifying and solving few of the issues arising from such mismatches between biology and statistics, focusing on the evolution of size. Given its nature, this thesis covered a broad range of subjects within the field of evolutionary quantitative genetics. Briefly, in this thesis: (1) I adopt a methodology to handle genetic constraints in a fairly phenotypic perspective, allowing to quantify the bias that would exist if such constraint was not accounted for; (2) I provide analytical proofs of several issues with applications of IPMs that incorporate inheritance and development, concluding that these will predict no evolutionary change regardless of whether it should, will, or has occurred; and (3) I build a two-sex individual-based model equivalent to an IPM that uses quantitative genetics theory to model trait transmission, which provides an addition to an ongoing controversy about the quantitative contribution of evolution in the response to selective harvesting in bighorn sheep, accounting for a large number of ecological complexities.

Bibliography

Agrawal, A.F. & Stinchcombe, J.R. 2009. How much do genetic covariances alter the rate of adaptation? *Proceedings of the Royal Society of London B: Biological Sciences* **276**: 1183–1191.

Allendorf, F.W., England, P.R., Luikart, G., Ritchie, P.A. & Ryman, N. 2008. Genetic effects of harvest on wild animal populations. *Trends in Ecology & Evolution* **23**: 327 – 337.

Allendorf, F.W. & Hard, J.J. 2009. Human-induced evolution caused by unnatural selection through harvest of wild animals. *Proceedings of the National Academy of Sciences* **106**: 9987–9994.

Anderson, M. 1995. *Sexual selection*. Princeton University Press, Princeton, New Jersey.

Arendt, J.D. 1997. Adaptive intrinsic growth rates: an integration across taxa. *The Quaterly Review of Biology* **72**: 149.

Arnold, S.F. 1994. Multivariate inheritance and evolution: a review of concepts. In: *Quantitative Genetics Studies of Behavioral Evolution* (C.R.B. Boake, ed), pp. 17–48. The University of Chicago Press.

Arnold, S.J., Bürger, R., Hohenlohe, P.A., Ajie, B.C. & Jones, A.G. 2008. Understanding the evolution and stability of the g-matrix. *Evolution* **62**: 2451–2461.

Arnold, S.J., Pfrender, M.E. & Jones, A.G. 2001. The adaptive landscape as a conceptual bridge between micro- and macroevolution. *Genetica* **112**: 9–32.

Audzijonyte, A., Kuparinen, A. & Fulton, E.A. 2013. How fast is fisheriesâĂŘinduced evolution? quantitative analysis of modelling and empirical studies. *Evolutionary Applications* **6**: 585–595.

Barfield, M., Holt, R.D. & Gomulkiewicz, R. 2011. Evolution in stage-structured populations. *The American Naturalist* **177**: 397–409.

Barnett, A.G., van der Pols, J.C. & Dobson, A.J. 2005. Regression to the mean: what it is and how to deal with it. *International Journal of Epidemiology* **34**: 215–20.

Bassar, R.D., Childs, D.Z., Rees, M., Tuljapurkar, S., Reznick, D.N. & Coulson, T. 2016. The effects of asymmetric competition on the life history of Trinidadian guppies. *Ecology Letters* **19**: 268–278.

Bell, G. 2010. Fluctuating selection: the perpetual renewal of adaptation in variable environments. *Philosophical Transactions of the Royal Society of London B: Biological Sciences* **365**: 87–97.

Benthem, K.J., Bruijning, M., Bonnet, T., Jongejans, E., Postma, E. & Ozgul, A. 2017. Disentangling evolutionary, plastic and demographic processes underlying trait dynamics: a review of four frameworks. *Methods in Ecology and Evolution* **8**: 75–85.

Bérénos, C., Ellis, P.A., Pilkington, J.G. & Pemberton, J.M. 2014. Estimating quantitative genetic parameters in wild populations: a comparison of pedigree and genomic approaches. *Molecular Ecology* **23**: 3434–3451.

Bermejo, J.L., Roehe, R., Schulze, V., Rave, G., Looft, H. & Kalm, E. 2003. Random regression to model genetically the longitudinal data of daily feed intake in growing pigs. *Livestock Production Science* **82**: 189–199.

Blanckenhorn, W. 2000. The evolution of body size: what keeps organisms small? *Quarterly Review of Biology* **75**: 385–407.

Bonenfant, C., Gaillard, J.M., Coulson, T., Festa-Bianchet, M., Loison, A., Garel, M., Loe, L.E., Blanchard, P., Pettorelli, N., Owen-Smith, N., Toit, J.D. & Duncan, P. 2009a. Empirical evidence of density-dependence in populations of large herbivores. vol. 41 of *Advances in Ecological Research*, pp. 313 – 357. Academic Press.

Bonenfant, C., Pelletier, F., Garel, M. & Bergeron, P. 2009b. Age-dependent relationship between horn growth and survival in wild sheep. *Journal of Animal Ecology* **78**: 161–171.

Bonnet, T., Wandeler, P., Camenisch, G. & Postma, E. 2017. Bigger is fitter? quantitative genetic decomposition of selection reveals an adaptive evolutionary decline of body mass in a wild rodent population. *PLOS Biology* **15**: 1–21.

Bradshaw, A.D. 1991. The Croonian Lecture, 1991 Genostasis and the limits to evolution. *Philosophical transactions of the Royal Society of London. Series B, Biological sciences* **333**: 289–305.

Bulmer, M.G. 1980. *The mathematical theory of quantitative genetics*. Clarendon Press, Oxford.

Campbell, D.T. & Kenny, D.A. 1999. *A primer on regression artifacts*. The Guilford Press, New York.

Castellani, M., Heino, M., Gilbey, J., Araki, H., Svåsand, T. & Glover, K.A. 2015. Ibsem: An individual-based atlantic salmon population model. *PLOS ONE* **10**: 1–35.

Caswell, H. 2001. *Matrix population models*. Oxford University Press, Oxford.

Caswell, H. & John, M. 1992. From the individual to the population in demographic models. In: *Individual-based models and approaches in ecology: populations, communities and ecosystems* (D.L. DeAngelis & L.J. Gross, eds). CRC Press.

Charmantier, A. & Garant, D. 2005. Environmental quality and evolutionary potential: lessons from wild populations. *Proceedings of the Royal Society of London B: Biological Sciences* **272**: 1415–1425.

Charmantier, A., Kruuk, L.E.B., Blondel, J. & Lambrechts, M.M. 2004. Testing for microevolution in body size in three blue tit populations. *Journal of Evolutionary Biology* **17**: 732–43.

Cheverud, J.M. 1988. A comparison of genetic and phenotypic correlations. *Evolution* **42**: 958–968.

Chevin, L.M. 2015. Evolution of adult size depends on genetic variance in growth trajectories: A comment on analyses of evolutionary dynamics using integral projection models. *Methods in Ecology and Evolution* **6**: 981–986.

Childs, D.Z., Coulson, T.N., Pemberton, J.M., Clutton-Brock, T.H. & Rees, M. 2011. Predicting trait values and measuring selection in complex life histories: Reproductive allocation decisions in Soay sheep. *Ecology Letters* **14**: 985–992.

Childs, D.Z., Rees, M., Rose, K.E., Grubb, P.J. & Ellner, S.P. 2003. Evolution of complex flowering strategies: an age- and size-structured integral projection model. *Proceedings of the Royal Society of London B: Biological Sciences* **270**: 1829–1838.

Childs, D.Z., Sheldon, B.C. & Rees, M. 2016. The evolution of labile traits in sex- and age-structured populations. *Journal of Animal Ecology* **85**: 329–342.

Clutton-Brock, T., Price, O., Albon, S. & Jewell, P. 1992. Early development and population fluctuations in soay sheep. *Journal of Animal Ecology* **61**: 381–396.

Clutton-Brock, T. & Sheldon, B.C. 2010. Individuals and populations: the role of long-term, individual-based studies of animals in ecology and evolutionary biology. *Trends in Ecology & Evolution* **25**: 562 – 573. Special Issue: Long-term ecological research.

Clutton-Brock, T.H., Grenfell, B.T., Coulson, T., MacColl, A.D.C., Illius, A.W., Forchhammer, M.C., Wilson, K., Lindström, J., Crawley, M.J. & Albon, S.D. 2004a. Population dynamics in soay sheep. In: *Soay sheep: dynamics and selection in an island population* (T.H. Clutton-Brock & J.M. Pemberton, eds). Cambridge University Press.

Clutton-Brock, T.H. & Pemberton, J.M. 2004a. Individuals and populations. In: *Soay sheep: dynamics and selection in an island population* (T.H. Clutton-Brock & J.M. Pemberton, eds). Cambridge University Press.

Clutton-Brock, T.H. & Pemberton, J.M. 2004b. *Soay Sheep Dynamics and Selection in an Island Population*. Cambridge University Press, Cambridge.

Clutton-Brock, T.H., Pemberton, J.M., Coulson, T., Stevenson, I.R. & MacColl, A.D.C. 2004b. The sheep of St Kilda. In: *Soay sheep: dynamics and selection in an island population* (T.H. Clutton-Brock & J.M. Pemberton, eds). Cambridge University Press.

Clutton-Brock, T.H., Stevenson, I.R., Marrow, P., MacColl, a.D., Houston, a.I. & McNamara, J.M. 1996. Population fluctuations, reproductive costs and life-history tactics in female Soay sheep. *Journal of Animal Ecology* **65**: 675–689.

Coltman, D.W., Festa-Bianchet, M., Jorgenson, J.T. & Strobeck, C. 2002. Age-dependent sexual selection in bighorn rams. *Proceedings of the Royal Society of London B: Biological Sciences* **269**: 165–172.

Coltman, D.W., O'Donoghue, P., Hogg, J.T. & Festa-Bianchet, M. 2005. Selection and genetic (co)variance in bighorn sheep. *Evolution; international journal of organic evolution* **59**: 1372–1382.

Coltman, D.W., O'Donoghue, P., Jorgenson, J.T., Hogg, J.T., Strobeck, C. & Festa-Bianchet, M. 2003. Undesirable evolutionary consequences of trophy hunting. *Nature* **426**: 655–658.

Cope, E.D. 1896. *The Primary Factors of Organic Evolution'*. Open Court Publishing, Chicago, IL.

Coulson, T. 2012. Integral projections models, their construction and use in posing hypotheses in ecology. *Oikos* **121**: 1337–1350.

Coulson, T.N., MacNulty, D.R., Stahler, D.R., VonHoldt, B., Wayne, R.K. & Smith, D.W. 2011. Modeling effects of environmental change on wolf population dynamics, trait evolution, and life history. *Science* **334**: 1275–8.

Coulson, T.N., Tuljapurkar, S. & Childs, D.Z. 2010. Using evolutionary demography to link life history theory, quantitative genetics and population ecology. *The Journal of Animal Ecology* **79**: 1226–40.

Crawley, M.J., Albon, S.D., Bazely, D.R., Milner, J.M., Pilkington, J.G. & Tuke, A.L. 2004. Vegetation and sheep population dynamics. In: *Soay sheep: dynamics and selection in an island population* (T.H. Clutton-Brock & J.M. Pemberton, eds). Cambridge University Press.

Darimont, C.T., Carlson, S.M., Kinnison, M.T., Paquet, P.C., Reimchen, T.E. & Wilmers, C.C. 2009. Human predators outpace other agents of trait change in the wild. *Proceedings of the National Academy of Sciences* **106**: 952–954.

De Jong, G. & Van Noordwijk, A.J. 1992. Acquisition and allocation of resources: genetic (co) variances, selection, and life histories. *The American Naturalist* **139**: 749–770.

de los Campos, G. & Gianola, D. 2007. Factor analysis models for structuring covariance matrices of additive genetic effects: a Bayesian implementation. *Genetics, selection, evolution* **39**: 481–494.

DeAngelis, D.L. & Grimm, V. 2014. Individual-based models in ecology after four decades. *F1000prime reports* **6**: 39.

DeAngelis, D.L. & Gross, L.J. (eds) 1992. *Individual-based models and approaches in ecology: populations, communities and ecosystems*. Chapman and Hall/CRC.

Dmitriew, C.M. 2011. The evolution of growth trajectories: what limits growth rate? *Biological reviews of the Cambridge Philosophical Society* **86**: 97–116.

Easterling, M.R., Ellner, S.P. & Dixon, P.M. 2000. Size-specific sensitivity: applying a new structured population model. *Ecology* **81**: 694–708.

Eldridge, W.H., Hard, J.J. & Naish, K.A. 2010. Simulating fishery-induced evolution in chinook salmon: the role of gear, location, and genetic correlation among traits. *Ecological Applications* **20**: 1936–1948.

Ellner, S.P. & Rees, M. 2006. Integral projection models for species with complex demography. *The American Naturalist* **167**: 410–428.

Endler, J. 1986. *Natural Selection in the Wild*. Monographs in population biology. Princeton University Press.

Estes, S. & Arnold, S.J. 2007. Resolving the paradox of stasis: models with stabilizing selection explain evolutionary divergence on all timescales. *The American Naturalist* **169**: 227–244.

Fairbairn, D.J. 1997. Allometry for sexual ssze dimorphism: pattern and process in the coevolution of body size in males and females. *Annual Review of Ecology and Systematics* **28**: 659–687.

Falconer, D. 1981. *Introduction to Quantitative Genetics*, 2nd edn. Longman, New York.

Festa-Bianchet, M. 1988. Birthdate and survival in bighorn lambs (ovis canadensis). *Journal of Zoology* **214**: 653–661.

Festa-Bianchet, M., Coltman, D.W., Turelli, L. & Jorgenson, J.T. 2004. Relative allocation to horn and body growth in bighorn rams varies with resource availability. *Behavioral Ecology* **15**: 305–312.

Festa-Bianchet, M., Coulson, T., Gaillard, J.M., Hogg, J.T. & Pelletier, F. 2006. Stochastic predation

events and population persistence in bighorn sheep. *Proceedings of the Royal Society of London B: Biological Sciences* **273**: 1537–1543.

Festa-Bianchet, M., Gaillard, J. & Jorgenson, J.T. 1998. Mass- and density-dependent reproductive success and reproductive costs in a capital breeder. *The American Naturalist* **152**: 367–379.

Festa-Bianchet, M., Jorgenson, J.T., Lucherini, M. & Wishart, W.D. 1995. Life history consequences of variation in age of primiparity in bighorn ewes. *Ecology* **76**: 871–881.

Festa-Bianchet, M. & King, W.J. 2007. Age–related reproductive effort in bighorn sheep ewes. *Ecoscience* **14**: 318–322.

Festa-Bianchet, M., Pelletier, F., Jorgenson, J.T., Feder, C. & Hubbs, A. 2014. Decrease in horn size and increase in age of trophy sheep in Alberta over 37 years. *Journal of Wildlife Management* **78**: 133–141.

Feulner, P.G.D., Gratten, J., Kijas, J.W., Visscher, P.M., Pemberton, J.M. & Slate, J. 2013. Introgression and the fate of domesticated genes in a wild mammal population. *Molecular Ecology* **22**: 4210–4221.

Fisher, R.A. 1918. The correlation between relatives on the supposition of mendelian inheritance. *Transactions of the Royal Society of Edinburgh* **52**: 399–433.

Fisher, R.A. 1930. *The genetical theory of natural selection*. Clarendon Press„ Oxford, U.K.

Franklin, O.D. & Morrissey, M.B. 2017. Inference of selection gradients using performance measures as fitness proxies. *Methods in Ecology and Evolution* **8**: 663–677.

Fussmann, G.F., Loreau, M. & Abrams, P.A. 2007. Eco-evolutionary dynamics of communities and ecosystems. *Functional Ecology* **21**: 465–477.

Galton, F. 1886. Regression Towards Mediocrity in Heriditary Stature. *Journal of the Anthropological Institute* **XV**: 246–263.

Gelman, A. 2006. Prior distributions for variance parameters in hierarchical models. *Bayesian Analysis* **1**: 515–533.

Gianola, D. & Sorensen, D. 2004. Quantitative genetic models for describing simultaneous and recursive relationships between phenotypes. *Genetics* **167**: 1407–1424.

Gjerde, B., Terjesen, B., Barr, Y., Lein, I. & Thorland, I. 2004. Genetic variation for juvenile growth and survival in Atlantic cod (Gadus morhua). *Aquaculture* **236**: 167–177.

Godfrey-Smith, P. 2007. Conditions for evolution by natural selection. *The Journal of Philosophy* **CIV**: 489–516.

Gould, S.J. & Eldredge, N. 1993. Punctuated equilibrium comes of age. *Nature* **366**: 223 EP –.

Grafen, A. 1988. On the uses of data on lifetime reproductive success. In: *Reproductive Success* (T.H. Clutton-Brock, ed), pp. 454–471. University of Chicago Press, Chicago, IL.

Grimm, V. 1999. Ten years of individual-based modelling in ecology: what have we learned and what could we learn in the future? *Ecological Modelling* **115**: 129 – 148.

Gunay, F., Alten, B. & Ozsoy, E.D. 2011. Narrow-sense heritability of body size and its response to different developmental temperatures in Culex quinquefasciatus (Say 1923). *Journal of Vector Ecology* **36**: 348–54.

Hadfield, J.D. 2008. Estimating evolutionary parameters when viability selection is operating. *Proceedings of the Royal Society of London B: Biological Sciences* **275**: 723–734.

Hadfield, J.D. 2010. MCMC methods for multi-response generalized linear mixed models: the MCMCglmm R package. *Journal of Statistical Software* **33**: 1–22.

Hadfield, J.D., Heap, E.A., Bayer, F., Mittell, E.A. & Crouch, N.M.A. 2013. Disentangling genetic and prenatal sources of familial resemblance across ontogeny in a wild passerine. *Evolution* **67**: 2701–2713.

Hadfield, J.D., Richardson, D.S. & Burke, T. 2006. Towards unbiased parentage assignment: combining genetic, behavioural and spatial data in a bayesian framework. *Molecular Ecology* **15**: 3715–3730.

Hadfield, J.D., Wilson, A.J., Garant, D., Sheldon, B.C. & Kruuk, L.E.B. 2010. The misuse of BLUP in ecology and evolution. *The American Naturalist* **175**: 116–25.

Haller, B.C. & Hendry, A.P. 2014. Solving the paradox of stasis: squashed stabilizing selection and the limits of detection. *Evolution* **68**: 483–500.

Hansen, T.F. 2012. Adaptive landscapes and macroevolutionary dynamics. In: *The adaptive landscape in evolutionary biology* (E.I. Svensson & R. Carlsbeek, eds). Oxford University Press.

Hansen, T.F., Armbruster, W., Carlson, M. & Pelabon, C. 2003. Evolvability and genetic constraints in Dalechampia Blossoms: genetic correlations and conditional evolvability. *Journal of Experimental Zoology* **296B**: 23–39.

Hansen, T.F. & Houle, D. 2004. Evolvability, stabilizing selection, and the problem of stasis. In: *Phenotypic integration* (M. Pigliucci & K. Preston, eds), pp. 130–150. Oxford University Press, Oxford.

Hansen, T.F., Pélabon, C. & Houle, D. 2011. Heritability is not evolvability. *Evolutionary Biology* **38**: 258–277.

Harris, R.B., Wall, W.A. & Allendorf, F.W. 2002. Genetic consequences of hunting: What do we know and what should we do? *Wildlife Society Bulletin (1973-2006)* **30**: 634–643.

Hedrick, P.W., Coltman, D.W., Festa-Bianchet, M. & Pelletier, F. 2014. Not surprisingly, no inheritance of a trait results in no evolution. *Proceedings of the National Academy of Sciences* **111**: E4810–E4810.

Henderson, C.R. 1975. Best linear unbiased estimation and prediction under a selection model. *Biometrics* **31**: 423–447.

Hendry, A.P., Gotanda, K.M. & Svensson, E.I. 2017. Human influences on evolution, and the ecological and societal consequences. *Philosophical Transactions of the Royal Society of London B: Biological Sciences* **372**.

Hereford, J. 2009. A quantitative survey of local adaptation and fitness trade-offs. *The American Naturalist* **173**: 579–588.

Hereford, J., Hansen, T.F. & Houle, D. 2004. Comparing strengths of directional selection: how strong is strong? *Evolution* **58**: 2133–2143.

Hine, E., Chenoweth, S.F., Rundle, H.D. & Blows, M.W. 2009. Characterizing the evolution of genetic variance using genetic covariance tensors. *Philosophical transactions of the Royal Society of London. Series B, Biological sciences* **364**: 1567–78.

Honek, A. 1993. Intraespecific variation in body size and fecundity in insects: a general relationship. *Oikos* **66**: 483–492.

Houle, D. 1992. Comparing evolvabiliy and variability of quantitative traits. *Genetics* **130**: 195–204.

Huchard, E., Charmantier, a., English, S., Bateman, a., Nielsen, J.F. & Clutton-Brock, T. 2014. Additive genetic variance and developmental plasticity in growth trajectories in a wild cooperative mammal. *Journal of Evolutionary Biology* **27**: 1893–1904.

Hunt, G. 2007. The relative importance of directional change, random walks, and stasis in the evolution of fossil lineages. *Proceedings of the National Academy of Sciences of the United States of America* **104**: 18404–8.

Hunter, D.C., Pemberton, J.M., Pilkington, J.G. & Morrissey, M.B. 2018. Quantification and decomposition of environment-selection relationships. *Evolution* **72**: 851–866.

Huston, M., DeAngelis, D. & Post, W. 1988. New computer models unify ecological theory. *BioScience* **38**: 682–691.

Hutchings, J.A. & Fraser, D.J. 2008. The nature of fisheries- and farming-induced evolution. *Molecular Ecology* **17**: 294–313.

Illius, A., Albon, S., Pemberton, J., Gordon, I. & Clutton-Brock, T. 1995. Selection for foraging efficiency during a population crash in soay sheep. *Journal of Animal Ecology* **64**: 481–492.

Jacquard, A. 1983. Heritability: one word, three concepts. *Biometrics* **39**: 465–477.

Jakobsen, J.H., Madsen, P., Jensen, J., Pedersen, L.G., Christensen, L.G. & Sorensen, D.A. 2002. Genetic parameters for milk production and persistency for danish holsteins estimated in random regression models using reml. *Journal of Dairy Science* **85**: 1607–1616.

Johnson, D.W. & Hixon, M.A. 2011. Sexual and lifetime selection on body size in a marine fish: the importance of life-history trade-offs. *Journal of Evolutionary Biology* **24**: 1653–1663.

Johnson, V.A., Biever, K.J., Haunold, A. & Schmidt, J.W. 1966. Inheritance of plant height, yield of grain, and other plant and seed characteristics in a cross of hard red winter wheat, Triticum aestivum L. *Crop Science* **6**: 336–338.

Johnston, S.E., Beraldi, D., McRae, A.F., Pemberton, J.M. & Slate, J. 2010. Horn type and horn length genes map to the same chromosomal region in soay sheep. *Heredity* **104**: 196 EP –.

Johnston, S.E., Gratten, J., Berenos, C., Pilkington, J.G., Clutton-Brock, T.H., Pemberton, J.M. & Slate, J. 2013. Life history trade-offs at a single locus maintain sexually selected genetic variation. *Nature* **502**: 93–5.

Jones, A.G., Arnold, S.J. & Bürger, R. 2004. Evolution and stability of the g-matrix on a landscape with a moving optimum. *Evolution* **58**: 1639–1654.

Jorgenson, J.T., Festa-Bianchet, M., Gaillard, J.M. & Wishart, W.D. 1997. Effects of age, sex, disease, and density on survival of bighorn sheep. *Ecology* **78**: 1019–1032.

Jorgenson, J.T., Festa-Bianchet, M. & Wishart, W.D. 1993. Harvesting bighorn ewes: consequences for population size and trophy ram production. *The Journal of Wildlife Management* **57**: 429–435.

Jorgenson, J.T., Festa-Bianchet, M. & Wishart, W.D. 1998. Effects of population density on horn development in bighorn rams. *The Journal of Wildlife Management* **62**: 1011–1020.

Kelly, C. & Price, T.D. 2005. Correcting for regression to the mean in behavior and ecology. *The American Naturalist* **166**: 700–707.

Kingsolver, J.G. & Pfennig, D.W. 2004. Individual-level selection as a cause of Cope's rule of phyletic size increase. *Evolution* **58**: 1608–1612.

Kirkpatrick, M. & Heckman, N. 1989. A quantitative genetic model for growth, shape, reaction norms, and other infinite-dimensional characters. *Journal of Mathematical Biology* **27**: 429–450.

Kirkpatrick, M., Hill, W.G. & Thompson, R. 1994. Estimating the covariance structure of traits during growth and aging, illustrated with lactations in dairy cattle. *Genetics Research* **64**: 57–69.

Kirkpatrick, M. & Lande, R. 1989. The evolution of maternal characters. *Evolution* **43**: 485–503.

Kirkpatrick, M., Lofsvold, D. & Bulmer, M. 1990. Analysis of the inheritance, selection and evolution of growth trajectories. *Genetics* **124**: 979–93.

Kirkpatrick, M. & Meyer, K. 2004. Direct estimation of genetic principal components. *Genetics* **168**: 2295–2306.

Knouft, J.H. & Page, L.M. 2003. The evolution of body size in extant groups of North American freshwater fishes: speciation, size distributions, and Cope's rule. *The American Naturalist* **161**: 413–421.

Kruuk, L., Charmantier, A. & Garant, D. 2014. The study of quantitative genetics in wild populations. In: *Quantitative Genetics in the Wild* (A. Charmantier, D. Garant & L.E. Kruuk, eds), pp. 1–15. Oxford University Press, Oxford, UK.

Kruuk, L.E.B. 2004. Estimating genetic parameters in natural populations using the "animal model". *Philosophical Transactions of the Royal Society of London. Series B, Biological Sciences* **359**: 873–890.

Kruuk, L.E.B. & Hadfield, J.D. 2007. How to separate genetic and environmental causes of similarity between relatives. *Journal of Evolutionary Biology* **20**: 1890–1903.

Kruuk, L.E.B., Slate, J., Pemberton, J.M., Sue, B., Guinness, F. & CluttonâĂŘBrock, T. 2002. Antler size in red deer: heritability and selection but no evolution. *Evolution* **56**: 1683–1695.

Kruuk, L.E.B., Slate, J. & Wilson, A.J. 2008. New Answers for Old Questions: The Evolutionary Quantitative Genetics of Wild Animal Populations. *Annual Review of Ecology Evolution and Systematics* **39**: 525–548.

Kuparinen, A. & Festa-Bianchet, M. 2017. Harvest-induced evolution: insights from aquatic and terrestrial systems. *Philosophical Transactions of the Royal Society of London B: Biological Sciences* **372**.

Kuparinen, A. & Merilä, J. 2007. Detecting and managing fisheries-induced evolution. *Trends in Ecology & Evolution* **22**: 652 – 659.

Lande, R. 1979. Quantitative genetic analysis of multivariate evolution, applied to brain: body size allometry. *Evolution* **33**: 401–416.

Lande, R. 1982. A quantitative genetic theory of life history evolution. *Ecology* **63**: 607–615.

Lande, R. & Arnold, S.J. 1983. The measurement of selection on correlated characters. *Evolution* **37**: 1210–1226.

Lande, R., Engen, S. & Sæther, B.E. 2017. Evolution of stochastic demography with life history tradeoffs in density-dependent age-structured populations. *Proceedings of the National Academy of Sciences* **114**: 11582–11590.

Larsson, K., van der Jeug, H.P., van der Veen, I.T. & Forslund, P. 1998. Body size declines despite positive directional selection on heritable size traits in a barnacle goose population. *Evolution* **52**: 1169–1184.

Legarra, A., Misztal, I. & Bertrand, J. 2004. Constructing covariance functions for random regression models for growth in Gelbvieh beef cattle. *Journal of Animal Science* **82**: 1564–1571.

Letcher, B.H., Coombs, J.A. & Nislow, K.H. 2011. Maintenance of phenotypic variation: repeatability, heritability and size-dependent processes in a wild brook trout population. *Evolutionary Applications* **4**: 602–615.

Lewis, R.M., Emmans, G.C., Dingwall, W.S. & Simm, G. 2002. A description of the growth of sheep and its genetic analysis. *Animal Science* **74**: 51–62.

Lewontin, R.C. 1970. The units of selection. *Annual Review of Ecology and Systematics* **1**: 1–18.

Little, T.D. 2013. *Longitudinal Structural Equation Modeling*. Methodology in Social Sciences. The Guilford Press, New York.

Loison, A., Festa-Bianchet, M., Gaillard, J.M., Jorgenson, J.T. & Jullien, J.M. 1999. Age-specific survival in five populations of ungulates:evidence of senescence. *Ecology* **80**: 2539–2554.

Lush, J.L. 1937. *Animal breeding plans*. Iowa State College Press, Ames, Iowa.

Lynch, M. & Walsh, B. 1998. *Genetics and analysis of quantitative traits*. Sinauer, Sunderland, MA.

Lynch, M. & Walsh, B. 2018. *Evolution and selection of quantitative traits*. Sinauer, Sunderland, MA.

Martin, A.M., Festa-Bianchet, M., Coltman, D.W. & Pelletier, F. 2016. Demographic drivers of age-dependent sexual selection. *Journal of Evolutionary Biology* **29**: 1437–1446.

Martin, J. & Pelletier, F. 2011. Measuring growth patterns in the field: effects of sampling regime and methods on standardized estimates. *Canadian Journal of Zoology* **89**: 529–537.

Martin, J.G.A. & Festa-Bianchet, M. 2011. Age–independent and age–dependent decreases in reproduction of females. *Ecology Letters* **14**: 576–581.

McArdle, J.J. 2009. Latent variable modeling of differences and changes with longitudinal data. *Annual review of psychology* **60**: 577–605.

McArdle, J.J. & McDonald, R.P. 1984. Some algebraic properties of the Reticular Action Model for moment structures. *British Journal of Mathematical and Statistical Psychology* **37**: 234–251.

Merilä, J., Sheldon, B.C. & Kruuk, L.E.B. 2001. Explaining statis: Microevolutionary studies in natural populations. *Genetica* **112-113**: 199–222.

Merow, C., Dahlgren, J.P., Metcalf, J.E., Childs, D.Z., Evans, M.E.K., Jongejans, E., Record, S., Rees, M., Salguero-Gómez, R. & Mcmahon, S.M. 2014. Advancing population ecology with integral projection models: A practical guide. *Methods in Ecology and Evolution* **5**: 99–110.

Meyer, K. 1998. Estimating covariance functions for longitudinal data using a random regression model. *Genetics, selection, evolution* **30**: 221–240.

Meyer, K. 2005. Estimates of genetic covariance functions for growth of Angus cattle. *Journal of animal breeding and genetics* **122**: 73–85.

Meyer, K. 2009. Factor-analytic models for genotype x environment type problems and structured covariance matrices. *Genetics Selection Evolution* **41**: 21.

Meyer, K. & Hill, W.G. 1997. Estimation of genetic and phenotypic covariance functions for longitudinal or 'repeated' records by restricted maximum likelihood. *Livestock Production Science* **47**: 185–200.

Meyer, K. & Kirkpatrick, M. 2005. Up hill, down dale: quantitative genetics of curvaceous traits. *Philosophical Transactions of the Royal Society of London B: Biological Sciences* **360**: 1443–1455.

Miller, B.L.W. & Sinervo, B. 2007. Heritable body size mediates apparent life-history trade-offs in a simultaneous hermaphrodite. *Journal of Evolutionary Biology* **20**: 1554–1562.

Milner, J.M., Albon, S.D., Illinus, A.W., Pemberton, J.M. & Clutton-Brock, T.H. 1999. Repeated selection of morphometric traits in the Soay sheep on St Kilda. *Journal of Animal Ecology* **68**: 472–488.

Milner, J.M., Albon, S.D., Kruuk, L.E.B. & Pemberton, J.M. 2004. Selection on phenotype. In: *Soay sheep: dynamics and selection in an island population* (T.H. Clutton-Brock & J.M. Pemberton, eds), pp. 190–216. Cambridge University Press.

Milner, J.M., Pemberton, J.M., Brotherstone, S. & Albon, S.D. 2000. Estimating variance components and heritabilities in the wild: a case study using the 'animal model' approach. *Journal of Evolutionary Biology* **13**: 804–813.

Mojica, J.P. & Kelly, J.K. 2010. Viability selection prior to trait expression is an essential component of natural selection. *Proceedings of the Royal Society B: Biological Sciences* **277**: 2945–2950.

Monteiro, L.S. & Falconer, D.S. 1966. Compensatory growth and sexual maturity in mice. *Animal Science* **8**: 179–192.

Morrissey, M.B. 2014. Selection and evolution of causally covarying traits. *Evolution* **68**: 1748–1761.

Morrissey, M.B. 2015. Evolutionary quantitative genetics of nonlinear developmental systems. *Evolution* **69**: 2050–2066.

Morrissey, M.B. & Hadfield, J.D. 2012. Directional selection in temporally replicated studies is remarkably consistent. *Evolution* **66**: 435–42.

Morrissey, M.B., Janeiro, M.J., Sparks, A.M., White, S., Pigeon, G., Teplitsky, C., Réale, D. & Milot, E. 2018. Into the wild: Wambam goes to canada. *Molecular Ecology* .

Morrissey, M.B., Kruuk, L.E.B. & Wilson, A.J. 2010. The danger of applying the breeder's equation in observational studies of natural populations. *Journal of Evolutionary Biology* **23**: 2277–2288.

Morrissey, M.B., Parker, D.J., Korsten, P., Pemberton, J.M., Kruuk, L.E.B. & Wilson, A.J. 2012a. The prediction of adaptive evolution: empirical application of the secondary theorem of selection and comparison to the breeder's equation. *Evolution* **66**: 2399–2410.

Morrissey, M.B., Parker, D.J., Korsten, P., Pemberton, J.M., Kruuk, L.E.B. & Wilson, A.J. 2012b. The prediction of adaptive evolution: empirical application of the secondary theorem of selection and comparison to the breeder's equation. *Evolution* **66**: 2399–2410.

Morrissey, M.B., Walling, C.a., Wilson, A.J., Pemberton, J.M., Clutton-Brock, T.H. & Kruuk, L.E.B. 2012c. Genetic analysis of life-history constraint and evolution in a wild ungulate population. *The American Naturalist* **179**: E97–114.

Mueller, L.D. 1997. Theoretical and empirical examination of density-dependent selection. *Annual Review of Ecology and Systematics* **28**: 269–288.

Nakagawa, S. & Freckleton, R.P. 2008. Missing inaction: the dangers of ignoring missing data. *Trends in Ecology and Evolution* **23**: 592–596.

Nakagawa, S. & Schielzeth, H. 2010. Repeatability for Gaussian and non-Gaussian data: a practical guide for biologists. *Biological Reviews of the Cambridge Philosophical Society* **85**: 935–56.

Neems, R.M., Lazarus, J. & McLachlan, A.J. 1998. Lifetime reproductive success in a swarming midge : trade-offs and stabilizing selection for male body size. *Behavioral Ecology* **9**: 279–286.

Noordwijk, A.J.V., Balen, J.H.V. & Scharloo, W. 1988. Heritability of body size in a natural population of the great tit (parus major) and its relation to age and environmental conditions during growth. *Genetical Research* **51**: 149–162.

Nussey, D.H., Coulson, T., Delorme, D., Clutton-Brock, T.H., Pemberton, J.M., Marco, F.B. & Gaillard, J.M. 2011. Patterns of body mass senescence and selective disappearance differ among three species of freeâĂŘliving ungulates. *Ecology* **92**: 1936–1947.

Nussey, D.H., Postma, E., Gienapp, P. & Visser, M.E. 2005. Selection on heritable phenotypic plasticity in a wild bird population. *Science* **310**: 304–306.

Orr, H.A. 2000. Adapation and the cost of complexity. *Evolution* **54**: 13–20.

Ozgul, A., Childs, D.Z., Oli, M.K., Armitage, K.B., Blumstein, D.T., Olson, L.E., Tuljapurkar, S. & Coulson, T. 2010. Coupled dynamics of body mass and population growth in response to environmental change. *Nature* **466**: 482–5.

Ozgul, A., Tuljapurkar, S., Benton, T.G., Pemberton, J.M., Clutton-Brock, T.H. & Coulson, T. 2009. The dynamics of phenotypic change and the shrinking sheep of St. Kilda. *Science* **325**: 464–7.

Pakkasmaa, S., Merilä, J. & O'Hara, R.B. 2003. Genetic and maternal effect influences on viability of common frog tadpoles under different environmental conditions. *Heredity* **91**: 117–24.

Palumbi, S.R. 2001. Humans as the world's greatest evolutionary force. *Science* **293**: 1786–1790.

Peiffer, J.A., Romay, M.C., Gore, M.A., Flint-Garcia, S.A., Zhang, Z., Millard, M.J., Gardner, C.A.C., McMullen, M.D., Holland, J.B., Bradbury, P.J. & Buckler, E.S. 2014. The genetic architecture of maize height. *Genetics* **196**: 1337–1356.

Pelletier, F., Clutton-Brock, T.H., Pemberton, J., Tuljapurkar, S. & Coulson, T. 2007. The evolutionary demography of ecological change: linking trait variation and population growth. *Science* **315**: 1571–1574.

Pelletier, F. & Festa-Bianchet, M. 2006. Sexual selection and social rank in bighorn rams. *Animal Behaviour* **71**: 649 – 655.

Pelletier, F., Festa-Bianchet, M. & Jorgenson, J.T. 2012. Data from selective harvests underestimate temporal trends in quantitative traits. *Biology Letters* **8**: 878–881.

Pelletier, F., Garant, D. & Hendry, A. 2009. Eco-evolutionary dynamics. *Philosophical Transactions of the Royal Society B: Biological Sciences* **364**: 1483–1489.

Pemberton, J. 2008. Wild pedigrees: the way forward. *Proceedings of the Royal Society of London B: Biological Sciences* **275**: 613–621.

Pemberton, J.M. 2010. Evolution of quantitative traits in the wild: mind the ecology. *Philosophical Transactions of the Royal Society B: Biological Sciences* **365**: 2431–2438.

Perez, K.O. & Munch, S.B. 2010. Extreme selection on size in the early lives of fish. *Evolution* **64**: 2450–2457.

Pigeon, G., Festa-Bianchet, M., Coltman, D.W. & Pelletier, F. 2016. Intense selective hunting leads to artificial evolution in horn size. *Evolutionary Applications* **9**: 521–530.

Pletcher, S.D. & Geyer, C.J. 1999. The genetic analysis of age-dependent traits: modeling the character process. *Genetics* **151**: 825–835.

Plummer, M. 2003. JAGS: A program for analysis of Bayesian graphical models using Gibbs sampling. In: *Proceedings of the 3rd International Workshop on Distributed Statistical Computing*.

Poissant, J., Davis, C.S., Malenfant, R.M., Hogg, J.T. & Coltman, D.W. 2012. Qtl mapping for sexually dimorphic fitness-related traits in wild bighorn sheep. *Heredity* **108**: 256–263.

Poissant, J., Wilson, A.J., Festa-Bianchet, M., Hogg, J.T. & Coltman, D.W. 2008. Quantitative genetics and sex-specific selection on sexually dimorphic traits in bighorn sheep. *Proceedings of the Royal Society of London B: Biological Sciences* **275**: 623–628.

Ponzi, E., Bonnet, T., Keller, L. & Muff, S. 2018. Heritability, selection, and the response to selection in the presence of phenotypic measurement error: effects, cures, and the role of repeated measurements. *bioRxiv* .

Postma, E. 2006. Implications of the difference between true and predicted breeding values for the study of natural selection and micro-evolution. *Journal of Evolutionary Biology* **19**: 309–20.

Postma, E. 2014. Four decades of estimating heritabilities in wild vertebrate populations: Improved methods, more data, better estimates? In: *Quantitative Genetics in the Wild. Oxford* (A. Charmantier, D. Garant & L.E.B. Kruuk, eds), pp. 16–33. Oxford University Press.

Price, G.R. 1970. Selection and covariance. *Nature* **227**: 520–521.

R Core Team 2014. *R: A Language and Environment for Statistical Computing*. R Foundation for Statistical Computing, Vienna, Austria. URL `http://www.R-project.org/`.

Rees, M., Childs, D.Z. & Ellner, S.P. 2014. Building integral projection models: a user's guide. *J. Anim. Ecol.* **83**: 528–545.

Rees, M. & Ellner, S.P. 2016. Evolving integral projection models: evolutionary demography meets eco-evolutionary dynamics. *Methods in Ecology and Evolution* **7**: 157–170.

Reeve, J.P. 2000. Predicting long-term response to selection. *Genetical Research* **75**: 83–94.

Robertson, A. 1966. A mathematical model of the culling process in dairy cattle. *Animal Production* **8**: 95–108.

Robertson, A. 1968. The spectrum of genetic variation. In: *Population biology and evolution* (R.C. Lewontin, ed). Syracuse University Press.

Robinson, M.R., Wilson, A.J., Pilkington, J.G., Clutton-Brock, T.H., Pemberton, J.M. & Kruuk, L.E.B. 2009. The impact of environmental heterogeneity on genetic architecture in a wild population of soay sheep. *Genetics* **181**: 1639–1648.

Roff, D.A. 1981. On being the right size. *The American Naturalist* **118**: 405–422.

Roff, D.A. 1986. Predicting body size with life history models. *BioScience* **36**: 316–323.

Roff, D.A. 1995. The estimation of genetic correlations from phenotypic correlations: a test of cheverud's conjecture. *Heredity* **74**: 481–490.

Roff, D.A. 1996. The evolution of genetic correlations: an analysis of patterns. *Evolution* **50**: 1392–1403.

Roff, D.A. 2000. Trade-offs between growth and reproduction : an analysis of the quantitative genetic evidence. *Journal of Evolutionary Biology* **13**: 434–445.

Roff, D.A. & Fairbairn, D.J. 2007. The evolution of trade-offs: where are we? *Journal of Evolutionary Biology* **20**: 433–47.

Rollinson, N. & Rowe, L. 2015. Persistent directional selection on body size and a resolution to the paradox of stasis. *Evolution* **69**: 2441–2451.

Russell, L. 1980. Sexual dimorphism, sexual selection, and adaptation in polygenic characters. *Evolution* **34**: 292–305.

Scheiner, S.M., Mitchell, R.J. & Callahan, H.S. 2000. Using path analysis to measure natural selection. *Journal of Evolutionary Biology* **13**: 423–433.

Schindler, S., Festa-Bianchet, M., Hogg, J.T. & Pelletier, F. 2017. Hunting, age structure, and horn size distribution in bighorn sheep. *Journal of Wildlife Management* **81**: 792–799.

Schindler, S., Neuhaus, P., Gaillard, J.M. & Coulson, T.N. 2013. The influence of nonrandom mating on population growth. *The American Naturalist* **182**: 28–41.

Schluter, D., Price, T.D. & Rowe, L. 1991. Conflicting selection pressures and life history trade-offs. *Proceedings of the Royal Society of London B: Biological Sciences* **246**: 11–17.

Schoener, T.W. 2011. The newest synthesis: Understanding the interplay of evolutionary and ecological dynamics. *Science* **331**: 426–429.

Sesana, R., Bignardi, A., Borquis, R., El Faro, L., Baldi, F., Albuquerque, L. & Tonhati, H. 2010. Random regression models to estimate genetic parameters for test-day milk yield in brazilian murrah buffaloes. *Journal of Animal Breeding and Genetics* **127**: 369–376.

Shimada, Y., Shikano, T., Murakami, N., Tsuzaki, T. & Seikai, T. 2007. Maternal and genetic effects on individual variation during early development in Japanese flounder Paralichthys olivaceus. *Fisheries Science* **73**: 244–249.

Shine, R. 1988. The evolution of large body size in females: a critique of Darwin's fecundity advantage model. *American Naturalist* **131**: 124–131.

Siepielski, A.M., DiBattista, J.D. & Carlson, S.M. 2009. It's about time: the temporal dynamics of phenotypic selection in the wild. *Ecology Letters* **12**: 1261–1276.

Simpson, G.G. 1944. *Tempo and mode in evolution*. Columbia University Press, New York.

Sinervo, B. & McAdam, A.G. 2008. Maturational costs of reproduction due to clutch size and ontogenetic conflict as revealed in the invisible fraction. *Proceedings of the Royal Society of London B: Biological Sciences* **275**: 629–638.

Sober, E. 1986. Force and disposition in evolutionary theory. In: *Minds, machines and evolution* (C. Hookway, ed), pp. 43–62. Cambridge University Press, Cambridge.

Sogard, S. 1997. Size-selective mortality in the juvenile stage of teleost fishes: a review. *Bulletin of Marine Science* **60**: 1129–1157.

Sokolovska, N., Rowe, L. & Johansson, F. 2000. Fitness and body size in mature odonates. *Ecological Entomology* **25**: 239–248.

Spitze, K. 1995. Quantitative genetics of zooplankton life histories. *Experientia* **51**: 454–464.

Stearns, S. 1989. Trade-offs in life-history evolution. *Functional ecology* **3**: 259–268.

Steppan, S.J., Phillips, P.C. & Houle, D. 2002. Comparative quantitative genetics : evolution of the G matrix **17**: 320–327.

Stinchcombe, J.R. & Kirkpatrick, M. 2012. Genetics and evolution of function valued traits: understanding environmentally responsive phenotypes. *Trends in ecology & evolution* **27**: 637–47.

Swain, D.P., Sinclair, A.F. & Mark Hanson, J. 2007. Evolutionary response to size-selective mortality in an exploited fish population. *Proceedings of the Royal Society of London B: Biological Sciences* **274**: 1015–1022.

Thompson, D.J. 1986. Heritability for body size in the isopo Asellus aquaticus (L.). *Crustaceana* **51**: 241–244.

Thompson, J.R. & Carter, R.L. 2007. An overview of normal theory structural measurement error models. *International Statistical Review* **75**: 183–198.

Thomson, C.E., Bayer, F., Crouch, N., Farrell, S., Heap, E., Mittell, E., Zurita-Cassinello, M. & Hadfield, J.D. 2017. Selection on parental performance opposes selection for larger body mass in a wild population of blue tits. *Evolution* **71**: 716–732.

Traill, L.W., Schindler, S. & Coulson, T. 2014. Demography, not inheritance, drives phenotypic change in hunted bighorn sheep. *Proceedings of the National Academy of Sciences of the United States of America* **111**.

van Noordwijk, A.J. & de Jong, G. 1986. Acquisition and allocation of resources: their influence on variation in life history tactics. *The American Naturalist* **128**: 137–142.

Villemereuil, P.D., Schielzeth, H., Nakagawa, S. & Morrissey, M. 2016. General methods for evolutionary quantitative genetic inference from generalised mixed models. *Genetics* **204**: 1281–1294.

Vindenes, Y. & Langangen, Ø. 2015. Individual heterogeneity in life histories and eco-evolutionary dynamics. *Ecology Letters* **18**: 417–432.

Visscher, P.M., Hill, W.G. & Wray, N.R. 2008. Heritability in the genomics era–concepts and misconceptions. *Nature reviews. Genetics* **9**: 255–66.

Walling, C., Morrissey, M.B., Foerster, K., Clutton-Brock, T.H., Pemberton, J.M. & Kruuk, L.E.B. 2014. A multivariate analysis of genetic constraints to life history evolution in a wild population of red deer. *Genetics* **198**: 1735–1749.

Walsh, B. & Blows, M.W. 2009. Abundant genetic variation + strong selection = multivariate genetic constraints: A geometric view of adaptation. *Annual Review of Ecology, Evolution, and Systematics* **40**: 41–59.

Wang, J. 2013. An improvement on the maximum likelihood reconstruction of pedigrees from marker data. *Heredity* **11**: 165–174.

Willis, J.H., Coyne, J.A. & Kirkpatrick, M. 1991. Can one predict the evolution of quantitative characters without genetics? *Evolution* **45**: 441–444.

Wilson, A.J. 2008. Why h2 does not always equal VA/VP? *Journal of Evolutionary Biology* **21**: 647–650.

Wilson, A.J., Kruuk, L.E.B. & Coltman, D.W. 2005. Ontogenetic patterns in heritable variation for body size: using random regression models in a wild ungulate population. *The American Naturalist* **166**: E177–E192.

Wilson, A.J., Pemberton, J.M., Pilkington, J.G., Clutton-Brock, T.H., Coltman, D.W. & Kruuk, L.E.B. 2007. Quantitative genetics of growth and cryptic evolution of body size in an island population. *Evolutionary Ecology* **21**: 337–356.

Wilson, A.J., Réale, D., Clements, M.N., Morrissey, M.B., Postma, E., Walling, C.A., Kruuk, L.E.B. & Nussey, D.H. 2010. An ecologist's guide to the animal model. *The Journal of Animal Ecology* **79**: 13–26.

Wright, S. 1921. Systems of mating. I. The biometric relations between parent and offspring. *Genetics* **6**: 111–123.

Wright, S. 1922. Coefficients of inbreeding and relationship. *The American Naturalist* **56**: 330–338.

Wright, S. 1931. Evolution in mendelian populations. *Genetics* **16**: 97–159.

Wright, S. 1934. The method of path coefficients. *The Annals of Mathematical Statistics* **5**: 161–215.

Wright, S. 1937. The distribution of gene frequencies in populations. *Proceedings of the National Academy of Sciences* **23**: 307–320.

Wright, S. 1960. Path coefficients and path regressions: alternative or complementary concepts? *Biometrics* **16**: 189–202.

Xu, J. & Wang, Q. 2013. Trade-off between adult body size and juvenile survival: an experimental test of parental effects in the mediterranean flour moth. *Australian Journal of Entomology* **52**: 403–406.

APPENDIX A

Supplementary material to Chapter 3

A.1 Supplementary tables

Table A.1.1: Coefficients of the bivariate model of lamb body mass and early pregnancy in Soay sheep ewes. Model description can be found in Equation (3.1), in the main text.

parameter		posterior mode	95% CrI
fixed effects			
body mass	intercept	13.710	(13.232; 14.270)
	density	-0.002	(-0.005; 0.001)
	density^2	0.000	(0.000; 0.000)
	twin	-2.909	(-3.216; -2.619)
	maternal age	0.377	(0.330; 0.436)
	maternal age^2	-0.109	(-0.127; -0.096)
	birth date	-0.061	(-0.072; -0.045)
	measurement date	0.083	(0.042; 0.119)
pregnancy	intercept	0.012	(-0.897; 0.677)
	density	-0.004	(-0.009; -0.001)
	density^2	0.000	(0.000; 0.000)
	twin	1.727	(1.023; 2.306)
	maternal age	-0.160	(-0.273; -0.026)
	maternal age^2	0.037	(-0.004; 0.068)
random effects			
breeding values	body mass	0.721	(0.184; 1.301)
	body mass:pregnancy	0.628	(-0.017; 1.505)
	pregnancy	1.632	(0.000; 5.930)
cohort	body mass	0.526	(0.264; 1.148)
	body mass:pregnancy	0.464	(0.115; 1.167)
	pregnancy	0.931	(0.115; 1.167)
maternal ID	body mass	0.626	(0.342; 1.017)
	body mass $\times$ pregnancy	0.001	(-0.143; 0.432)
	pregnancy	0.003	(0.000; 0.889)
residuals	body mass	1.788	(1.368; 2.224)
	body mass $\times$ pregnancy	1.038	(0.697; 1.254)
	pregnancy	1.000	(1.000; 1.000)

A.2 Details on solving derivatives and integrals

Estimating average trait values (Eqn. 3.3, main text) and variances (Eqn. 3.4), main text) on the expected scale implies solving integrals of high dimensionality in the context of the path analysis, and particularly when these equations are applied to the vector-valued function $\boldsymbol{f(l)}$ in Equation (3.11).

In such circumstances, solving integrals using Monte Carlo simulations is particularly useful as the error is independent from the integrand dimensionality, but mainly because other numerical methods are likely to fail. Monte Carlo integration relies on the fact that the integral $\int_L g(l)f(l)dl$ (or $\int_L g^{-1}(l)f(l)dl$ if applied to an inverse link function) corresponds to the expectation of g, $\mathbb{E}_f[g(L)]$. As a consequence, a random sample of latent values, L, generated using its density f can be used to approximate de empirical average of g,

$$\bar{g} \approx \frac{1}{n}\sum_{i=1}^{n} g(l_i), \tag{A.1}$$

where n is the number of draws from L. $\bar{g}$ is also an approximation to $\int_L g(l)f(l)dl$. This approximation converges to the real value of the integral, by the law of large numbers as $n \to \infty$ (Robert & Casella, 2005). I sampled $n_{MC} = 2000$ values from the distribution of the latent traits on which I evaluated $\boldsymbol{f(l)}$. Since the statistical models were fitted in a Bayesian framework, this procedure was applied to $n_{post} = 2000$ posterior independent samples.

For lower dimensional integrals, and particularly to obtain Φ (average derivative of the expected values with respect to the latent ones) in Equation (3.6), in the main text, I used function *cuhre* from R package **R2Cuba** that implements a deterministic algorithm that uses cubature rules of polynomial degree, also allowing for multidimensional integration.

Likewise, the differentiation in the calculation of extended selection gradients (Eqn. 3.12, main text) was accomplished by numerical linear approximation,

$$W'(l) \approx \frac{W(l+h) - W(l)}{h}, \tag{A.2}$$

where h is some small value. So, the extended selection gradient for mass would be obtained by evaluating W for a certain value of latent mass l and at for $l + h$. This procedure was applied to $n_{MC} = 2000$ values from the distribution of the latent distributions on which I evaluated $\boldsymbol{f(l)}$ times $n_{post} = 2000$ posterior independent samples.

APPENDIX B

Supplementary material to Chapter 4

B.1 Deriving biometric relationships from growth models

B.1.1 Development

The principles of path analysis McArdle & McDonald (1984) were applied to variance-covariance matrices for growth and path coefficient matrices matching Figures 4.1a and 4.1b (main text), both for the general scenario and for the simplification suggested in the main text. In the latter, the obtained variances and covariances in true size across ages are 1 and for the observed size, variances are 1 and covariances r^2.

General 4-age example

Latent true size model I define a variance-covariance matrix for growth, $\boldsymbol{V}$, that includes both the variances on growth, ${\sigma^2}_g$, and the measurement error on observed size, ${\sigma^2}_\epsilon$, as well as a path coefficient matrix, $\boldsymbol{b}$, as follows

$$\boldsymbol{V} = \begin{bmatrix} {\sigma^2}_{g_1} & 0 & 0 & 0 & 0 & 0 & 0 & 0 \\ 0 & {\sigma^2}_{g_2} & 0 & 0 & 0 & 0 & 0 & 0 \\ 0 & 0 & {\sigma^2}_{g_3} & 0 & 0 & 0 & 0 & 0 \\ 0 & 0 & 0 & {\sigma^2}_{g_4} & 0 & 0 & 0 & 0 \\ 0 & 0 & 0 & 0 & {\sigma^2}_{\epsilon_1} & 0 & 0 & 0 \\ 0 & 0 & 0 & 0 & 0 & {\sigma^2}_{\epsilon_2} & 0 & 0 \\ 0 & 0 & 0 & 0 & 0 & 0 & {\sigma^2}_{\epsilon_3} & 0 \\ 0 & 0 & 0 & 0 & 0 & 0 & 0 & {\sigma^2}_{\epsilon_4} \end{bmatrix} \quad \boldsymbol{b} = \begin{bmatrix} 0 & 0 & 0 & 0 & 0 & 0 & 0 & 0 \\ b_{\tilde{z}_1} & 0 & 0 & 0 & 0 & 0 & 0 & 0 \\ 0 & b_{\tilde{z}_2} & 0 & 0 & 0 & 0 & 0 & 0 \\ 0 & 0 & b_{\tilde{z}_3} & 0 & 0 & 0 & 0 & 0 \\ r_1 & 0 & 0 & 0 & 0 & 0 & 0 & 0 \\ 0 & r_2 & 0 & 0 & 0 & 0 & 0 & 0 \\ 0 & 0 & r_3 & 0 & 0 & 0 & 0 & 0 \\ 0 & 0 & 0 & r_4 & 0 & 0 & 0 & 0 \end{bmatrix}.$$

These two matrices are built to match the path diagrams in Figure 4.1a (main text), so that the tracing rules of path analysis can be applied to obtain variances and covariances in size among ages. Particularly, a phenotypic variance-covariance matrix for size among ages, $\boldsymbol{\Sigma}$, is obtained

using

$$\boldsymbol{\Sigma} = \boldsymbol{\varphi} \boldsymbol{V} \boldsymbol{\varphi}^T \tag{a1}$$

and

$$\boldsymbol{\varphi} = (\boldsymbol{I} - \boldsymbol{b})^{-1}, \tag{a2}$$

where $\boldsymbol{\varphi}$ is a matrix with the regressions of each age on every other age and $\boldsymbol{I}$ is an identity matrix of order equal to the number of different ages. The phenotypic variance-covariance matrix for true sizes is therefore given by

$$\boldsymbol{\Sigma_z} = \begin{pmatrix} \sigma^2_{g_1} & \sigma^2_{g_1} b_{z_1} & \sigma^2_{g_1} b_{z_1} b_{z_2} & \sigma^2_{g_1} b_{z_1} b_{z_2} b_{z_3} \\ \sigma^2_{g_1} b_{z_1} & \sigma^2_{g_1} b^2_{z_1} + \sigma^2_{g_2} & \sigma^2_{g_1} b^2_{z_1} b_{z_2} + \sigma^2_{g_2} b_{z_2} & \sigma^2_{g_1} b^2_{z_1} b_{z_2} b_{z_3} + \sigma^2_{g_2} b_{z_2} b_{z_3} \\ \sigma^2_{g_1} b_{z_1} b_{z_2} & \sigma^2_{g_1} b^2_{z_1} b_{z_2} + \sigma^2_{g_2} b_{z_2} & \sigma^2_{g_1} b^2_{z_1} b^2_{z_2} + \sigma^2_{g_2} b^2_{z_2} + \sigma^2_{g_3} & \sigma^2_{g_1} b^2_{z_1} b^2_{z_2} b_{z_3} + \sigma^2_{g_2} b^2_{z_2} b_{z_3} + \sigma^2_{g_3} b_{z_3} \\ \sigma^2_{g_1} b_{z_1} b_{z_2} b_{z_3} & \sigma^2_{g_1} b^2_{z_1} b_{z_2} b_{z_3} + \sigma^2_{g_2} b_{z_2} b_{z_3} & \sigma^2_{g_1} b^2_{z_1} b^2_{z_2} b_{z_3} + \sigma^2_{g_2} b^2_{z_2} b_{z_3} + \sigma^2_{g_3} b_{z_3} & \sigma^2_{g_1} b^2_{z_1} b^2_{z_2} b^2_{z_3} + \sigma^2_{g_2} b^2_{z_2} b^2_{z_3} + \sigma^2_{g_3} b^2_{z_3} + \sigma^2_{z_4} \end{pmatrix}, \tag{A1}$$

and the phenotypic variance-covariance matrix for observed sizes is as follows

$$\boldsymbol{\Sigma_x} = \begin{pmatrix} \sigma^2_{g_1} r^2_1 + \sigma^2_{\epsilon_1} & \sigma^2_{g_1} b_{z_1} r_1 r_2 & \sigma^2_{g_1} b_{z_1} b_{z_2} r_1 r_3 & \sigma^2_{g_1} b_{z_1} b_{z_2} b_{z_3} r_1 r_4 \\ \sigma^2_{g_1} b_{z_1} r_1 r_2 & \sigma^2_{g_1} b^2_{z_1} r^2_2 + \sigma^2_{g_2} r^2_2 + \sigma^2_{\epsilon_2} & \sigma^2_{g_1} b^2_{z_1} b_{z_2} r_2 r_3 + \sigma^2_{g_2} b_{z_2} r_2 r_3 & \sigma^2_{g_1} b^2_{z_1} b_{z_2} b_{z_3} r_2 r_4 + \sigma^2_{g_2} b_{z_2} b_{z_3} r_2 r_4 \\ \sigma^2_{g_1} b_{z_1} b_{z_2} r_1 r_3 & \sigma^2_{g_1} b^2_{z_1} b_{z_2} r_2 r_3 + \sigma^2_{g_2} b_{z_2} r_2 r_3 & \sigma^2_{g_1} b^2_{z_1} b^2_{z_2} r^2_3 + \sigma^2_{g_2} b^2_{z_2} r^2_3 + \sigma^2_{g_3} r^2_3 + \sigma^2_{\epsilon_3} & \sigma^2_{g_1} b^2_{z_1} b^2_{z_2} b_{z_3} r_3 r_4 + \sigma^2_{g_2} b^2_{z_2} b_{z_3} r_3 r_4 + \sigma^2_{g_3} b_{z_3} r_3 r_4 \\ \sigma^2_{g_1} b_{z_1} b_{z_2} b_{z_3} r_1 r_4 & \sigma^2_{g_1} b^2_{z_1} b_{z_2} b_{z_3} r_2 r_4 + \sigma^2_{g_2} b_{z_2} b_{z_3} r_2 r_4 & \sigma^2_{g_1} b^2_{z_1} b^2_{z_2} b_{z_3} r_3 r_4 + \sigma^2_{g_2} b^2_{z_2} b_{z_3} r_3 r_4 + \sigma^2_{g_3} b_{z_3} r_3 r_4 & \sigma^2_{g_1} b^2_{z_1} b^2_{z_2} b^2_{z_3} r^2_4 + \sigma^2_{g_2} b^2_{z_2} b^2_{z_3} r^2_4 + \sigma^2_{g_3} b^2_{z_3} r^2_4 + \sigma^2_{g_4} r^2_4 + \sigma^2_{\epsilon_4} \end{pmatrix}. \tag{A2}$$

Observed size model implemented into IPMs Similarly to the true underlying model, I set the variance-covariance matrix with variances in growth and the matrix with the path coefficients estimated with the standard approach used in IPMs (matching Fig. 4.1b in the main text), respectively, as

$$\boldsymbol{V_{IPM}} = \begin{bmatrix} s^2_{g_1} & 0 & 0 & 0 \\ 0 & s^2_{g_2} & 0 & 0 \\ 0 & 0 & s^2_{g_3} & 0 \\ 0 & 0 & 0 & s^2_{g_4} \end{bmatrix} \qquad \boldsymbol{b_{IPM}} = \begin{bmatrix} 0 & 0 & 0 & 0 \\ b_{x_1} & 0 & 0 & 0 \\ 0 & b_{x_2} & 0 & 0 \\ 0 & 0 & b_{x_3} & 0 \end{bmatrix}.$$

As such, the resulting phenotypic variance-covariance matrix for size at age is

$$\boldsymbol{\Sigma_{x_{IPM}}} = \begin{pmatrix} s^2_{g_1} & s^2_{g_1} b_{x_1} & s^2_{g_1} b_{x_1} b_{x_2} & s^2_{g_1} b_{x_1} b_{x_2} b_{x_3} \\ s^2_{g_1} b_{x_1} & s^2_{g_1} b^2_{x_1} + s^2_{g_2} & s^2_{g_1} b^2_{x_1} b_{x_2} + s^2_{g_2} b_{x_2} & s^2_{g_1} b^2_{x_1} b_{x_2} b_{x_3} + s^2_{g_2} b_{x_2} b_{x_3} \\ s^2_{g_1} b_{x_1} b_{x_2} & s^2_{g_1} b^2_{x_1} b_{x_2} + s^2_{g_2} b_{x_2} & s^2_{g_1} b^2_{x_1} b^2_{x_2} + s^2_{g_2} b^2_{x_2} + s^2_{g_3} & s^2_{g_1} b^2_{x_1} b^2_{x_2} b_{x_3} + s^2_{g_2} b^2_{x_2} b_{x_3} + s^2_{g_3} b_{x_3} \\ s^2_{g_1} b_{x_1} b_{x_2} b_{x_3} & s^2_{g_1} b^2_{x_1} b_{x_2} b_{x_3} + s^2_{g_2} b_{x_2} b_{x_3} & s^2_{g_1} b^2_{x_1} b^2_{x_2} b_{x_3} + s^2_{g_2} b^2_{x_2} b_{x_3} + s^2_{g_3} b_{x_3} & s^2_{g_1} b^2_{x_1} b^2_{x_2} b^2_{x_3} + s^2_{g_2} b^2_{x_2} b^2_{x_3} + s^2_{g_3} b^2_{x_3} + s^2_{g_4} \end{pmatrix}. \quad \text{(A3)}$$

Simplified 4-age example

Analogous matrices for the simplified example set in the main text are shown here. In this example, size-dependent growth coefficients for any age a are one ($b_{z_a} = 1, \forall a$), the variance in true growth at age one is one ($\sigma^2_{g_1} = 1$) and the subsequent are zero ($\sigma^2{}_{g_a} = 0, a > 1$). Finally, the square root of the repeatabilities (r_a) and the variances in measured size ($\sigma^2{}_{\epsilon_a}$) take the same value, r and $1 - r^2$, respectively.

Latent true size model The matrices with true variances and path coefficients correspond to

$$\boldsymbol{V} = \begin{bmatrix} 1 & 0 & 0 & 0 & 0 & 0 & 0 & 0 \\ 0 & 0 & 0 & 0 & 0 & 0 & 0 & 0 \\ 0 & 0 & 0 & 0 & 0 & 0 & 0 & 0 \\ 0 & 0 & 0 & 0 & 0 & 0 & 0 & 0 \\ 0 & 0 & 0 & 0 & 1-r^2 & 0 & 0 & 0 \\ 0 & 0 & 0 & 0 & 0 & 1-r^2 & 0 & 0 \\ 0 & 0 & 0 & 0 & 0 & 0 & 1-r^2 & 0 \\ 0 & 0 & 0 & 0 & 0 & 0 & 0 & 1-r^2 \end{bmatrix} \qquad \boldsymbol{b} = \begin{bmatrix} 0 & 0 & 0 & 0 & 0 & 0 & 0 & 0 \\ 1 & 0 & 0 & 0 & 0 & 0 & 0 & 0 \\ 0 & 1 & 0 & 0 & 0 & 0 & 0 & 0 \\ 0 & 0 & 1 & 0 & 0 & 0 & 0 & 0 \\ r & 0 & 0 & 0 & 0 & 0 & 0 & 0 \\ 0 & r & 0 & 0 & 0 & 0 & 0 & 0 \\ 0 & 0 & r & 0 & 0 & 0 & 0 & 0 \\ 0 & 0 & 0 & r & 0 & 0 & 0 & 0 \end{bmatrix},$$

resulting in the following phenotypic variance-covariance matrix for size at age, where the upper left 4×4 block corresponds to true sizes and the lower right to observed sizes

$$\boldsymbol{\Sigma} = \begin{bmatrix} 1 & 1 & 1 & 1 & r & r & r & r \\ 1 & 1 & 1 & 1 & r & r & r & r \\ 1 & 1 & 1 & 1 & r & r & r & r \\ 1 & 1 & 1 & 1 & r & r & r & r \\ r & r & r & r & 1 & r^2 & r^2 & r^2 \\ r & r & r & r & r^2 & 1 & r^2 & r^2 \\ r & r & r & r & r^2 & r^2 & 1 & r^2 \\ r & r & r & r & r^2 & r^2 & r^2 & 1 \end{bmatrix}.$$

Observed size model implemented into IPMs Similar matrices estimated by the methods normally used in IPMs are given below

$$\boldsymbol{V_{IPM}} = \begin{bmatrix} 1 & 0 & 0 & 0 \\ 0 & 1-r^4 & 0 & 0 \\ 0 & 0 & 1-r^4 & 0 \\ 0 & 0 & 0 & 1-r^4 \end{bmatrix} \qquad \boldsymbol{b_{IPM}} = \begin{bmatrix} 0 & 0 & 0 & 0 \\ r^2 & 0 & 0 & 0 \\ 0 & r^2 & 0 & 0 \\ 0 & 0 & r^2 & 0 \end{bmatrix},$$

resulting in a variance-covariance matrix for size across ages as follows

$$\boldsymbol{\Sigma_{IPM}} = \begin{bmatrix} 1 & r^2 & r^{2^2} & r^{2^4} \\ r^2 & 1 & r^2 & r^{2^2} \\ r^{2^2} & r^2 & 1 & r^2 \\ r^{2^4} & r^{2^2} & r^2 & 1 \end{bmatrix}.$$

B.1.2 Inheritance

As for development, the principles of path analysis were applied to the variance-covariance matrix with the path coefficient matrix, in this case matching Figures 4.5a and 4.5b from the main text.

The cross-age structure of the inheritance function

Expressions for true parent-offspring regressions Let the additive genetic, $\boldsymbol{G_{PO}}$, and the residual, $\boldsymbol{E_{PO}}$, variance-covariance matrices matching Figure 4.5a be defined as

$$\boldsymbol{G_{PO}} = \begin{bmatrix} \sigma^2_{a\,J} & \sigma_{a\,J,A} & \frac{\sigma^2_{a\,J}}{2} & \frac{\sigma_{a\,J,A}}{2} \\ \sigma_{a\,J,A} & \sigma^2_{a\,A} & \frac{\sigma_{a\,J,A}}{2} & \frac{\sigma^2_{a\,A}}{2} \\ \frac{\sigma^2_{a\,J}}{2} & \frac{\sigma_{a\,J,A}}{2} & \sigma^2_{a\,J} & \sigma_{a\,J,A} \\ \frac{\sigma_{a\,J,A}}{2} & \frac{\sigma^2_{a\,A}}{2} & \sigma_{a\,J,A} & \sigma^2_{a\,A} \end{bmatrix} \qquad \boldsymbol{E_{PO}} = \begin{bmatrix} \sigma^2_{e\,J} & \sigma_{e\,J,A} & 0 & 0 \\ \sigma_{e\,J,A} & \sigma^2_{e\,A} & 0 & 0 \\ 0 & 0 & \sigma^2_{e\,B} & \sigma_{e\,J,A} \\ 0 & 0 & \sigma_{e\,J,A} & \sigma^2_{e\,A} \end{bmatrix},$$

where $\sigma^2_{a\,J}$ and $\sigma^2_{e\,J}$ correspond to the additive genetic and environmental variances in size as a juvenile, respectively; and $\sigma^2_{a\,A}$ and $\sigma^2_{e\,A}$ correspond to similar quantities for variance in growth. Note that, in both matrices, the upper left 2×2 square corresponds to parental quantities, whereas the bottom right corresponds to offspring's and the off-diagonals to the correlation between them. In G_{PO}, the genetic covariance of a parent with its offspring was taken as $\frac{1}{2}$ Lynch & Walsh (1998).

Assuming that, regardless of the generation, the regression of adult size on juvenile size is given by b, a matrix of path coefficients $\boldsymbol{b}$ can be defined as

$$\boldsymbol{b} = \begin{bmatrix} 0 & 0 & 0 & 0 \\ b & 0 & 0 & 0 \\ 0 & 0 & 0 & 0 \\ 0 & 0 & b & 0 \end{bmatrix}.$$

The resulting phenotypic variance-covariance matrix for size is given by

$$\boldsymbol{\Sigma_{PO}} = \begin{bmatrix} \sigma^2_{z\,J} & \sigma^2_{z\,J}b + \sigma_{z\,J,A} & \frac{\sigma^2_{a\,J}}{2} & \frac{\sigma^2_{a\,J}}{2}b + \frac{\sigma_{a\,J,A}}{2} \\ \sigma^2_{z\,J}b + \sigma_{z\,J,A} & \sigma^2_{z\,J}b^2 + 2\sigma_{z\,J,A}b + \sigma^2_{z\,A} & \frac{\sigma^2_{a\,J}}{2}b + \frac{\sigma_{a\,J,A}}{2} & \frac{\sigma^2_{a\,J}}{2}b^2 + \sigma_{a\,J,A}b + \frac{\sigma^2_{a\,A}}{2} \\ \frac{\sigma^2_{a\,J}}{2} & \frac{\sigma^2_{a\,J}}{2}b + \frac{\sigma_{a\,J,A}}{2} & \sigma^2_{z\,J} & \sigma^2_{z\,J}b + \sigma_{z\,J,A} \\ \frac{\sigma^2_{a\,J}}{2}b + \frac{\sigma_{a\,J,A}}{2} & \frac{\sigma^2_{a\,J}}{2}b^2 + \sigma_{a\,J,A}b + \frac{\sigma^2_{a\,A}}{2} & \sigma^2_{z\,J}b + \sigma_{z\,J,A} & \sigma^2_{z\,J}b^2 + 2\sigma_{z\,J,A}b + \sigma^2_{z\,A} \end{bmatrix}.$$

Considering that the estimator for the slope of a linear regression is just the quotient of the covariance between the response and the predictor by the variance of the predictor, the parent-offspring regressions, β_{O_J,P_J} and β_{O_A,P_A}, are easily calculated using $\boldsymbol{\Sigma_{PO}}$, as well as the other two true regressions discussed in the main text.

Expressions for parent-offspring regressions recovered by IPMs Similarly to what was done for the theoretical values, a residual variance-covariance matrix, $\boldsymbol{E_{PO_{IPM}}}$, and a matrix with path coefficients, $\boldsymbol{b_{PO_{IPM}}}$,

$$\boldsymbol{E_{PO_{IPM}}} = \begin{bmatrix} s^2_{g_J} & 0 & 0 & 0 \\ 0 & s^2_{g_A} & 0 & 0 \\ 0 & 0 & s^2_{g_J} & 0 \\ 0 & 0 & 0 & s^2_{g_A} \end{bmatrix} \qquad \boldsymbol{b_{PO_{IPM}}} = \begin{bmatrix} 0 & 0 & 0 & 0 \\ b_{dev} & 0 & 0 & 0 \\ 0 & b_{inh} & 0 & 0 \\ 0 & 0 & b_{dev} & 0 \end{bmatrix},$$

were defined so to match the path diagram in Figure 4.5b (main text). s^2 was used to denote variances, and in matrix $\boldsymbol{b_{PO_{IPM}}}$, b_{dev} and b_{inh} correspond to coefficients for ontogenic development and cross-age inheritance, respectively. Using Equations (a1) and (a2), a phenotypic variance-covariance matrix for size,

$$\boldsymbol{\Sigma_{PO_{IPM}}} = \begin{pmatrix} s^2_{g_J} & s^2_{g_J} b_{dev} & s^2_{g_J} b_{dev}b_{inh} & s^2_{g_J} b_{dev}{}^2 b_{inh} \\ s^2_{g_J} b_{dev} & s^2_{g_J} b_{dev}{}^2 + s^2_{g_A} & s^2_{g_J} b_{dev}{}^2 b_{inh} + s^2_{g_A} b_{inh} & s^2_{g_J} b_{dev}{}^3 b_{inh} + s^2_{g_A} b_{dev} b_{inh} \\ s^2_{g_J} b_{dev} b_{inh} & s^2_{g_J} b_{dev}{}^2 b_{inh} & s^2_{g_J} + s^2_{g_J} b_{dev}{}^2 b_{inh}{}^2 + s^2_{g_A} b_{inh}{}^2 & s^2_{g_J} b_{dev} + s^2_{g_J} b_{dev}{}^3 b_{inh}{}^2 + s^2_{g_A} b_{dev} b_{inh}{}^2 \\ s^2_{g_J} b_{dev}{}^2 b_{inh} & s^2_{g_J} b_{dev}{}^3 b_{inh} + s^2_{g_A} b_{dev} b_{inh} & s^2_{g_J} b_{dev} + s^2_{g_J} b_{dev}{}^3 b_{inh}{}^2 + s^2_{g_A} b_{dev} b_{inh}{}^2 & s^2_{g_J} b_{dev}{}^2 + s^2_{g_J} b_{dev}{}^4 b_{inh}{}^2 + s^2_{g_A} b_{dev}{}^2 b_{inh}{}^2 + s^2_{g_A} \end{pmatrix}, \quad \text{(B.1)}$$

is obtained. According to this matrix, the parent-offspring regression, regardless of the ontogenic stage, is given by $b_{dev} \cdot b_{inh}$,

$$\beta_{O_J,P_{J\,IPM}} = \frac{s^2_{g_J} b_{dev} b_{inh}}{s^2_{g_J}} = b_{dev} b_{inh} \quad \text{(A2a)}$$

$$\beta_{O_A,P_{A\,IPM}} = \frac{s^2_{g_J} b_{dev}{}^3 b_{inh} + s^2_{g_A} b_{dev} b_{inh}}{s^2_{g_J} b_{dev}{}^2 + s^2_{g_J}} = b_{dev} b_{inh}. \quad \text{(A2b)}$$

As pointed out in the main text, an IPM recovers the true values for the regression of juvenile size on adult size (β_{O_J,O_A} and β_{P_J,P_A}, or just $\beta_{J,A}$) and also for offspring juvenile size on parent adult size (β_{O_J,P_A}), as they are estimated directly from the data. As a result, b_{dev} and b_{inh} correspond to true $\beta_{J,A}$ and β_{O_J,P_A}, respectively, and therefore the product $\beta_{J,A} \cdot \beta_{O_J,P_A}$ corresponds to the IPM's estimator of the parent-offspring regression for both juveniles and adults.

B.2 Supplementary tables and figures

B.2.1 Tables

Table B.2.1: Covariances among ages i and j ($j > i$) in true and observed sizes. σ^2_g correspond to variances in growth, b_z to path coefficients, and r to the square root of the repeatabilities. The subscripts $1, 2, ...$ denote corresponding ages.

Covariance(age i, age j)	true latent size (z)	observed size (x)
$cov(1,j)$	$\sigma^2_{g_1} \prod_{i=1}^{j-1} b_{z_i}$	$\sigma^2_{g_1} \prod_{i=1}^{j-1} b_{z_i}\ r_i r_j$
$cov(2,j)$	$\sigma^2_{g_1} b^2_{z_1} \prod_{i=2}^{j-1} b_{z_i} + \sigma^2_{g_2} \prod_{i=2}^{j-1} b_{z_i}$	$\sigma^2_{g_1} b^2_{z_1} \prod_{i=2}^{j-1} b_{z_i}\ r_i r_j + \sigma^2_{g_2} \prod_{i=2}^{j-1} b_{z_i}\ r_i r_j$
$cov(3,j)$	$\sigma^2_{g_1} b^2_{z_1} b^2_{z_2} \prod_{i=3}^{j-1} b_{z_i} + \sigma^2_{g_2} b^2_{z_2} \prod_{i=3}^{j-1} b_{z_i}$	$\sigma^2_{g_1} b^2_{z_1} b^2_{z_2} \prod_{i=3}^{j-1} b_{z_i}\ r_i r_j + \sigma^2_{z_2} b^2_{z_2} \prod_{i=3}^{j-1} b_{z_i}\ r_i r_j + \sigma^2_{g_3} \prod_{i=3}^{j-1} b_{z_i}\ r_i r_j$
$cov(...,j)$	...	...

Table B.2.2: Covariances in size among ages i and j ($j > i$) recovered by typically-constructed IPMs. s_g^2 correspond to variances growth and b to path coefficients. The subscripts $1, 2, ...$ denote corresponding ages.

Covariance(age i, age j)	observed size (x)
$cov(1,j)$	$s_{g_1}^2 \prod_{i=1}^{j-1} b_{x_i}$
$cov(2,j)$	$s_{g_1}^2 b_{x_1}^2 \prod_{i=2}^{j-1} b_{x_i} + s_{g_2}^2 \prod_{i=2}^{j-1} b_{x_i}$
$cov(3,j)$	$s_{g_1}^2 b_{x_1}^2 b_{x_2}^2 \prod_{i=3}^{j-1} b_{x_i} + s_{g_2}^2 b_{x_2}^2 \prod_{i=3}^{j-1} b_{x_i} + s_{g_3}^2 \prod_{i=3}^{j-1} b_{x_i}$
$cov(...,j)$	...

B.2.2 Figures

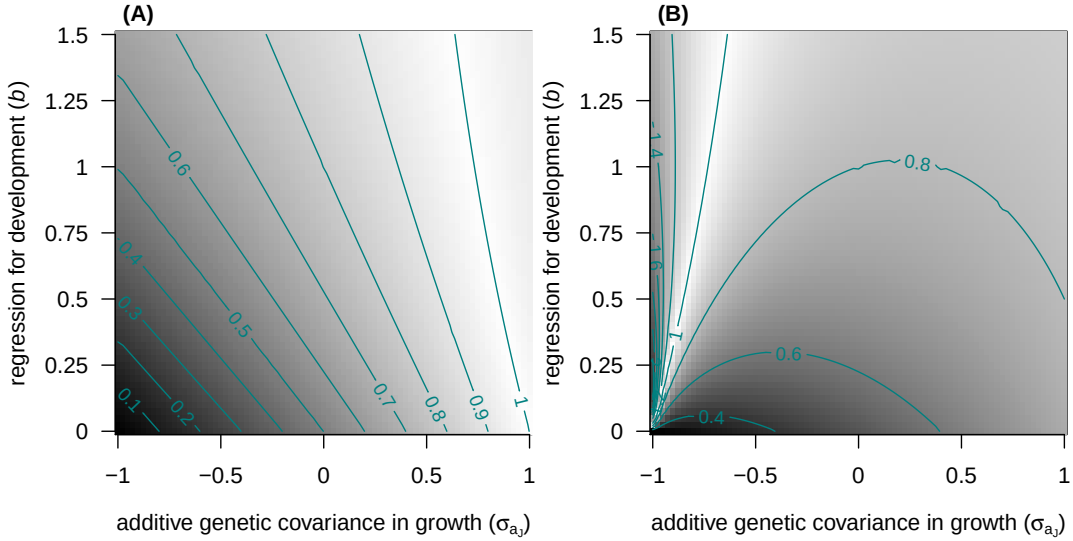

Figure B.2.1: Proportion of parent-offspring regression recovered by IPMs, in juveniles, **(A)**, and adults, **(B)**, as a function of the size-dependent growth regression (b) and the additive genetic covariance in growth ($\sigma_{a_{J,A}}$). The remaining parameters were set to $\sigma^2_{a_J} = 1$, $\sigma^2_{a_A} = 1$, $\sigma^2_{e_J} = 1$, $\sigma^2_{e_A} = 1$, and $\sigma_{e_{J,A}} = 0$. The true values were used as reference.

APPENDIX C

Supplementary material to Chapter 5

C.1 Code for the factor analytic models

Table C.1.1: JAGS code for the factor analytic model described in equation (5.3) including a single additive genetic axis, `fa(1)`.

```
---------------------------------------------------------------------------------------------
modelCode<-"
model {
##### A. Breeding values
#unknown parents
for(i in 1:NKnownNeither) {a.mum[i]~dnorm(0,tau_a)}
for(i in (NKnownNeither+NKnownMum+1):(NKnownNeither+NKnownMum+NKnownDad)) {a.mum[i]~dnorm(0,tau_a)}
for(i in 1:(NKnownNeither+NKnownMum)) {a.dad[i]~dnorm(0,tau_a)}
#known parents
for(i in (NKnownNeither+1):(NKnownNeither+NKnownMum)) {a.mum[i]<-a[mum[i]]}
for(i in (NKnownNeither+NKnownMum+NKnownDad+1):Nped) {a.mum[i]<-a[mum[i]]}
for(i in (NKnownNeither+NKnownMum+1):Nped) {a.dad[i]<-a[dad[i]]}
#offspring
for(i in 1:Nped) {a[i]~dnorm((a.mum[i]+a.dad[i])/2,tau_a2)}
#bv for the sheep being modelled
for(i in 1:N) {fa[i]<-a[id[i]]} #id in phenotypic data

##### B. the model
# state model
for(i in 1:N) {
fe[i]~dnorm(0, 1)
for(j in 1:Nage){
z[i,j]~dnorm(mu[j]+beta*dens[i]+lambda_a[j]*fa[i]+lambda_e[j]*fe[i] + u[Mum[i]] + w[cohort[i]],
tau[agecat[j]])
}
}
# observation model
for(k in 1:n.obs){y[k]~dnorm(z[id2[k],age[k]], meas.tau[age[k]])}

##### C. Prior distributions
tau_a[1]<-1
tau_a2[1]<-2

beta~dnorm(0,0.00001)
for (i in 1:Nmum) {u[i]~dnorm(0,tauMum)}
for (i in 1:Ncohort) {w[i]~dnorm(0,tauCohort)}
tauMum~dgamma(0.001,0.001)
sigmaMum<-1/tauMum
tauCohort~dgamma(0.001,0.001)
sigmaCohort<-1/tauCohort

for (j in 1:Nage){
mu[j]~dnorm(0,0.00001)
meas.tau[j]<-1000
meas.sigma[j]<-1/meas.tau[j]
lambda_a[j]~dnorm(0,0.00001)
lambda_e[j]~dnorm(0,0.00001)
}
for (j in 1:4){
tau[j]~dgamma(0.001,0.001)
sigma[j]<-1/tau[j]
}
}
"
---------------------------------------------------------------------------------------------
```

Table C.1.2: JAGS code for the factor analytic model described in equation (5.3) including two additive genetic axes, `fa(2)`.

```
-----------------------------------------------------------------------------------------------
modelCode<-"
model {
##### A. Breeding values
#unknown parents
for (j in 1:2){
for(i in 1:NKnownNeither) {a.mum[i,j]~dnorm(0,tau_a[j])}
for(i in (NKnownNeither+NKnownMum+1):(NKnownNeither+NKnownMum+NKnownDad)) {a.mum[i,j]~dnorm(0,tau_a[j])}
for(i in 1:(NKnownNeither+NKnownMum)) {a.dad[i,j]~dnorm(0,tau_a[j])}
#known parents
for(i in (NKnownNeither+1):(NKnownNeither+NKnownMum)) {a.mum[i,j]<-a[mum[i],j]}
for(i in (NKnownNeither+NKnownMum+NKnownDad+1):Nped) {a.mum[i,j]<-a[mum[i],j]}
for(i in (NKnownNeither+NKnownMum+1):Nped) {a.dad[i,j]<-a[dad[i],j]}
#offspring
for(i in 1:Nped) {a[i,j]~dnorm((a.mum[i,j]+a.dad[i,j])/2,tau_a2[j])}}
#genetic common factors for the sheep being modelled
for(i in 1:N) {fa1[i]<-a[id[i],1]} #id
for(i in 1:N) {fa2[i]<-a[id[i],2]} #id

##### B. the model
# state model
for(i in 1:N) {
fe[i]~dnorm(0, 1)
for(j in 1:Nage){
z[i,j]~dnorm(mu[j]+beta*dens[i]+lambda_a[j,1]*fa1[i]+lambda_a[j,2]*fa2[i]+lambda_e[j]*fe[i] +
u[Mum[i]] + w[cohort[i]], tau[agecat[j]])
}
}
# observation model
for(k in 1:n.obs){y[k]~dnorm(z[id2[k],age[k]], meas.tau[age[k]])}

##### C. Prior distributions
tau_a[1]<-1
tau_a2[1]<-2
tau_a[2]<-1
tau_a2[2]<-2

beta~dnorm(0,0.00001)
for (i in 1:Nmum) {u[i]~dnorm(0,tauMum)}
for (i in 1:Ncohort) {w[i]~dnorm(0,tauCohort)}
tauMum~dgamma(0.001,0.001)
sigmaMum<-1/tauMum
tauCohort~dgamma(0.001,0.001)
sigmaCohort<-1/tauCohort

for (j in 1:Nage){
mu[j]~dnorm(0,0.00001)
meas.tau[j]<-1000
meas.sigma[j]<-1/meas.tau[j]
lambda_a[j,1]~dnorm(0,0.00001)
lambda_e[j]~dnorm(0,0.00001)
}
lambda_a[1,2]<-0
for (j in 2:Nage) {lambda_a[j,2]~dnorm(0,0.00001)}
for (j in 1:4){
tau[j]~dgamma(0.001,0.001)
sigma[j]<-1/tau[j]
}
}
"
-----------------------------------------------------------------------------------------------
```

C.2 Model outputs

Table C.2.1: Parameter estimates from the multivariate model (`mvt`) on horn length fitted to the bighorn sheep males from the population of Ram Mountain. Values correspond to posterior means and lower (ll) and upper (ul) limits of 95% HPD credible intervals. Additive genetic and phenotypic (co)variances and correlations are available in Appendix C.4.

parameter	mean	ll	ul
fixed effects			
yearling	21.43	20.24	22.62
2 years-old	37.55	36.32	38.85
3 years-old	52.13	50.87	53.51
4 years-old	63.77	62.38	65.19
5 years-old	72.67	71.25	74.27
6 years-old	79.01	77.44	80.65
7 years-old	82.59	80.87	84.44
8 years-old	84.74	82.98	86.86
population density (yearlings) $(\times 100)$	6.39	1.59	11.96
population density (2 year-olds) $(\times 100)$	-3.10	-5.23	-0.87
population density (3 year-olds) $(\times 100)$	-4.93	-7.54	-1.93
population density (older) $(\times 100)$	-6.55	-9.63	-2.94
random effects			
maternal ID	3.85	0.65	7.26
cohort	11.41	3.69	19.98
year of measurement	1.10	0.41	2.00

Table C.2.2: Parameter estimates from the random regression model (`rr`) on horn length fitted to the bighorn sheep males from the population of Ram Mountain. Values correspond to posterior means and lower (ll) and upper (ul) limits of 95% HPD credible intervals. Additive genetic and phenotypic (co)variances and correlations are available in Appendix C.4.

parameter	mean	ll	ul
fixed effects			
yearling	21.66	20.30	23.12
2 years-old	38.27	36.65	39.72
3 years-old	53.23	51.61	55.08
4 years-old	65.18	63.25	67.01
5 years-old	74.10	72.18	76.02
6 years-old	80.29	78.36	82.26
7 years-old	83.51	81.38	85.69
8 years-old	85.22	82.83	87.69
population density (yearlings) $(\times 100)$	6.56	1.88	11.35
population density (2 year-olds) $(\times 100)$	-3.50	-5.39	-1.67
population density (3 year-olds) $(\times 100)$	-5.41	-8.14	-2.86
population density (older) $(\times 100)$	-7.98	-11.28	-4.74
random effects			
breeding values			
intercept	20.57	0.00	43.68
age	3.84	0.00	6.42
age^2	0.12	0.05	0.20
intercept $\times$ *age*	-4.36	-8.27	0.30
intercept $\times$ age^2	-1.10	-1.87	-0.22
age $\times$ age^2	0.65	0.17	1.19
permanent environment			
intercept	15.88	0.00	33.93
age	0.61	0.00	2.57
age^2	0.01	0.00	0.04
intercept $\times$ *age*	1.74	-0.73	5.41
intercept $\times$ age^2	-0.07	-0.67	0.47
age $\times$ age^2	0.04	-0.04	0.31
maternal ID	0.85	0.00	2.72
cohort	13.00	4.75	23.14
year of measurement	1.20	0.48	2.16
residual			
population density (yearlings)	1.46	0.41	2.73
population density (2 year-olds)	2.36	1.51	3.20
population density (3 year-olds)	1.51	0.83	2.36
population density (older)	1.87	1.30	2.49

Table C.2.3: Estimates of the age-specific parameters from the factor analytic model with a single additive genetic common factor (`fa(1)`) on horn length fitted to the bighorn sheep males from the population of Ram Mountain. Values correspond to posterior means and lower (ll) and upper (ul) limits of 95% HPD credible intervals of age-specific intercepts (μ), factor loadings associated to the additive genetic common factor (λ_a) and factor loadings associated to the permanent environment common factor (λ_e). Additive genetic and phenotypic (co)variances and correlations are available in Appendix C.4.

	μ			λ_a			λ_e		
age	mean	ll	ul	mean	ll	ul	mean	ll	ul
yearling	22.36	21.60	23.21	2.52	0.19	4.53	-2.86	-4.08	-1.60
2 years-old	38.22	37.06	39.43	3.39	-0.76	7.05	-6.66	-6.91	-3.58
3 years-old	52.29	50.95	53.55	2.75	-2.25	7.48	-6.66	-8.15	-4.78
4 years-old	63.22	61.69	64.69	1.91	-4.39	7.06	-7.92	-9.56	-5.91
5 years-old	71.91	70.33	73.37	0.70	-5.25	5.96	-7.92	-9.85	-6.37
6 years-old	78.02	76.29	79.53	-0.53	-6.15	4.79	-7.77	-9.93	-5.97
7 years-old	81.44	79.68	83.19	-2.67	-6.74	0.75	-5.61	-8.44	-2.84
8 years-old	83.67	81.77	85.49	-2.94	-6.67	0.58	-5.34	-7.91	-2.19

Table C.2.4: Estimates of the non-age-specific parameters from the factor analytic model with a single additive genetic common factor (`fa(1)`) on horn length fitted to the bighorn sheep males from the population of Ram Mountain. Values correspond to posterior means and lower (ll) and upper (ul) limits of 95% HPD credible intervals.

parameter	mean	ll	ul
fixed effects			
population density (yearlings) $(\times 100)$	-1.14	-3.32	1.19
population density (2 year-olds) $(\times 100)$	-0.08	-3.08	3.38
population density (3 year-olds) $(\times 100)$	1.00	-2.80	5.28
population density (older) $(\times 100)$	2.69	-2.05	7.32
random effects			
maternal ID	0.13	0.00	0.63
cohort	0.12	0.00	0.52
year of measurement	0.26	0.00	1.17
residual			
population density (yearlings)	4.51	3.23	5.95
population density (2 year-olds)	2.92	1.63	4.30
population density (3 year-olds)	3.33	1.99	4.90
population density (older)	2.82	2.00	3.76

Table C.2.5: Estimates of the age-specific parameters from the factor analytic model with two additive genetic common factor (`fa(2)`) on horn length fitted to the bighorn sheep males from the population of Ram Mountain. Values correspond to posterior means and lower (ll) and upper (ul) limits of 95% HPD credible intervals of age-specific intercepts (μ), factor loadings associated to the additive genetic common factors (λ_a) and factor loadings associated to the permanent environment common factor (λ_e). Additive genetic and phenotypic (co)variances and correlations are available in Appendix C.4.

	μ			λ_{a1}			λ_{a2}			λ_e		
age	mean	ll	ul	mean	ll	ul	mean	ll	ul	mean	ll	ul
yearling	22.32	21.49	23.12	3.22	1.23	4.64	0.00	0.00	0.00	-2.54	-4.12	-1.15
2 years-old	38.13	36.92	39.25	4.11	1.52	6.67	0.58	-1.01	2.10	-6.47	-6.60	-3.15
3 years-old	52.19	50.97	53.70	3.38	0.20	6.98	0.63	-2.59	3.19	-6.47	-7.89	-4.56
4 years-old	63.14	61.64	64.62	2.91	-0.90	7.51	-0.24	-4.21	3.63	-7.59	-9.13	-5.63
5 years-old	71.85	70.23	73.36	2.25	-2.06	6.80	-1.19	-5.39	3.07	-7.49	-9.35	-5.47
6 years-old	78.13	76.43	79.79	1.84	-2.80	6.33	-2.05	-6.06	2.31	-7.20	-9.31	-4.71
7 years-old	81.95	79.84	83.82	0.86	-3.43	5.81	-3.51	-6.81	0.40	-5.16	-7.83	-1.62
8 years-old	84.82	82.41	87.46	2.19	-3.29	7.31	-4.60	-7.73	-1.17	-4.76	-8.39	-0.91

Table C.2.6: Estimates of the non-age-specific parameters from the factor analytic model with two additive genetic common factors (`fa(2)`) on horn length fitted to the bighorn sheep males from the population of Ram Mountain. Values correspond to posterior means and lower (ll) and upper (ul) limits of 95% HPD credible intervals.

parameter	mean	ll	ul
fixed effects			
population density (yearlings) $(\times 100)$	-0.74	-3.12	1.56
population density (2 year-olds) $(\times 100)$	0.66	-2.76	3.94
population density (2 year-olds) $(\times 100)$	1.78	-2.11	5.82
population density (older) $(\times 100)$	3.38	-1.36	8.06
random effects			
maternal ID	0.11	0.00	0.51
cohort	0.08	0.00	0.37
year of measurement	0.18	0.00	0.87
residual			
population density (yearlings)	3.37	1.18	5.54
population density (2 year-olds)	2.26	0.00	3.63
population density (3 year-olds)	2.93	1.40	4.46
population density (older)	2.06	1.41	2.76

Table C.2.7: Estimates of the age-specific parameters from the antedependence model (`ant`) on horn length fitted to the bighorn sheep males from the population of Ram Mountain. Values correspond to posterior means and lower (ll) and upper (ul) limits of 95% HPD credible intervals of age-specific intercepts (μ), age-specific slopes on previous horn length (β_{dev}) and residual variances (σ_r^2). Phenotypic (co)variance and correlation matrices are available in Appendix C.4.

	μ			β_{dev}			σ_r^2		
age	mean	ll	ul	mean	ll	ul	mean	ll	ul
yearling	16.97	10.67	23.49				6.62	3.78	9.66
2 years-old	15.10	12.35	17.57	1.03	0.92	1.15	4.59	3.22	6.11
3 years-old	19.56	15.93	23.04	0.87	0.77	0.96	3.59	2.36	4.89
4 years-old	19.04	13.99	24.38	0.87	0.76	0.97	3.05	1.67	4.38
5 years-old	18.83	12.38	25.26	0.86	0.76	0.96	3.27	1.69	4.90
6 years-old	16.74	9.33	23.42	0.87	0.78	0.98	2.32	1.13	3.77
7 years-old	26.67	12.16	41.10	0.71	0.53	0.90	3.36	1.39	5.93
8 years-old	35.18	20.66	50.88	0.60	0.40	0.78	3.53	1.28	6.33

Table C.2.8: Estimates of the non-age-specific parameters from the antedependence model (`ant`) on horn length fitted to the bighorn sheep males from the population of Ram Mountain. Values correspond to posterior means and lower (ll) and upper (ul) limits of 95% HPD credible intervals.

parameter	mean	ll	up
fixed effects			
inheritance	0.09	-0.04	0.21
population density (yearlings) $(\times 100)$	-4.95	-8.95	-0.63
population density (2 year-olds) $(\times 100)$	1.44	-1.93	4.62
population density (3 year-olds) $(\times 100)$	1.77	-1.47	5.18
population density (older) $(\times 100)$	2.45	-1.37	6.03
random effects			
permanent environment	1.22	0.32	2.20
maternal ID	0.12	0.00	0.42
cohort	0.80	0.00	2.38
year of measurement	4.63	1.78	7.97

Table C.2.9: Estimates of the age-specific parameters from an IPM-like antedependence model on horn length fitted to the bighorn sheep males from the population of Ram Mountain. This model differs from one shown in the main text as its inheritance function is of parental horn length at conception, rather than at 3 years-old. Values correspond to posterior means and lower (ll) and upper (ul) limits of 95% HPD credible intervals of age-specific intercepts (μ), age-specific slopes on previous horn length (β_{dev}) and residual variances (σ_r^2)..

	μ			β_{dev}			σ_r^2		
age	mean	ll	ul	mean	ll	ul	mean	ll	ul
yearling	31.64	26.06	37.53				5.02	2.47	7.84
2 years-old	14.40	11.97	16.99	1.07	0.96	1.18	4.96	3.46	6.39
3 years-old	18.09	14.66	21.67	0.91	0.82	1.00	3.82	2.52	5.11
4 years-old	16.87	12.42	22.08	0.91	0.81	1.00	3.21	1.86	4.72
5 years-old	16.59	9.97	22.19	0.89	0.80	1.00	3.41	1.92	5.33
6 years-old	14.41	7.93	21.00	0.90	0.81	0.99	2.33	1.14	3.79
7 years-old	23.94	8.73	37.68	0.75	0.58	0.95	3.53	1.44	6.30
8 years-old	32.54	18.27	48.77	0.63	0.43	0.81	3.57	1.37	6.48

Table C.2.10: Estimates of the non-age-specific parameters from an IPM-like antedependence model on horn length fitted to the bighorn sheep males from the population of Ram Mountain. This model differs from one shown in the main text as its inheritance function is of parental horn length at conception, rather than at 3 years-old. Values correspond to posterior means and lower (ll) and upper (ul) limits of 95% HPD credible intervals.

parameter	mean	ll	up
fixed effects			
inheritance	-0.14	-0.22	-0.07
population density (yearlings) $(\times 100)$	-6.38	-11.09	-1.54
population density (2 year-olds) $(\times 100)$	3.04	-1.42	7.09
population density (3 year-olds) $(\times 100)$	3.62	-0.48	8.13
population density (older) $(\times 100)$	4.40	0.07	8.61
random effects			
permanent environment	0.86	0.09	1.64
maternal ID	0.10	0.00	0.38
cohort	0.44	0.00	1.32
year of measurement	4.63	1.99	7.52

C.3 Additive genetic and permanent environment variation across ages

Table C.3.1: Additive genetic and permanent environment contributions to the phenotypic variance across the horn length ontogeny of males from the bighorn sheep population of Ram Mountain. Absolute values, σ^2_a and σ^2_e, proportions of phenotypic variance, h^2 and e^2, and coefficients of variation, CV_a and CV_e, are shown for the different models.

		yearling	2 years-old	3 years-old	4 years-old	5 years-old	6 years-old	7 years-old	8 years-old
σ^2_a	mvt	11.22 (5.54;16.95)	27.19 (19.07;36.44)	30.77 (21.18;40.56)	37.58 (25.17;51.42)				
	rr	10.03 (4.78; 15.47)	19.22 (10.99; 27.74)	29.80 (15.45; 43.03)	36.28 (16.65; 53.09)	36.12 (12.02; 54.74)	29.76 (5.83; 51.42)	20.57 (0.00; 43.68)	14.91 (0.14; 40.45)
	fa(1)	7.78 (0.00; 15.51)	15.25 (0.00; 33.36)	12.60 (0.00; 33.73)	9.90 (0.00; 31.87)	6.21 (0.00; 23.40)	5.52 (0.00; 22.85)	10.20 (0.00; 31.73)	11.57 (0.00; 34.13)
	fa(2)	11.08 (0.00; 19.57)	19.82 (0.38; 38.21)	17.18 (0.01; 40.73)	17.30 (0.01; 45.94)	16.60 (0.00; 47.14)	18.23 (0.01; 52.91)	22.37 (0.03; 55.29)	36.27 (0.74; 76.46)
	ant*	2.46 (-1.02; 6.32)	4.89 (-2.02; 12.44)	4.99 (-2.23; 12.87)	4.78 (-2.11; 13.02)	4.44 (-1.98; 12.84)	4.06 (-2.49; 11.50)	2.43 (-1.35; 7.55)	1.08 (-0.58; 3.44)
h^2	mvt	0.29 (0.12;0.45)	0.50 (0.32;0.68)	0.53 (0.35;0.71)	0.57 (0.38;0.74)				
	rr	0.32 (0.15; 0.51)	0.46 (0.26; 0.65)	0.57 (0.34; 0.77)	0.59 (0.35; 0.82)	0.57 (0.28; 0.82)	0.50 (0.17; 0.81)	0.38 (0.00; 0.72)	0.28 (0.00; 0.70)
	fa(1)	0.35 (0.00; 0.65)	0.31 (0.00; 0.65)	0.20 (0.00; 0.51)	0.12 (0.00; 0.39)	0.08 (0.00; 0.31)	0.07 (0.00; 0.30)	0.21 (0.00; 0.60)	0.24 (0.00; 0.68)
	fa(2)	0.50 (0.07; 0.86)	0.40 (0.02; 0.74)	0.27 (0.00; 0.59)	0.22 (0.00; 0.53)	0.21 (0.00; 0.56)	0.24 (0.00; 0.66)	0.40 (0.01; 0.87)	0.54 (0.11; 0.97)
	ant*	0.18 (-0.08; 0.43)	0.19 (-0.07; 0.45)	0.16 (-0.07; 0.39)	0.14 (-0.06; 0.36)	0.12 (-0.05; 0.32)	0.11 (-0.04; 0.29)	0.08 (-0.03; 0.22)	0.05 (-0.02; 0.14)
CV_a**	mvt	0.15 (0.11;0.19)	0.14 (0.12;0.16)	0.11 (0.09;0.13)	0.10 (0.08;0.12)				
	rr	0.14 (0.10; 0.18)	0.12 (0.09; 0.14)	0.11 (0.08; 0.13)	0.10 (0.07; 0.12)	0.09 (0.06; 0.11)	0.07 (0.04; 0.10)	0.05 (0.02; 0.09)	0.04 (0.01; 0.08)
	fa(1)	0.12 (0.03; 0.19)	0.10 (0.01; 0.16)	0.06 (0.00; 0.11)	0.04 (0.00; 0.09)	0.03 (0.00; 0.07)	0.02 (0.00; 0.06)	0.03 (0.00; 0.07)	0.04 (0.00; 0.07)
	fa(2)	0.15 (0.06; 0.21)	0.11 (0.05; 0.18)	0.08 (0.02; 0.13)	0.06 (0.01; 0.11)	0.05 (0.01; 0.10)	0.05 (0.00; 0.09)	0.05 (0.01; 0.10)	0.07 (0.02; 0.11)
σ^2_e	mvt	12.54 (9.60;15.64)	27.70 (20.83;34.51)	32.21 (22.85;41.69)	39.37 (27.56;51.42)	44.29 (31.51;59.39)	44.77 (29.99;62.78)	36.66 (19.99;54.84)	32.34 (17.27;52.88)
	rr	4.97 (0.73; 9.37)	5.06 (0.51; 10.65)	6.24 (0.12; 14.80)	8.05 (0.07; 20.65)	10.24 (0.02; 26.27)	12.79 (0.00; 29.89)	15.88 (0.00; 33.93)	19.94 (0.01; 40.77)
	fa(1)	8.73 (2.24; 16.23)	29.34 (10.75; 46.27)	46.47 (24.50; 65.72)	65.46 (40.46; 88.54)	66.04 (44.29; 89.37)	64.10 (42.61; 90.62)	34.91 (11.42; 60.68)	31.78 (8.63; 56.99)
	fa(2)	6.99 (0.06; 14.13)	19.82 (9.17; 42.41)	17.18 (19.33; 60.80)	17.30 (31.01; 82.38)	16.60 (27.94; 84.05)	18.23 (19.44; 83.16)	22.37 (0.00; 53.92)	36.27 (0.01; 58.20)
e^2	mvt	0.44 (0.28;0.59)	0.63 (0.48;0.78)	0.66 (0.50;0.82)	0.71 (0.56;0.85)	0.73 (0.59;0.87)	0.73 (0.58;0.87)	0.69 (0.53;0.85)	0.66 (0.48;0.83)
	rr	0.16 (0.02; 0.32)	0.12 (0.01; 0.27)	0.12 (0.00; 0.30)	0.13 (0.00; 0.35)	0.17 (0.00; 0.43)	0.22 (0.00; 0.53)	0.30 (0.00; 0.64)	0.39 (0.00; 0.71)
	fa(1)	0.41 (0.13; 0.77)	0.62 (0.28; 0.94)	0.74 (0.43; 0.97)	0.83 (0.57; 0.97)	0.88 (0.65; 0.97)	0.88 (0.66; 0.97)	0.72 (0.33; 0.96)	0.68 (0.25; 0.95)
	fa(2)	0.33 (0.00; 0.67)	0.54 (0.19; 0.90)	0.68 (0.35; 0.95)	0.75 (0.43; 0.97)	0.76 (0.41; 0.97)	0.73 (0.31; 0.98)	0.55 (0.08; 0.95)	0.42 (0.00; 0.84)
CV_e	mvt	0.16 (0.14; 0.18)	0.14 (0.12; 0.16)	0.11 (0.09; 0.13)	0.10 (0.08; 0.12)	0.10 (0.08; 0.11)	0.09 (0.07; 0.10)	0.07 (0.06; 0.09)	0.07 (0.05; 0.09)
	rr	0.10 (0.05; 0.15)	0.06 (0.02; 0.09)	0.05 (0.01; 0.08)	0.04 (0.01; 0.08)	0.04 (0.01; 0.08)	0.04 (0.00; 0.07)	0.05 (0.00; 0.07)	0.05 (0.00; 0.08)
	fa(1)	0.13 (0.08; 0.19)	0.14 (0.09; 0.18)	0.13 (0.10; 0.16)	0.13 (0.10; 0.15)	0.12 (0.10; 0.14)	0.10 (0.08; 0.12)	0.07 (0.05; 0.10)	0.07 (0.04; 0.09)
	fa(2)	0.12 (0.05; 0.19)	0.13 (0.08; 0.17)	0.13 (0.09; 0.15)	0.12 (0.09; 0.15)	0.11 (0.08; 0.13)	0.09 (0.06; 0.12)	0.06 (0.02; 0.10)	0.06 (0.01; 0.10)

* derived from the model, not estimated.
** not shown for the `ant` model because it implied the calculation of square roots of negative values (some posterior samples for the cross-age parent-offspring regression).

C.4 P and G matrices estimates

This appendix contains additive genetic and phenotypic covariance and correlation matrices derived from the multivariate, random regression, factor analytic (`fa(1)` and `fa(2)`), and antedependence models. To see how the **P** and **G** matrices were derived from model parameters see the Methods section in the main text.

Table C.4.1: Additive genetic covariance and correlation matrix of male horn length across ages in the bighorn population of Ram Mountain, estimated with the multivariate model (`mvt`). The diagonal correspond to variances in horn length at different ages, the upper diagonal to covariances and the lower diagonals to correlations. Values correspond to means of the corresponding posterior distributions.

	1	2	3	4
1	11.22	14.95	15.07	16.75
2	0.86	27.19	27.72	30.65
3	0.82	0.96	30.77	33.05
4	0.83	0.96	0.97	37.58

Table C.4.2: Additive genetic covariance and correlation matrix of male horn length across ages in the bighorn population of Ram Mountain, estimated by the random regression model (`rr`). The diagonal correspond to variances in horn length at different ages, the upper diagonal to covariances and the lower diagonals to correlations. Values correspond to means of the corresponding posterior distributions.

	1	2	3	4	5	6	7	8
1	10.03	12.42	13.66	13.76	12.72	10.53	7.20	2.73
2	0.90	19.22	23.46	25.16	24.30	20.89	14.93	6.41
3	0.80	0.98	29.80	32.67	32.06	27.99	20.45	9.44
4	0.73	0.95	0.99	36.28	36.00	31.84	23.78	11.83
5	0.68	0.93	0.98	1.00	36.12	32.43	24.91	13.57
6	0.63	0.89	0.95	0.98	0.99	29.76	23.84	14.66
7	0.54	0.79	0.86	0.89	0.93	0.96	20.57	15.11
8	0.22	0.35	0.41	0.45	0.50	0.58	0.73	14.91

Table C.4.3: Additive genetic covariance and correlation matrix of male horn length across ages in the bighorn population of Ram Mountain, estimated by the factor analytic model with a single additive genetic common factor (`fa(1)`). The diagonal correspond to variances in horn length at different ages, the upper diagonal to covariances and the lower diagonals to correlations. Values correspond to means of the corresponding posterior distributions.

	1	2	3	4	5	6	7	8
1	7.78	10.79	9.47	7.52	4.21	0.76	-5.73	-6.38
2	0.96	15.25	13.60	11.09	6.62	1.94	-7.08	-7.99
3	0.87	0.90	12.60	10.73	7.04	3.13	-4.75	-5.54
4	0.71	0.74	0.84	9.90	7.18	4.35	-1.84	-2.43
5	0.39	0.43	0.53	0.69	6.21	4.89	1.52	1.21
6	-0.10	-0.07	0.03	0.19	0.50	5.52	4.88	4.88
7	-0.86	-0.82	-0.72	-0.56	-0.25	0.25	10.20	10.58
8	-0.88	-0.84	-0.75	-0.59	-0.27	0.23	0.93	11.57

Table C.4.4: Additive genetic covariance and correlation matrix of male horn length across ages in the bighorn population of Ram Mountain, estimated by the factor analytic model with two additive genetic common factors (`fa(2)`). The diagonal correspond to variances in horn length at different ages, the upper diagonal to covariances and the lower diagonals to correlations. Values correspond to means of the corresponding posterior distributions.

	1	2	3	4	5	6	7	8
1	11.08	14.24	12.15	10.91	8.80	7.46	3.93	8.35
2	0.94	19.82	17.67	15.82	12.56	10.20	4.19	8.59
3	0.83	0.93	17.18	16.20	13.58	11.39	5.45	8.32
4	0.71	0.79	0.90	17.30	15.98	14.88	10.42	13.42
5	0.56	0.60	0.72	0.90	16.60	16.61	14.36	17.59
6	0.41	0.41	0.51	0.72	0.89	18.23	17.75	21.53
7	0.10	0.02	0.07	0.30	0.53	0.74	22.37	26.71
8	0.30	0.18	0.17	0.35	0.53	0.70	0.92	36.27

Table C.4.5: Phenotypic covariance and correlation matrix of male horn length across ages in the bighorn population of Ram Mountain, estimated with the multivariate model (`mvt`). The diagonal correspond to variances in horn length at different ages, the upper diagonal to covariances and the lower diagonals to correlations. Values correspond to means of the corresponding posterior distributions.

	1	2	3	4	5	6	7	8
1	28.94	30.07	28.83	29.26	28.72	27.46	21.60	19.41
2	0.84	44.11	42.43	44.36	43.44	41.07	31.66	29.36
3	0.77	0.92	48.61	49.19	48.84	46.85	36.50	33.95
4	0.73	0.89	0.94	55.77	54.69	53.13	42.79	39.14
5	0.68	0.84	0.90	0.94	60.70	57.93	49.11	45.30
6	0.65	0.79	0.86	0.91	0.95	61.17	51.57	46.38
7	0.55	0.65	0.72	0.79	0.87	0.91	53.06	46.30
8	0.51	0.63	0.70	0.75	0.83	0.85	0.91	48.74

Table C.4.6: Phenotypic covariance and correlation matrix of male horn length across ages in the bighorn population of Ram Mountain, estimated by the random regression model (`rr`). The diagonal correspond to variances in horn length at different ages, the upper diagonal to covariances and the lower diagonals to correlations. Values correspond to means of the corresponding posterior distributions.

	1	2	3	4	5	6	7	8
1	31.50	30.89	31.80	31.55	30.16	27.63	23.94	19.11
2	0.85	41.68	42.67	44.56	43.77	40.31	34.18	25.38
3	0.78	0.91	52.60	53.43	53.31	49.53	42.08	30.96
4	0.72	0.88	0.94	61.25	58.80	55.28	47.64	35.87
5	0.67	0.85	0.92	0.94	63.29	57.57	50.87	40.10
6	0.64	0.81	0.89	0.92	0.94	59.47	51.75	43.65
7	0.58	0.72	0.79	0.83	0.87	0.92	53.38	46.52
8	0.47	0.54	0.59	0.64	0.70	0.78	0.88	51.78

Table C.4.7: Phenotypic covariance and correlation matrix of male horn length across ages in the bighorn population of Ram Mountain, estimated by the factor analytic model with a single additive genetic common factor (`fa(1)`). The diagonal correspond to variances in horn length at different ages, the upper diagonal to covariances and the lower diagonals to correlations. Values correspond to means of the corresponding posterior distributions.

	1	2	3	4	5	6	7	8
1	21.53	26.97	29.67	31.31	27.95	23.95	10.88	9.36
2	0.84	48.01	50.67	54.90	50.42	44.81	23.75	21.27
3	0.81	0.92	62.90	66.03	62.45	57.48	34.55	31.81
4	0.76	0.89	0.94	78.69	73.07	69.10	45.16	42.26
5	0.69	0.84	0.91	0.95	75.57	70.06	49.01	46.39
6	0.61	0.76	0.85	0.91	0.94	72.94	51.87	49.64
7	0.34	0.49	0.63	0.73	0.81	0.87	48.43	43.84
8	0.30	0.45	0.59	0.70	0.78	0.85	0.92	46.67

Table C.4.8: Phenotypic covariance and correlation matrix of male horn length across ages in the bighorn population of Ram Mountain, estimated by the factor analytic model with two additive genetic common factors (`fa(2)`). The diagonal correspond to variances in horn length at different ages, the upper diagonal to covariances and the lower diagonals to correlations. Values correspond to means of the corresponding posterior distributions.

	1	2	3	4	5	6	7	8
1	21.81	27.69	29.23	30.76	28.32	26.20	17.38	21.00
2	0.85	48.11	50.80	54.43	50.55	46.68	30.30	32.86
3	0.79	0.92	63.10	66.22	62.88	58.77	39.42	39.77
4	0.74	0.89	0.94	78.24	73.97	70.72	50.70	50.76
5	0.69	0.83	0.91	0.96	76.36	72.07	54.63	55.00
6	0.65	0.78	0.86	0.93	0.96	74.16	56.90	58.02
7	0.50	0.59	0.68	0.78	0.85	0.90	54.10	54.29
8	0.56	0.59	0.62	0.71	0.78	0.84	0.92	65.21

Table C.4.9: Phenotypic covariance and correlation matrix of male horn length across ages in the bighorn population of Ram Mountain, implied by the antedependence model (`ant`). The diagonal correspond to variances in horn length at different ages, the upper diagonal to covariances and the lower diagonals to correlations. Values correspond to means of the corresponding posterior distributions.

	1	2	3	4	5	6	7	8
1	13.38	13.81	12.02	10.45	9.03	7.90	5.70	3.47
2	0.74	25.66	22.33	19.41	16.76	14.66	10.56	6.42
3	0.60	0.81	29.85	25.93	22.38	19.57	14.10	8.56
4	0.50	0.67	0.83	32.41	27.97	24.44	17.60	10.69
5	0.42	0.56	0.70	0.84	34.26	29.92	21.54	13.06
6	0.36	0.48	0.60	0.72	0.86	35.29	25.39	15.38
7	0.29	0.39	0.48	0.57	0.68	0.79	28.70	17.36
8	0.20	0.27	0.34	0.40	0.48	0.55	0.70	21.05

APPENDIX D

Supplementary material to Chapter 6

D.1 Supplementary figures

Appendix D.1 includes figures of model predictions, for breeding success and survival, plotted against observed data. The predictions shown correspond to predicted values for each individual used to estimate the model averaged by age.

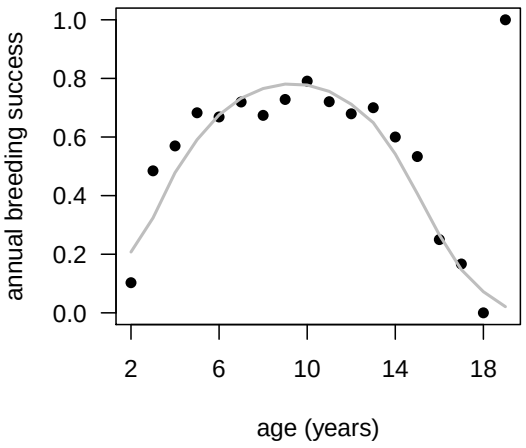

Figure D.1.1: Observed and predicted annual breeding success in bighorn ewes of Ram Mountain. Black dots correspond to observed data, whereas the grey line corresponds to model predictions. The predictions are based on the model represented in Equation (6.1), for which parameter estimates are shown in Tab. 6.1 (both in the main text).

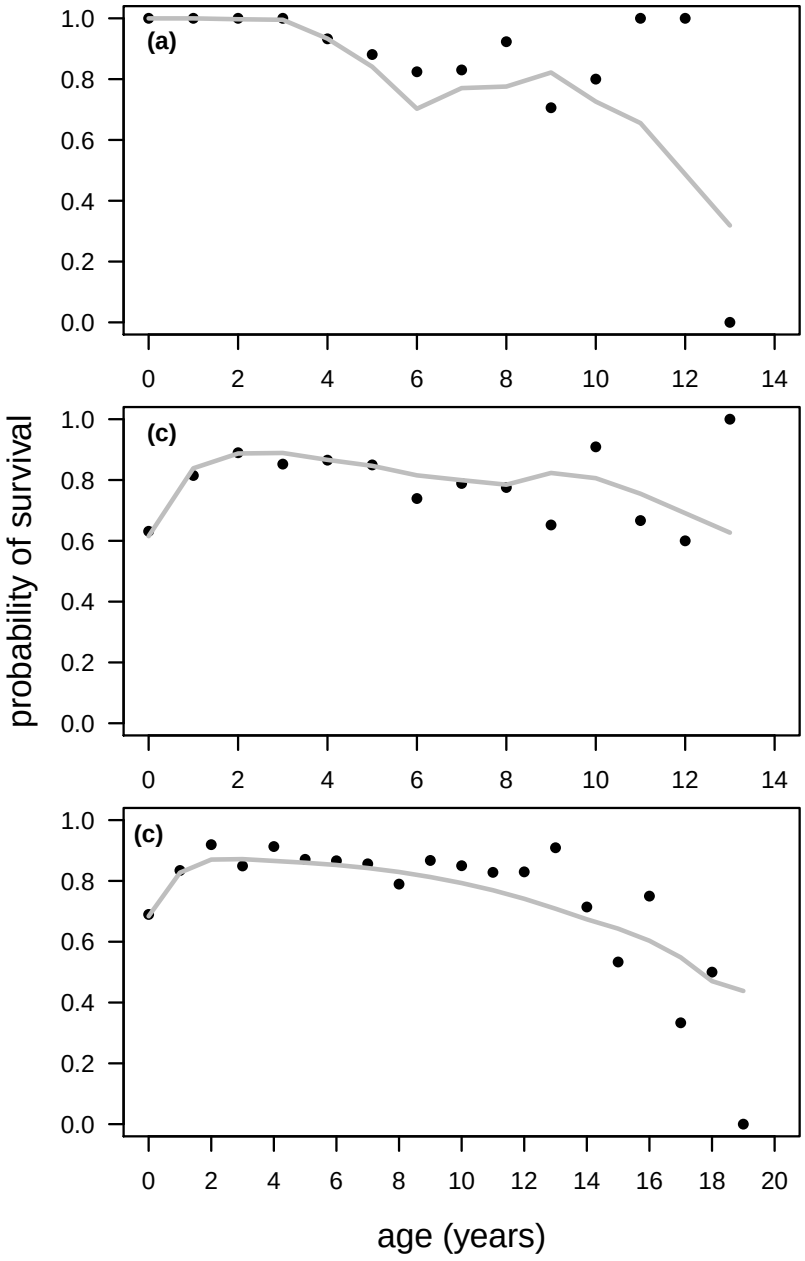

Figure D.1.2: Observed and predicted annual survival probability as a function of age in the bighorn sheep population of Ram Mountain; male harvest survival (a), and male (b) and female (c) winter survival are shown. Black dots correspond to observed values, whereas grey lines are predicted values for the individuals in the population, averaged by age. The corresponding models are described by Equations 6.5, 6.7, and 6.6, and the corresponding parameter estimates are shown in Tab. 6.2 (main text).

D.2 Model code

Table D.2.1: JAGS code for the multinomial model fitting annual male breeding success, as described in Equations (6.2)-(6.4).

```
---------------------------------------------------------------------------------------------
modelCode<-"
model{
for(y in 1:n.years){
#ramYearData[,,1]: ID
#ramYearData[,,3]: age
#ramYearData[,,4]: number of lambs
#ramYearData[,,5]: horn length
#ramYearData[,,6]: maternal ID
#ramYearData[,,7]: cohort
ramYearData[y,1:(n.rams[y]),4]~dmulti(p[1:(n.rams[y]),y],totalRS[y])
for(i in 1:(n.rams[y])){
p[i,y] <- p.prime[i,y] / sum(p.prime[1:(n.rams[y]),y])
p.prime[i,y]<-exp(betaAge[1]*(ramYearData[y,i,3]-mid.age)+
                    betaHorn[1]*(ramYearData[y,i,5]-mid.horn)+
                    betaInt*(ramYearData[y,i,3]-mid.age)*(ramYearData[y,i,5]-mid.horn)+
                    ramb[ramYearData[y,i,1]]+cohortb[ramYearData[y,i,7]]+
                    mumb[ramYearData[y,i,6]])
}
}


betaAge[1]~dnorm(0,0.0001)
#betaAge[2]~dnorm(0,0.0001)
betaHorn[1]~dnorm(0,0.0001)
#betaHorn[2]~dnorm(0,0.0001)
betaInt~dnorm(0,0.0001)


# random effect for rams
ramTau~dgamma(0.001,0.001)
mumTau~dgamma(0.001,0.001)
cohortTau~dgamma(0.001,0.001)
for (i in 1:n.rams.total) {ramb[i]~dnorm(0,ramTau)}
for (i in 1:n.mums) {mumb[i]~dnorm(0,mumTau)}
for (i in 1:n.cohorts) {cohortb[i]~dnorm(0,cohortTau)}
ramVar<-1/ramTau
mumVar<-1/mumTau
cohortVar<-1/cohortTau
}
"
---------------------------------------------------------------------------------------------
```

D.3 Model checks

Before actual analyses, results from simulations running for 1000 years (iterations) were analysed against observed parameters from the bighorn sheep population inhabiting Ram Mountain. These simulations were used to identify the duration of the burn-in period and to inspect population density and structure, horn length dynamics and the vital rates against observed values. I present both results from simulations without and with an inheritance mechanism.

D.3.1 Scenario with no inheritance

Population size stabilizes very fast, potentially in less than 100 iterations, an indication that the starting values of 50 females and 50 males were not very distant from the values at equilibrium (Fig. D.3.1). The age structure recovered in the simulations is very similar to the observed in the bighorn sheep population at Ram Mountain, for both females and males (Fig. D.3.2, D.3.3). Overall, in scenarios in which the inheritance mechanism is switched off, a burn-in of 200 years is likely to be sufficient.

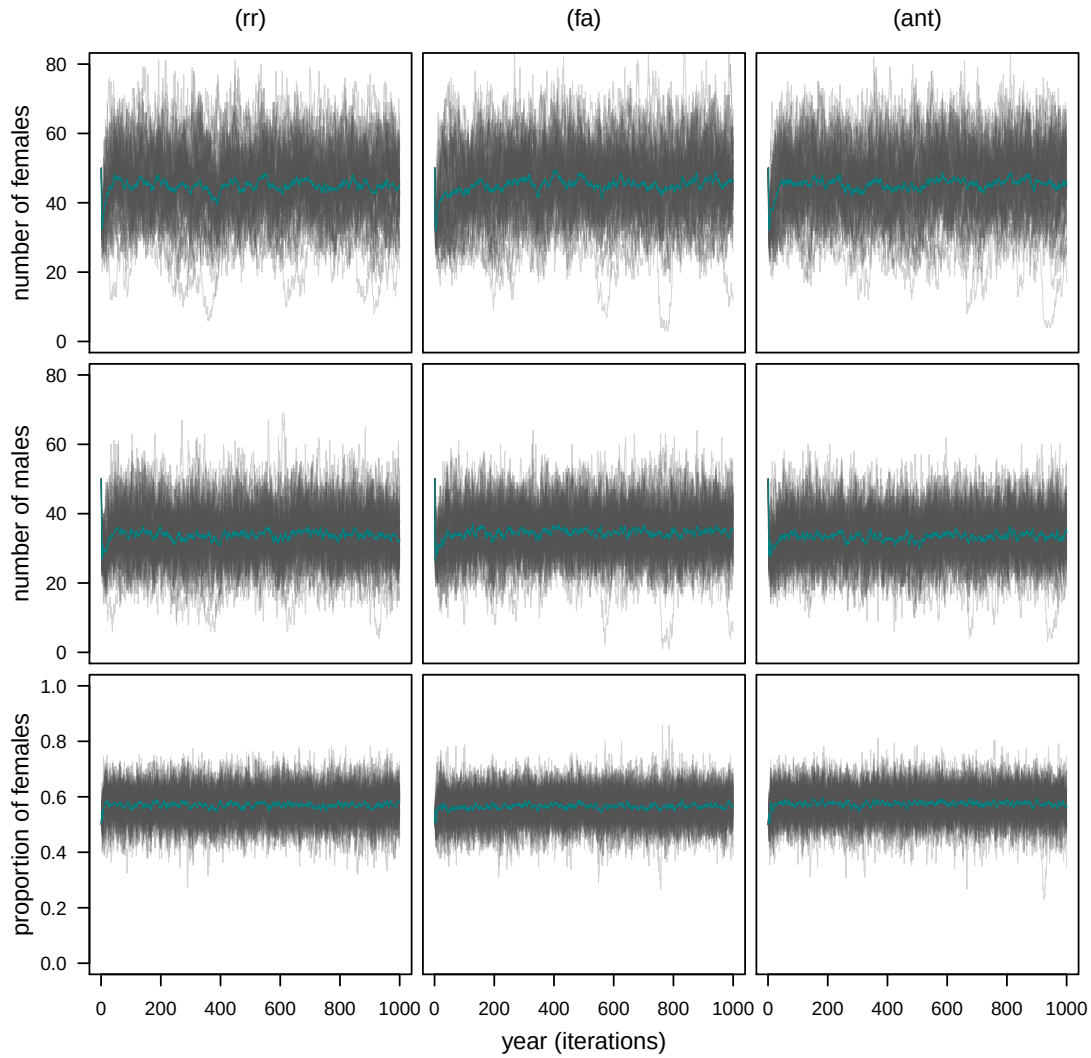

Figure D.3.1: Population dynamics and sex ratio obtained along 1000 iterations in a scenario with no inheritance mechanism built-in. Results are shown for each approach to modelling horn length trajectories, random regression (`rr`), factor analysis (`fa`), and the antedependence model (`ant`). Grey lines correspond to 50 individual simulations, whereas the line in teal corresponds to the average of those simulations.

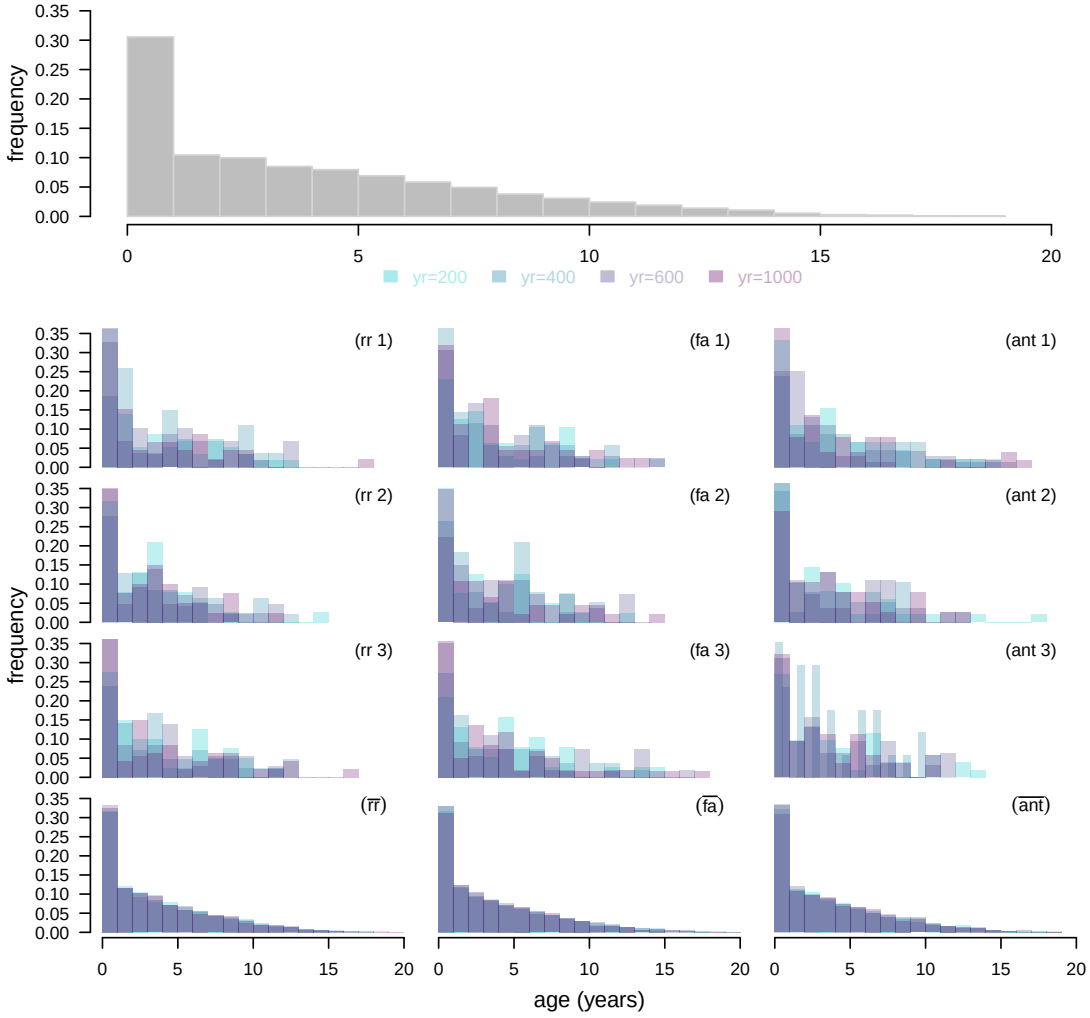

Figure D.3.2: Female population structured by age, observed in the bighorn sheep population of Ram Mountain (top panel) and simulated over 1000 years (iterations), in a scenario with no inheritance mechanism built-in (lower panels). Simulation results are shown for the three approaches to modelling size trajectories, random regression (`rr`), factor analytic (`rr`) and antedependence (`ant`) models, for three independent simulations, as examples, and the average of 50 simulations. In each plot different colours represent age structure at different years (iterations), suggesting that not only simulated results match the the observed age structure, but also that this match occurs at least as soon as after 200 iterations.

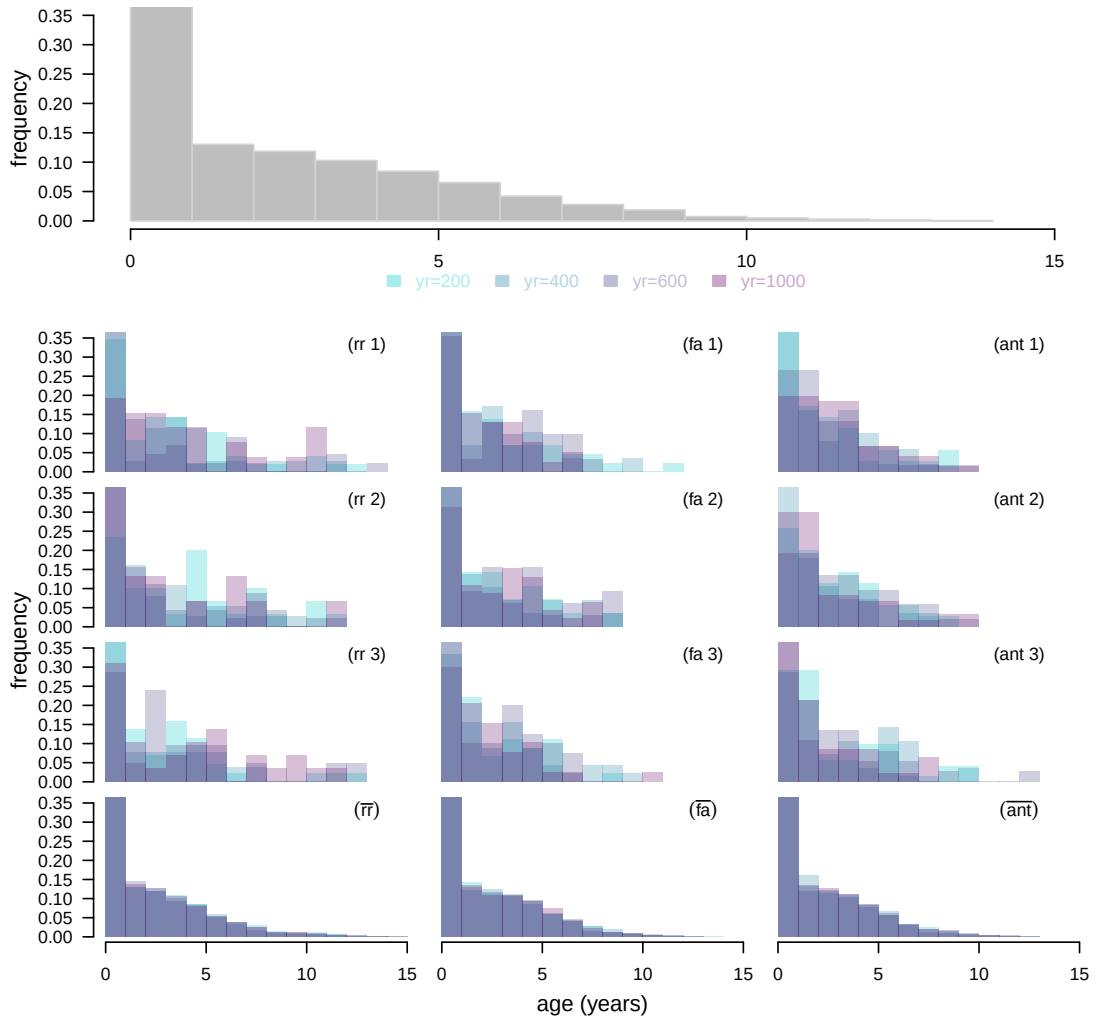

Figure D.3.3: Male population structured by age, observed in the bighorn sheep population of Ram Mountain (top panel) and simulated over 1000 years (iterations), in a scenario with no inheritance mechanism built-in (lower panels). Simulation results are shown for the three approaches to modelling size trajectories, random regression (`rr`), factor analytic (`rr`) and antedependence (`ant`) models, for three independent simulations, as examples, and the average of 50 simulations. In each plot different colours represent age structure at different years, suggesting that not only simulated results match the the observed age structure, but also that this match occurs at least as soon as after 200 iterations.

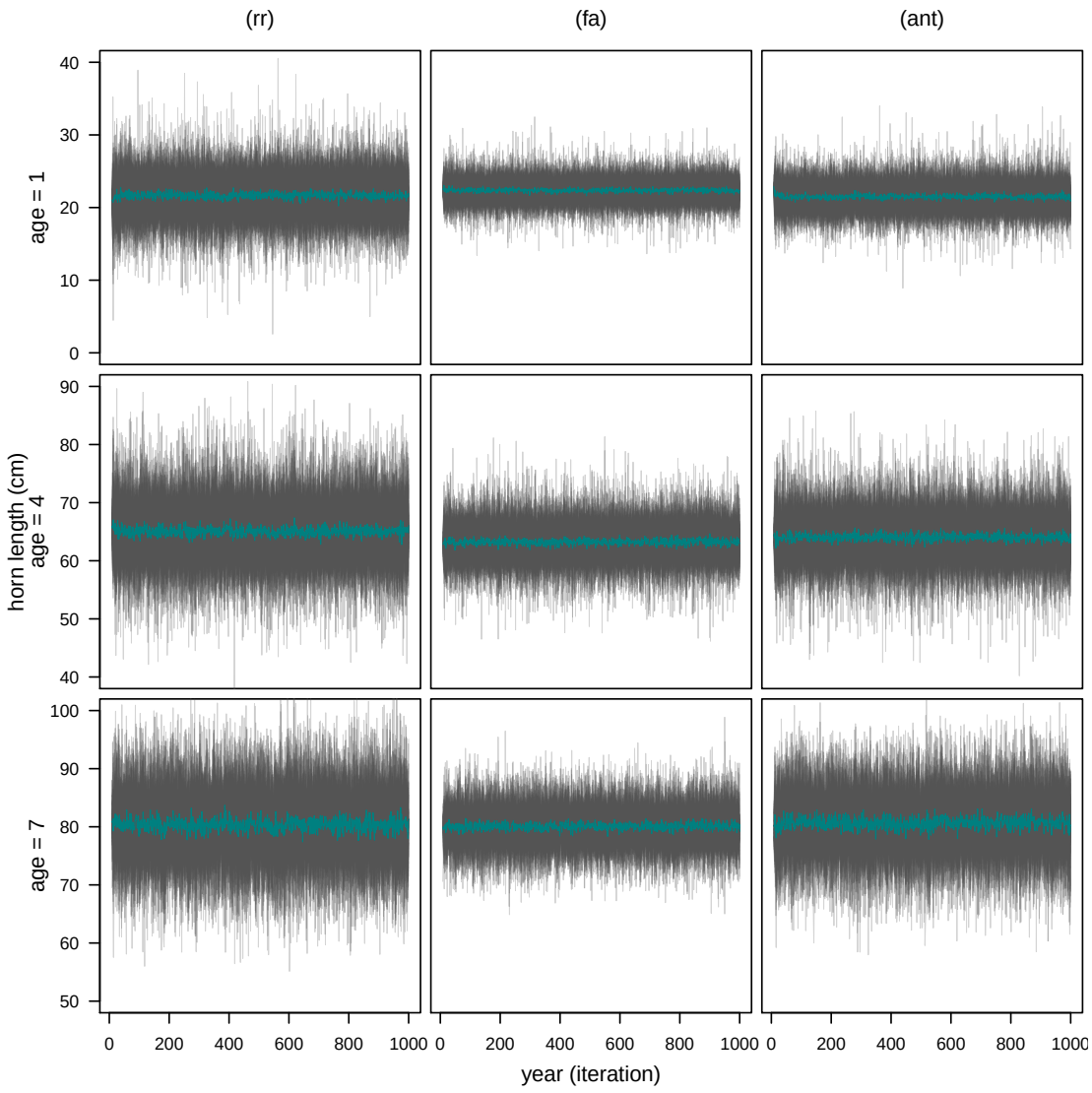

Figure D.3.4: Horn length dynamics over 1000 years (iterations) under a scenario with no inheritance mechanism built-in. Results are shown for 3 different ages and the three approaches to modelling horn length trajectories, random regression (`rr`), factor analytic (`fa`) and antedependence (`ant`) models. Grey lines correspond to 50 individual simulations, whereas the line in teal correspond to the average of those simulations.

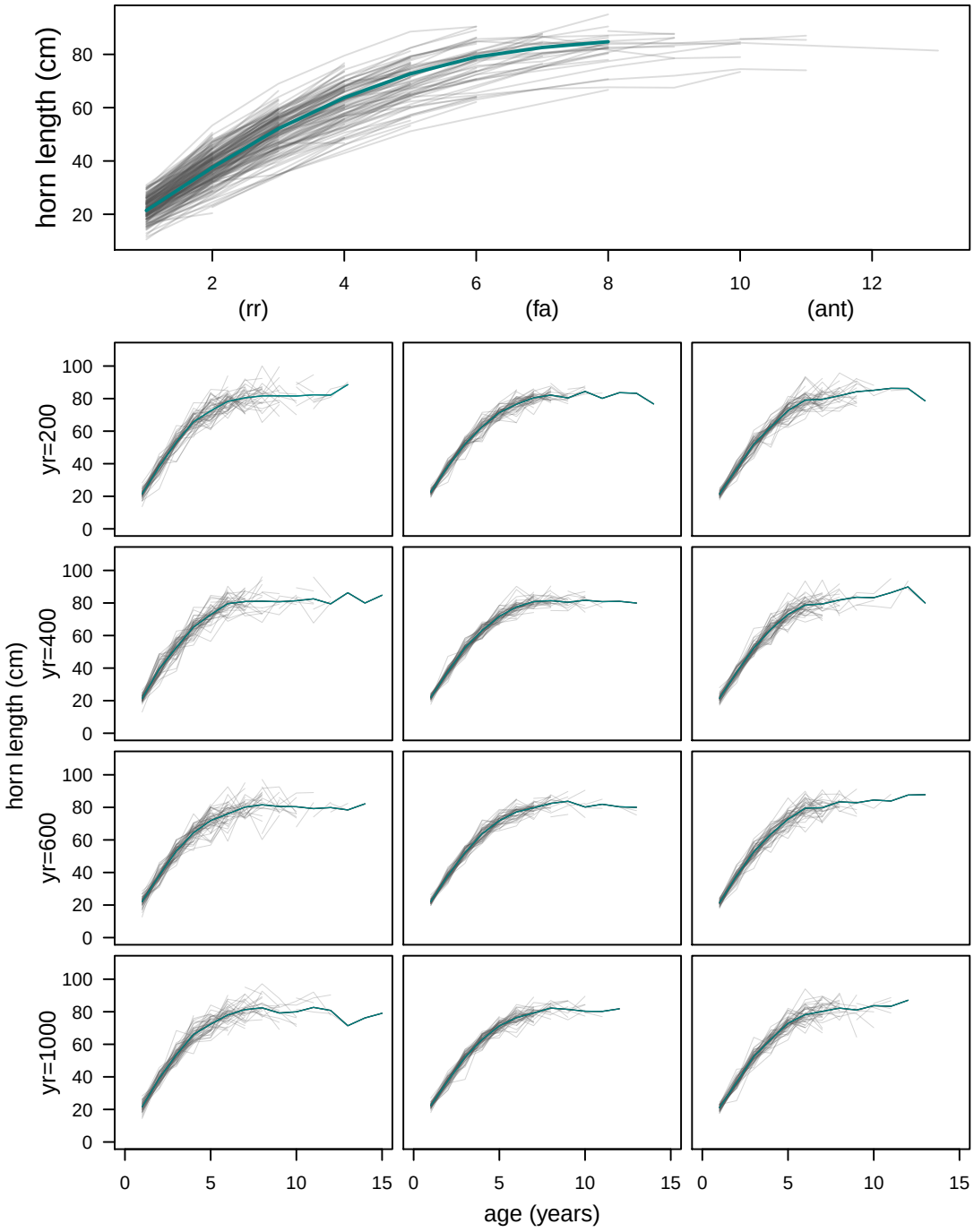

Figure D.3.5: Male horn length ontogenetic trajectories, observed in the bighorn sheep population of Ram Mountain (upper panel) and simulated over 1000 years (iterations) under a scenario with no inheritance mechanism built-in (lower panels). Results are shown for four different t and for the three approaches to modelling size trajectories, random regression (`rr`), factor analytic (`rr`) and antedependence (`ant`) models. Grey lines correspond to individual trajectories (observed data) and to averages of simulations (simulated data), whereas lines in teal correspond to overall averages.

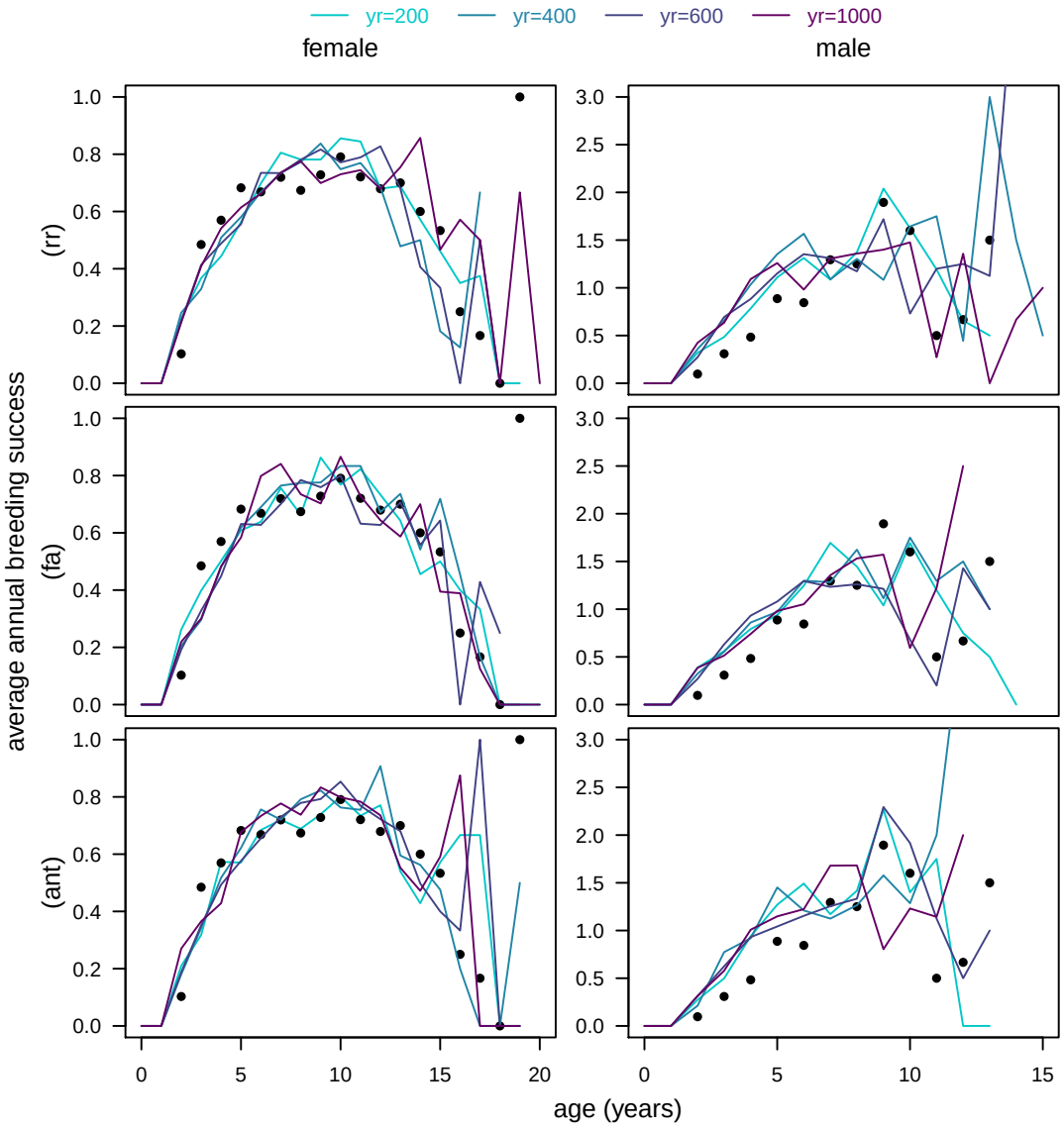

Figure D.3.6: Observed and simulated average breeding success as a function of age in a scenario with no inheritance mechanism built-in. Results are shown for the three approaches used to modelling size trajectories, random regression (`rr`), factor analytic (`rr`) and antedependence (`ant`) models, and correspond to averages of 50 independent simulations. Each simulation was run for 1000 iterations, and results are shown for years 200, 400, 600 and 1000. Black points correspond to observed values.

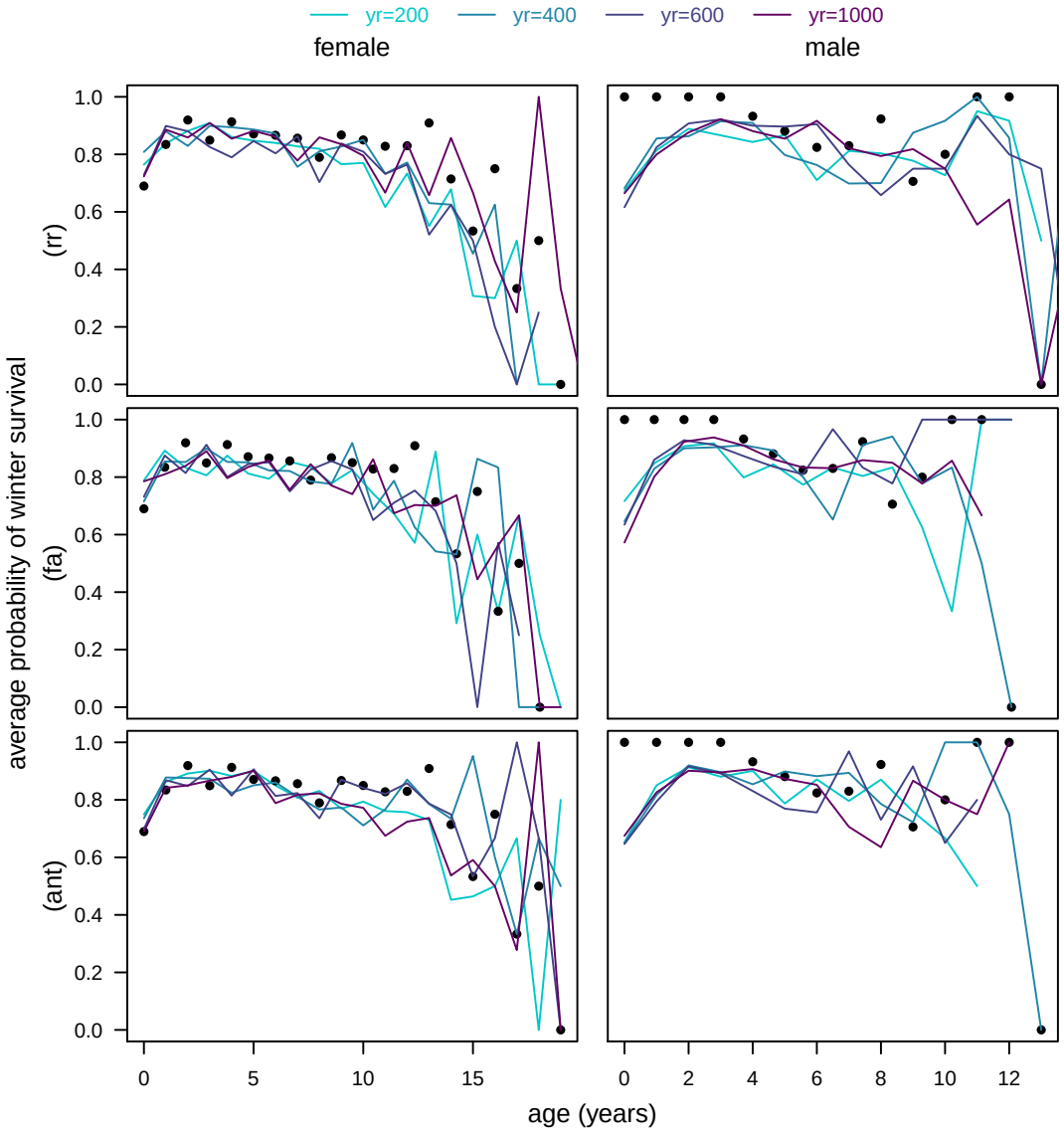

Figure D.3.7: Observed and simulated average winter survival as a function of age in a scenario with no inheritance mechanism built-in. Results are shown for the three approaches used to modelling size trajectories, random regression (`rr`), factor analytic (`rr`) and antedependence (`ant`) models, and correspond to averages of 50 independent simulations. Each simulation was run for 1000 iterations, and results are shown for iterations 200, 400, 600 and 1000. Black points correspond to observed values.

D.3.2 Scenario with inheritance

Population size stabilizes very fast, potentially in less than 200 iterations (Fig. D.3.8). The age structure recovered in the simulations is very similar to the observed in the bighorn sheep population at Ram Mountain, for both females and males (Fig. D.3.9, D.3.10). Horn length and breeding value

dynamics seem to have reasonably stabilised after 1000 iterations (Fig. D.3.11, D.3.12). Overall, in scenarios with an inheritance mechanism, a burn-in of 1000 years is likely to be sufficient.

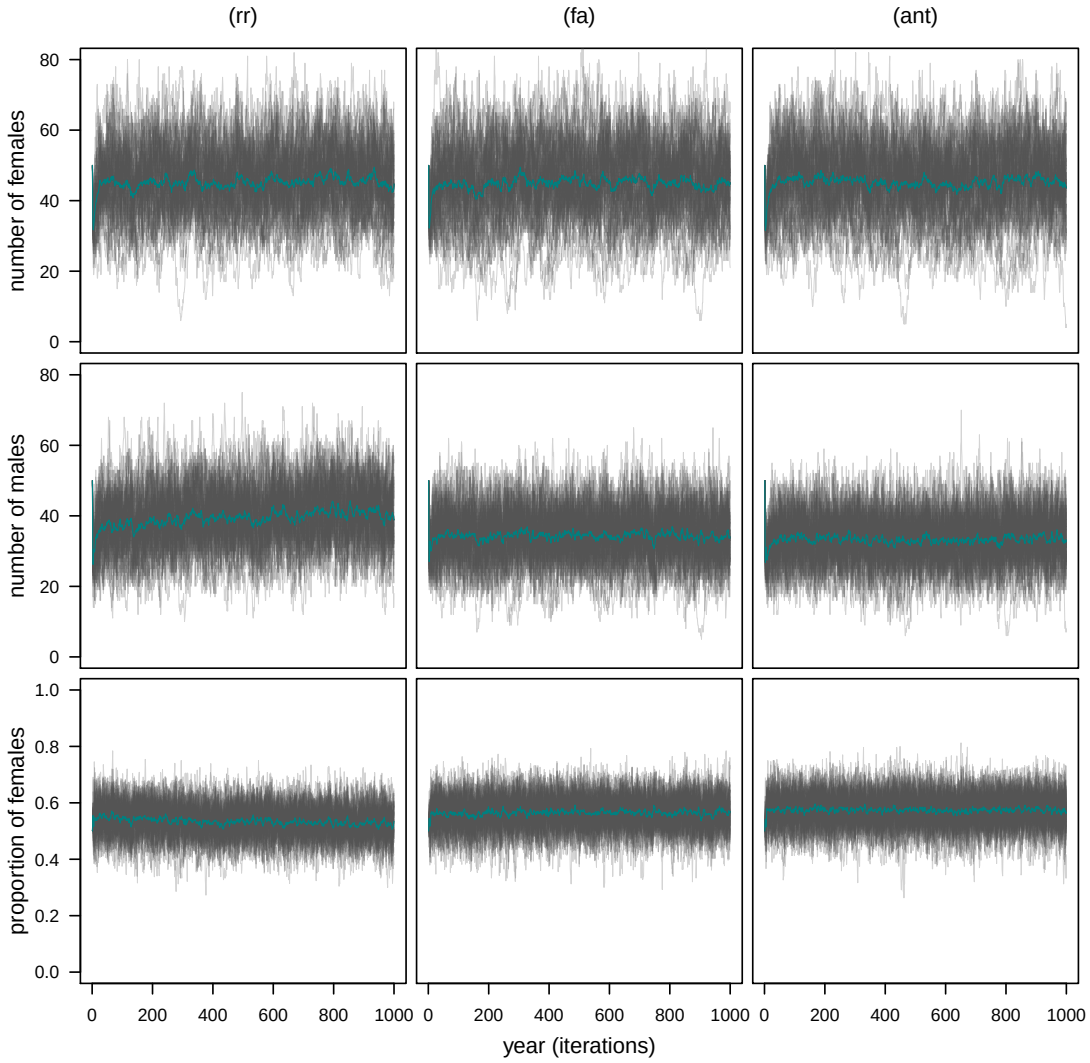

Figure D.3.8: Population dynamics and sex ratio obtained along 1000 years (iterations) with an inheritance mechanism built-in. Results are shown for each approach to modelling horn length trajectories, random regression (`rr`), factor analysis (`fa`), and the antedependence model (`ant`). Grey lines correspond to 50 individual simulations, whereas the line in teal corresponds to the average of those simulations.

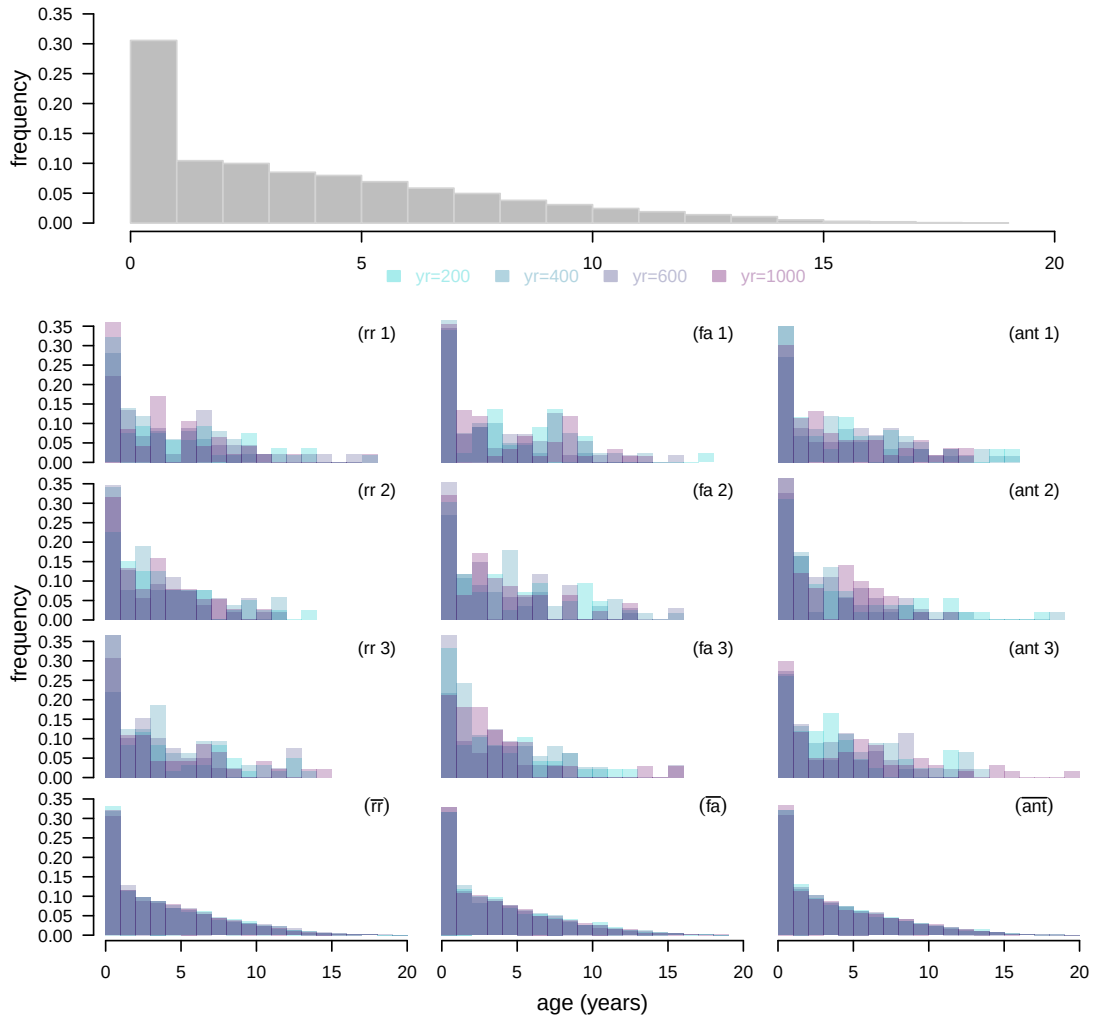

Figure D.3.9: Female population structured by age, observed in the bighorn sheep population of Ram Mountain (top panel) and simulated over 1000 years (iterations) (lower panels), in a scenario with an inheritance mechanism built-in. Simulation results are shown for the three approaches to modelling size trajectories, random regression (`rr`), factor analytic (`rr`) and antedependence (`ant`) models, for three independent simulations, as examples, and the average of 50 simulations. In each plot different colours represent age structure at different *t*, suggesting that not only simulated results match the observed age structure, but also that this match occurs at least as soon as after 200 iterations.

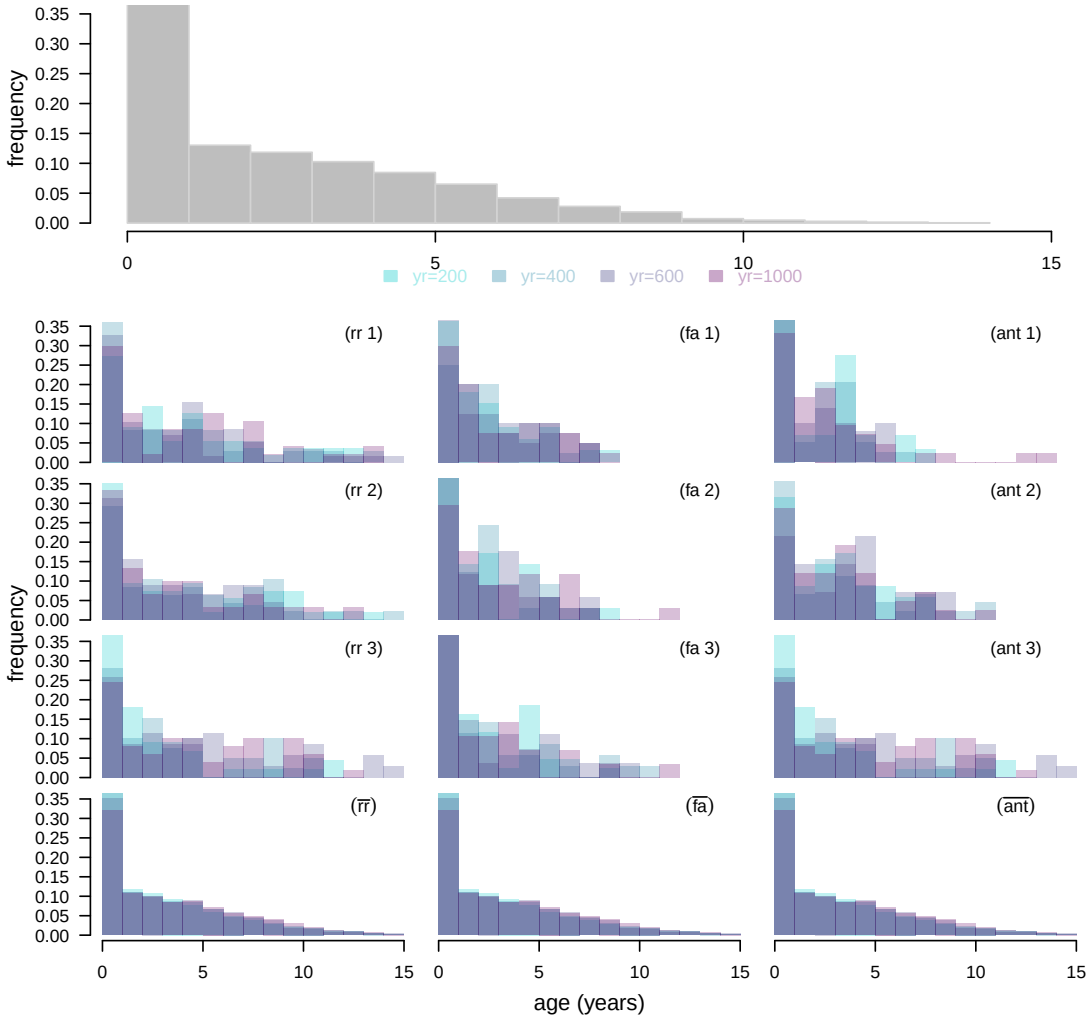

Figure D.3.10: Male population structured by age, observed in the bighorn sheep population of Ram Mountain (top panel) and simulated over 1000 iterations (lower panels), in a scenario with an inheritance mechanism built-in. Simulation results are shown for the three approaches to modelling size trajectories, random regression (`rr`), factor analytic (`rr`) and antedependence (`ant`) models, for three independent simulations, as examples, and the average of 50 simulations. In each plot different colours represent age structure at different t, suggesting that not only simulated results match the observed age structure, but also that this match occurs at least as soon as after 200 iterations.

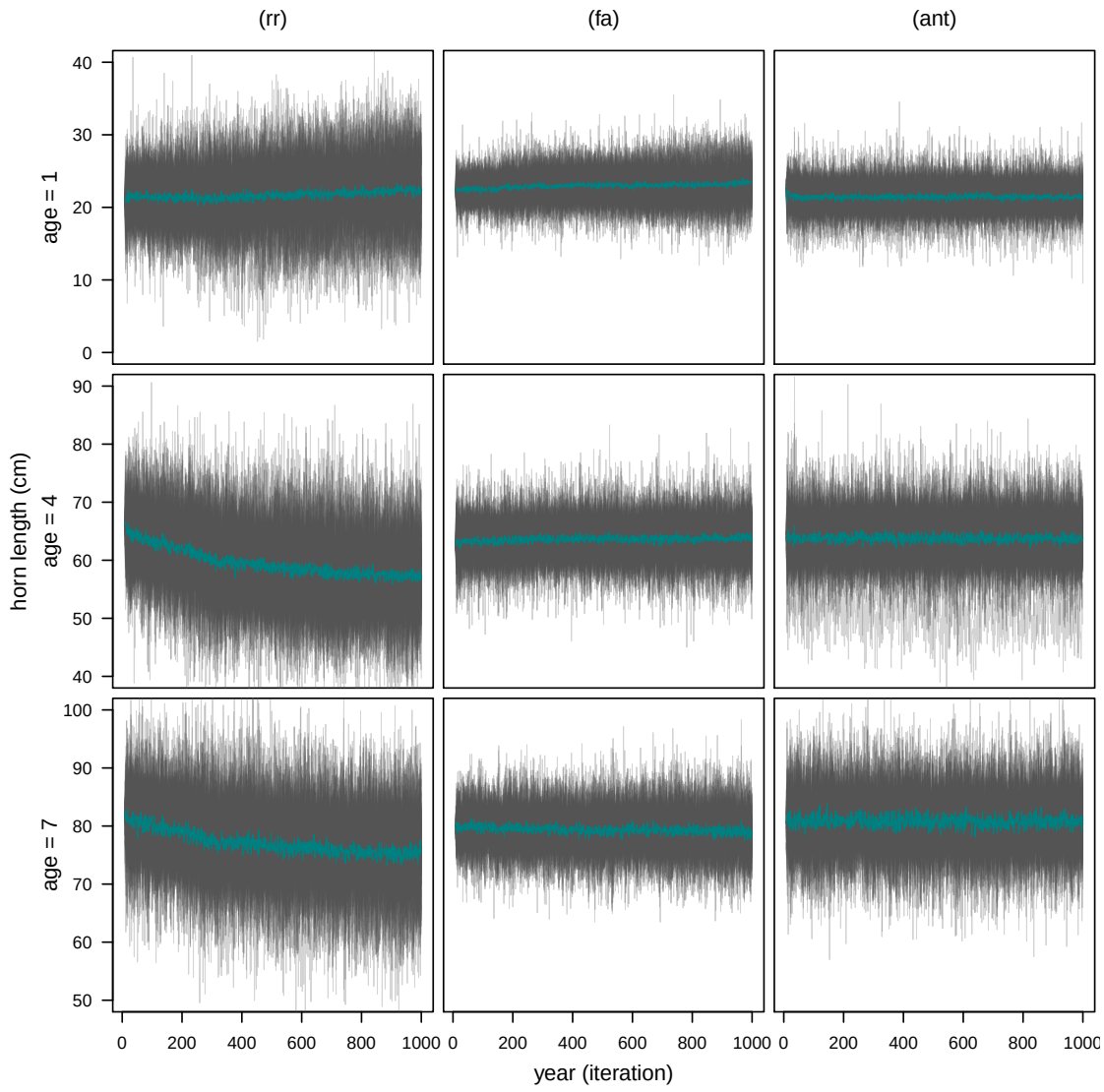

Figure D.3.11: Male horn length dynamics over 1000 years (iterations) in a scenario with an inheritance mechanism built-in. Results are shown for 3 different ages and the three approaches to modelling horn length trajectories, random regression (`rr`), factor analytic (`rr`) and antedependence (`ant`) models. Grey lines correspond to 50 individual simulations, whereas the line in teal correspond to the average of those simulations.

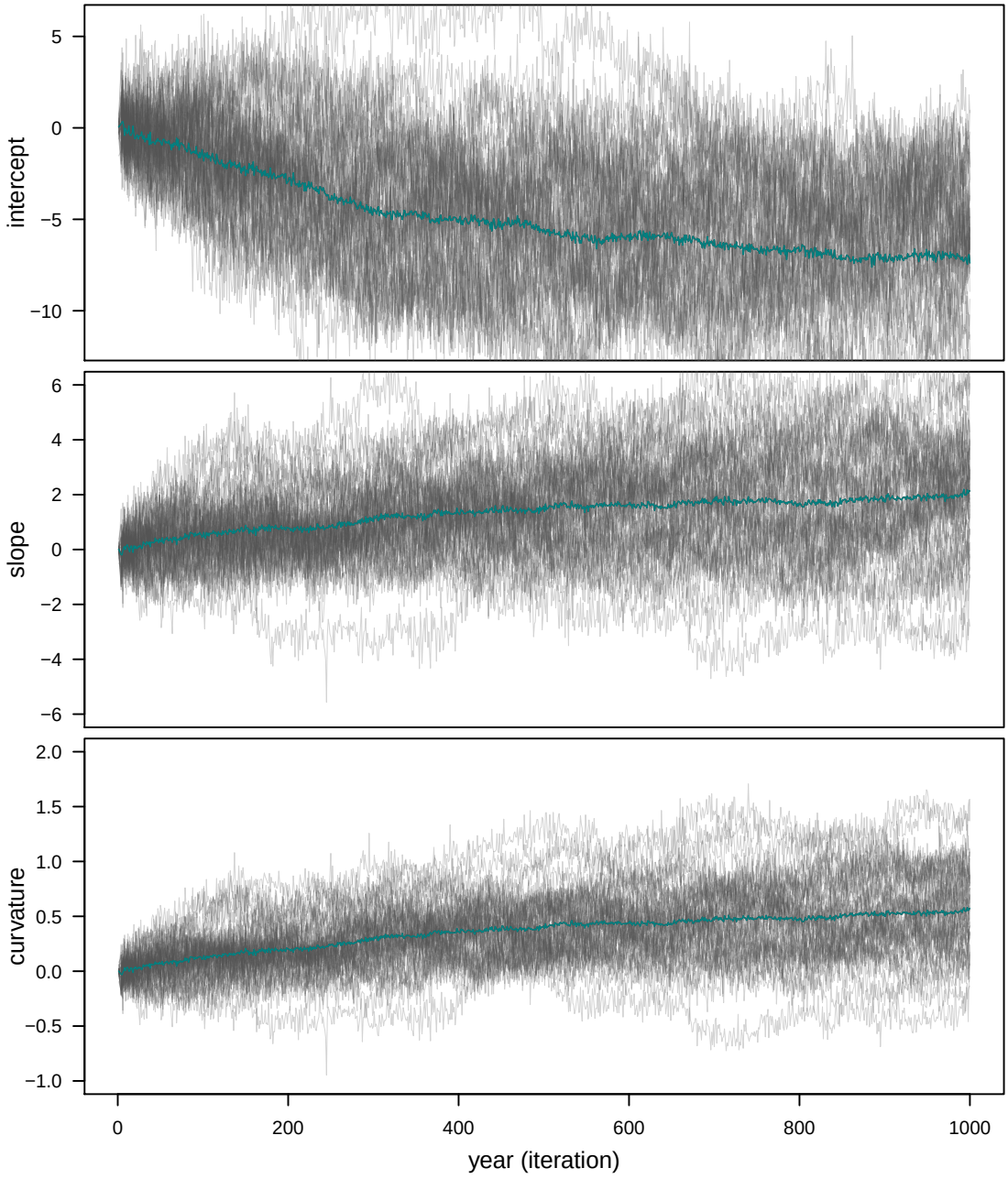

Figure D.3.12: Breeding values dynamics, including intercepts, slopes and curvatures, over 1000 years (iterations) for the random regression model. Grey lines correspond to 50 individual simulations, whereas the line in teal correspond to the average of those simulations.

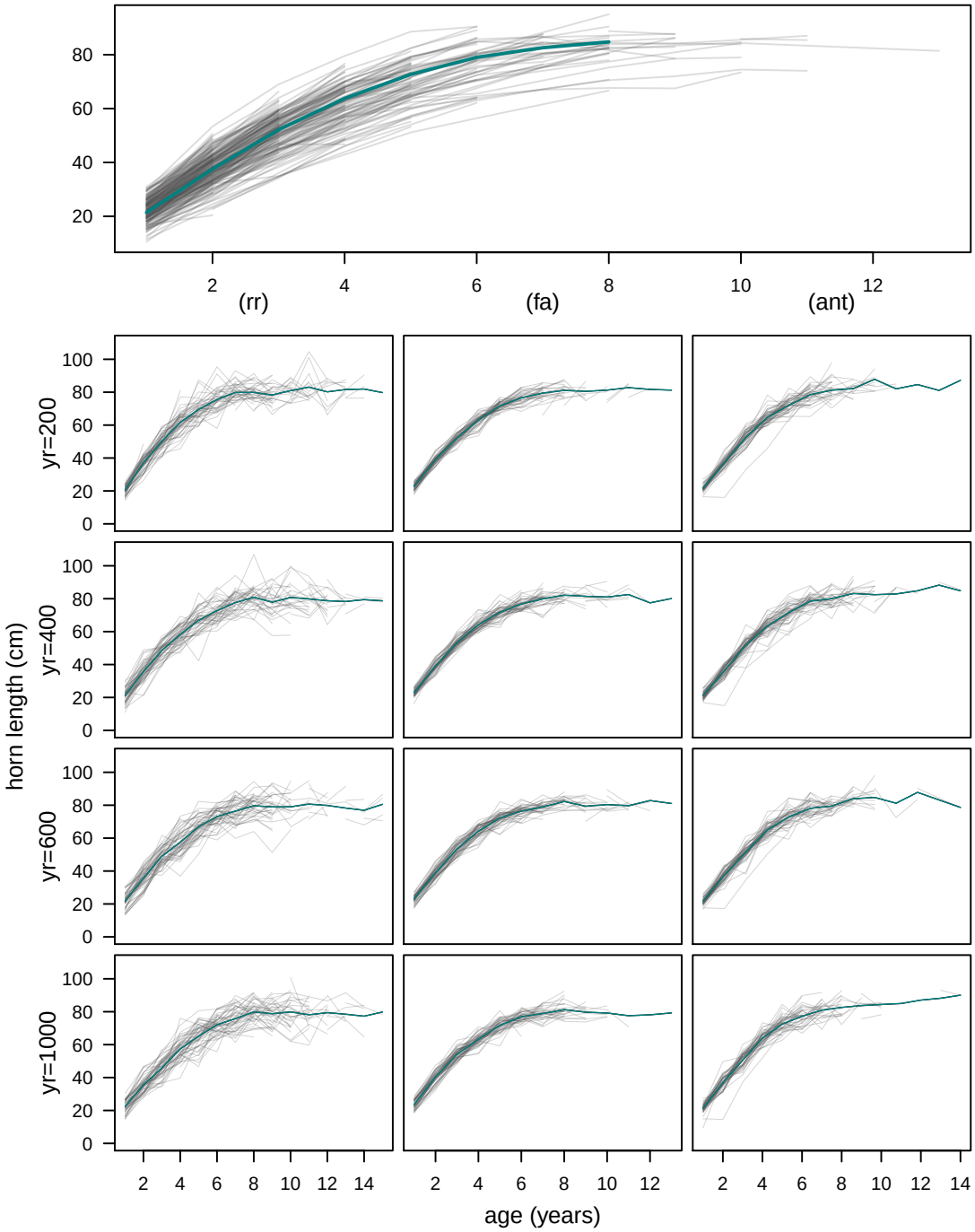

Figure D.3.13: Male horn length trajectories, observed in the bighorn population of Ram Mountain (upper panel) and simulated for 1000 years (iterations) under a scenario with an inheritance mechanism built-in (lower panels). Results are shown for four different years and the three approaches to modelling size trajectories, random regression (`rr`), factor analytic (`rr`) and antedependence (`ant`) models. Grey lines correspond to individual trajectories (observed data) and to averages of individual simulations (simulated data), whereas lines in teal correspond to overall averages.

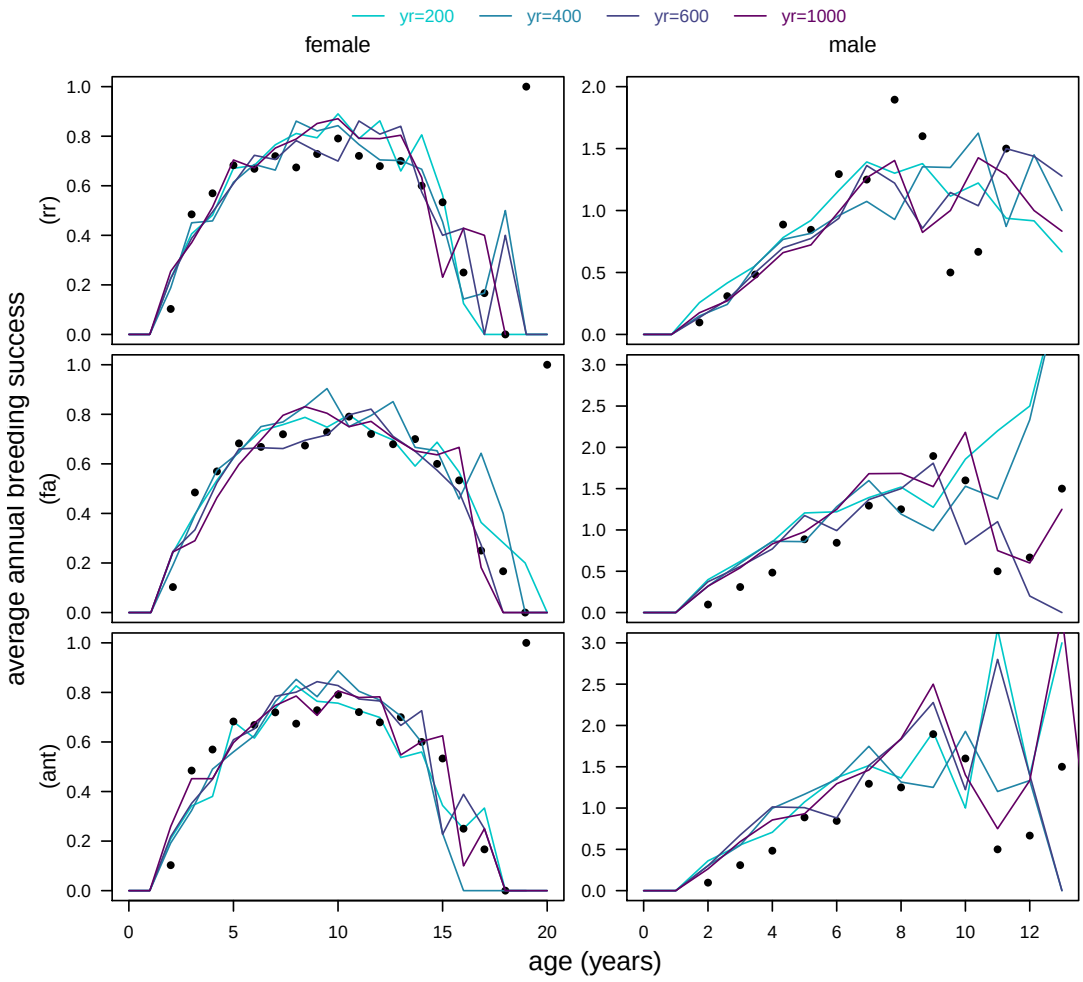

Figure D.3.14: Observed and simulated average breeding success as a function of age in a scenario with an inheritance mechanism built-in. Results are shown for the three approaches used to modelling size trajectories, random regression (`rr`), factor analytic (`rr`) and antedependence (`ant`) models, and correspond to averages of 50 independent simulations. Each simulation was run for 1000 iterations, and results are shown for iterations (years) 200, 400, 600 and 1000. Black points correspond to observed values.

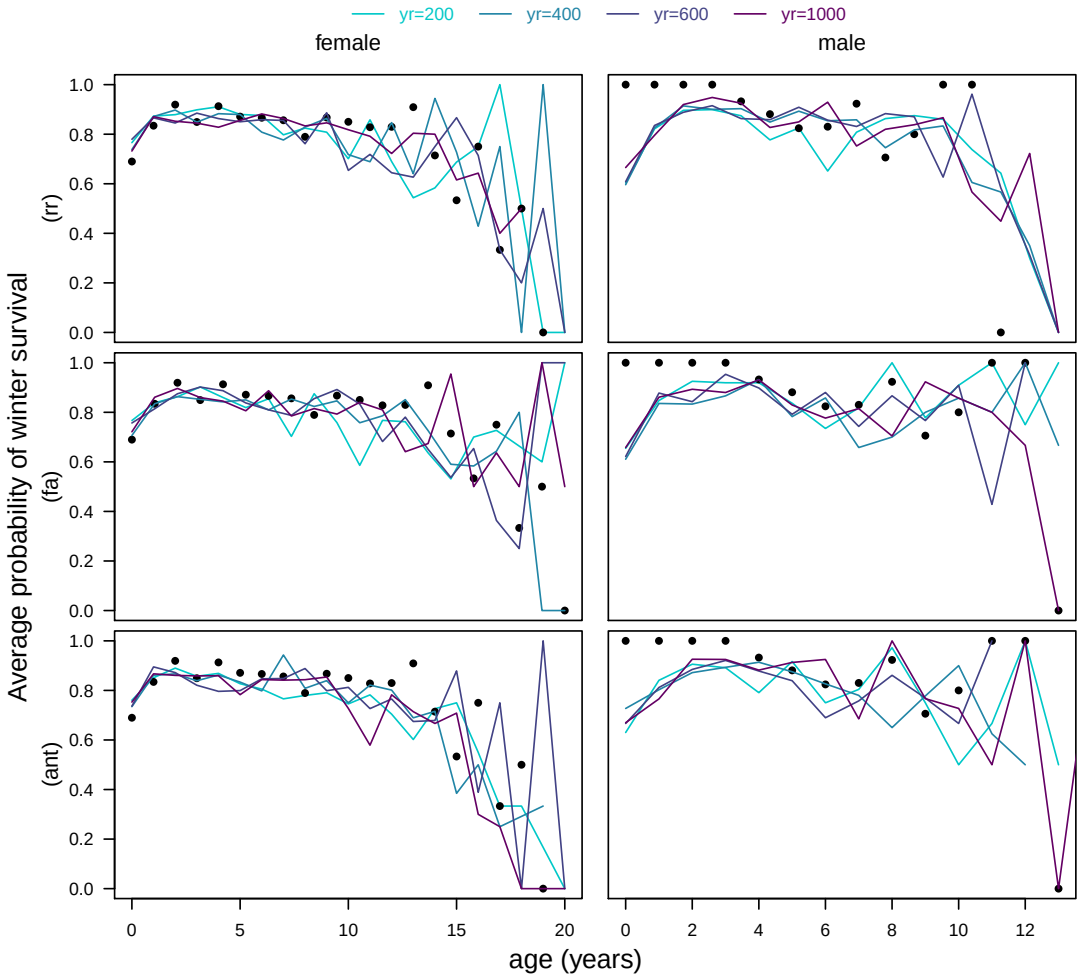

Figure D.3.15: Observed and simulated winter survival as a function of age in a scenario with an inheritance mechanism built-in. Results are shown for the three approaches used to modelling size trajectories, random regression (`rr`), factor analytic (`rr`) and antedependence (`ant`) models, and correspond to averages of 50 independent simulations. Each simulation was run for 1000 iterations, and results are shown for iterations (years) 200, 400, 600 and 1000. Black points correspond to observed values.

Bibliography

Lynch, M. & Walsh, B. 1998. *Genetics and analysis of quantitative traits*. Sinauer, Sunderland, MA.

McArdle, J.J. & McDonald, R.P. 1984. Some algebraic properties of the Reticular Action Model for moment structures. *British Journal of Mathematical and Statistical Psychology* **37**: 234–251.

Robert, C.P. & Casella, G. 2005. *Monte Carlo statistical methods*, 2nd edn. Springer texts in statistics. Springer, Berlin. URL `https://cds.cern.ch/record/1187871`.